UNIVERSITY OF OKLAHOMA

GRADUATE COLLEGE

# PERMIAN LOESS AND EQUATORIAL GLACIATION IN EASTERN EQUATORIAL PANGEA

A DISSERTATION

SUBMITTED TO THE GRADUATE FACULTY

in partial fulfillment of the requirements for the

Degree of

DOCTOR OF PHILOSOPHY

By

LILY S. PFEIFER
Norman, Oklahoma
2020

# PERMIAN LOESS AND EQUATORIAL GLACIATION IN EASTERN EQUATORIAL PANGEA

A DISSERTATION APPROVED FOR THE
SCHOOL OF GEOSCIENCES

BY THE COMMITTEE CONSISTING OF

Dr. Gerilyn S. Soreghan, Chair

Dr. Michael J. Soreghan

Dr. Megan E. Elwood Madden

Dr. Kelly K. Feille

# TABLE OF CONTENTS

Supplemental Materials

## ACKNOWLEDGEMENTS

I am eternally grateful for my advisor—Dr. Lynn Soreghan—who has provided many years of support, mentorship, encouragement, and unforgettable experiences. She is the ultimate role model, and I am privileged to have had the opportunity to learn from her throughout my graduate career! Thanks to my committee—Drs. Lynn Soreghan, Mike Soreghan, Megan Elwood-Madden, and Kelly Feille for challenging and guiding me through the writing and defense of my dissertation. To Drs. Stéphane Pochat and Jean Van Den Driessche, for our long-lived international collaboration, many successful summers in the dust of the Salagou, and more to come. I am especially thankful for Dr. Linda Hinnov's patient mentorship in cyclostratigraphy! To Drs. Gary Weissmann, Roberto Ibarra, Mike Soreghan, and Kelly Feille for expanding my perspectives in science education. And to Christian Zeeden and colleagues at the Leibniz Institute for Applied Geophysics (LIAG) for their contributions to Chapter II.

Chapters I, II, and IV of this dissertation are derived from articles published in Geological Society of America Bulletin, Frontiers in Earth Science, and Journal of Geoscience Education, respectively (note copyright statements on the cover page for each chapter). A special thanks goes to our many reviewers and editors at these journals (named in the Acknowledgements section for each chapter) for their assistance improving these manuscripts for publication.

To my fantastic research group—especially Alicia Bonar, Steve Adams—you are the best. Thank you also to my long-term mentors (Drs. Jeff Trop, Chris Daniel), and to all my wonderful family and friends (geos and non-geos) for their encouragement and interest in my work, including a significant thank you to my amazing husband, Clayton—I could not have done this without your patience and unwavering support! Thanks to our 2018–2019 NSF IRES student participants (Lory Alaniz, Brooke Birkett, Stepfan Huntsman, Jada Langston, Jessica Mueller, Emily Simpson, Vee Smith, Karen Yeager) for field work and data collection in France, and especially to Brooke Birkett for her continued work on Chapter IV. Thanks also to Dr. Lindsey Hunt and undergraduate students Zach Tomlinson and Autumn Roche for assistance with grain-size analysis and microprobe work. A huge thanks to the incredibly helpful and efficient School of Geosciences staff on the 7$^{th}$ floor (Ashley, Ginger, Leah, Rebecca)! Thanks to the University of Oklahoma Office of Human Research Participant Protection/ Institutional Review Board for training and support relevant to Chapter IV (IRB No. 9330).

This work was supported by the National Science Foundation (NSF) under International Research Experiences for Students (IRES) grant OISE-1658614 (principal investigators Drs. Lynn and Mike Soreghan) and also EAR-1338331 (Sedimentary Geology and Paleobiology Program; PI Dr. Lynn Soreghan). Additional support was provided by the Eberly Family Chair in Geosciences at OU (Dr. Lynn Soreghan). Financial support for partially offsetting publication costs for Chapter I was provided from the Office of the Vice President for Research and the Office of the Provost (OU). I am also grateful for financial support received through the Robberson Conference Presentation & Creative Exhibition Travel Grant (Graduate College, OU) to attend and present at national conferences (GSA, AGU) as well as the financial support I have received through the Sally R. Thomas Endowed Scholarship, the Bill K. and Donna Reed Fellowship, and the Cecil Von Hagen Endowed Scholarship to complete this degree.

## ABSTRACT

Carboniferous-Permian strata in basins within and proximal-to the Central Pangean Mountains (CPM) archive regional paleoequatorial climate during a unique interval in geological history (Pangean assembly, ice-age apex-and-collapse, megamonsoon inception). Whether these strata preserve a periglacial signal—or are periglacial in origin—remains debated. With a focus on upper Paleozoic (Upper Carboniferous – Permian) strata from the Lodève Basin, south-central Massif Central, France (eastern equatorial Pangea), this dissertation aims to address these questions through detailed sedimentology and analytical methods such as sediment geochemistry, detrital zircon geochronology, and cyclostratigraphy (time series analysis of magnetic susceptibility data). The purpose of this abstract is to illuminate relationships among the four chapters of this dissertation. Each chapter to follow is formatted for publication in various peer-reviewed scientific journals.

Ancient (Upper Carboniferous-Permian) loess deposits represent semiarid paleoclimates that—relative to the Quaternary Earth—are unusual in terms of their (paleo)equatorial occurrence (Chan and Archer, 2003; Muhs and Bettis, 2003; Soreghan et al., 2008a). Voluminous loess deposits are well recognized in the Upper Carboniferous-Permian record of western equatorial Pangea (e.g., Murphy, 1987; Johnson, 1989; Kessler et al., 2001; Soreghan et al., 2002, 2008a, 2014b; Soreghan and Soreghan, 2007; Mack and Dinterman, 2002; Tramp et al., 2004; Sweet et al., 2013; Giles et al., 2013; Foster et al., 2014), where they have been interpreted as derived from periglacial processes (Soreghan et al., 2008, 2009, 2014a). **Chapter I** aims to test the hypothesis that lower Permian strata in *eastern* equatorial Pangea (eastern CPM) might record a similar paleoclimatic significance. Through detailed sedimentology, provenance, and geochemical analysis of the Permian Salagou Formation (Lodève Basin, France), we interpret that the ~1.5-km-thick Salagou Formation involves eolian transport of fine-grained (silt-sized) sediment and ultimate deposition as loess, and as dust preserved in shallow, ephemeral lacustrine environments. Coarse-grained protoliths and geochemical proxies that correspond to a low degree of chemical weathering and cool (~4°C) mean annual temperatures suggest that silt generation is most consistent with glacial and periglacial processes in the Variscan Mountains (eastern CPM). These results further support a revised model for early Permian climate, showing continuity of a globally unique distribution of dust across low-latitude upland regions of the supercontinent, where a semiarid tropics may have hosted significant ice at moderate elevation.

Analysis and modeling of magnetic susceptibility data through a ~1000-m paleoloess section from the Salagou Formation **(Chapter II**) yields distinctive Milankovitch-scale paleoclimatic variability through the middle to late Cisuralian (ca. 285-275 Ma), including evidence of a predominant orbital eccentricity-scale cyclicity (~10-m-thick) and subordinate obliquity and precession-scale variability (~3.5 and ~1.8 m-thick). Application of methods designed for cyclic stratigraphy with uncertain timescales indicates depositional rates between 9 to 14 cm/kyr from the lower-upper Salagou Formation. We propose—with the support of laboratory rock magnetic data—that the rock magnetic signal is pedogenically driven, and that the Salagou Formation records ~10 million years of astronomically-forced climatic cyclicity. These results are consistent with eccentricity-scale loessite–paleosol cyclicity in the deep-time record of western equatorial Pangea 100 kyr-scale (Soreghan et al., 1997, 2002; Soreghan M.J. et al., 2014; Tramp et al., 2004), and—more recently— the lower Guadalupian record of mid-

latitude eastern Pangea (Huang et al., 2020). Furthermore, this study demonstrates the ability to recognize cyclic trends through extended stratigraphic successions of deep-time loessite using a portable MS meter. These methods are conducive for rapid and convenient *in situ* data acquisition.

Moving slightly lower in the section of the Lodève Basin, to the lower Permian (lower Cisuralian) Usclas Formation, **Chapter III** probes the mechanisms of formation of delicate impressions in lacustrine strata. These sediments accumulated in the paleoequatorial and intramontane Lodève Basin during peak icehouse conditions (Late Paleozoic Ice Age). Evidence for periglacial and proglacial conditions at paleoequatorial latitudes (though controversial) have been hypothesized in both western (Ancestral Rocky Mountains; Soreghan et al., 2008ab; 2014ab) and eastern Pangea (Variscan paleomountains; Julien, 1895; Becq-Giraudon and Van Den Driessche, 1994; Becq-Giraudon et al., 1996; **Chapter I** - Pfeifer et al., 2020). Our experimental replication of delicate, stellate features that occur here in the Usclas Formation corroborates the interpretation that they are ice-crystal molds. This work records ephemeral freezing in equatorial Pangea, calling for a reevaluation of climate conditions in eastern equatorial Pangea. Ephemeral freezing at low latitudes and low-moderate altitudes (< 2 km), implies either cold tropical temperatures (~5°C cooler than the Last Glacial Maximum) and/or lapse rates that exceeded those of the Last Glacial Maximum.

The work involved in this dissertation was funded by the NSF-IRES (International Research Experiences for Students) program, and thus involved annual recruitment, participation, and mentorship of U.S. undergraduate geoscience cohorts (predominantly first-generation college students, largely from historically underrepresented groups in STEM). **Chapter IV** discusses how activating Multicontext pedagogy—a model that recognizes and includes a broader spectrum of "knowing and doing" (Ibarra, 2001; Chávez and Longerbeam, 2016; Weissmann et al., 2019)—resulted in measurable advances in self-efficacy and field/analytical competencies, especially for higher-context students, from the first to second year of the program. Academic culture—especially in STEM—tends to favor the "low-context" approach of scientific inquiry (task-oriented, linear, individuated), but many students bring different cultural values from personal or community-based experiences that tend to be higher-context (process-oriented, systems-thinking, integrated). This work shows how recognizing and adapting to a broader spectrum of culturally-based learning perspectives enhances program quality – even for a short ~four-week field season.

CHAPTER I

# LOESS IN EASTERN EQUATORIAL PANGEA ARCHIVES A DUSTY ATMOSPHERE AND POSSIBLE UPLAND GLACIATION



Citation:
*Pfeifer, L.S., Soreghan, G.S., Pochat, S., and Van Den Driessche, J. (2020). Loess in eastern equatorial Pangea archives a dusty atmosphere and possible upland glaciation, Geological Society of America Bulletin, doi: https://doi.org/10.1130/B35590.1.*

# LOESS IN EASTERN EQUATORIAL PANGEA ARCHIVES A DUSTY ATMOSPHERE AND POSSIBLE UPLAND GLACIATION


## ABSTRACT

Carboniferous–Permian strata in basins within the Central Pangean Mountains in France archive regional paleoequatorial climate during a unique interval in geological history (Pangea assembly, ice-age collapse, megamonsoon inception). The voluminous (~1.5 km) succession of exclusively fine- grained red beds that comprises the Permian Salagou Formation (Lodève Basin, France) has long been interpreted to record either lacustrine or fluvial deposition, primarily based on a local emphasis of subaqueous features in the upper ~25% of the section. In contrast, data presented here indicate that the lower-middle Salagou Formation is dominated by up to 15-m-thick beds of internally massive red mudstone with abundant pedogenic features (microscale) and no evidence of channeling. Up-section, limited occurrences of ripple and hummocky cross-stratification, and mudcracks record the intermittent in- fluence of shallow water, but with no channeling nor units with grain sizes exceeding coarse silt. These data suggest that the most parsimonious interpretation for the Salagou Formation involves eolian transport of the sediment and ultimate deposition as loess in shallow, ephemeral lacustrine environments. Provenance analyses of the Salagou Formation indicate coarse-grained protoliths and, together with geochemical proxies (chemical index of alteration [CIA] and $\tau_{Na}$) that correspond respectively to a low degree of chemical weathering and a mean annual temperature of ~4 °C, suggest that silt generation in this case is most consistent with cold-weathering (glacial and associated periglacial) processes in the Variscan highlands. Together with previous studies that detailed voluminous Permian loess in western equatorial Pangea, this work shows a globally unique distribution of dust at low latitudes that can be linked either directly to glaciated alpine terranes or to reworked and deflated deposits of other types (e.g., fluvial outwash) where fine-grained material was originally generated from glacial grinding in alpine systems. These results further support a revised model for early Permian climate, in which extratropical ice sheets coexisted with a semiarid tropics that may have hosted significant ice at moderate elevation.


## INTRODUCTION

Ancient (pre-Quaternary) loess deposits record valuable information about paleoclimate and are well recognized in the Upper Paleozoic record of western equatorial Pangea (e.g., Murphy, 1987; Johnson, 1989; Kessler et al., 2001; Soreghan et al., 2002, 2008a, 2014b; Soreghan and Soreghan, 2007; Mack and Dinterman, 2002; Tramp et al., 2004; Sweet et al., 2013; Giles et al., 2013; Foster et al., 2014). The paleoclimatic significance of voluminous Upper Paleozoic loess, particularly in equatorial latitudes, remains debated: Some argue for a periglacial derivation (glacial grinding and eolian deflation; Soreghan and Soreghan, 2007, 2008; Soreghan et al., 2008b, 2009, 2014a, 2014b), and others argue for a peridesert origin (e.g., reworking of eolian dunes; Johansen, 1988). In either case, loess deposits represent semiarid conditions that—relative to Quaternary Earth—are unusual for equatorial regions (Chan and Archer, 2003; Muhs and Bettis, 2003; Soreghan et al., 2008a). Global paleogeography in the late Paleozoic was governed by the assembly of Pangea, and formation of the low-latitude Central Pangean Mountains, which spanned from the Variscan-Hercynian system of Europe (Ziegler et al., 1979; Ziegler, 1996) west to the Appalachian-Ouachita-Marathon uplifts of North America.

Interpretations of loess production in the deep-time record vary; however, if late Paleozoic loess in the western United States has an inferred origin in low-latitude, upland periglacial processes (e.g. Soreghan and Soreghan, 2007; Sweet and Soreghan, 2008; Soreghan et al., 2008a, 2008b, 2009, 2014a, 2014b), then deposits in the Central Pangean Mountains in eastern equatorial Pangea (western Europe) might reflect similar controls on sedimentation across the low-latitude upland regions of the supercontinent.

Carboniferous–Permian strata in basins that formed as a result of postorogenic collapse of the Variscan Mountains (eastern Central Pangean Mountains) in France preserve an unusually complete record of highland-proximal sedimentation in the late Paleozoic. In this paper, we document the sedimentology of the Permian Salagou Formation, an ~1.5-km-thick monotonous succession of exclusively fine-grained red beds in the Lodève Basin (Massif Central, south-central France), long interpreted to record either fluvial floodplain or lacustrine depositional settings. This work presents new interpretations for these strata that have implications for our understanding of paleoequatorial climate during the decline of the late Paleozoic icehouse, and it also contributes to our repertoire of methods for recognizing well-lithified, diagenetically altered loessite in the deep-time record.

## GEOLOGIC BACKGROUND

### Geologic Setting

The Variscan orogeny was a complex arc-continent collision (Matte, 1986) involving long-lived (ca. 500–290 Ma) convergence and extensive crustal shortening (>600 km), followed by mid-late Carboniferous gravitational collapse of the overthickened crust (e.g., Ménard and Molnar, 1988; Burg et al., 1994). Several discrete Carboniferous–Permian continental rift basins in the French Massif Central (Fig. 1) record subsequent development of extensional detachment faults as well as extensional reactivation of long-lived Variscan faults (Van Den Driessche and Brun, 1989; Malavieille et al., 1990; Burg et al., 1994). These basins remained within the equatorial belt throughout the late Paleozoic and archive regional paleoequatorial climate during the collapse of the late Paleozoic icehouse.

The late Paleozoic Pangean supercontinent disrupted zonal oceanic and atmospheric circulation patterns and led to extreme climate conditions (Parrish, 1993). Globally, the Carboniferous to Permian transition is characterized by an overall trend of increased aridity at equatorial latitudes—from widespread peat accumulation in the Carboniferous to arid-climate strata such as eolian siliciclastic and evaporitic facies in the Permian (Parrish, 1993; Tabor and Poulsen, 2008). Late Paleozoic Gondwanan glaciation is supported by abundant geologic evidence and is inferred to reflect several fundamental forcing mechanisms that cooled Earth, such as low $pCO_2$ and solar luminosity (Crowley et al., 1991; Montañez et al., 2007), potentially augmented by elevated sulfate aerosols produced by explosive volcanism (Soreghan et al., 2019). Hypothesized upland glaciation in the Variscan paleomountains of eastern equatorial Pangea was originally posited by Julien (1895), followed by several others (Grangeon, 1960; Dewolf, 1988; Sabrier et al., 1993; Becq-Giraudon and Van Den Driessche, 1994; Becq-Giraudon et al., 1996), but it remains controversial and not generally accepted. Paleoaltitude estimates for the Variscan Mountains range widely (<1000 to >5000 m; e.g., Becq-Giraudon and Van Den Driessche, 1994; Becq-Giraudon et al., 1996; Keller and Hatcher, 1999; Fluteau et al., 2001; Schneider et al., 2006; Roscher and Schneider, 2006).

## Lodève Basin

The Graissessac-Lodève Basin, southern-most Massif Central (Fig. 1), is one of several extensional continental basins that recorded late-stage Variscan collapse. It remained in equatorial latitudes (~5°S to ~15°N throughout the late Paleozoic; Domeier and Torsvik, 2014; Muttoni and Kent, 2019) and preserves one of the thickest, most complete, and well-exposed records of Upper Paleozoic strata in Europe, and it is well correlated to other European Carboniferous– Permian basins (Körner et al., 2003), such as the St. Affrique and Rodez basins to the north (e.g., Hübner et al., 2011). Sediment was sourced from the west and southwest basin margins (Odin, 1986; Pochat and Van Den Driessche, 2011), primarily from rapid (1–17 mm/yr) exhumation of the Montagne Noire metamorphic core complex ca. ~300–285 Ma (Pfeifer et al., 2016). The lower (Upper Carboniferous–Lower Permian) "gray facies" accumulated in inferred ever-wet, fluvial-alluvial, deltaic and deep-lacustrine environments, and it transitions up section to the Permian "red facies," composed of continental red beds interpreted to record deposition in fluvial floodplain, deltaic, and playa-lake environments (e.g., Fig. 1; Odin, 1986; Gand et al., 1997; Körner et al., 2003; Pochat et al., 2005; Schneider et al., 2006; Roscher and Schneider, 2006; Lopez et al., 2008; Pochat and Van Den Driessche, 2011). This gray-to-red transition (Lower Permian) is widely interpreted to reflect increased aridity and seasonality during the collapse of the late Paleozoic icehouse (Körner et al., 2003; Schneider et al., 2006; Roscher and Schneider, 2006; Lopez et al., 2008; Michel et al., 2015a), but others posit that this shift records a tectonic evolution (enlargement of the extensional basin) with superimposed climatic variation (Pochat and Van Den Driessche, 2011). Lodève Basin strata subsequently underwent deep (~3 km) burial and high geothermal heat flow (up to 610 °C in the western Graissessac Basin; Copard et al., 2000) and thus are moderately to severely diagenetically overprinted. Diagenesis precludes paleoenvironmental reconstructions (e.g., $pCO_2$) based on paleopedological isotopic analyses and clay mineralogy (e.g., Schneider et al., 2006; Quast et al., 2006; Michel, 2009; Michel et al., 2015a).

## Salagou Formation

The Permian Salagou Formation consists of an estimated 1500–1700 m of fine-grained red beds. They resemble the voluminous fine-grained Permian red beds of western equatorial Pangea (e.g., Soreghan et al., 2008a) studied in many regions of the southwestern and midcontinental United States that have been interpreted as ancient loess deposits (Murphy, 1987; Johnson, 1989; Kessler et al., 2001; Soreghan et al., 2002; Mack and Dinterman, 2002; Tramp et al., 2004; Soreghan and Soreghan, 2007; Sweet et al., 2013; Giles et al., 2013; Foster et al., 2014). The Salagou Formation is thought to have accumulated over several million years, but dates remain in flux. The Rabejac Formation, immediately below the Salagou Formation, is middle Artinskian in age, based on the age of the lowest ash bed in the Salagou Formation (284.4 Ma; Michel et al., 2015a) and tetrapod footprints (Schneider et al., 2019). Magnetostratigraphy from Evans (2012) indicated that the Salagou Formation lies within the Kiaman superchron (>262 Ma), confirmed by U-Pb dating on inferred tuffs in the lower– mid-Salagou Octon Member (Michel et al., 2015a) ranging from 284.4 to 282.9 Ma, but the latter dates have been disputed (Pochat and Van Den Driessche, 2015; Michel et al., 2015b).

Previous studies of the Salagou Formation have recognized two primary members within the formation: the Octon Member (lower–middle Salagou, ~1200 m) and the Merifons Member

(upper Salagou, ~600 m), wherein the Merifons transition is defined by a sudden increase in thin silt to fine sand calcareous interbeds (e.g., Körner, 2006; Schneider et al., 2006). At the western margin of the basin, there is an abrupt transition from "dry" (playa) red beds (Salagou Formation) to "wet" (alluvial-fluvial) red beds (upper Merifons Member to La Lieude Formation and La Tour-sur-Orb fanglomerates), but no chronostratigraphic data exist for the La Lieude Formation aside from the tetrapod track ichnofauna that provides a Guadalupian age (Schneider et al., 2010, 2019). These coarse-grained deposits are stratigraphically above the majority of the Salagou Formation (~1.5 km of the Octon Member to lower Merifons Member described in this paper).

A predominance of features in the upper ~25% of the Salagou Formation (Merifons Member) bears evidence of waterlain deposition, leading to prevailing interpretations that advocate either fluvial floodplain or playa-lake deposition (Odin, 1986; Pochat et al., 2005; Schneider et al., 2006; Lopez et al., 2008; Pochat and Van Den Driessche, 2011). Yet, the majority of the section below this point (Octon Member–lower Merifons Member) is internally structureless and lacks evidence for fluvial deposition (e.g., channelization, cross-stratification, unidirectional paleocurrent indicators, evidence for floodplain deposition such as climbing ripples, or even laminae). Environmental interpretations include (1) a semiarid, fluctuating shallow playa lake (Merifons Member; westernmost part of basin) that graded eastward into a vast, sporadically flooded plain (Odin, 1986), (2) a playa floodplain with ephemeral lakes and Vertisol to calcic Vertisol horizons, where desiccation features represent overbank deposits or sheetflood events that mobilized fine detritus (Schneider et al., 2006; Lopez et al., 2008; Michel et al., 2015a), and (3) a large, oxic lake (Pochat et al., 2005; Pochat and Van Den Driessche, 2011), where the consistent orientation of wave ripples in the upper part of the formation records stable climate, S-SW–directed wind (present-day coordinates), and estimated water depths of ~6–50 m during the mid- to Late Permian (Pochat et al., 2005; Pochat and Van Den Driessche, 2011).

## METHODS

### Facies Analysis

In total, a 1015 m section of the Salagou Formation (concatenation of nine 70–200 m sections; Fig. 2) was measured and described at decimeter scale to assess spatial and temporal variations in the stratigraphy. Hand samples for grain-size analysis and thin-section petrography were collected every 5–10 m. Suspected paleosols were described following terminology from Brewer (1976), Mack et al. (1993), and Retallack (2001). The Salagou Formation has not been measured and described at decimeter scale detail previously, though it has appeared in theses (Körner, 2006 [in German]). Prior estimates of its thickness (~2000 m; Pochat et al., 2005; Schneider et al., 2006) derived from its map pattern (Fig. 2) may be overestimated.

### Relative Grain-Size Analysis

Owing to sample lithification that precluded disaggregation, relative grain-size analysis (quartz size fraction; Table 1) was conducted for both the massive red mudstone facies and the Montagne Noire basement (source) lithologies using two-dimensional (2-D) backscatter-electron (BSE) image analysis techniques modified from M. Soreghan and Francus (2004). We focused

on quartz because of its resistance to chemical alteration and its application in interpreting wind-strength fluctuations within loess-paleosol successions (Porter and An, 1995; Xiao et al., 1995; M. Soreghan and Francus, 2004). Twelve digital BSE images per sample were acquired (at 760x; images 500 μm across) using a Cameca SX100 electron probe micro-analyzer. For several granitic basement samples, images were acquired at lower magnification (at 125x; images 2000 μm across) to accommodate larger quartz grains, and even then, quartz grains were commonly larger than the field of view (see for example Appendix 1[1]). If quartz was not distinct from plagioclase or dolomite (based on texture or grayscale), identification of each quartz grain was done with energy dispersive spectroscopy (EDS). The silica-rich matrix of the Salagou Formation precluded automated differentiation of quartz and matrix by BSE contrast (as in M. Soreghan and Francus, 2004), so images were first processed by manually tracing quartz grains before being scanned into Image J (National Institute of Health freeware package) to measure the cross-sectional areas. Particle size distribution results depend on the method used: Laser diffraction (e.g., with laser particle-size analysis [LPSA]) enables measurement of three-dimensional (3-D) grain size, whereas image analysis techniques on 2-D sample slices are fine-skewed and cannot resolve the finest (<2 μm) phases (Soreghan and Francus, 2004; Varga et al., 2018). Additionally, this analysis focused exclusively on the quartz grains, to assess relative variations through the section, rather than absolute grain size. Stereological corrections to predict 3-D volume from a 2-D measurement are difficult in "multidispersal" systems that include a range of grain sizes and shapes (Sahagian and Proussevitch, 1998; M. Soreghan and Francus, 2004). To understand quartz grain-size results cast in a "truer" distribution, we applied a stereological correction for 2-D to 3-D conversion (Johnson, 1994), which did not substantially affect grain-size statistics (mean and mode increased by an average of 0.5 μm and 0.8 μm, respectively; see Table 1).

**Geochemistry**

Whole-rock geochemistry (Table 2) was acquired from the lower (n = 3), middle (n = 3), and upper (n = 4) Salagou Formation. Additional samples included detailed sampling (n = 4, 30 cm apart) of a profile in the middle Salagou Formation that displayed inferred macroscopic pedogenic features and a set (n = 5) of predominant source-rock lithologies (schist, granite, and tuff from the Montagne Noire dome). The chemical index of alteration (CIA; Nesbitt and Young, 1982; Price and Velbel, 2003; Joo et al., 2018) represents major-element proportions ($Al_2O_3/[Al_2O_3 + CaO + Na_2O + K_2O]$) and is a proxy for the intensity of chemical weathering. We consider that grain size can affect CIA values (e.g., Whitmore et al., 2004; Hatano et al., 2019), but results allow for comparison of inferred pedogenic horizons and parent loess (in the basin), and assessment of the degree of chemical weathering in the paleohighlands (at the source). Similarly, the index of sodium depletion fraction ($\tau_{Na}$) assesses surface soil chemical weathering intensity by measuring the depletion of Na relative to immobile Zr with the equation $\tau_{Na} = (Na/Zr)_{soil}/(Na/Zr)_{protolith} - 1$ (Rasmussen et al., 2011; Yang et al., 2016). The $\tau_{Na}$–mean annual temperature (MAT) empirical transfer function ($MAT = -24.2 \times \tau_{Na} - 0.9$) proposed by Yang et al. (2016) represents the dependence of surface chemical weathering intensity ($\tau_{Na}$) on air temperature (MAT) and thus offers a quantitative method with which to estimate paleotemperatures (±2.7 °C) from deep-time records.

## SEDIMENTOLOGIC DATA

### Attributes of Salagou Formation Source Lithologies: Montagne Noire Dome

Pfeifer et al. (2016) used detrital zircon geochronology and sandstone petrography to assess provenance of the Salagou Formation (Fig. 3). Detrital zircon analysis of three Salagou Formation samples (lower, middle, upper) all yielded a principal age peak of 460 Ma. The middle and upper Salagou Formation exhibited age distributions that included equally dominant age peaks at 287 and 294 Ma, respectively, whereas the basal sample from the Salagou Formation had a subordinate age peak at 311 Ma. These samples are quartzofeldspathic (31%–44% feldspar; 9:1 plagioclase:potassium), with subordinate proportions of metamorphic lithics (14%–17%). These data record a predominant source within the Montagne Noire metamorphic core complex, a Variscan paleohigh located <30 km W-SW of the Lodève Basin. The Montagne Noire dome consists of a deformed and metamorphosed Neoproterozoic to Lower Paleozoic series (schist and gneiss) intruded by Ordovician granites, and later by ca. 320–295 Ma granitoids. New quartz grain-size and geochemical data (CIA) for several of the predominant source lithologies are shown in Tables 1 and 2, respectively. Average (Neoproterozoic) schist (n = 2) CIA is 70, with mean quartz grain sizes of 31–56 μm. Average Carboniferous– Permian granite (n = 2) CIA is 59, and quartz grain sizes in most cases were too large for imaging on the probe, but two of the finer granite samples had mean quartz grain sizes of 175 and 191 μm, respectively. A Cambrian tuff from the study area (n = 1) exhibited a mean quartz grain size of 127 μm. We attempted a volumetric estimation for the CIA mode of the source as a whole using the geochemistry and hypothesized ratio (70% schist and 30% granite) of these units in the source terrane and derived a CIA of ~66. However, we lacked geochemical data for other lithologies that were also actively eroding sources, as recorded by predominant peaks in detrital zircon data (e.g., the Ordovician orthogneiss). Unaltered CIA values of gneiss are typically quite low (~50; Tijani et al., 2006), so we would expect a more comprehensive estimation of volumetric CIA for the source terrane as a whole to be <66.

### Attributes of the Salagou Formation

#### *Massive Red Mudstone Facies*

***Description.*** The massive red to reddish-brown (5YR 5/8–5/6) mudstone facies (Fig. 4) is the most prevalent lithofacies, making up 90% of the lower-to-middle and 70% of the upper Salagou Formation. It occurs in tabular, laterally continuous beds that range in thickness from a few centimeters up to 15–20 m, and it exhibits abrupt, nonerosive contacts with interbedded units. This facies is internally structureless and fractures in a blocky manner. It is well cemented and lacks grading, laminations, and preferred sedimentary fabric in thin section (Fig. 5). Modal analysis of nonmatrix grains (n =7; Fig. 3) showed ~50% quartz, ~35% plagioclase feldspar (albite), and ~15% lithics (metamorphic). Quartz grains are subangular, moderately sorted, and silt sized (mean overall 23 μm, mean range 19–28 μm; Table 1). Most samples have a high proportion (~50%) of fine-grained matrix consisting predominantly of illite with subordinate chlorite (and heavy minerals rutile, apatite, and hematite; Appendix 1 [see footnote 1]). These observations reinforce previous work (Michel, 2009), wherein X-ray diffraction (XRD) of the <2 μm fraction of the Octon Member (lower Salagou Formation) yielded clay compositions of illite

and quartz with subordinate components of minerals from the chlorite-kandite group (undifferentiated). Other cements included silica, potassium feldspar, calcite, and dolomite. CIA values from the massive red mudstone in the upper, middle, and lower Salagou ranged from 60 to 66 (Table 2; average 63).

***Interpretation.*** The fine (mud) grain size, thick and internally structureless beds, and local pedogenic overprinting (see below) of the massive red mudstone facies lead us to interpret these as loess deposits (e.g., Pye, 1987; Tsoar and Pye, 1987; Johnson, 1989; Muhs, 2007; Soreghan and Soreghan, 2007, 2008a, 2008b; Sweet et al., 2013; Foster et al., 2014). Quartz grain-size means (19–28 μm; Table 1) are uniform throughout the section. Note that mean grain sizes from the Salagou Formation are limited to the 2-D analysis of quartz grains and therefore cannot be compared in an absolute manner to "typical" loess size distributions (e.g., 2–50 μm; Muhs, 2018), which represent an analysis of the full particle distribution on disaggregated material. However, of all quartz grains analyzed (n = 1846), 97% were in the silt (~4–62 μm) range (78% were in the range of medium silt, 6–30 μm). Studies on Quaternary loess recognize considerable variability in both composition and grain size among loess bodies wherein predominant $SiO_2$ ranges from 45% to 75% and grain size (typically 60%–90% within 2–50 μm) fines with distance from source (Pye, 1987; Liu, 1988; Muhs and Bettis, 2003; Porter, 2001; Muhs et al., 2004; Muhs, 2018). This facies shares attributes with Upper Paleozoic loessite of the western United States, which are also mineralogically immature, angular to subangular, and feldspar rich (Johnson, 1989; Soreghan and Soreghan, 2007; Soreghan et al., 2008a), although it is possible that some albite in the Salagou Formation is authigenic (e.g., Schneider et al., 2006).

In ancient loessite, proportions of clay-sized material and/or true clay minerals also vary, increasing (up to 30%–50%) with distance from source and within pedogenically modified horizons (e.g., Soreghan et al., 2002; Tramp et al., 2004; Soreghan and Soreghan, 2007). Similar to formerly termed "graywacke" sandstone (e.g., Dickinson, 1970, and others; see also Garzanti, 2017), "graywacke" mudstone in the Salagou Formation is difficult to evaluate given the apparently clay-rich matrix. Modern fine-fraction dust (very fine silt particles that are clay agglomerates) can reflect lacustrine deflation (e.g., diatomaceous material such as that of the Bodélé depression; e.g., Smalley et al., 2005), and "clay pellets" such as those recognized in the matrix of Triassic loessite (e.g., Wilkins et al., 2018). However, no evidence of clay pellets occurs in thin sections of mudstone from the Salagou Formation. Given the history of elevated temperature and burial in the Lodève Basin, combined with the well-documented volcanic centers in the greater region (see below; e.g. Soreghan et al., 2019; Michel et al., 2015a), the illite-dominant matrix likely reflects transformation from formerly smectitic clay—a common product of altered volcanic glass, feldspar, mafic silicates, and other aluminosilicates (Chamley, 1989; Tabor and Myers, 2015). Smectite forms in areas with moderate to low rainfall, and poor drainage, or in dry low latitudes (Chamley, 1989). Perhaps seasonal, shallow lacustrine conditions in the Lodève Basin sustained an environment sufficiently wet to convert fine ash to smectite. Subordinate chlorite was either sourced locally from chlorite-rich schists in the Montagne Noire dome, or it was also an alteration product of a distal (muscovite-rich) source.

The illite-rich pseudomatrix in the Salagou Formation likely represents long-range suspension of fine volcanic material that had a separate provenance from local coeval source terranes in the Montagne Noire dome ("coarser" Q-F-Lm fraction; Fig. 3). Recent work (Wilson et al., 2019) inferred distal volcanic sources as a substantial component in Lower Triassic loessite from the North Sea that exhibited similarly illite-enriched compositions. Additional work

(clay mineralogy, geochemistry, and geochronology) is required to pinpoint the correlative volcanic source(s), but late Paleozoic ice age explosive (ignimbritic) volcanism peaked ca. 300–290 Ma (associated with Variscan orogenic collapse) near the paleo-equator (Soreghan et al., 2019, and references within). Discrete tuffs (284–282 Ma; Michel et al., 2015a) occur throughout the lower–middle Salagou Formation, so it is reasonable to infer that long-distance sourcing of volcanic aerosol dust defines the fine detrital matrix in the Salagou Formation.

The consistently low CIA values (average 63) of the massive red mudstone facies are similar to those of Upper Paleozoic loessite of western equatorial Pangea (average 59–60; Soreghan et al., 2002; Soreghan et al., 2008a), with values between those of unweathered granite and average shale (50–70; Nesbitt and Young, 1982). Furthermore, CIA values of the interpreted loessite approximate the modal CIA of the basement sources (59–70), reflecting a low degree of chemical weathering. CIA values from the Lodève Basin have been reported previously (Schneider et al., 2006; Lopez et al., 2008) and were similarly interpreted to reflect weak chemical weathering, attributed to maximum aridity in the upper Octon Member (roughly in the middle Salagou Formation).

### *Pedogenic Intervals within the Massive Red Mudstone Facies*

***Description.*** Large (~10+ cm), randomly oriented, semiradial slickensides exist locally within the massive red mudstone facies (Fig. 4). The color (5YR 5/8–5/6) of these units and the mineralogy of clay matrix do not change from that in the massive mudstone facies, but the proportion of clay-rich matrix is on average slightly higher (Fig. 5). Discontinuous nodular bedding, and reduction halos around irregular, vertical traces that are abruptly truncated also occur within this facies. Micromorphologic attributes of samples from these localities include birefringent clay concentrations, wedge-shaped peds, circumgranular cracks, clay coatings on grains, calcium carbonate nodules, and porphyroskelic (Retallack, 2001) fabrics (e.g., Fig. 5). CIA values from these intervals average 66, and $\tau_{Na}$ is −0.22 (Fig. 6).

***Interpretation.*** Randomly oriented slickensides and rare root traces in the massive red mudstone facies are interpreted to reflect pedogenesis, an interpretation further confirmed by the micromorphological and geochemical characteristics. The lack of horizonation in these soil profiles reflects a combination of incipient soil development that persisted despite the continuous accumulation of eolian dust, and destruction of (any) primary horizonation by shrink-swell pedoturbation. The high clay content (illite matrix, likely smectite prior to diagenesis) and defining (macro and micro) attributes of interpreted pedogenic horizons are most closely analogous to modern Vertisols (Driese and Foreman, 1992; Ahmad, 1983; Gray and Nickelsen, 1989; Mack et al., 1993). Seasonal wetting and drying cause shearing and slickensides in the B horizon and desiccation cracks (described in following section) during dry seasons (Gray and Nickelsen, 1989; Mack et al., 1993), as well as microscale features such as wedge-shaped peds (Mack et al., 1993), clay coatings on peds or detrital grains (Nettleton and Sleeman, 1985; Driese and Foreman, 1992), and concentrated masses (globules) of hematite (Brewer, 1976), most of which are observable in thin section in these samples (Fig. 5). Horizons with interpreted pedogenically altered zones have elevated CIAs (average 66; Fig. 6) compared with those in the interpreted parent loessite (average 63), consistent with enhanced weathering during ephemerally wet intervals. Studies of Paleozoic loessite in the western United States revealed similar patterns, with elevated CIAs (up to 75) and aluminum in intercalated pedogenic horizons (Soreghan et al.,

2002; Tramp et al., 2004; Soreghan et al., 2008a). Locally (lower–middle Salagou Formation), discontinuous nodular bedding and carbonate micronodules in thin section represent incipient soil development (e.g., weakly developed Calcisols) or the reworking of loess during wetter periods (Johnson, 1989; Mack et al., 1993; Michel, 2009). Water availability modulates the relative effectiveness of many pedogenic processes (Retallack, 2001; Sheldon and Tabor, 2009). Vertisol development typically indicates seasonal precipitation (Tabor and Myers, 2015); in the modern–Pliocene record, these form in regions (semiarid tropics) that receive ∼400/500–1000 mm of annual precipitation (e.g., Lepre, 2019). The presence of interpreted Vertisols in the Salagou Formation coupled with abundant evidence for intermittent shallow water (e.g., interbedded units described below) suggest seasonal precipitation (∼400 mm+) consistent with in situ Na depletion. Thus, the $\tau_{Na}$ of −0.22 corresponds with a MAT of 4.4 °C during pedogenesis (Fig. 6; Yang et al., 2016).

### *Interbedded Facies*

***Description.*** Thin (1–10 cm), resistant, planar and continuous beds of mudstone cap meter(s)-thick packages of the massive mudstone facies and comprise up to 10% of the lower–middle and 30% of the upper Salagou Formation (Fig. 2). Bedding thicknesses of the intervening massive red mudstone facies decrease substantially in the upper part of the Salagou Formation, controlled by the increased occurrence of interbedded units. Calcareous mudstone interbeds (Figs. 4E–4F) commonly exhibit downwardly tapering polygonal desiccation cracks (commonly ∼10–20 cm in diameter and penetrating downward typically 1–3 cm but up to 8 cm) with up-curled edges, as well as rare asymmetrical/symmetrical ripples (average wavelength of 3–4 cm, <1 cm amplitude; Pochat et al., 2005) and fissile mud drapes. Platy laminated mudstone interbeds (Figs. 4H–4I) occur regularly only in the upper Salagou Formation. They are typically 3–5 cm (up to 10 cm) thick, they are invariably reduced (buff to blue), and they exhibit platy fracturing along very thin (millimeter-scale) pervasive laminations. Hummocky cross-stratification (HCS) and asymmetrical/symmetrical wave ripples are common, and basal/upper contacts are abrupt.

***Interpretation.*** Desiccation features also indicate that drying of saturated sediment or shallow water (clay shrinking) was common. Variable depths of crack penetration (1–8 cm) might relate to the intensity of seasonal precipitation (Tabor and Myers, 2015). Ripples and HCS record wind perturbation of a seasonally wet shallow lacustrine environment, but in the predominant red mudstone facies, there is no evidence of graded or laminated beds consistent with deep subaqueous deposition. The uniformly silt-sized grains and overall similar characteristics of these interbedded facies to the massive red mudstone facies suggest sediment was similarly delivered by eolian processes, wherein ephemeral standing water effectively trapped settling dust. The sedimentary structures (laminations, ripples, desiccation features) and well-defined bedding that differentiate interbedded units from the predominant massive mudstone facies record subaqueous reworking and sorting of the sediment.

## DISCUSSION

### Recognition of Permian Loess in Eastern Equatorial Pangea

We postulate that the Salagou Formation facies exhibit characteristics most consistent with eolian transport and ultimate deposition as loess, with subordinate reworking of eolian-transported dust (clay and silt) into shallow lacustrine environments. Previous depositional interpretations of the Salagou Formation have focused primarily on the "interbedded" facies that contain positive evidence for the influence of water. However, the volumetric predominance of the massive mudstone (70%–90% of the unit) has proven relatively enigmatic owing to the absence of evidence for fluvial attributes such as channels, erosional scours, cross-stratification, or climbing ripple cross-stratified units. The uniform mud size also calls into question a fluvial interpretation. Although a general up-section increase occurs in interbedded units and sedimentary structures reflective of subaqueous deposition, the frequency and extent of interbedded units are vastly subordinate to the proportion of massive mudstone. Asymmetric ripples inferred to record Permian winds invariably are also associated with symmetrical ripples in the same bed (Pochat et al., 2005), and HCS and gutter casts represent combined flow during shallow-lacustrine storm events. Provenance based on detrital zircon geochronology and petrography indicates sediment sourcing from the Montagne Noire (located W-SW of the basin; Pfeifer et al., 2016), but the transport mechanism for the vast volume of fine-grained sediment has not been previously identified.

### Silt Generation

If the Salagou Formation is predominantly loess—whether deposited directly from the air as loess, or eolian-transported dust with final deposition in shallow, ephemeral lakes—then its great thickness (~1.5 km based on our measurements; Fig. 2) represents generation of an enormous amount of silt-sized quartz (in addition to fine-grained feldspar, metamorphic lithics, very fine-grained clay-rich matrix, and accessory phases). Several processes, including salt, chemical, or tectonic weathering, saltation-induced abrasion, weathering of silt-rich protoliths, fluvial comminution, deflation of silt-rich (e.g., deltaic, floodplain) sources, and glacial grinding, are considered potentially capable of producing silt-sized grains, but their relative efficacy remains debated. Building on previous discussions by Soreghan et al. (2008a), Muhs (2013), and others, we reviewed the suitability of these processes and examined them in context of the Salagou Formation.

Nahon and Trompette (1982) considered tropical (chemical) weathering in modern systems as a primary mechanism to generate silt, but many subsequent studies suggested limited production of silt by these means (Pye and Mazzullo, 1994; Assallay et al., 1998; Wright, 2002, 2007). CIA values of the Salagou Formation loess (average 63), paleosols (average 66), and basement (maximum ~66; see discussion above) are consistently low and overlap within error. Together with the preservation of labile phases ($\tau_{Na}$ of −0.22 and abundant plagioclase feldspar throughout the Salagou Formation), the geochemical data (Fig. 6) are inconsistent with a tropical weathering origin (Nesbitt and Young, 1996) and indicate sediment was sourced from a region dominated by physical weathering and/ or high altitude (e.g., Johnson, 1989; Soreghan et al., 2008a, 2014b).

Weathering of silt-rich protoliths such as siltstone, slate, phyllite, and volcanic rocks can release large quantities of "ready-made" silt (Kuenen, 1969; Blatt, 1987, 1989; Muhs and Bettis, 2003; Soreghan et al., 2016). In both mechanical and chemical weathering, granitic and gneissic sources tend to generate sand-sized quartz twice the size of quartz from schist (Blatt, 1967; Borrelli et al., 2014), although others suggest granite can release significant silt (e.g. Wright, 2007; discussion to follow). Detrital zircon data (Fig. 3) reveal a Carboniferous–Permian age population (310–285 Ma) that persists throughout deposition of the Salagou Formation and records derivation from coarse-grained (175– 191 μm; Table 1) granitic protoliths of this age from the Montagne Noire dome. The absence of volcanic lithics in framework modes of the Salagou Formation (Fig. 3), together with the sizes of both quartz (19–28 μm; Table 1) and zircon (>>30 μm) grains, indicates the exclusively local provenance of Carboniferous–Permian detrital zircon as opposed to contributions from distal penecontemporaneous volcanic ash (inferred constituent of the illite-abundant matrix). Detrital zircon ages were obtained with a 30 μm laser spot size, so dated grains were >30 μm, and many were broken or rounded rather than the prismatic and euhedral shapes typical of volcanic grains. Other volcanic units in the immediate source area include Cambrian tuffs, which are minimally exposed and exhibit a coarse quartz grain size (127 μm; Table 1). Finally, the finest average quartz grain sizes from the Montagne Noire Neoproterozoic schists (31–56 μm) exceed those (19–28 μm) measured in all samples of the loessite (Table 1).

Experimental studies (Goudie et al., 1979; Wright and Smith, 1993; Wright, 2007) have demonstrated that some silt but mostly sand (>70%) can be produced from parent rock in cases wherein (1) salt is available, and (2) the parent rock is susceptible to disaggregation (e.g., porous sandstone; Smith et al., 2002). The Salagou Formation contains little to no sand-sized grains, and the source (Montagne Noire) is composed of granite, schist, and gneiss. Dust deflated from sabkha-playa systems would have an evaporitic (e.g., gypsiferous) or diatomaceous component (e.g., the Bodélé depression; Koren et al., 2006; Bristow and Moller, 2018). Previous workers have recognized pedogenic gypsum in the uppermost Salagou Formation (Merifons Member; Michel et al., 2015a), but it is neither abundant nor widespread. Hence, salt weathering is not a tenable solution for production of fines in this system.

The importance of silt generation in the form of "desert" loess—quartz fragmentation resulting from saltation-induced intergranular collisions—remains disputed (e.g., Smalley, 1990; Wright, 2001; Smith et al., 2002; Smalley et al., 2019). For example, some suggest that the large accumulations in the Chinese Loess Plateau originated in proximal deserts (Liu et al., 1994; Porter, 2001), whereas others suggest a glacial origin in the mountains of high Asia, followed by desert "storage" and ultimate deflation (e.g., Assallay et al., 1998; Smalley et al., 2005; Stevens et al., 2013; Li et al., 2018; Smalley et al., 2019). Formation of the silt in Permian–Pennsylvanian loessite in western Pangea was similarly linked initially to saltation abrasion in coeval sand dunes, owing primarily to the low-latitude setting (e.g., Johansen, 1988), but later work has called this into question. The quartzofeldspathic composition of these deposits is incompatible with coeval quartz-rich eolian sands, and silt from reworked dunes is commonly coarser (e.g., Johnson, 1989) or finer (Stuut et al., 2009) than typical "loess-size" grains (Whalley et al., 1987; Assallay et al., 1998; Bullard et al., 2004). Finally, the volumetrics of the loessite significantly exceed those of (potential) coeval eolian sandstone (Soreghan et al., 2008a, and references within). There is very little loess-sized silt documented in association with erg systems (e.g., Smalley and Vita-Finzi, 1968; Smalley and Krinsley, 1978; Tsoar and Pye, 1987; Smalley, 1990; Assallay et al., 1998; Muhs and Bettis, 2003; Smalley et al., 2005; Muhs, 2013;

Smalley et al., 2019), consistent with experimental studies that call into question the efficacy of making significant volumes of loess-sized quartz silt from saltation abrasion of eolian sand (Kuenen, 1959; Bullard et al., 2004; Swet et al., 2019; Adams and Soreghan, 2020). In the case of the Salagou Formation, grain-size modes, feldspar-rich compositions, and sheer volume are similarly incompatible with a desert loess origin, especially considering the lack of coeval eolian sandstone in the greater region.

Mechanical comminution in high-energy fluvial systems has also been suggested as a means to produce silt, but experimental results show limited (and fine, 2–20 μm) silt production (e.g., Kuenen, 1959; Moss et al., 1981; Wright and Smith, 1993; Smith and Swart, 2002). Silt-rich rivers occur primarily in regions either producing (high altitude, glacier proximal) or storing (e.g., Yellow River, Chinese Loess Plateau) large volumes of loess. Even in fluvial systems draining the Chinese Loess Plateau, particle sizes can include >50% sand-sized grains (Jia et al., 2016). The importance of river systems in the distribution and concentration of loess prior to eolian deflation is recognized for most large Quaternary loess deposits (Smalley, 1995; Gallet et al., 1998; Wright, 2001), but silt produced by fluvial comminution alone is not consistent with the distribution of major loess deposits. Additionally, in the Lodève Basin study region, no evidence exists for coeval fluvial or deltaic systems, albeit highland-proximal systems are rarely preserved. These arguments suggest a minimal, if any, role for fluvial comminution in generating the fines in the Salagou Formation.

In summary, the effectiveness of salt weathering, tropical weathering, eolian and fluvial comminution, and derivation from precursor silt-rich units in producing abundant silt is limited, but moreover it is inconsistent with data from the Salagou Formation, especially in light of the comparably coarse grain size of known protoliths. Glacial grinding and associated periglacial processes (e.g., frost shattering) are effective mechanisms to comminute bedrock into large volumes of loess-sized silt (see Bryan, 1945; Kuenen, 1969; Smalley and Vita-Finzi, 1968; Boulton, 1978; Pye, 1987; Smalley, 1990, 1995; Wright et al., 1998; Assallay et al., 1998; Muhs and Bettis, 2003; Wright, 2001, 2007; Soreghan et al., 2008a, 2016; Muhs, 2013, 2018; Smalley et al., 2019). Smalley (1990, 1995) noted that most significant Quaternary loess relates to glacial processes (either directly or through an intermediate step) owing to the ease with which glacial systems produce the characteristic loess grain size (Boulton, 1978; Assallay et al., 1998). The great volume of loess-sized silt in the Salagou Formation, the coarse-grained protoliths, and mineralogical and geochemical data that reflect minimal chemical weathering are all most consistent with silt generation in a region dominated by physical, cold-weathering processes and/or at high altitude.

## Late Paleozoic Climatic Significance

A possible glacial or periglacial origin for equatorial loess has significant bearing on the late Paleozoic climate system. Both true loessite and reworked loessite (e.g., marine carbonates with eolian-transported silt) have been documented across western equatorial Pangea (e.g., Soreghan et al., 2008a). Loess in the Salagou Formation—and correlatives in nearby basins (e.g., St. Affrique; Hübner et al., 2011)—whether blown in during glaciation or after being reworked, is interpreted to have been originally generated by glacial and periglacial mechanisms in the Variscan paleohighlands of eastern equatorial Pangea. Evidence for upland glaciation has been previously hypothesized for Upper Carboniferous deposits of the Lodève-Graissessac Basin (e.g. Julien, 1895; Grangeon, 1960; Dewolf, 1988; Sabrier et al., 1993; Becq-Giraudon and Van Den

Driessche, 1994; Becq-Giraudon et al., 1996) but poorly accepted due to both the low paleolatitude (0–15°N) of the Variscan Mountains, and the difficulty of inferring glaciation from highlands that are now eroded; no evidence of ice-contact facies has yet been documented, so only periglacial facies are potentially preserved.

Recent recognition of younger (Lower– Upper Triassic, greenhouse) occurrences of loessite in both Europe and North America (e.g., Chan, 1999; Wilkins et al., 2018; Lawton et al., 2018; Wilson et al., 2019) raises the possibility of recycling of premade silt or erosion of volcanic origins. Gondwanan (continental) ice sheets persisted following "peak" ice (ca. 299 Ma) through the Sakmarian (ca. 290 Ma), decreased substantially through the Artinskian (ca. 283 Ma), and then persisted only in Australia through the Wuchiapingian (Soreghan et al., 2019). If equatorial upland (alpine) glaciation existed, we posit it might have persisted through the Sakmarian–Artinskian. Detrital zircon data from the Salagou Formation (Pfeifer et al., 2016) record the youngest (maximum depositional) age populations from the lower (287 ± 4 Ma), mid-upper (285 ± 3 Ma), and upper (291 ± 8 Ma) parts of the formation, and U-Pb isotope dilution–thermal ionization mass spectrometry dates on inferred tuffs in the lower-mid-Salagou Octon Member (Michel et al., 2015a) range from 284 to 283 Ma (±0.1 Ma). Therefore, despite weak age control of the uppermost Salagou Formation (262 Ma absolute youngest; Evans, 2012), these ages indicate that most of the Salagou Formation silt was generated during icehouse conditions. We cannot reject the possibility of a subordinate recycled or distal component, but these data substantiate the interpretation that loess generation and accumulation were essentially coeval with glacial conditions (within 10–15 m.y. of peak ice) and occurred relatively quickly, consistent with the extremely rapid 1–17 mm/yr exhumation of the source terrane (Pfeifer et al., 2016).

Glaciation has also been hypothesized for uplands of western equatorial Pangea (e.g., Uncompahgre uplift, Ancestral Rocky Mountains, 0–11°) in regions where inferred proglacial depositional systems can be traced toward epeiric shorelines, providing crude constraints on minimum elevations for ice-contact deposition persisting to within 1200–1600 m elevation (Soreghan et al., 2014a), an interpretation that calls for globally cooler paleotemperatures than those previously modeled for low latitudes in the late Paleozoic (Soreghan et al., 2014b). The $\tau_{Na}$ values (−0.19) from loessite in western equatorial Pangea (Maroon Formation, Colorado; Yang et al., 2016) together with $\tau_{Na}$ values (−0.22) from loessite in eastern equatorial Pangea (this study) correspond to MATs between 3.7 and 4.4 ± 2.7 °C at equatorial latitudes during deposition of Upper Pennsylvanian–Permian loess (Fig. 6). This estimated MAT is consistent with glaciation at moderate elevation (Variscan Mountains) in low-latitude Pangea.

Together with studies that document Pennsylvanian–Permian loessite in western equatorial Pangea (Murphy, 1987; Johnson, 1989; Kessler et al., 2001; Soreghan et al., 2002, 2008a, 2014b; Soreghan and Soreghan, 2007; Mack and Dinterman, 2002; Tramp et al., 2004; Sweet et al., 2013; Giles et al., 2013; Foster et al., 2014), this work documents widespread low-latitude accumulations of eolian dust in the Permian. We posit that the confluence of conditions necessary to generate and distribute such a remarkable volume of silt required widespread glaciation of upland regions near the equator (Central Pangean Mountains) and semiarid conditions in this low-latitude region of accumulation, which—from a Quaternary perspective—is unusual. Major loess deposits of the Pliocene–Pleistocene that relate to glacial or periglacial processes occur in temperate, middle- to high-latitude regions (e.g., Muhs and Bettis, 2003; Li et al., 2019) and have been recognized as a "sedimentary extreme" (Chan and Archer, 2003) of unusually high silt production (Muhs and Bettis, 2003). Likewise, the volume and unique

distribution (at equatorial latitudes) of the Pennsylvanian–Permian loess record represent a depositional and climatic extreme. We postulate that widespread loess/dust preservation during this interval—a signal that now spans across low-latitude Pangea—calls for a globally cooler Earth during the time(s) archived by the widespread, first-cycle loess. Evans (2003) classified ice distribution through Earth history into two categories—exclusively high latitudes during the Phanerozoic and exclusively low latitudes during the Precambrian. However, the icehouse mode for the late Paleozoic is perhaps better characterized by climate simulations (Feulner, 2017) that model a range of global MAT from 1.4 °C to 12 °C during the late Carboniferous (relative to 10–15 °C MAT during Pliocene–Pleistocene glaciations) and align with evidence for upland glaciation in equatorial Pangea (simulated MAT ~0–10 °C throughout western and central equatorial Pangea under $CO_2$ of 150 ppm and a cold summer orbital configuration in Gondwanaland; Feulner, 2017).

## CONCLUSION

The Salagou Formation is interpreted to record eolian transport and subsequent deposition as both true loess and as dust that was ultimately trapped in seasonally shallow lakes. The loess interpretation is based primarily on sedimentological characteristics (massive and homogeneous in macroscale observations to entirely fine-grained material with common pedogenic features in microscale observations) and a lack of evidence for fluvial deposition or suitable alternative interpretations for delivering such a large volume (~1.5 km) of silt to the basin. The methods applied here (facies and petrographic analysis, geochemical assessment of parent loess and subordinate pedogenically altered horizons, and grain-size analysis of both the source lithologies and derived sediment) are applicable for recognizing well-lithified and diagenetically altered ancient loessite. This is the first documentation of Upper Paleozoic loessite in eastern equatorial Pangea and thus represents an important contribution in an increasingly recognized record of pre-Quaternary loess for the late Paleozoic ice age. The Salagou Formation, together with analogous Upper Paleozoic loess deposits that have been documented in western equatorial Pangea, records widespread accumulations of eolian-transported material into low-latitude basins. Provenance data, relatively feldspar-rich compositions, and geochemical proxies (CIA and $\tau_{Na}$-MAT values) suggest that the most parsimonious interpretation is that bulk silt generation reflects cold-weathering (glacial and periglacial) processes in the Variscan Mountains (0–15°N). The global recognition of substantial loess deposits at low latitudes has significant implications for our understanding of the late Paleozoic equatorial climate system, which was semiarid and potentially cold enough at times to host ice (at elevation) at the equator.

## ACKNOWLEDGMENTS

This chapter is derived from an article published in *Geological Society of America Bulletin*, 2020, copyright Geological Society of America, available online: *doi.org/10.1130/B35590.1*. This work was supported by the National Science Foundation (NSF) under International Research Experiences for Students (IRES) grant OISE-1658614 (principal investigators G.S. Soreghan, M.J. Soreghan) and also EAR-1338331 (Sedimentary Geology and Paleobiology Program; to G.S. Soreghan). Thanks go to M.J. Soreghan and L.E. Hunt for grain-size analysis and microprobe work, N.G. Heavens for suggestions, and to our 2018–2019 NSF IRES student participants (L. Alaniz, B. Birkett, S. Huntsman, J. Langston, J. Mueller, E. Simpson, V. Smith,

K. Yeager). Thanks also go to our reviewers (J. Schneider and anonymous reviewer) and editors (B. Pratt and R. Strachan) for their assistance with improving this work. Financial support for partially offsetting publication costs was provided from the Office of the Vice President for Research and the Office of the Provost, University of Oklahoma.

**Supplemental Material.** Provided in dissertation section "Supplemental Material for Ch. I". Also available at https://doi.org/10.1130/GSAB.S.12268736.

## FIGURES AND TABLES

**Table 1.** Results of quartz grain size analysis (μm), Salagou Formation, Lodève Basin, France

| | | | | | 3D corrected* | | |
|---|---|---|---|---|---|---|---|
| | Grains (#) | Mode | Median | Mean | Mode | Median | Mean |
| Salagou Formation | | | | | | | |
| Mid-Upper | 120 | 16 | 17 | 21 | 18 | 18 | 21 |
| Mid-Upper | 595 | 17 | 17 | 19 | 9 | 18 | 19 |
| Middle | 312 | 10 | 17 | 21 | 10 | 18 | 22 |
| Lower-Mid | 565 | 10 | 23 | 28 | 11 | 24 | 29 |
| Lower | 254 | 13 | 22 | 28 | 21 | 23 | 29 |
| ALL | 1846 | 17 | 19 | 23 | 17 | 19 | 24 |
| Difference* | | | | | 0.5 | 0.7 | 0.8 |
| | | | | | | | |
| Montagne Noire | | | | | | | |
| Granite 1 | 106 | 209 | 185 | 191 | | | |
| Granite 2 | 115 | 152 | 163 | 175 | | | |
| Schist 1 | 219 | 25 | 32 | 31 | | | |
| Schist 2 | 223 | 51 | 55 | 56 | | | |
| Tuff | 120 | 108 | 122 | 127 | | | |

*Note:* Values in table are statistical distributions of quartz grain-size analysis results by backscattered electron image analysis for the Salagou Formation (upper), and for the Montagne Noire dome (lower; Variscan basement, interpreted source terrane). Dark gray—results with application of the stereological correction from Johnson (1994). Locations within the Salagou Formation are depicted on Figure 2 (lower-middle is Octon Member; upper is Merifons Member).

*Johnson (1994)

**Table 2.** Whole rock geochemistry, Salagou Formation, Lodève Basin, France

| | Lower* Loess | Middle* Loess | Upper* Loess | Avg Loess | Middle Paleosol | Schist Basement | Granite Basement | UCC Standard[†] | NAQL Standard[§] | mmNASC Standard[#] |
|---|---|---|---|---|---|---|---|---|---|---|
| **$SiO_2$** | 59.5 | 61.9 | 61.2 | 60.9 | 58.4 | 81.0 | 75.6 | 66.0 | 80.2 | 60.4 |
| **$Al_2O_3$** | 20.2 | 19.6 | 19.1 | 19.6 | 21.7 | 8.6 | 14.1 | 15.2 | 10.8 | 16.6 |
| **$Fe_2O_3$** | 7.8 | 6.3 | 7.0 | 7.0 | 7.9 | 5.2 | 0.9 | 4.5 | 2.4 | 8.1 |
| **CaO** | 0.3 | 1.3 | 1.4 | 1.0 | 0.3 | 0.3 | 0.1 | 4.2 | 1.1 | 2.3 |
| **MgO** | 3.48 | 2.31 | 3.25 | 3.01 | 2.69 | 1.43 | 0.28 | 2.20 | 0.90 | 6.35 |
| **$Na_2O$** | 2.36 | 4.16 | 3.32 | 3.28 | 3.32 | 0.71 | 1.24 | 3.90 | 1.60 | 1.80 |
| **$K_2O$** | 5.43 | 3.57 | 3.66 | 4.22 | 4.79 | 1.89 | 7.16 | 3.40 | 2.50 | 3.17 |
| **$TiO_2$** | 0.76 | 0.72 | 0.83 | 0.77 | 0.74 | 0.72 | 0.42 | 0.50 | 0.70 | 0.91 |
| Zr | 164 | 165 | 162 | 164 | 173 | 678 | 242 | 190 | 302 | 165 |
| La | 31.6 | 21.6 | 5.3 | 19.5 | 23.3 | 21.7 | 15.1 | 30.0 | 27.9 | 32.0 |
| Th | 6.6 | 3.5 | 1.1 | 3.7 | 5.1 | 3.3 | 2.6 | 10.7 | 8.6 | 10.3 |
| Sc | 9.0 | 5.3 | 2.0 | 5.4 | 7.3 | 3.5 | 2.0 | 11.0 | 7.8 | 18.0 |
| **CIA** | 66 | 60 | 62 | 63 | 66 | 70 | 59 | 46 | 60 | 61 |

*Note:* Summary of whole-rock geochemistry (wt. %) and calculated chemical index of alteration (CIA) values for the Salagou Formation and also for rock types of the Montagne Noire dome (Variscan basement, interpreted source terrane). Samples from inferred "loess" and "paleosol" units are labeled accordingly. The oxides are in percent, and the trace elements are in ppm. UCC—upper continental crust; NAQL—North American Quaternary loess; mmNASC—metamorphosed North American shale composite (for comparison).

*Lower, Middle, Upper refer to position in the Salagou Fm. (see map on Fig. 2; lower-middle is Octon Mbr. and upper is Merifons Mbr.)

[†]Taylor and McLennan (1985).

[§]Taylor et al. (1983).

[#]Gromet et al. (1984).

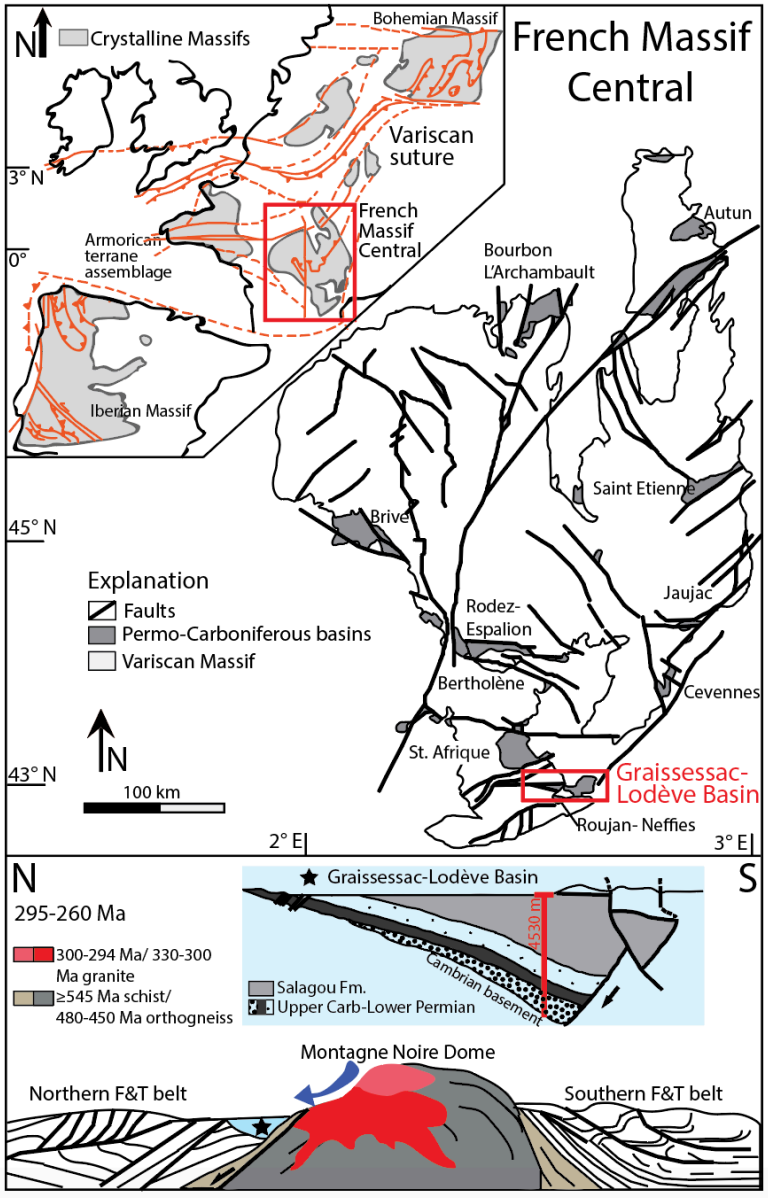


**Figure 1.** Structural map of the Massif Central showing the location of Carboniferous– Permian continental rift basins (dark gray) that formed as a result of extension associated with gravity collapse of the Variscan Mountains ca. 300 Ma. Inset: Late Paleozoic reconstruction of western Europe during the Variscan orogeny (ca. 320–300 Ma) showing the crystalline massifs (gray) and peri-Gondwanan arc terranes wedged between Laurasia and Gondwana. Cross section: Carboniferous–Permian strata in the Graissessac-Lodève Basin cover ~150 km2 and are bordered to the south by the Montagne Noire metamorphic core complex—a Variscan paleohigh that sourced the sediment in the basin (Pfeifer et al., 2016). Montagne Noire dome is color-coded by generalized ages of the predominant geologic units within the structure. The lower (Upper Carboniferous–Lower Permian) "gray facies" include a coarse, basal conglomerate, and fluvial-alluvial, deltaic, and lacustrine sands and muds. Transition up section to the Permian "red facies" begins with fluvial-lacustrine sandstone, mudstone, and conglomerate, and transitions up section to exclusively fine-grained (mudstone-siltstone) strata in the Salagou Formation. F&T—fold-and-thrust. Figure is modified after Pfeifer et al. (2016).

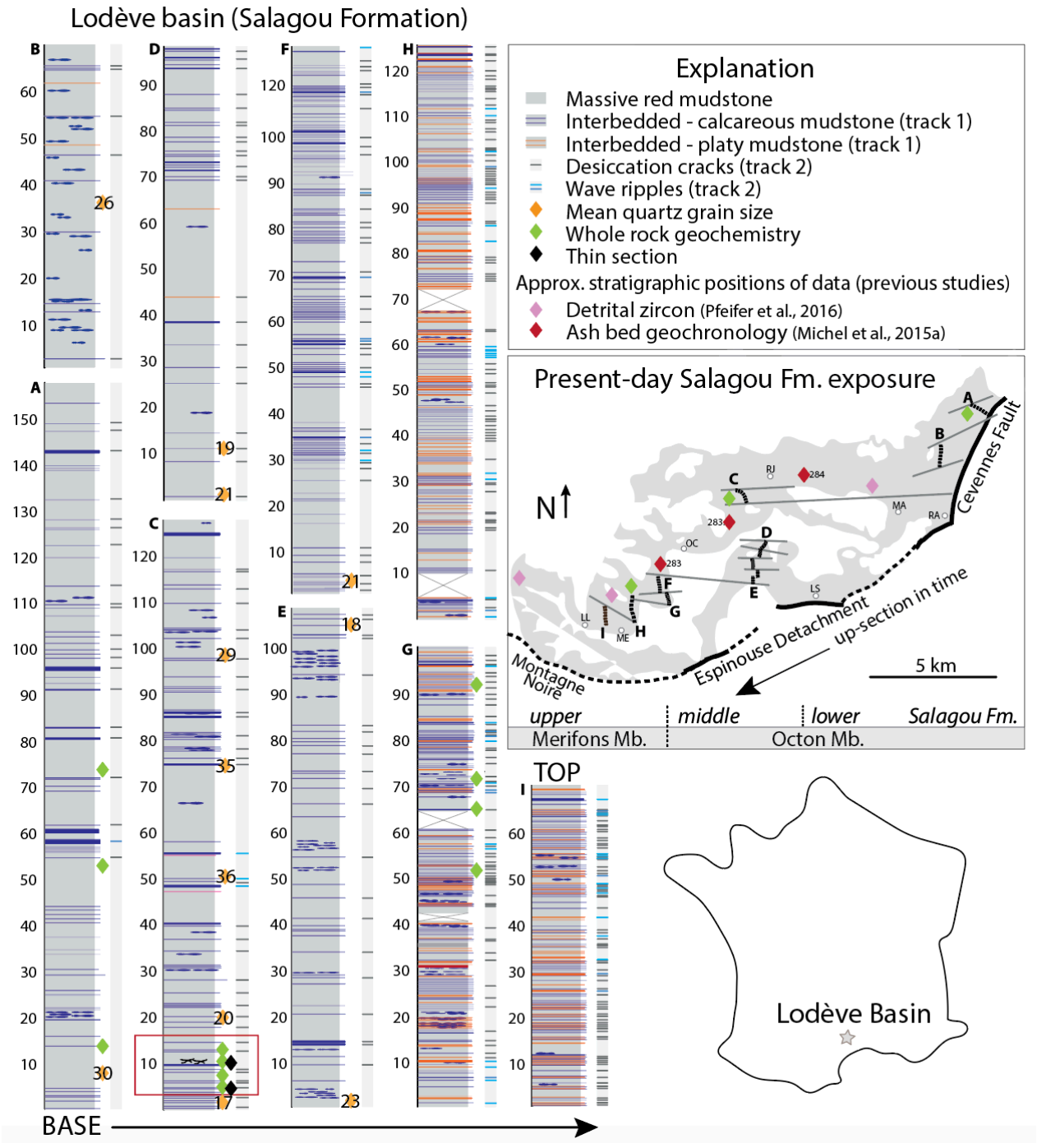
Lodève basin (Salagou Formation)
Explanation
Massive red mudstone
Interbedded - calcareous mudstone (track 1)
Interbedded - platy mudstone (track 1)
Desiccation cracks (track 2)
Wave ripples (track 2)
Mean quartz grain size
Whole rock geochemistry
Thin section
Approx. stratigraphic positions of data (previous studies)
Detrital zircon (Pfeifer et al., 2016)
Ash bed geochronology (Michel et al., 2015a)
Present-day Salagou Fm. exposure
N
Cevennes Fault
Espinouse Detachment
up-section in time
5 km
Montagne Noire
upper
middle
lower
Salagou Fm.
Merifons Mb.
Octon Mb.
TOP
BASE
Lodève Basin

**Figure 2** ***(previous page)*****.** Stratigraphic logs of the Salagou Formation (Lodève Basin), ~1000 m total. Base of section is on the bottom left, and top of section is at the top right. The wide column depicts the lithologies, and the second track (thinner column) denotes sedimentary structures (both at decimeter-scale resolution). Locations of data are shown with symbols in the key; mean quartz grain size (n > 100) for each sample is reported in microns with a number overlying the orange symbols. Red box indicates the position of the detailed pedogenic profile featured in Figures 4–6 and Table 2 ("paleosol" geochemistry). Inset map: Outcrop pattern of the Salagou Formation. Modern Lac Salagou and other Quaternary basalt/Mesozoic cover are shown in white. Approximate locations of villages for reference are shown with white points: Rabieux (RA), Mas Audran (MA), Rabejac (RJ), Octon (OC), Liausson (LS), Merifons (ME), and la Lieude (LL). This shows map-scale concatenation of segments of section (dashed black lines). Moving from the east to the west is generally moving from the base to the top of the section. See bottom bar for how our "lower," "middle," and "upper" formation designations relate to the Octon and Merifons Members (e.g., Schneider et al., 2006) and generally where this transition occurs (just east of Octon [OC]). Sequential sections were correlated laterally using map-scale projections of strike (dark gray). This approach might result in some unrepresented gaps between sections (poor exposure; most severe in the middle Salagou Formation). Estimated missing section totals <~500 m. Southward dip of bedding is consistent but ranges from ~5°S to 20°S (steeper toward S-bounding detachment fault).

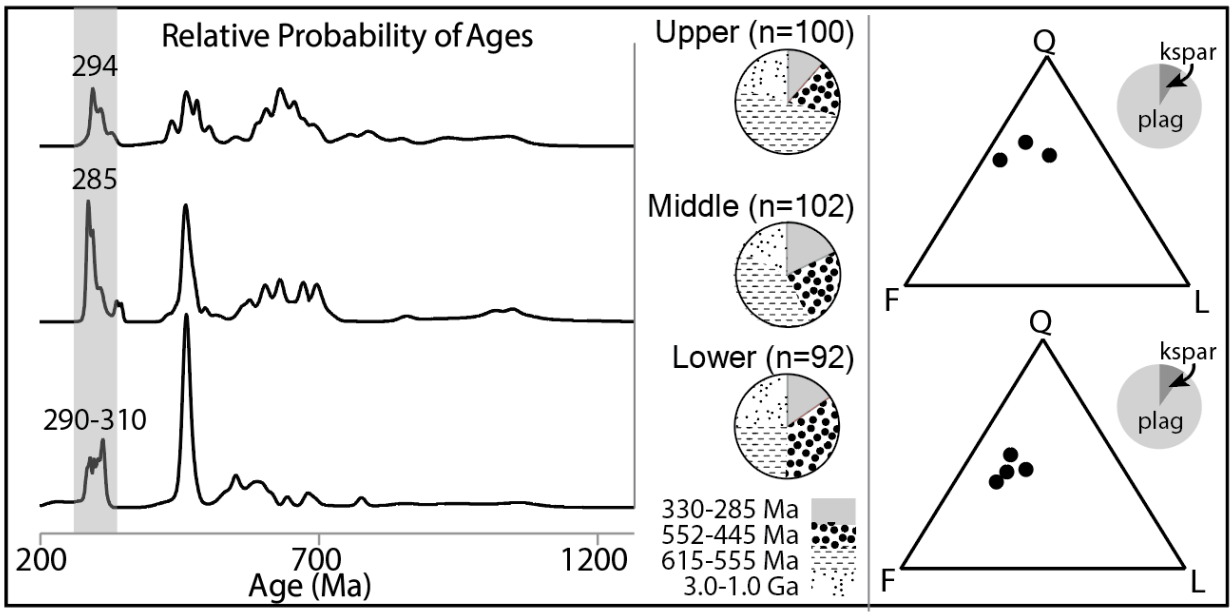


**Figure 3.** Summary of provenance data for the Salagou Formation (from Pfeifer et al., 2016). Left: Normalized probability plots of detrital zircon ages (and corresponding pie charts) from the lower, middle, and upper Salagou Formation, highlighting the youngest, late Paleozoic age peak. Right: Quartz-feldspar-lithics (QFL) ternary diagrams of framework modes from the lower and upper Salagou Formation (corresponding pie charts emphasize the high proportion of plagioclase [plag] relative to potassium feldspar [kspar], 9:1).


**Figure 4.** (A–I) Outcrop photos of representative facies. The massive red mudstone facies is characterized by massive, thick (15–20 m) bedding (A–B), and areas with interpreted incipient pedogenesis include radial slickensides (C) and blocky fracturing (D). The interbedded facies (G) include: thin beds of calcareous mudstone (E) with common desiccation cracks (F; note curled-up edges), and platy-fractured mudstone with millimeter-scale laminae, commonly with two-dimensional wave ripples (H–I).

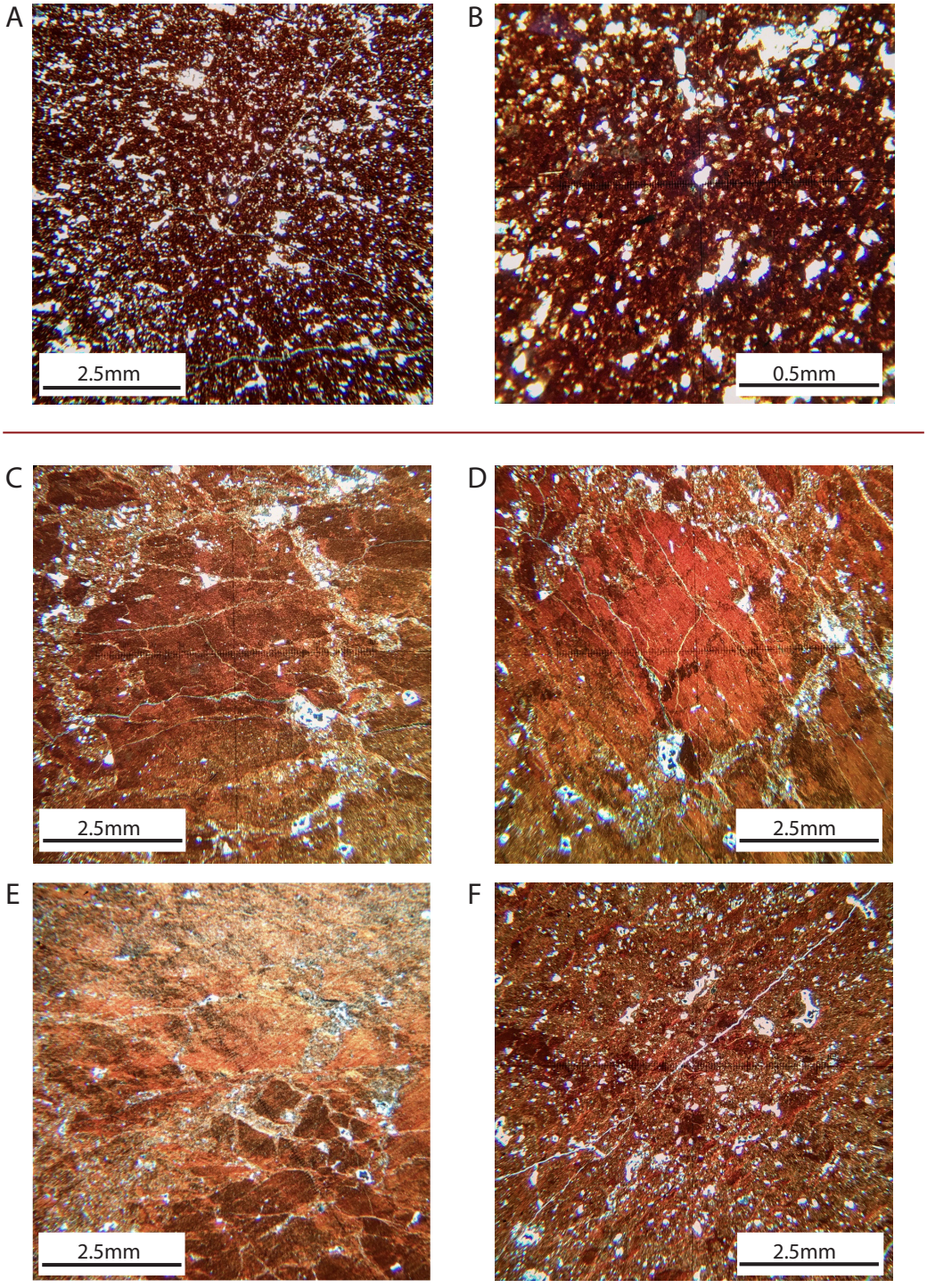


**Figure 5.** (A–F) Thin section photomicrographs of representative facies. The massive red mudstone is internally structureless (no preferred fabric) and composed of subangular, moderately sorted, silt-sized quartz in an illite-rich matrix (A–B). Micromorphologic attributes in pedogenic horizons include, for example, regions of birefringent clay (C–D), blocky peds (E), and porphyroskelic fabric (F). Other features not shown here: circumgranular cracks, clay coatings on grains, and calcium carbonate nodules. Top of thin section is oriented to top of page in all photos except for D, wherein stage is rotated ~45° (top of slide oriented to the left page).

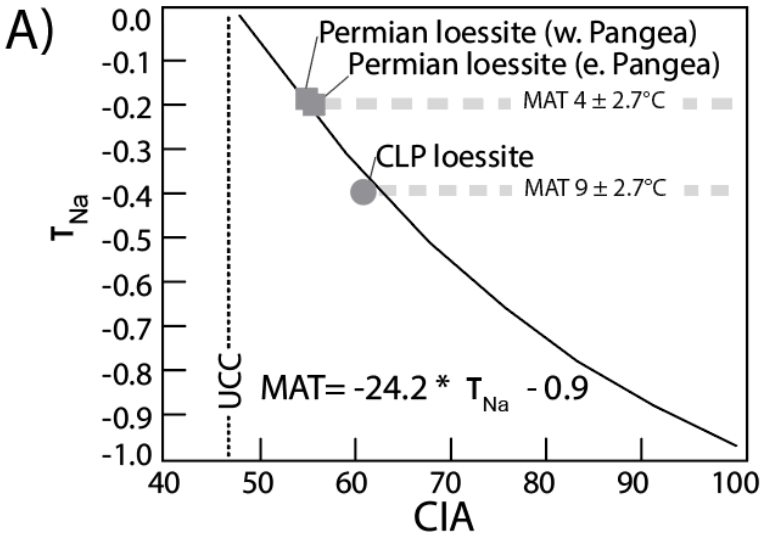
A)
Permian loessite (w. Pangea)
Permian loessite (e. Pangea)
MAT 4 ± 2.7°C
CLP loessite
MAT 9 ± 2.7°C
UCC
MAT= -24.2 * T_Na - 0.9
T_Na
CIA
0.0
-0.1
-0.2
-0.3
-0.4
-0.5
-0.6
-0.7
-0.8
-0.9
-1.0
40
50
60
70
80
90
100

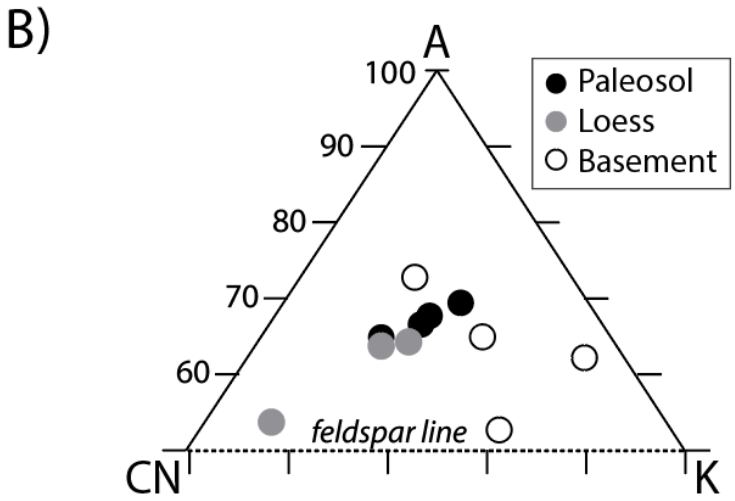
B)
A
100
90
80
70
60
Paleosol
Loess
Basement
feldspar line
CN
K

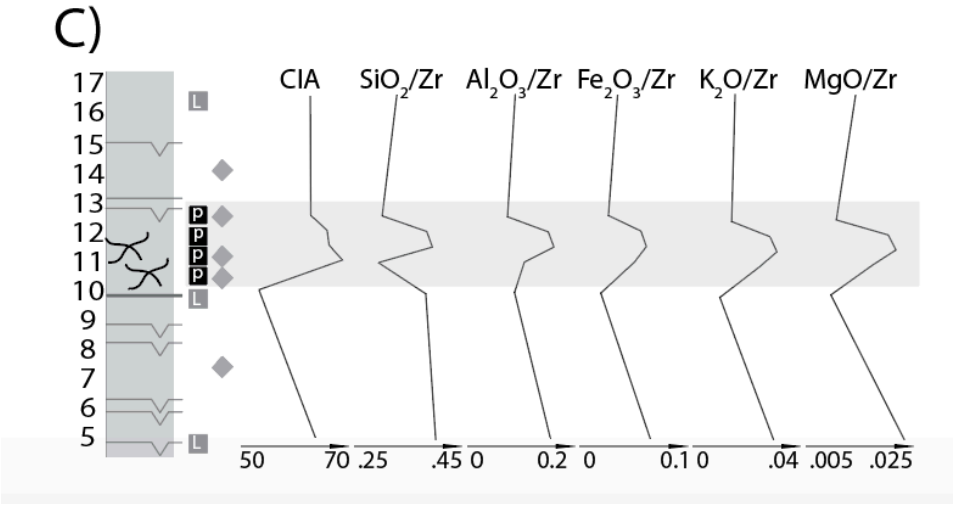
C)
CIA
SiO2/Zr
Al2O3/Zr
Fe2O3/Zr
K2O/Zr
MgO/Zr
17
16
15
14
13
12
11
10
9
8
7
6
5
L
P
50
70
.25
.45
0
0.2
0
0.1
0
.04
.005
.025

**Figure 6** ***(previous page)*****.** Summary of geochemical results from interpreted paleosol (lower-middle Salagou Formation), with position shown by the red box in Figure 2. (A) Correlation of weathering indices after Yang et al. (2016)—chemical index of alteration (CIA) and sodium depletion fraction ($\tau_{Na}$). Results from the Salagou Formation are indicated with the gray square. CIA-$\tau_{Na}$ values from the Permian Maroon Formation, western equatorial Pangea (M. Soreghan et al., 2014b) are almost identical. CIA-$\tau_{Na}$ values from the Chinese Loess Plateau (CLP; Yang et al., 2016) and upper continental crust (UCC; Taylor and McLennan, 1985) are shown for comparison. Mean annual temperature (MAT) values (calculated with the $\tau_{Na}$-MAT transfer function proposed by Yang et al., 2016) are displayed adjacent to respective samples. (B) CIA ternary diagram (from feldspar line) showing the distribution between massive red mudstone, interpreted paleosols, and representative basement lithologies. Basement lithology high in Al is the schist. A—aluminum, CN—calcium and sodium, and K—potassium. CIA values are displayed on left side of diagram. (C) Detailed plots for selected paleosol profile showing graphic log and trends in geochemical parameters normalized to zircon. Geochemical samples are denoted with squares, and thin section samples are denoted with diamonds. "Loess" (nonshaded area, "L"-labeled samples) is interpreted for areas that show minimal macro- or micro-evidence for pedogenesis (e.g., contains desiccation cracks, less clay, no peds), and "paleosol" (shaded area, "P"-labeled samples) is inferred based on the slickensided macromorphologies (Figs. 4C–4D) wherein micromorphologies (Figs. 5C–5F) contain pedogenic fabrics.

## REFERENCES CITED


Adams, S.M., and Soreghan, G.S., 2020, A test of the efficacy of sand saltation for silt production: Implications for the interpretation of loess: Geology, v. 48, https://doi.org/10.1130/G47282.1.

Ahmad, N., 1983, Vertisols, in Wilding, L.P., Smeck, N.E., and Hall, G.F., eds., Pedogenesis and Soil Taxonomy II: The Soil Orders: New York, Elsevier, Developments in Soil Science 11B, p. 91–123, https://doi.org/10.1016/ S0166-2481(08)70614-7.

Assallay, A.M., Rogers, C.D.F., Smalley, I.J., and Jefferson, I.F., 1998, Silt: 2–62 μm: Earth-Science Reviews, v. 45, p. 61–88, https://doi.org/10.1016/ S0012-8252(98)00035-X.

Becq-Giraudon, J.F., and Van Den Driessche, J., 1994, Dépôts périglaciaires dans le Stephano-Autunien du Massif Central: Témoin de l'effondrement gravitaire d'un haut plateau Hercynien: Comptes Rendus de l'Academie des Sciences Paris, v. 318, p. 675–682.

Becq-Giraudon, J.F., Montenat, C., and Van Den Driessche, J., 1996, Hercynian high-altitude phenomena in the French Massif Central: Tectonic implications: Palaeogeography, Palaeoclimatology, Palaeoecology, v. 122, p. 227–241, https://doi.org/10.1016/0031-0182(95)00081-X.

Blatt, H., 1967, Provenance determination and the recycling of sediments: Journal of Sedimentary Petrology, v. 37, p. 1031–1044.

Blatt, H., 1987, Oxygen isotopes and the origin of quartz: Journal of Sedimentary Petrology, v. 57, p. 373–377, https://doi .org/10.1306/212F8B34-2B24-11D7- 8648000102C1865D.

Blatt, H., 1989, Flux of siliciclastic grains in sediments: Jour- nal of Geological Education, v. 37, p. 243–249, https:// doi.org/10.5408/0022-1368-37.4.243.

Borrelli, L., Perri, F., Critelli, S., and Gulla, G., 2014, Characterization of granitoid and gneissic weathering profiles of the Mucone River basin (Calabria, Italy): Catena, v. 113, p. 325–340, https://doi.org/10.1016/ j.catena.2013.08.014 (corrigendum: https://doi.org/10.1016/j.catena.2014.03.011).

Boulton, G.S., 1978, Boulder shapes and grain-size distributions of debris as indicators of transport paths through a glacier and till genesis: Sedimentology, v. 25, p. 773–799, https://doi.org/10.1111/j.1365-3091.1978.tb00329.x.

Brewer, R., 1976, Fabric and Mineral Analysis of Soils: New York, Krieger, 482 p.

Bristow, C.S., and Moller, T.H., 2018, Testing the auto-abrasion hypothesis for dust production using diatomite dune sediments from the Bodélé depression in Chad: Sedimentology, v. 65, no. 4, p. 1322–1330, https://doi.org/10.1111/sed.12423.

Bryan, K., 1945, Glacial versus desert origin of loess: American Journal of Science, v. 243, p. 245–246, https://doi.org/10.2475/ajs.243.5.245.

Bullard, J.E., McTainsh, G.H., and Pudmenzky, C., 2004, Aeolian abrasion and modes of fine particle production from natural red dune sands: An experimental study: Sedimentology, v. 51, p. 1103–1125, https://doi.org/10.1111/j.1365-3091.2004.00662.x.

Burg, J.P., Van Den Driessche, J., and Brun, J.P., 1994, Syn- to post-thickening extension in the Variscan belt of Western Europe; modes and structural consequences: Comptes Rendus de l'Academie des Sciences Paris, v. 319, p. 1019–1032.

Chamley, H., 1989, Clay Sedimentology: New York, Springer-Verlag, 623 p., https://doi.org/10.1007/978-3-642- 85916-8.

Chan, M.A., 1999, Triassic loessite of north-central Utah: Stratigraphy, petrophysical character, and paleoclimate implications: Journal of Sedimentary Research, v. 69, p. 477–485, https://doi.org/10.2110/jsr.69.477.

Chan, M.A., and Archer, A.W., 2003, Introduction: A look at extreme depositional systems, in Chan, M.A., and Archer, A.W., eds., Extreme Depositional Environments: Mega End Members in Geologic Time: Geological Society of America Special Paper 370, p. 1–4, https://doi.org/10.1130/0-8137-2370-1.1.

Copard, Y., Disnar, J.R., Becq-Giraudon, J.F., and Boussafir, M., 2000, Evidence and effects of fluid circulation on organic matter in intramontane coalfields (Massif Central, France): International Journal of Coal Geology, v. 44, p. 49–68, https://doi.org/10.1016/S0166-5162(99)00049-X.

Crowley, T.J., Baum, S.K., and Hyde, W.T., 1991, Climate model comparison of Gondwanan and Laurentide glaciations: Journal of Geophysical Research, ser. D, Atmospheres, v. 96, p. 9217–9226, https://doi.org/10.1029/91JD00530.

Dewolf, Y., 1988, Stratified slope deposits, in Clark, M.J., ed., Advances in Periglacial Geomorphology: New York, Wiley, p. 91–110.

Dickinson, W.R., 1970, Interpreting detrital modes of graywacke and arkose: Journal of Sedimentary Petrology, v. 40, p. 695–707.

Domeier, M., and Torsvik, T.H., 2014, Plate tectonics in the late Paleozoic: Geoscience Frontiers, 5, p. 303–350, http://doi.org/10.1016/j.gsf.2014.01.002.

Driese, S.G., and Foreman, J.L., 1992, Paleopedology and paleoclimatic implications of late Ordovician Vertic paleosols: Juniata Formation, southern Appalachians: Journal of Sedimentary Petrology, v. 62, no. 1, p. 71–83. Evans, D.A., 2003, A fundamental Precambrian–Phanerozoic shift in Earth's glacial style?: Tectonophysics, v. 375, p. 353–385, https://doi.org/10.1016/S0040-1951(03)00345-7.

Evans, M.E., 2012, Magnetostratigraphy of the Lodève Basin, France: Implications for the Permo-Carboniferous reversed superchron and the geocentric axial dipole: Studia Geophysica et Geodaetica, v. 56, p. 725–734, https://doi.org/10.1007/s11200-010-0082-y.

Feulner, G., 2017, Formation of most of our coal brought Earth close to global glaciation: Proceedings of the National Academy of Sciences of the United States of America, v. 26, p. 1–5, https://doi.org/10.1073/ pnas.1712062114.

Fluteau, F., Besse, J., Broutin, J., and Ramstein, G., 2001, The Late Permian climate. What can be inferred from climate modelling concerning Pangea scenarios and Hercynian range altitude?: Palaeogeography, Palaeoclimatology, Palaeoecology, v. 167, p. 39–71, https://doi.org/10.1016/S0031-0182(00)00230-3.

Foster, T.M., Soreghan, G.S., Soreghan, M.J., Benison, K.C., and Elmore, R.D., 2014, Climatic and paleogeographic significance of eolian sediment in the Middle Permian Dog Creek Shale (midcontinent U.S.): Palaeo- geography, Palaeoclimatology, Palaeoecology, v. 402, p. 12–29, https://doi.org/10.1016/j.palaeo.2014.02.031.

Gallet, S., Jahn, B., Lano, B.V.V., Dia, A., and Rossello, E., 1998, Loess geochemistry and its implications for particle origin and composition of the upper continental crust: Earth and Planetary Science Letters, v. 156, p. 157–172, https://doi.org/10.1016/S0012-821X(97)00218-5.

Gand, G., Garric, J., and Lapeyrie, J., 1997, Biocénoses à Triopsidés (Crustacea, Branchiopoda) du Permien du bassin de Lodève (France): Geobios, v. 30, no. 5, p. 673–700, https://doi.org/10.1016/S0016- 6995(97)80157-X.
Garzanti, E., 2017, The maturity myth in sedimentology and provenance analysis: Journal of Sedimentary Research, v. 87, p. 353–365, https://doi.org/10.2110/jsr.2017.17.
Giles, J.M., Soreghan, M.J., Benison, K.C., Soreghan, G.S., and Hasiotis, S.T., 2013, Lakes, loess, and paleosols in the Permian Wellington Formation of Oklahoma, USA: Implications for paleoclimate and paleogeography of the midcontinent: Journal of Sedimentary Research, v. 83, p. 825–846, https://doi.org/10.2110/jsr.2013.59.
Goudie, A.S., Cooke, R.U., and Doornkamp, J.C., 1979, The formation of silt from quartz dune sand from salt- weathering processes in deserts: Journal of Arid Environments, v. 2, p. 105–112, https://doi.org/10.1016/ S0140-1963(18)31786-5.
Grangeon, M., 1960, Observations sur la sedimentation Houillere: Bulletin de la Société Géologique de France, v. S7-II, p. 630–650, https://doi.org/10.2113/gssgfbull.S7-II.5.630.
Gray, M.B., and Nickelsen, R.P., 1989, Pedogenic slickensides, indicators of strain and deformation processes in redbed sequences of the Appalachian foreland: Geology, v. 17, p. 72–75, https://doi.org/10.1130/0091- 7613(1989)017<0072:PSIOSA>2.3.CO;2.
Gromet, L.P., Dymek, R.F., Haskin, L.A., and Korotev, R.L., 1984, North American shale composite: Its compilation, major and trace element characteristics: Geochimica et Cosmochimica Acta, v. 48, p. 2469–2482, https://doi.org/10.1016/0016-7037(84)90298-9.
Hatano, N., Yoshida, K., and Sasao, E., 2019, Effects of grain size on the chemical weathering index: A case study of Neogene fluvial sediments in southwest Japan: Sedimentary Geology, v. 386, p. 1–8, https://doi.org/10.1016/j.sedgeo.2019.03.017.
Hübner, N., Körner, F., and Schneider, J., 2011, Tectonics, climate and facies of the Saint Affrique Basin and correlation with the Lodève Basin (Permian, Southern France): German Journal of Geology, v. 162, no. 2, p. 157–170, https://doi.org/10.1127/1860-1804/2011/0162-0157.
Jia, X., Li, Y., and Wang, H., 2016, Bed sediment particle size characteristics and its sources implication in the desert reach of the Yellow River: Environmental Earth Sciences, v. 75, no. 11, p. 950, https://doi.org/10.1007/ s12665-016-5760-9.
Johansen, S.J., 1988, Origins of Upper Paleozoic quartzose sandstones, American Southwest: Sedimentary Geology, v. 56, p. 153–166, https://doi.org/10.1016/0037-0738(88)90052-8.
Johnson, M.R., 1994, Thin section grain size analysis re- visited: Sedimentology, v. 41, p. 985–999, https://doi.org/10.1111/j.1365-3091.1994.tb01436.x.
Johnson, S., 1989, The significance of loessite in the Maroon Formation (Middle Pennsylvanian to Lower Permian), Eagle Basin, northwest Colorado: Journal of Sedimentary Petrology, v. 59, p. 789–791.
Joo, Y.J., Madden, M.E.E., and Soreghan, G.S., 2018, Anomalously low chemical weathering in fluvial sediment of a tropical watershed (Puerto Rico): Geology, v. 46, no. 8, p. 691–694, https://doi.org/10.1130/G40315.1.
Julien, A., 1895, Ancient glaciers de la periode Houillere dans le plateau central de la France: Annuaire du Club Alpin Français, v. 21, p. 1–28.
Keller, G.R., and Hatcher, R.D.J., 1999, Some comparisons of the structure and evolution of the southern Appalachian–Ouachita orogen and portions of the Trans-European suture zone

region: Tectonophysics, v. 314, no. 1–3, p. 43–68, https://doi.org/10.1016/S0040-1951(99)00236-X.
Kessler, J.L.P., Soreghan, G.S., and Wacker, H.J., 2001, Equatorial aridity in western Pangea: Lower Permian loessite and dolomitic paleosols in northeastern New Mexico: Journal of Sedimentary Research, v. 71, p. 818–833, https://doi.org/10.1306/2DC4096B-0E47-11D7-8643000102C1865D.
Koren, I., Kaufman, Y.J., Washington, R., Todd, M.C., Rudich, Y., Martins, J.V., and Rosenfeld, D., 2006, The Bodélé depression: A single spot in the Sahara that provides most of the mineral dust to the Amazon forest: Environmental Research Letters, v. 1, no. 1, p. 1–5, https://doi.org/10.1088/1748-9326/1/1/014005.
Körner, F., 2006, Klima- und Sedimentationsmuster des peri-tethyalen, kontinentalen Perms—Interdisziplinäre Studien an redbeds des Lodève Beckens [Ph.D. thesis]: Freiburg, Germany, Universität Freiburg, 261 p.
Körner, F., Schneider, J.W., Hoernes, S., Gand, G., and Kleeburg, R., 2003, Climate and continental sedimentation in the Permian of the Lodève Basin (southern France), in Decandia, F.A., Cassinis, G., and Spina, A., eds., Late Paleozoic to Early Mesozoic Events of Mediterranean Europe, and Additional Regional Reports: Bolletino della Società Geologica Italiana Volume Speciale 2, p. 185–191.
Kuenen, P.H., 1959, Experimental abrasion: Fluviatile action on sand: American Journal of Science, v. 257, p. 172– 190, https://doi.org/10.2475/ajs.257.3.172.
Kuenen, P.H., 1969, Origin of quartz silt: Journal of Sedimentary Petrology, v. 39, p. 1631–1633, https://doi .org/10.1306/74D71ED3-2B21-11D7- 8648000102C1865D.
Lawton, T.F., Ruiz-Urena, J.E., Solari, L.A., Terrazas, C.T., Juárez-Arriaga, E., and Ortega-Obregón, C., 2018, Provenance of Upper Triassic–Middle Jurassic strata of the Plomosas uplift, east-central Chihuahua, Mexico, and possible sedimentologic connections with Colorado Plateau depositional systems, in Ingersoll, R.V., Lawton, T.F., and Graham, S.A., eds., Tectonics, Sedimentary Basins, and Provenance: A Celebration of the Career of William R. Dickinson: Geological Society of America Special Paper 540, p. 481–508, https://doi.org/10.1130/2018.2540(22).
Lepre, C.J., 2019, Constraints on Fe-oxide formation in monsoonal Vertisols of Pliocene Kenya using rock magnetism and spectroscopy: Geochemistry Geophysics Geosystems, v. 20, no. 11, p. 4998–5013, https://doi.org/10.1029/2019GC008276.
Li, J., Song, Z., Ruan, L., Yang, L., Van Zwieten, L., Hu, Z., and Wang, H., 2019, The contribution of Asian dust in the pedogenesis of Ultisols in southeastern China determined by soil grain size: Journal of Soils and Sediments, v. 19, p. 232–240, https://doi.org/10.1007/ s11368-018-2012-5.
Li, L., Chen, J., Chen, Y., Hedding, D.W., Li, T., Li, L., Liu, X., Zeng, F., Wu, W., Zhao, L., and Li, G., 2018, Uranium isotopic constraints on the provenance of dust on the Chinese Loess Plateau: Geology, v. 46, no. 9, p. 747–750, https://doi.org/10.1130/G45130.1.
Liu, C., Masuda, A., Okada, A., Yabuki, S., and Zi-Li, F., 1994, Isotope geochemistry of Quaternary deposits from the arid lands in northern China: Earth and Planetary Science Letters, v. 127, p. 25–38, https://doi.org/10.1016/0012-821X(94)90195-3.
Liu, T.S., 1988, Loess in China II: Berlin, Springer, 224 p.
Lopez, M., Grand, G., Garric, J., Körner, F., and Schneider, J., 2008, The playa environments of the Lodève Permian basin (Languedoc-France): Journal of Iberian Geology, v. 34, no. 1, p. 29–56.

Mack, G.H., and Dinterman, P.A., 2002, Depositional environments and paleogeography of the Lower Permian (Leonardian) Yeso and correlative formations in New Mexico: The Mountain Geologist, v. 39, p. 75–88.
Mack, G.H., James, W.C., and Monger, H.C., 1993, Classification of paleosols: Geological Society of America Bulletin, v. 105, p. 129–136, https://doi.org/10.1130/0016-7606(1993)105<0129:COP>2.3. CO;2.
Malavieille, J., Guihot, P., Costa, S., Lardeaux, J.M., and Gardien, V., 1990, Collapse of the thickened Variscan crust in the French Massif Central: Mont Pilat extensional shear zone and Saint-Étienne Upper Carboniferous basin: Tectonophysics, v. 177, p. 139–149, https:// doi.org/10.1016/0040-1951(90)90278-G.
Matte, P., 1986, Tectonics and plate tectonic models for the Variscan belt of Europe: Tectonophysics, v. 126, p. 329– 374, https://doi.org/10.1016/0040-1951(86)90237-4.
Ménard, G., and Molnar, P., 1988, Collapse of a Hercynian Tibetan Plateau into a late Palaeozoic European Basin and Range province: Nature, v. 334, p. 235–237, https://doi.org/10.1038/334235a0.
Michel, L.A., 2009, Petrographic, Petrologic, and Isotopic Study of Paleosol Carbonates from the Permo-Pennsylvanian Lodève Basin, France [Ph.D. thesis]: Dallas, Texas, Southern Methodist University, 253 p.
Michel, L., Tabor, N., Montañez, I., Schmitz, M., and Davydov, V., 2015a, Chronostratigraphy and paleoclimatology of the Lodève Basin, France: Evidence for a pan-tropical aridification event across the Carboniferous-Permian boundary: Palaeogeography, Palaeoclimatology, Palaeoecology, v. 430, p. 118–131, https:// doi.org/10.1016/j.palaeo.2015.03.020.
Michel, L., Schmitz, M., Tabor, N., Montañez, I., and Davydov, V., 2015b, Reply to the comment on "Chronostratigraphy and paleoclimatology of the Lodève Basin, France: Evidence for a pan-tropical Aridification event across the Carboniferous-Permian boundary": Palaeogeography, Palaeoclimatology, Palaeoecology, v. 441, p. 1000–1004, https://doi.org/10.1016/j.palaeo.2015.03.020.
Moss, A.J., Green, P., and Hutka, J., 1981, Static breakage of granitic detritus by ice and water in comparison with breakage by flowing water: Sedimentology, v. 28, p. 261–272, https://doi.org/10.1111/j.1365-3091.1981. tb01679.x.
Muhs, D.R., 2007, Loess deposits, origins and properties, in Elias, S.A., ed., Encyclopedia of Quaternary Science, Volume 3: Amsterdam, Elsevier, p. 1405–1418.
Muhs, D.R., 2013, Loess and its geomorphic, stratigraphic, and paleoclimatic significance in the Quaternary, in Lancaster, N., Sherman, D.J., and Baas, A., eds., Treatise on Geomorphology, Volume 11: Aeolian Geomorphology: San Diego, California, Academic Press, p. 149–183, https://doi.org/10.1016/B978-0-12- 374739-6.00302-X.
Muhs, D.R., 2018, The geochemistry of loess: Asian and North American deposits compared: Journal of Asian Earth Sciences, v. 155, p. 81–115, https://doi.org/10.1016/j.jseaes.2017.10.032.
Muhs, D.R., and Bettis, E.A., 2003, Quaternary loess-paleosol sequences as an example of climatic extremes, in Chan, M.A., and Archer, A.W., eds., Extreme Depositional Environments: Mega End Members in Geologic Time: Geological Society of America Special Publication 370, p. 53–74, https://doi.org/10.1130/0-8137-2370-1.53.

Muhs, D.R., McGeehin, J.P., Beann, J., and Fisher, E., 2004, Holocene loess deposition and soil formation as competing processes, Matanuska Valley, southern Alaska: Quaternary Research, v. 61, p. 265–276, https://doi.org/10.1016/j.yqres.2004.02.003.

Murphy, K., 1987, Eolian Origin of Upper Paleozoic Red Siltstones at Mexican Hat and Dark Canyon, Southeastern Utah [M.S. thesis]: Lincoln, Nebraska, University of Nebraska, p. 127.

Muttoni, G., Kent, D.V., 2019, Adria as promontory of Africa and its conceptual role in the Tethys Twist and Pangea B to Pangea A transformation in the Permian: Rivista Italiana di Paleontogia e Stratigrafia, v. 125, p. 249–269, https://doi.org/10.13130/2039-4942/11437.

Nahon, D., and Trompette, R., 1982, Origin of siltstones; glacial grinding versus weathering: Sedimentology, v. 29, p. 25–35, https://doi.org/10.1111/j.1365-3091.1982. tb01706.x.

Nesbitt, H.W., and Young, G.M., 1982, Early Proterozoic climates and plate motions inferred from major element chemistry of lutites: Nature, v. 299, p. 715–717, https:// doi.org/10.1038/299715a0.

Nesbitt, H.W., and Young, G.M., 1996, Petrogenesis of sediments in the absence of chemical weathering: Effects of abrasion and sorting on bulk composition and mineralogy: Sedimentology, v. 43, p. 341–358, https://doi.org/10.1046/j.1365-3091.1996.d01-12.x.

Nettleton, W.D., and Sleeman, J.R., 1985, Morphology of Vertisols, in Douglas, L.A., and Thompson, M.L., eds., Soil Micromorphology and Soil Classification: Soil Science Society of America Special Publication 15, p. 165–196.

Odin, B., 1986, Les Formations Permiennes, Autunien Supérieur à Thuringienne, du Bassin de Lodève (Hérault, France) [Ph.D. thesis]: Aix-en-Provence and Marseille, France, Université Aix-Marseille III, 392 p.

Parrish, J., 1993, Climate of the supercontinent Pangea: Chicago Journals, v. 101, no. 2, p. 215–233.

Pfeifer, L.S., Soreghan, G.S., Pochat, S., Van Den Driessche, J., and Thomson, S.N., 2016, Permian exhumation of the Montagne Noire core complex recorded in the Graissessac-Lodève Basin, France: Basin Research, v. 30, p. 1–14, https://doi.org/10.1111/bre.12197.

Pochat, S., and Van Den Driessche, J., 2011, Filling sequence in late Paleozoic continental basins: A chimera of climate change? A new light shed given by the Graissessac-Lodève basin (SE France): Palaeogeography, Palaeoclimatology, Palaeoecology, v. 302, p. 170–186, https://doi.org/10.1016/j.palaeo.2011.01.006.

Pochat, S., and Van Den Driessche, J., 2015, Comment on "Chronostratigraphy and paleoclimatology of the Lodève Basin, France: Evidence for a pan-tropical aridification event across the Carboniferous-Permian boundary," by Michel, L.A., Tabor, N.J., Montañez, I.P., Schmitz, M.D., Davydov, V.I.: Palaeogeography, Palaeoclimatology, Palaeoecology, v. 430, p. 118–131, https://doi.org/10.1016/j.palaeo.2015.03.020.

Pochat, S., Van Den Driessche, J., Mouton, V., and Guillocheau, F., 2005, Identification of Permian paleowind direction from wave-dominated lacustrine sediments (Lodève Basin, France): Sedimentology, v. 52, p. 809–825, https://doi.org/10.1111/j.1365-3091.2005.00697.x.

Porter, S.C., 2001, Chinese loess record of monsoon climate during the last glacial-interglacial cycle: Earth-Science Reviews, v. 54, p. 115–128, https://doi.org/10.1016/ S0012-8252(01)00043-5.

Porter, S.C., and An, Z., 1995, Correlation between climate events in the North Atlantic and China during the last glaciation: Nature, v. 375, p. 305–308, https://doi.org/10.1038/375305a0.
Price, J.R., and Velbel, M.A., 2003, Chemical weathering indices applied to weathering profiles developed on heterogeneous felsic metamorphic parent rocks: Chemical Geology, v. 202, p. 397–416, https://doi.org/10.1016/ j.chemgeo.2002.11.001.
Pye, K., 1987, Aeolian Dust and Dust Deposits: London, Academic Press, 334 p.
Pye, K., and Mazzullo, J., 1994, Effects of tropical weathering on quartz grain shape: An example from northeastern Australia: Journal of Sedimentary Research, v. 64, p. 500–507.
Quast, A., Hoefs, J., and Paul, J., 2006, Pedogenic carbonates as a proxy for palaeo-$CO_2$ in the Palaeozoic atmosphere: Palaeogeography, Palaeoclimatology, Palaeoecology, v. 242, p. 110–125, https://doi.org/10.1016/ j.palaeo.2006.05.017.
Rasmussen, C., Brantley, S., Richter, D.B., Blum, A., Dixon, J., and White, A.F., 2011, Strong climate and tectonic control on plagioclase weathering in granitic terrain: Earth and Planetary Science Letters, v. 301, p. 521– 530, https://doi.org/10.1016/j.epsl.2010.11.037.
Retallack, G.J., 2001, Soils of the Past: An Introduction to Paleopedology: Oxford, UK, Blackwell Science, Ltd., 520 p., https://doi.org/10.1002/9780470698716
Roscher, M., and Schneider, J., 2006, Permo-Carboniferous climate: Early Pennsylvanian to Late Permian climate development of central Europe in a regional and global context, in Lucas, S.G., Cassinis, G., and Schneider, J.W., eds., Non-Marine Permian Biostratigraphy and Biochronology: Geological Society [London] Special Publication 265, p. 95–136, https://doi.org/10.1144/ GSL.SP.2006.265.01.05.
Sabrier, R., Delfaud, J., Causse, F., Marocco, R., and Toutin-Morin, N., 1993, Utilisation des associations de minéraux argileux pour la reconstitution des paléotopographies: Mégatoposéquence actuelle d'Equateur, Orogène pyrénéen à l' Oligo-miocène, Chaîne varisque du Var au Permien: Bulletin de l'Institut de Géologie du Bassin d'Aquitaine, v. 53, p. 13–26.
Sahagian, D.L., and Proussevitch, A.A., 1998, 3D particle size distribution from 2D observations: Stereology for natural applications: Journal of Volcanology and Geothermal Research, v. 84, p. 173–196, https://doi.org/10.1016/S0377-0273(98)00043-2.
Schneider, J., Körner, F., Roscher, M., and Kroner, U., 2006, Permian climate development in the northern peri-Tethys area: The Lodève Basin, French Massif Central, compared in a European and global context: Palaeogeography, Palaeoclimatology, Palaeoecology, v. 240, p. 161–183, https://doi.org/10.1016/ j.palaeo.2006.03.057.
Schneider, J.W., Lucas, S.G., Werneburg, R., and Rößler, R., 2010, Euramerican late Pennsylvanian/Early Permian arthropleurid/tetrapod associations—Implications for the habitat and paleobiology of the largest terrestrial arthropod, in Lucas, S.G., Schneider, J.W., and Spielmann, J.A., eds., Carboniferous-Permian Transition in Canõn del Cobre, Northern New Mexico: New Mexico Museum of Natural History and Science Bulletin, v. 49, p. 49–70.
Schneider, J.W., Lucas, S.G., Scholze, F., Voigt, S., Marchetti, L., Werneburg, R., Golubev, V.K., Barrick, J.E., Klein, H., Oplu, S., Nemyrovska, T., Ronchi, A., Day, M.O., Silantiev, V.V., Rößler, R., Saber, H., Linnemann U., Zharinova, V., and Shen, S.-Z., 2019, Late Paleozoic–early Mesozoic continental biostratigraphy— Links to the Standard

Global Chronostratigraphic Scale: Palaeoworld (in press), https://doi.org/10.1016/j.palwor.2019.09.001.
Sheldon, N.D., and Tabor, N.J., 2009, Quantitative paleoenvironmental and paleoclimatic reconstruction using paleosols: Earth Science Reviews, v. 95, no. 1–52, https://doi.org/10.1016/j.earscirev.2009.03.004.
Smalley, I.J., 1990, Possible formation mechanisms for the modal coarse silt quartz particles in loess: Quaternary International, v. 7–8, p. 23–27, https://doi.org/10.1016/1040-6182(90)90035-3.
Smalley, I.J., 1995, Making the material; the formation of silt-sized primary mineral particles for loess deposits: Quaternary Science Reviews, v. 14, p. 645–651, https://doi.org/10.1016/0277-3791(95)00046-1.
Smalley, I.J., and Krinsley, D.H., 1978, Loess deposits associated with deserts: Catena, v. 5, p. 53–66, https://doi.org/10.1016/S0341-8162(78)80006-X.
Smalley, I.J., and Vita-Finzi, C., 1968, The formation of fine particles in sandy deserts and the nature of 'desert' loess: Journal of Sedimentary Petrology, v. 38, p. 768–774.
Smalley, I.J., Kumar, R., Dhand, K.O.H., Jefferson, I.F., and Evans, R.D., 2005, The formation of silt material for terrestrial sediments: Particularly loess and dust: Sedimentary Geology, v. 179, p. 321–328, https://doi.org/10.1016/j.sedgeo.2005.06.011.
Smalley, I.J., Marshall, J., Fitzsimmons, K., Whalley, W.B., and Ngambi, S., 2019, Desert loess: A selection of relevant topics: Geologos, v. 25, no. 1, p. 91–102, https://doi.org/10.2478/logos-2019-0007.
Smith, B.J., Wright, J.S., and Whalley, W.B., 2002, Sources of non-glacial, loess-size quartz silt and the origins of "desert loess": Earth-Science Reviews, v. 59, p. 1–26, https://doi.org/10.1016/S0012-8252(02)00066-1.
Smith, R.M.H., and Swart, R., 2002, Changing fluvial environments and vertebrate taphonomy in response to climatic drying in a mid-Triassic rift valley fill: The Omingonde Formation (Karoo Supergroup) of central Namibia: Palaios, v. 17, p. 249–267, https://doi.org/10.1669/0883-1351(2002)017<0249:CFEAVT>2.0.CO;2.
Soreghan, G.S., Soreghan, M.J., and Hamilton, M.A., 2008a, Origin and significance of loess in late Paleozoic western Pangaea: A record of tropical cold: Palaeogeography, Palaeoclimatology, Palaeoecology, v. 268, p. 234–259, https://doi.org/10.1016/j.palaeo.2008.03.050.
Soreghan, G.S., Soreghan, M.J., Poulsen, C.J., Young, R.A., Sweet, D.E., and Davogustto, O.C., 2008b, Anomalous cold in Pangaean tropics: Geology, v. 36, p. 659–662, https://doi.org/10.1130/G24822A.1.
Soreghan, G.S., Soreghan, M.J., Sweet, D.E., and Moore, K.D., 2009, Hot fan or cold outwash? Hypothesized proglacial deposition in the Upper Paleozoic Cutler Formation, western tropical Pangea: Journal of Sedimentary Research, v. 79, p. 495–522, https://doi.org/10.2110/jsr.2009.055.
Soreghan, G.S., Sweet, D.E., and Heavens, N.G., 2014a, Upland glaciation in tropical Pangaea: Geologic evidence and implications for late Paleozoic climate modeling: The Journal of Geology, v. 122, p. 137–163, https://doi.org/10.1086/675255.
Soreghan, G.S., Joo, Y.J., Madden, M.E.E., and Van Deventer, S.C., 2016, Silt production as a function of climate and lithology under simulated comminution: Quaternary International, v. 399, p. 218–227, https:// doi.org/10.1016/j.quaint.2015.05.010.

Soreghan, G.S., Soreghan, M.J., and Heavens, N.G., 2019, Explosive volcanism as a key driver of the late Paleozoic ice age: Geology, v. 47, no. 7, p. 600–604, https://doi.org/10.1130/G46349.1.

Soreghan, M.J., and Francus, P., 2004, Processing backscattered electron digital images of thin section, in Francus, P., ed., Image Analysis, Sediments and Paleoenvironments: Berlin, Springer, p. 203–225.

Soreghan, M.J., and Soreghan, G.S., 2007, Whole-rock geochemistry of Upper Paleozoic loessite, western Pangea: Implications for paleo-atmospheric circulation: Earth and Planetary Science Letters, v. 255, p. 117–132, https://doi.org/10.1016/j.epsl.2006.12.010.

Soreghan, M.J., Soreghan, G.S., and Hamilton, M.A., 2002, Paleowinds inferred from detrital zircon geochronology of Upper Paleozoic loessite, western equatorial Pangea: Geology, v. 30, p. 695–698, https://doi.org/10.1130/0091-7613(2002)030<0695:PIFDZG>2.0.CO;2.

Soreghan, M.J., Heavens, N., Soreghan, G.S., Link, P.K., and Hamilton, M.A., 2014b, Abrupt and high-magnitude changes in atmospheric circulation recorded in the Permian Maroon Formation, tropical Pangea: Geological Society of America Bulletin, v. 126, p. 569–584, https://doi.org/10.1130/B30840.1.

Stevens, T., Carter, A., Watson, T.P., Vermeesch, P., Ando, S., Bird, A.F., Lu, H., Garzanti, E., Cottam, M.A., and Sevastjanova, I., 2013, Genetic linkage between the Yellow River, the Mu Us desert and the Chinese Loess Plateau: Quaternary Science Reviews, v. 78, p. 355–368, https:// doi.org/10.1016/j.quascirev.2012.11.032.

Stuut, J.B., Smalley, I.J., and O'Hara-Dhand, K., 2009, Aeolian dust in Europe: African sources and European deposits: Quaternary International, v. 198, p. 234–245, https://doi.org/10.1016/j.quaint.2008.10.007.

Sweet, A.C., Soreghan, L.S., Sweet, D.E., Soreghan, M.J., and Madden, A.S., 2013, Permian dust in Oklahoma: Source and origin for middle Permian (Flowerpot-Blaine) redbeds in western tropical Pangaea: Sedimentary Geology, v. 284–285, p. 181–196, https://doi.org/10.1016/j.sedgeo.2012.12.006.

Sweet, D.E., and Soreghan, G.S., 2008, Polygonal cracking in coarse clastics records cold temperatures in the equatorial Fountain Formation (Pennsylvanian–Permian, Colorado): Palaeogeography, Palaeoclimatology, Palaeoecology, v. 268, no. 3–4, p. 193–204, https://doi.org/10.1016/j.palaeo.2008.03.046.

Swet, N., Elperin, T., Kok, J.F., Martin, R.L., Yizhaq, H., and Katra, I., 2019, Can active sands generate dust particles by wind-induced processes?: Earth and Planetary Science Letters, v. 506, p. 371–380, https://doi.org/10.1016/j.epsl.2018.11.013.

Tabor, N.J., and Myers, T.S., 2015, Paleosols as indicators of paleoenvironment and paleoclimate: Annual Review of Earth and Planetary Sciences, v. 43, p. 333–363, https://doi.org/10.1146/annurev-earth-060614-105355.

Tabor, N.J., and Poulsen, C.J., 2008, Paleoclimate across the late Pennsylvanian–Early Permian tropical palaeo-latitudes: A review of climate indicators, their distribution, and relation to palaeophysiographic climate factors: Palaeogeography, Palaeoclimatology, Palaeo-ecology, v. 268, p. 293–310, https://doi.org/10.1016/ j.palaeo.2008.03.052.

Taylor, S.R., and McLennan, S.M., 1985, The Continental Crust; Its Composition and Evolution: An Examination of the Geochemical Record Preserved in Sedimentary Rocks: Oxford, UK, Blackwell Science Publications, 312 p.

Taylor, S.R., McLennan, S.M., and McCulloch, M.T., 1983, Geochemistry of loess, continental crustal composition and crustal model ages: Geochimica et Cosmochimica Acta, v. 47, p. 1897–1905, https://doi.org/10.1016/0016-7037(83)90206-5.

Tijani, M.N., Okunlola, O.A., and Abimbola, A.F., 2006, Lithogenic concentrations of trace metals in soils and saprolites over crystalline basement rocks: A case study from SW Nigeria: Journal of African Earth Sciences, v. 46, no. 5, p. 427–438, https://doi.org/10.1016/ j.jafrearsci.2006.08.003.

Tramp, K.L., Soreghan, G.S., and Elmore, R.D., 2004, Paleoclimatic inferences from paleopedology and magnetism of the Permian Maroon Formation loessite (Colorado, USA): Geological Society of America Bulletin, v. 116, p. 671–686, https://doi.org/10.1130/B25354.1.

Tsoar, H., and Pye, K., 1987, Dust transport and the question of desert loess formation: Sedimentology, v. 34, p. 139–153, https://doi.org/10.1111/j.1365-3091.1987. tb00566.x.

Van Den Driessche, J., and Brun, J.P., 1989, Un modèle cinématique de l'extension paleozoique superieur dans le sud du Massif Central: Comptes Rendus de l'Academie des Sciences Paris, v. 309, p. 1607–1613.

Varga, G., Kovacs, J., Szalai, Z., Cserhati, C., and Ujvari, G., 2018, Granulometric characterization of paleosols in loess series by automated static image analysis: Sedimentary Geology, v. 370, p. 1–14.

Whalley, W.B., Smith, B.J., McAlister, J.J., and Edwards, A.J., 1987, Aeolian abrasion of quartz particles and the production of silt-size fragments: Preliminary results in Frostick, L., and Reid, I., eds., Desert Sediments: Ancient and Modern: Geological Society of America Special Publication 35, p. 129–138, https:// doi.org/10.1144/GSL.SP.1987.035.01.09.

Whitmore, G.P., Crook, K.A.W., and Johnson, D.P., 2004, Grain size control of mineralogy and geochemistry in modern river sediment, New Guinea collision, Papua New Guinea: Sedimentary Geology, v. 171, p. 129– 157, https://doi.org/10.1016/j.sedgeo.2004.03.011.

Wilkins, A., Hurst, A., Wilson, M., and Archer, S., 2018, Palaeo-environment in an ancient low-latitude, arid lacustrine basin with loessite: The Smith Bank Formation (Early Triassic) in the central North Sea, UK continental shelf: Sedimentology, v. 65, p. 335–359, https://doi.org/10.1111/sed.12382.

Wilson, M.J., Hurst, A., Wilkins, A.D., Wilson, L., and Bowen, L., 2019, Mineralogical evidence for multiple dust sources in an early Triassic loessite: Sedimentology, v. 67, p. 239–260, https://doi.org/10.1111/sed.12641.

Wright, J., 2001, "Desert" loess versus "glacial" loess: Quartz silt formation, source areas and sediment pathways in the formation of loess deposits: Geomorphology, v. 36, p. 231–256, https://doi.org/10.1016/ S0169-555X(00)00060-X.

Wright, J., 2002, Granitoid weathering profiles as a source of loessic silt: Transactions of the Japanese Geomorphological Union, v. 23, no. 5, p. 769–793.

Wright, J., 2007, An overview of the role of weathering in the production of quartz silt: Sedimentary Geology, v. 202, p. 337–351, https://doi.org/10.1016/ j.sedgeo.2007.03.024.

Wright, J., and Smith, B., 1993, Fluvial comminution and the production of loess-sized quartz silt: A simulation study: Geografiska Annaler, Ser. A, Physical Geography, v. 75, no. 1–2, p. 25–34, https://doi.org/10.1080/04353676.1993.11880380.

Wright, J., Smith, B., and Whalley, B., 1998, Mechanisms of loess-sized quartz silt production and their relative effectiveness: Laboratory simulations: Geomorphology, v. 23, p. 15–34, https://doi.org/10.1016/ S0169-555X(97)00084-6.

Xiao, J., Porter, S.C., An, Z., Kumai, H., and Yoshikawa, S., 1995, Grain size of quartz as an indicator of winter monsoon strength on the Loess Plateau of central China during the last 130,000 yr: Quaternary Research, v. 43, p. 22–29, https://doi.org/10.1006/qres.1995.1003.

Yang, J., Cawood, P.A., Du, Y., Li, W., and Yan, J., 2016, Reconstructing Early Permian tropical climates from chemical weathering indices: Geological Society of America Bulletin, v. 128, no. 5–6, p. 739–751, https:// doi.org/10.1130/B31371.1.

Ziegler, A.M., Scotese, C.R., McKerrow, W.S., Johnson, M.E., and Bambach, R.K., 1979, Paleozoic paleogeography: Annual Review of Earth and Planetary Sciences, v. 7, p. 473–502, https://doi.org/10.1146/annurev. ea.07.050179.002353.

Ziegler, P.A., 1996, Geodynamic processes govern development of rifted basins, in Roure, F., Ellouz, N., Shien, V.S., and Skvortsov, L., eds., Geodynamic Evolution of Sedimentary Basins: Moscow, p. 19–67.

CHAPTER II

# ROCK MAGNETIC CYCLOSTRATIGRAPHY OF PERMIAN LOESS IN EASTERN EQUATORIAL PANGEA (SALAGOU FORMATION, SOUTH-CENTRAL FRANCE)



Citation:
*Pfeifer, L.S., Hinnov, L., Zeeden, C., Rolf, C., Laag, C., and Soreghan, G.S. (2020). Rock magnetic cyclostratigraphy of Permian loess in eastern equatorial Pangea (Salagou Formation, south-central France), Frontiers in Earth Science, 8, 241, doi: 10.3389/feart.2020.00241.*

# ROCK MAGNETIC CYCLOSTRATIGRAPHY OF PERMIAN LOESS IN EASTERN EQUATORIAL PANGEA (SALAGOU FORMATION, SOUTH-CENTRAL FRANCE)


## ABSTRACT

We present the findings from analysis and modeling of a stratigraphic series of magnetic susceptibility (MS) data measured with a portable MS meter from the Permian Salagou Formation loessite (south-central France). The results reveal discernible Milankovitch-scale paleoclimatic variability throughout the Salagou Formation, recording astronomically forced climate change in deep-time loessite of eastern equatorial Pangea. Optimal sedimentation rates are estimated to have ranged between 9.4 cm/kyr (lower Salagou Formation) and 13 cm/kyr (mid-upper Salagou Formation). A persistent 10-m-thick cyclicity is present that likely represents orbital eccentricity-scale (~100 kyr) variability through the middle to late Cisuralian (ca. 285—275 Ma). Subordinate, higher frequency cycles with thicknesses of ~3.3–3.5 and ~1.8 m appear to represent obliquity and precession-scale variability. If the driver of magnetic enhancement is pedogenic, then the ~10 m thick cyclicity that is consistent over ~1000 m of section may represent the thickness of loessite–paleosol couplets in the Salagou Formation. Laboratory rock magnetic data show generally low magnetic enhancement compared to analogous Eurasian Quaternary loess deposits. This is related to the predominance of hematite (substantially weaker signal than magnetite or maghemite) in the Salagou Formation which may be explained by different conditions of formation (e.g., syn depositional processes, more arid, and/or oxidizing climate conditions) than in present Eurasia and/or post depositional oxidation of magnetite and maghemite.


## INTRODUCTION

Loess-paleosol sequences of the Chinese Loess Plateau (CLP; thickness of ~200 m) and other regions (e.g., Li et al., 2019) are widely regarded as high-resolution and continuous continental records of global Pleistocene climate change (e.g., Liu, 1985; Heller and Liu, 1986; Kukla, 1987; Kukla et al., 1988; Kukla and An, 1989; Maher and Thompson, 1991, 1992; Evans and Heller, 2001; Yang and Ding, 2004; Muhs, 2007; Maher and Possolo, 2013; Maher, 2016). These quasi-cyclic loess-paleosol deposits commonly record a combination of glacial-interglacial oscillations and changes in monsoonal precipitation, and trends in their magnetic susceptibility (MS) correlate with marine-based oxygen isotope records of continental ice volume (Heller and Liu, 1982; Kukla et al., 1988; Shackleton et al., 1990; Parrish, 1993; Porter, 2001; Porter et al., 2001; Basarin et al., 2014; Ahmed and Maher, 2017; Zeeden et al., 2018).

Thick loessite deposits have also been associated with the Late Paleozoic Ice Age (e.g., Murphy, 1987; Johnson, 1989; Kessler et al., 2001; Mack and Dinterman, 2002; Soreghan et al., 2002; Tramp et al., 2004; Soreghan and Soreghan, 2007; Soreghan et al., 2008a,b; Soreghan G. S. et al., 2014; Soreghan M. J. et al., 2014; Giles et al., 2013; Sweet et al., 2013; Foster et al., 2014; Pfeifer et al., 2020). Voluminous paleo-loess accumulated in low latitudes of western and eastern Pangea and are exposed today in the western United States (exceeding 700 m thick) and western Europe (up to ~1500 m thick in southern France). Loessite– paleosol intercalations in the deep-time record of western equatorial Pangea have been posited to represent icehouse

glacial- interglacial oscillations on a 100 kyr-scale (Soreghan et al., 1997, 2002; Soreghan M. J. et al., 2014; Tramp et al., 2004), as well as higher frequency climatic signals occurring on obliquity and possibly precession scales (Soreghan M. J. et al., 2014). Recently, a radioisotopically-dated lower Guadalupian cyclic lacustrine record from the Junggar Basin of eastern Pangea (30—32°N paleolatitude) was discovered to exhibit astronomical frequencies (Huang et al., 2020). Importantly, this new evidence supports the hypothesis explored in this work for presumably analogous Milankovitch cycles recorded in the thick (~1000 m) record of upper Paleozoic loess in eastern equatorial Pangea.

The objectives of this work are to (1) document Permian climatic variability and assess Milankovitch characteristics using MS data from the Salagou Formation loessite obtained with a portable MS meter, (2) leverage laboratory rock magnetic measurements to better understand the origin of the magnetic signal, and (3) compare this upper Paleozoic record with analogous successions from the Eurasian Quaternary record.

## GEOLOGICAL SETTING

The Permian Salagou Formation is an exclusively fine-grained and internally massive deposit of red mudstone with local pedogenic overprinting and water-reworked interbeds that accumulated in the Lodève continental rift basin at equatorial latitudes (0–3°N; Domeier and Torsvik, 2014; Muttoni and Kent, 2019). Its characteristics are most consistent with eolian transport and deposition either as loess, or as dust deposited in a seasonal, shallow lacustrine environment (Pfeifer et al., 2020). The provenance of the Salagou Formation is the Montage Noire Dome, a local uplift of Variscan basement composed of gneiss, schist, and granite (Fig. 1; Pfeifer et al., 2016). The recognition of great volumes of loess-sized silt, together with known coarse-grained granitic protoliths and deposition during global icehouse conditions, are all most consistent with a hypothesis of upland glaciation in this region (Pfeifer et al., 2020).

The late Artinskian to mid-Kungurian (upper Rotliegend I; Kiersnowski, 2013) age of the lower Salagou Formation (Octon Member) is well constrained by U-Pb ID-TIMS dates from ash layers (Michel et al., 2015; Fig. 2). Chronostratigraphic constraints for the top of the formation (Merifons Member) are lacking, so the extent of Guadalupian deposition (cf. Schneider et al., 2006; Pochat and Van Den Driessche, 2011) is unclear. The Octon Member (basal to mid-upper Salagou) makes up the majority of the Salagou Formation and consists primarily of massive red mudstone with loessitic characteristics (Pfeifer et al., 2020). The MS data for this study were collected from the Octon Member to lower Merifons Member (Figs. 1, 2; red bar), which represents deposition through the mid-late Cisuralian (ca. 285–275 Ma).

Magnetic susceptibility has been used as a proxy for climatic signals in both Plio-Pleistocene loess, the Chinese “red clay,” and Permian loessite recording climate-dependent pedogenesis and dust influx (e.g., Heller and Liu, 1984; Maher and Taylor, 1988; Soreghan et al., 1997, 2002; Soreghan M. J. et al., 2014; Tramp et al., 2004). MS measures the concentration and grain size of ferrimagnetic minerals which consist primarily of magnetite, secondarily of maghemite, and supplemented by hematite (e.g., Maher, 1986; Kukla and An, 1989; Porter et al., 2001; Muhs, 2007; Ahmed and Maher, 2017). In saturated, gleyed (reduced) and thus Fe-leached soils, MS values in parent loess can exceed those in pedogenic intervals (e.g., see Muhs, 2007 and the references within; Beget et al., 1990; Hayward and Lowell, 1993; Chlachula, 2003). But otherwise, in situ precipitation of ultra-fine-grained ferrimagnetic material [e.g., super-paramagnetic (SP) magnetite or maghemite] during warmer and wetter interglacial conditions

has been widely recognized as a driver of elevated MS in pedogenically altered intervals compared to unaltered parent loess (deposited during arid and dusty glacial periods, and/or phases of monsoonal interference). This is true for both the CLP (cf. Heller and Liu, 1984; Maher and Taylor, 1988; Zhou et al., 1990; Maher and Thompson, 1991, 1992; Zheng et al., 1991; Maher et al., 1994; Porter et al., 2001; Ahmed and Maher, 2017), where bulk MS of paleosols is ~4–10x higher than in loess (Heller and Liu, 1984, 1986; Liu et al., 1993) and in lower Permian loessite of western equatorial Pangea where bulk MS is commonly ~1.5– 2x (and up to 9x) higher in paleosols relative to loess (Soreghan et al., 1997, 2002; Cogoini et al., 2001; Tramp et al., 2004; Soreghan G. S. et al., 2014). The origin of the magnetic signal in Permian loessite of western equatorial Pangea (e.g., Maroon Formation, CO) is dominantly hematite, but is also driven locally by the inferred presence of submicron SP magnetite (Soreghan et al., 1997; Cogoini et al., 2001; Jia, 2020).

Rock magnetism of Quaternary loess (and loess-based paleosols) has been used as a proxy (directly proportional) for mean annual precipitation (MAP) of ~300–1500 mm/year (e.g., Porter, 2001; Maher and Possolo, 2013; Maher, 2016; Gao et al., 2019). Depending on the parent material, amount of biological mixing, carbonate leaching, and clay illuviation, soils less penetrable by precipitation in areas with MAP > ~600 mm may result in water-logged conditions. Together with the presence of organic matter, this promotes anoxia and post-depositional dissolution of (fine) magnetic minerals.

## DATA AND METHODS

### Magnetic Susceptibility Sampling

#### *Sampling Magnetic Susceptibility in the Field (KT-10)*

A detailed sedimentological investigation of the Salagou Formation (Pfeifer et al., 2020) included measurement and description (at a decimeter scale) of ~1000 total meters of stratigraphic section exposed at the surface (Fig. 3). One MS reading (each flanked by free air measurements) was taken every 0.5 m through the entire formation with the Terraplus KT-10 Plus v2 handheld MS meter that includes a pin and circular coil for uneven surfaces. In mathematical terms, MS (k) is the ratio of the intensity of magnetization (I) to the magnetic field (H) responsible for the magnetization. It is calculated with the KT-10 Plus handheld meter based on the difference in frequency between the rock and free air with a sensitivity of 1 x $10^{-6}$ SI units (KT-10 manual, 2017). Results (k) in dimensionless units of $10^{-3}$ are reported as a curve constructed from the individual MS values at 0.5 m increments through each section.

The Salagou Formation was measured and described over nine stratigraphic sections (Fig. 3A). Most sections are continuous (from the top of one to the base of the next) and can be concatenated for analysis. However, there is ~500 m of missing section (inaccessible in outcrop) between the lowermost section (Section 1; Fig. 3A) and the remainder of the formation (Sections 2–9; Fig. 3A), necessitating the need to analyze Section 1 separately. Thus, time series analysis was done in two large segments (as noted in Fig. 3A, lower horizontal bar): the lower (165 m of continuous Section 1; results in Fig. 5) and the mid-upper (775 m of eight concatenated Sections 2–9; results in Fig. 6).

### *Sampling for Laboratory Magnetic Measurements*

Two sets of samples were collected from the middle Salagou Formation (Fig. 3A) for laboratory rock magnetic analysis (section "Laboratory Magnetic Measurements") at two different increments. In the first set (Fig. 3B), a 10 g sample was collected at a 5 m resolution for ~80 m of section. The second set (Fig. 3C) is higher resolution (a 10 g sample collected every 30 cm) but covers a shorter interval (~10.2 m total).

## Time Series Analysis and Modeling

Time series analysis of the MS stratigraphic series was carried out in MATLAB and Astrochron for R (Meyers, 2014) (see Supplementary Appendix S1 for commands). MATLAB functions were used to display the stratigraphic series, and for spectral analysis and evolutionary spectrograms to assess the distribution of variability as a function of frequency (cycles/meter) and along stratigraphic position to assess potential changes in sedimentation rate. A low-pass Taner filter was applied to pre-whiten the stratigraphic series, for clarity in evaluating stratigraphic cyclicity potentially related to orbital eccentricity.

The absence of an adequately precise time scale (Fig. 2) motivated the application of objective modeling with the average spectral misfit (ASM) method provided in Astrochron (Meyers and Sageman, 2007). The ASM method searches for astronomical frequencies in well-sampled stratigraphic series across a range of plausible sedimentation rates. For each test sedimentation rate, the stratigraphic series is converted to a time series and compared against an astronomical target (in kyr). Here the astronomical target is a collection of astronomical frequencies based on a precession frequency of k = 56.6 arcsec/year estimated for 298 Ma (Berger and Loutre, 1994) and assuming Solar System fundamental frequencies $s_i$, $g_i$ from Laskar et al. (2004; Table 1).The sedimentation rate yielding time frequencies in the data that most closely match those of the astronomical target (with Monte Carlo testing for assessing significance) is taken as the "optimal sedimentation rate."

## Laboratory Magnetic Measurements

More elaborate rock magnetic analysis was carried out for representative sections from the middle Salagou Formation (Figs. 3B,C) to determine the origin of the magnetic signal and strengthen the validity of MS as a proxy for the ancient paleoclimate record. The analyses were done at the rock and paleomagnetic laboratory of the Leibniz Institute for Applied Geophysics (LIAG) in Grubenhagen, Germany. The samples were dried, homogenized, weighed, and filled into non-magnetic plastic boxes of 6.4 $cm^3$. The MS for all samples was measured using a frequency- and field-variable Magnon VSM susceptibility bridge at 505 Hz (low frequency susceptibility; $\chi$lf) and at 5050 Hz (high frequency susceptibility; $\chi$hf), both at a field of 400 A/m. These measurements were also used to detect the frequency dependence of the MS, which can be expressed as simple difference ($\Delta\chi$ or $\%\chi$fd). The temperature-dependent MS was determined using an AGICO MFK1-FA Kappabridge and the CS4 furnace, covering a temperature range of 20–700°C (Fig. 4). Additionally, the system was rinsed by Argon provided in a constant flux and pressure. Thermally stable furnace holders were measured in an empty state and subtracted, based on their MS rusting of the full-range heating. The applied field strength was set to 400 A/m.

## RESULTS

### Sedimentology

Pfeifer et al. (2020) conducted detailed sedimentological analysis of the Salagou Formation. The dominant facies consist of thick and internally structureless mudstone beds (Fig. 3A, gray; interpreted as loess deposits) with local pedogenic overprinting. There is a general up-section increase in interbedded units (calcareous mudstone, commonly with desiccation features and laminated mudstone, commonly with ripples) that reflect intermittent subaqueous deposition (Fig. 3A, navy). Interpreted pedogenic intervals are nested within the loessite, defined in outcrop primarily by large (~10+ cm), randomly oriented, semi-radial slickensides (Figs. 3B,C). Micromorphologic attributes of samples from these localities include higher proportions of clay, wedge-shaped peds, clay coatings on grains, and porphyroskelic fabrics. Geochemical analyses reveal elevated chemical index of alteration (CIA) values from these intervals (compared to neighboring loessite). These features, together with a lack of horizonation, are most analogous to modern Vertisols which are typically indicative of environments with seasonal precipitation (e.g., Mack et al., 1993).

### Magnetic Susceptibility Measurements by KT-10

Table 2 summarizes the statistics of MS data obtained by portable MS meter, reporting the mean and standard deviation of susceptibility readings overall and by section (#1–9; Fig. 3A). Overall, the mean measurement of k (MS) for the Salagou formation is 0.253 ± 0.100 (x $10^{-3}$). The section with the lowest readings (uppermost Salagou; Section 9) averages 0.179 ± 0.034 ($\times 10^{-3}$) and the section with the highest readings (middle Salagou; Section 5) averages 0.366 ± 0.092 ($\times 10^{-3}$).

***Lower Salagou Formation –*** A repeating pattern appears in the MS series (Fig. 5A), defined by a predominant peak at 0.1 cycles/m (10 m wavelength) in the power spectrum (Fig. 5B) and warm colors in the spectrogram (Fig. 5C). Prominent, shorter frequencies of 0.29 cycles/cm (3.45 m) and 0.57 cycles/m (1.75 m) are also consistent through the section. ASM analysis estimates an optimal sedimentation rate of ~9.4 cm/kyr and indicates that astronomical forcing is statistically significant (P = 0.002; Fig. 5D).

***Mid-Upper Salagou Formation –*** Analysis of the mid-upper Salagou Formation (Fig. 6) reveals a strong, very low-frequency signal—especially in the middle part of the section—coincident with observed ~100–130 m (large-amplitude variations) in the MS series (Fig. 6A). The most significant cyclicity is ~0.1 cycles/m (0.13–0.08 cycles/m), i.e., 10 m thick cycles. Subordinate, higher frequency peaks at 0.28–0.31 and 0.55 cycles/m appear intermittently throughout the series. ASM analysis estimates an optimal sedimentation rate of 13 cm/kyr and indicates that astronomical forcing is statistically significant (P = 0.002; Fig. 6D).

### Laboratory Magnetic Measurements

Temperature (Fig. 4) and frequency-dependent susceptibility measurements from the representative section (Figs. 3B,C) indicate that the origin of the magnetic signal is primarily

driven by hematite, as evinced by the decrease of the MS at its Curie temperature at 675°C, with a varying but generally minor contribution of magnetite at a Curie temperature of 580°C (Fig. 4).

## DISCUSSION

### Calibration of Magnetic Susceptibility Measurements by KT-10

The data acquired by portable MS meter (see Section "Cyclicity in the Salagou Formation") demonstrate the tool's ability to recognize cyclic trends through extended stratigraphic successions of loessite. This methodology is relatively rapid, convenient, and inexpensive, but it is important to calibrate in situ outcrop MS data with rock magnetic analysis from the laboratory. The correlation between MS acquired by the portable MS meter in the field and detailed rock magnetic data acquired in the laboratory ($\chi$lf and $\Delta\chi$) is weak ($r^2 = 0.1758$; Fig. 3C), but a simple t-test indicates with 95% confidence that the relationships between $\chi$lf and field MS, and $\Delta\chi$ and field MS, are both highly significant (P-values < 0.05). The standard deviations in most sections (Table 2; Sections 1–3 and 7–9) for MS readings obtained with the portable meter ($0.179 \times 10^{-3} – 0.234 \times 10^{-3}$) are between $0.034 \times 10^{-3} – 0.064 \times 10^{-3}$, which further supports reproducibility. Prior to taking measurements through a section, several readings were recorded on the same sample to understand variability in the magnetic signal by lithology, and the tool always measured within $0.05 \times 10^{-3}$. For example, in Section 3 (Fig. 3A), six measurements were taken on calcareous interbeds for a mean reading of $0.158 \pm 0.037 \times 10^{-3}$ and 11 measurements were taken on pedogenic slickensides for a mean reading of $0.232 \pm 0.055 \times 10^{-3}$. In comparison to the average loess reading for this same section ($0.220 \pm 0.056 \times 10^{-3}$), this demonstrates the reliability of the tool to capture magnetic signal variations in different lithologies as well as reproducibility of readings on the same sample.

However, there are limitations with in situ MS measurements. The poor correlation between field and laboratory data may be caused by inhomogeneous volumes measured in the field (e.g., uneven surfaces or fractures/cavities in outcrop). Elevated mean MS readings from the portable meter ($0.303 \times 10^{-3} – 0.366 \times 10^{-3}$) in the middle Salagou formation (Table 2; Sections 4–6) have especially high standard deviations ($0.092 \times 10^{-3} – 0.135 \times 10^{-3}$) compared to other sections. It is possible that elevated values in the middle Salagou Formation relate to a decline in calcareous cement observable in this interval.

### Origin of the Magnetic Signal and Comparison to Quaternary Eurasian Loess

The direct relationship between $\chi$lf and $\Delta\chi$ (Fig. 7; frequency dependence) demonstrates that magnetic enhancement (increased $\chi$) is triggered by ultrafine SP particles close to the domain transition boundary. The production of SP magnetic grains can occur either in situ via pedogenic processes (Singer et al., 1996; Maher, 1998), by incorporation of detrital particles (e.g., Reynolds et al., 2001), and/or through conversion of magnetic mineral species during fluid or burial diagenesis (Katz et al., 1998; Woods et al., 2002). Given the burial history of the basin ($T_{max}$ up to 500–600°C; Copard et al., 2000), we cannot dismiss the possibility that some SP particles may have formed as a result of diagenesis, but minimal evidence occurs for fluid flow or veining in the Salagou Formation exposures. We prefer the interpretation of primarily pedogenically formed magnetic particles for the following reasons: (1) Association with evidence for pedogenesis, namely Vertic features (section "Sedimentology"), and elevated clay

mineral content and CIA (compared to parent loessite). Lindquist et al. (2011) show that the seasonal wetting and drying typical of Vertisols facilitate the formation of ferrimagnetic SP minerals. (2) There is no evidence for gleying: The Vertic characteristics of Salagou Formation paleosols are inconsistent with ever-wet conditions (Tabor and Myers, 2015). Numerous studies on recent and modern soils show consistently that non-water-logged (gleyed) soils have higher MS and greater abundances of pedogenically produced ultra-fine-grained ferrimagnetic material than in surrounding loess (cf. Heller and Liu, 1984; Maher and Taylor, 1988; and other references in section "Geological Setting"). Furthermore, (3) the alignment of $\chi$lf and $\Delta\chi$ with other Eurasian loess (Fig. 7) suggests pedogenic control on the magnetic signal (see also discussion below) as opposed to trends typical of diagenesis.

Rock magnetic data from the Salagou Formation shows magnetic enhancement, but distinctly lower $\chi$lf and lower $\Delta\chi$ compared to reference data (Fig. 7) from the Pliocene red clay on the CLP (Song et al., 2007) and a loess-paleosol sequence in Romania (Zeeden et al., 2016). A systematically lower $\chi$lf and $\Delta\chi$ relates to the predominance of hematite, which generally exhibits a weaker magnetic signal than magnetite and maghemite. The dominance of hematite and lower contribution of magnetite and maghemite in the Salagou Formation is similar to that found in Permian loessite from western equatorial Pangea (Soreghan et al., 1997; Cogoini et al., 2001; Jia, 2020), but unusual relative to Quaternary loess deposits. This difference may be attributable to syn-depositional processes (e.g., eolian sorting or dilution from rapid deposition of quartz and other non-iron-bearing minerals), more arid and/or oxidizing climate conditions preferring hematite formation over magnetite genesis or preservation (Maher, 1998), weak or stifled pedogenesis (documented sedimentologically; section "Sedimentology"), and/or post-depositional oxidation (of magnetite and maghemite). Eolian sorting is unlikely, because instead of the direct relationship between $\chi$lf and $\Delta\chi$ in the Salagou Formation (Fig. 7), sorting tends to generate an inverse pattern (high $\chi$lf with low $\Delta\chi$; e.g., Matasova and Kazansky, 2004). Similarly, hematite precipitates formed during post-depositional processes tend to generate a magnetic signal with an inconsistent pattern between $\chi$lf and $\Delta\chi$. The well-defined alignment of $\chi$lf and $\Delta\chi$ between these datasets (Fig. 7) strongly suggests that the magnetic signal in the Salagou Formation is driven by pedogenesis. If there is no post-depositional (diagenetic) conversion of magnetite/maghemite to hematite, then the low contribution of magnetite in the Salagou Formation loess compared to Eurasian Quaternary loess might reflect substantially different paleoclimatic settings in the Permian of France.

If changes in the magnetic signal are pedogenically driven, then samples in this dataset represent a range of pedogenic alteration, where samples with more magnetic enhancement are more enriched in ultrafine particles of hematite. However, the average bulk $\chi$ from interpreted paleosol ($1.3 \pm 0.3 \times 10^{-3}$) and loess ($1.5 \pm 0.4 \times 10^{-3}$) units in the Salagou Formation overlap within error. This is atypical of Quaternary Eurasian loess, and even compared to ancient loessite from western equatorial Pangea wherein the magnetic signal of paleosols— also driven primarily by hematite—is 1.5–2 higher than in the parent loess. But the rock magnetic measurements in the Salagou Formation ($1–1.5 \times 10^{-3}$) are overall much lower compared to the Permian loessitic paleosols of western equatorial Pangea (~$2–6 \times 10^{-3}$; Soreghan et al., 1997, 2002; Cogoini et al., 2001; Tramp et al., 2004; Soreghan G. S. et al., 2014), so it seems that the Salagou Formation preserves distinctively low concentrations of magnetite or maghemite in comparison even to time-equivalent loessite on the other (western) side of Pangea.

## Cyclicity in the Salagou Formation

In the lower Salagou MS series (Fig. 5), the persistent frequency at 0.1 cycles/m indicates a 10 m thick cyclicity. Higher frequencies at 0.29 and 0.57 cycles/m indicate 3.5 and 1.75 m thick cycles, respectively. This nested cyclicity, i.e., five to six shorter cycles within each 10 m "bundle," also appears in the MS series (Fig. 5A). If the predominant (10 m thick) cyclicity represents the orbital eccentricity, then this section (160 m) represents a duration of ~1.6 Myr, and the well-defined 3.5 and 1.75 m cycling represents the obliquity and precession index, respectively. There is also a very low frequency corresponding to a 44-m cycle, i.e., a candidate for 405 kyr orbital eccentricity.

In the mid-upper Salagou MS series (Fig. 6), there is long- term amplitude variation that is potentially associated with the decreased presence of calcareous cement in the middle part of the section (resulting in elevated MS values) and/or missing or repeated strata in the concatenation of successive sections (Fig. 3A). Regardless, the predominant cyclicity is ~9.4 m thick, which appears to be broadened by variable sedimentation rates along the series, with multiple closely spaced spectral peaks from 0.13 to 0.08 cycles/m (7–12 m thick cycles). Higher frequencies at 0.28–0.31 and 0.55 cycles/m translate to ~3.3 and 1.8 m thick cycles, respectively. If the predominant 9.4 m cycles represent short orbital eccentricity, then this section (775 m) represents 7.8 Myr of sedimentation. It is possible that ~3.3 and 1.8 m thick cycles represent obliquity and precession (respectively) but are inconsistent through the section and locally poorly defined.

The ASM analysis confirms that astronomical frequencies are present and statistically significant (P-values < 0.05 for both MS series), rejecting the null hypothesis of no astronomical forcing for specific sedimentation rates of 9.4 cm/kyr (lower Salagou) and 13 cm/kyr (mid-upper Salagou). The up-section increase of optimal (ASM-based) sedimentation rates from 9.4 to 13 cm/kyr suggests that the Salagou Formation represents a duration of 9–10 Myr. This result is similar to estimates for the Salagou Formation from previous work (11–17 cm/kyr; Pochat and Van Den Driessche, 2011) as well as average sedimentation rates for the middle Permian Lucaogou Formation of northwest China (8.9–10.3 cm/kyr; Huang et al., 2020). It is slightly faster than lower Permian loess deposition in western equatorial Pangea (>700 m over ~9 Myr so ≥7.8 cm/kyr; Johnson, 1989; Tramp et al., 2004; Soreghan M. J. et al., 2014), and on the lower end of sedimentation rates proposed for the Plio-Pleistocene CLP (Stevens and Lu, 2009).

If the driver of magnetic enhancement is pedogenesis (see section "Origin of the Magnetic Signal and Comparison to Quaternary Eurasian Loess"), then these data demonstrate fluctuation between loess accumulation and soil formation with loessite–paleosol couplets around 10 m thick in the Salagou Formation, which is similar to the lower Permian loessite of western equatorial Pangaea (Soreghan M. J. et al., 2014). Irregular cyclicity (e.g., 100–130 m; Fig. 5A) may reflect long-term variability in atmospheric circulation, hydroclimate, and/or changes in sedimentation rates.

## CONCLUSION

This study documents statistically significant astronomically forced climate change recorded in deep-time loessite of low-latitude Pangea. The results are as follows:

- Spectral analysis of handheld MS stratigraphic data shows a persistent 10 m thick cyclicity through the Permian Salagou Formation that denotes orbital eccentricity-scale

(~100 kyr) variability. Accordingly, subordinate, higher frequency cycles, at ~3.3–3.5 and ~1.8 m thick (most prominent in the lower Salagou Formation) likely represent 35 kyr obliquity and 17–21 kyr precession index-scale variations.

- Average spectral misfit analysis supports the interpretation of the presence of astronomical forcing frequencies, which are statistically significant in the MS series for optimal sedimentation rates of 9.4 cm/kyr (lower Salagou Formation) and 13 cm/kyr (mid-upper Salagou Formation): similar to the Permian of northwest China (~9–10 cm/kyr) and the western United States (~8 cm/kyr).
- Rock magnetic data from the Salagou Formation indicates magnetic enhancement wherein we interpret that magnetic particles (hematite) likely formed by pedogenesis, possibly with a diagenetic overprint.
- The uniquely low magnetic signal in the Salagou Formation compared to analogous Eurasian Quaternary loess deposits relates to the predominance of hematite, which generally has a much weaker magnetic signal than magnetite and maghemite, and may be explained by differing conditions of formation (e.g., syn depositional processes, more arid and/or oxidizing climate conditions) than in present Eurasia (not unexpected), and/or post depositional oxidation of magnetite and maghemite.
- The portable MS meter allows for rapid and convenient in situ data acquisition. This study demonstrates the ability to recognize cyclic trends through extended stratigraphic successions of loessite using this method when calibrated with detailed rock magnetic analysis from the laboratory.

The evidence demonstrates that the Salagou Formation records climatic variability over a time interval of 9–10 Myr during the early Permian (middle to late Cisuralian). If the driver of magnetic enhancement is pedogenic, then the ~10 m thick cyclicity that is consistent over ~1000 m of section may represent the thickness of loessite–paleosol couplets in the Salagou Formation.

## ACKNOWLEDGMENTS

This chapter is derived from an article published in *Frontiers in Earth Science*: *Geomagnetism and Paleomagnetism Specialty section,* 2020, available online: *doi: 10.3389/feart.2020.00241*. This work was supported by the National Science Foundation under International Research Experiences for Students (IRES) grant OISE-1658614 (awarded to PIs G.S. and M.J. Soreghan) and also EAR-1338331 (Sedimentary Geology and Paleobiology Program to G.S.). We thank M.J. Soreghan for suggesting collection of handheld MS data and our 2018 NSF IRES student participants for assistance with data collection (L. Alaniz, E. Simpson, V. Smith, and K. Yeager). We thank Stephane Pochat and Jean Van Den Driessche for field assistance and collaboration. We thank Kathrin Worm for support in the magnetic laboratory. This is IPGP contribution number 4143. Thank you to reviewers Rui Zhang and Diana Jordanova, and editor Hagay Amit.

**Supplemental Material.** Provided in dissertation section "Supplemental Material for Ch. II". Also available at https://www.frontiersin.org/articles/10.3389/feart.2020.00241/full#supplementary-material

## FIGURES AND TABLES

**Table 1.** Periodicities (in kyr) of orbital eccentricity (from Laskar et al., 2004). Precession index, and obliquity are from Earth's precession frequency ($k$) = 56.6 arcsec/year modeled at 298 Ma (Berger and Loutre, 1994).

| Astronomical parameter | Frequency (arcsec/year) | Period (kyr) |
|---|---|---|
| **Eccentricity** | | |
| $g_2$–$g_5$ | 3.194548 | 405.091 |
| $g_3$–$g_2$ | 9.916 | 131.0 |
| $g_4$–$g_2$ | 10.464 | 123.4 |
| $g_3$–$g_5$ | 13.110548 | 98.9 |
| $g_4$–$g_5$ | 13.658548 | 94.5 |
| **Precession index** | | |
| $k$+ $g_5$ | 60.857452 | 21.296 |
| $k$+ $g_2$ | 64.052 | 20.234 |
| $k$+ $g_3$ | 73.968 | 17.521 |
| $k$+ $g_4$ | 74.516 | 17.392 |
| **Obliquity** | | |
| $k$+ $s_6$ | 30.252145 | 44.840 |
| $k$+ $s_3$ | 37.750 | 34.331 |
| $k$+ $s_4$ | 38.755 | 33.441 |
| $k$+ $s_2$ | 49.55 | 26.155 |

*Note: g* and *s* are Solar System fundamental frequencies from Laskar et al. (2004), and subscripts refer to the planets in order (2–6): Venus, Earth, Mars, Jupiter, Saturn.

**Table 2.** Basic statistics of MS measurements by KT-10 (field data) depicted in Figure 3A as curves constructed from individual MS values.

| Section no. | Mean ($10^{-3}$) | St. dev ($10^{-3}$) | # Readings | Total m | Interval (m) |
|---|---|---|---|---|---|
| 9 | 0.179 | 0.034 | 138 | 70 | 0.51 |
| 8 | 0.222 | 0.064 | 226 | 125 | 0.55 |
| 7 | 0.234 | 0.062 | 179 | 100 | 0.56 |
| 6 | 0.345 | 0.135 | 227 | 121.5 | 0.54 |
| 5 | 0.366 | 0.092 | 220 | 111 | 0.50 |
| 4 | 0.303 | 0.097 | 159 | 100 | 0.63 |
| 3 | 0.220 | 0.057 | 259 | 131.5 | 0.51 |
| 2 | 0.205 | 0.038 | 137 | 70 | 0.51 |
| 1 | 0.198 | 0.046 | 314 | 160 | 0.51 |
| ALL | 0.253 | 0.100 | 1859 | 989 | 0.53 |

*Note:* This table reports the mean and standard deviation of MS measurements overall, and also by section (#1–9; corresponding with the stratigraphic columns in Figure 3A). The number of readings (measurements) for each section is also reported, as well as the sampling interval. Note: the aim was to take a measurement every 0.5 m, but sampling intervals are slightly wider than 0.5 m because of unexposed parts of the section.

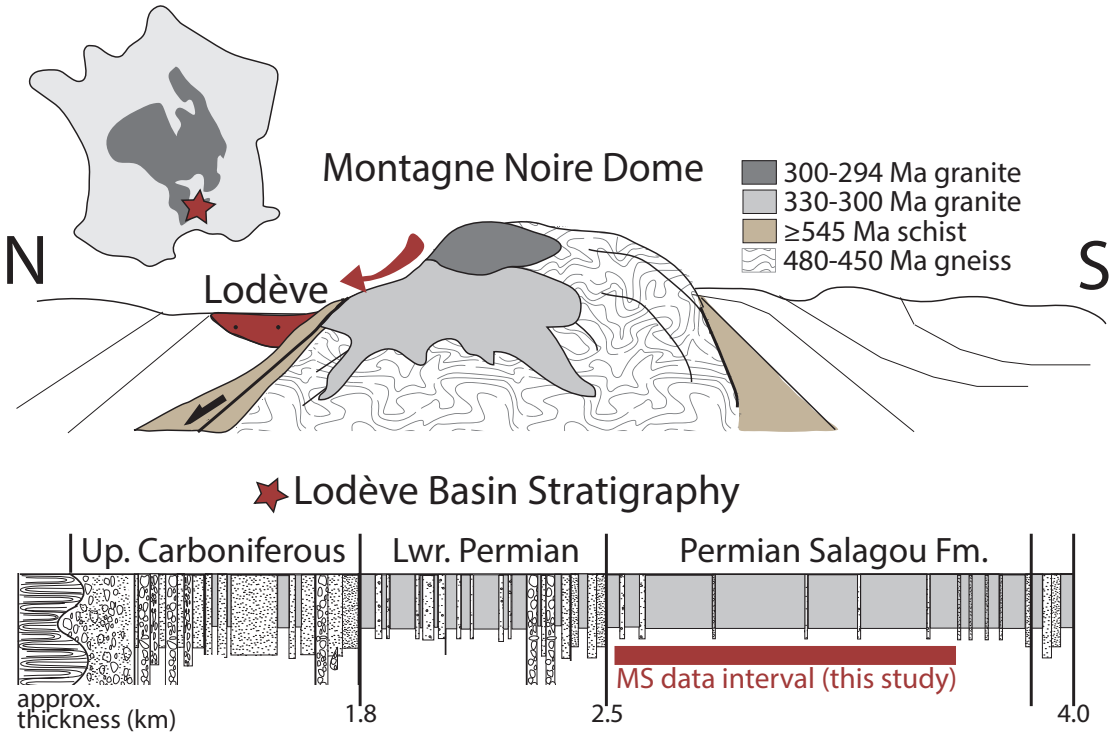


**Figure 1.** Geological setting of the Lodève Basin in south-central France (southern Massif Central). The N-S cross section depicts the generalized position of the Lodève basin in relation to several source lithologies in the Montagne Noire Dome (interpreted source of sediment in the Lodève Basin; Pfeifer et al., 2016). The generalized stratigraphic column (adapted from Pochat and Van Den Driessche, 2011) of the upper Carboniferous – Permian strata in the Lodève Basin, depicting the stratigraphic interval of focus in this study with a red bar.

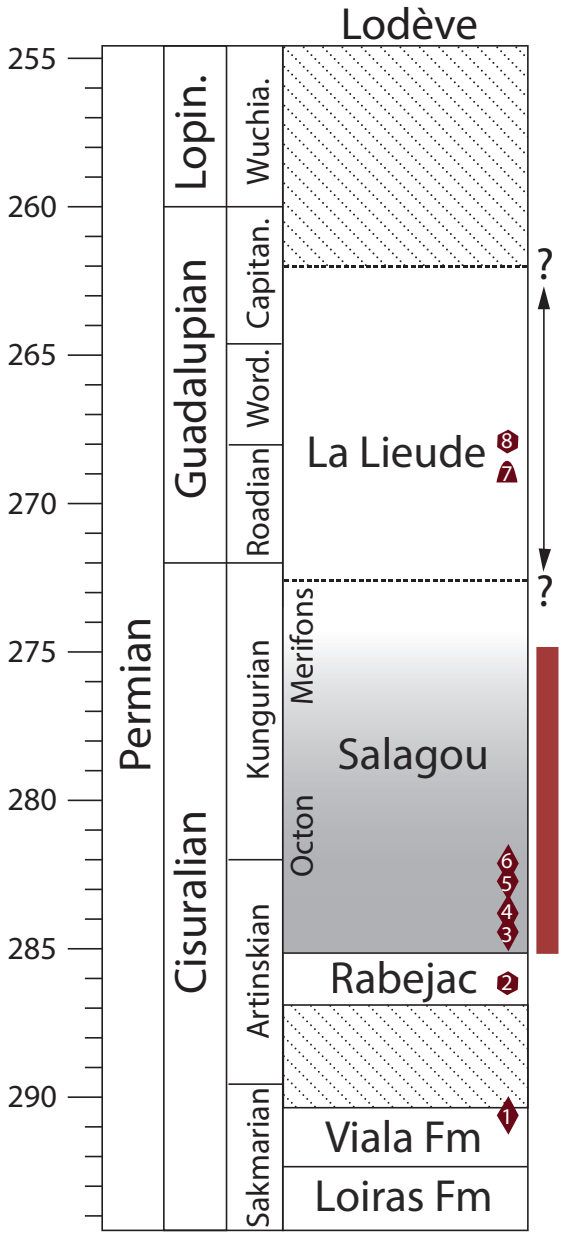


**Figure 2.** A summary of the current Permian chronostratigraphic constraints of the Salagou Formation (Lodève Basin). The section where MS data were measured in this study is highlighted in gray and also indicated with the red bar. Note that the upper age of the Salagou Formation is very poorly constrained. Icon shapes indicate different types of age data, numbered 1–8 according to the sources from which they are derived; Specifically: (1) U/Pb ID-TIMS on ash 291.0 ± 0.2 from the upper Viala Formation (Michel et al., 2015), (2) tetrapod tracks, Dromopus–Erpetopus biochron boundary, ~290–284 Ma (Schneider, pers. commun. 2020); (3–6) U/Pb ID-TIMS on ash (in stratigraphic order: 284.4 ± 0.1, 284.5 ± 0.1, 283.5 ± 0.1, 282.9 ± 0.1) from the Octon Member of the Salagou Formation (Michel et al., 2015), (7) magnetostratigraphic data from the La Lieude Formation that suggests proximity to the end of the "Kiaman" or Permo-Carboniferous Reversed Superchron (PCRS), ca. 262 Ma (Evans, 2012), and (8) tetrapod track ichnofauna from the La Lieude Formation consistent with a Guadalupian age (Schneider et al., 2010, 2019).

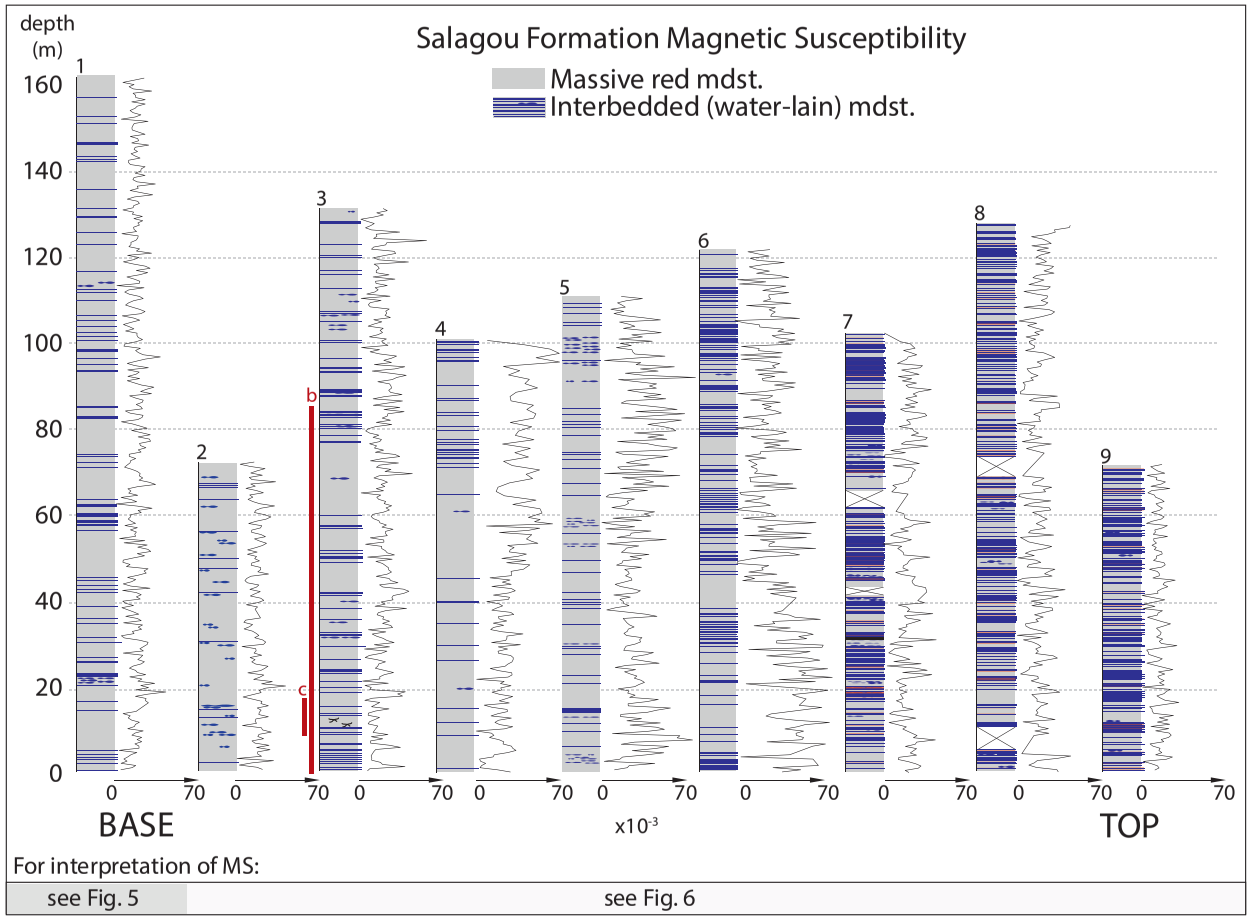
depth
(m)
Salagou Formation Magnetic Susceptibility
Massive red mdst.
Interbedded (water-lain) mdst.
160
140
120
100
80
60
40
20
0
1
2
3
4
5
6
7
8
9
b
c
0
70
BASE
TOP
x10-3
For interpretation of MS:
see Fig. 5
see Fig. 6

(a)

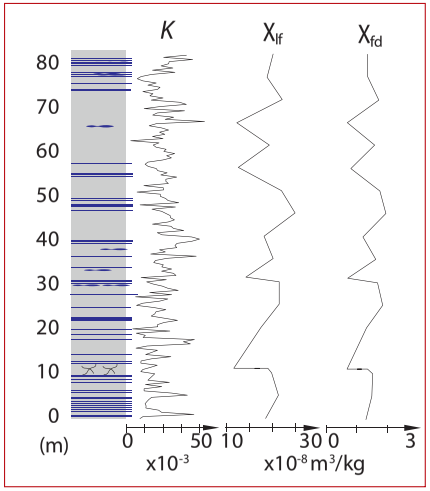
K
Xlf
Xfd
80
70
60
50
40
30
20
10
0
(m)
0
50
10
30
3
x10-3
x10-8 m3/kg

(b)

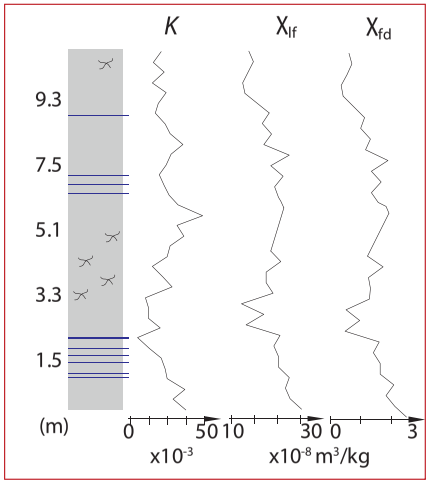
K
Xlf
Xfd
9.3
7.5
5.1
3.3
1.5
(m)
0
50
10
30
3
x10-3
x10-8 m3/kg

(c)

**Figure 3** ***(previous page)*****.** Rock magnetic data from the Salagou Formation. (A) Stratigraphy with handheld (outcrop) MS data (in units of $10^{-3}$). Section are numbered for reference and correspondence to Table 2. The dotted lines indicate depth intervals (see meter marks at left). The red bars on Section #3 represent the locations of detailed profiles sampled at two different intervals for detailed rock magnetic data (B,C; see insets). Bar at bottom of page indicates which stratigraphic section correspond with each interpreted MS series in Figure 5 (#1 only) and Figure 6 (#2–9). (B,C) Focused view showing the stratigraphy and outcrop MS again, but also displaying rock magnetic data obtained for these intervals. Specifically, mass normalized low-field MS ($\chi$lf) at 505 Hz in $10^{-8}$ $m^3$/kg and delta $\chi$ ($\chi$fd). (B) An 80-m section sampled at 5-m intervals. Note the pedogenic interval ~11 m. The correlation between MS measured in the field to $\chi$lf is negligible ($r^2 = 0.0059$), but the relationship between the two datasets is highly significant (P-value < 0.05). (C) A 10-m section sampled at 30-cm intervals. Note the pedogenic interval ~3–5 m. The correlation between MS measured in the field to $\chi$lf is weak ($r^2 = 0.1758$), but the relationship between the two datasets is highly significant (P-value < 0.05).

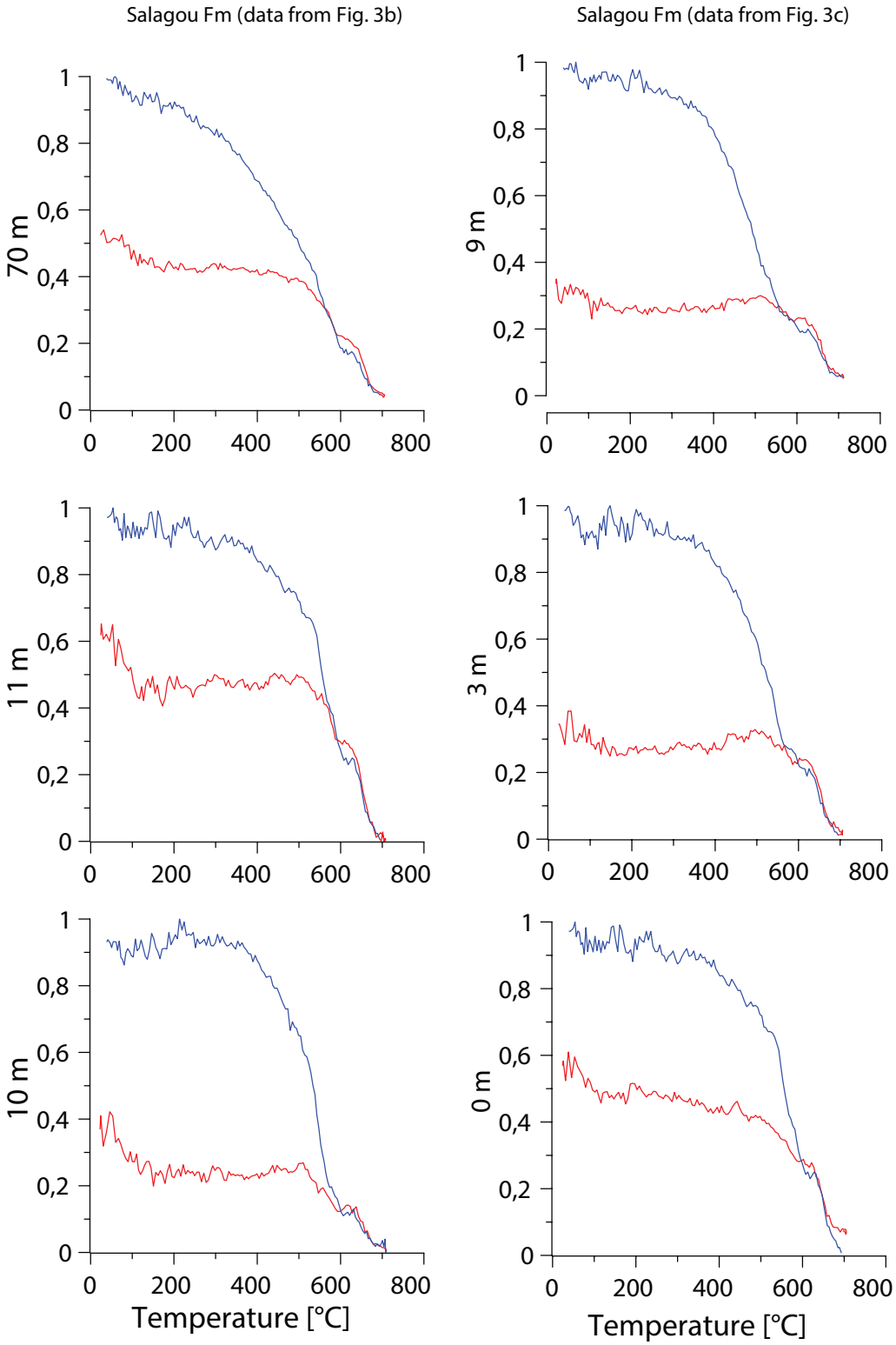


**Figure 4.** Temperature-dependent susceptibilities of datasets for selected samples from discussed sections in Figures 3B,C. Heating (red) and cooling curves (blue) are plotted against χlf, scaled to a maximum of 1 for comparison. Note that an χlf decrease at the Curie temperature of magnetite (580°C) tends to be less expressed than the clear χlf decrease at the Curie temperature of hematite (675°C).

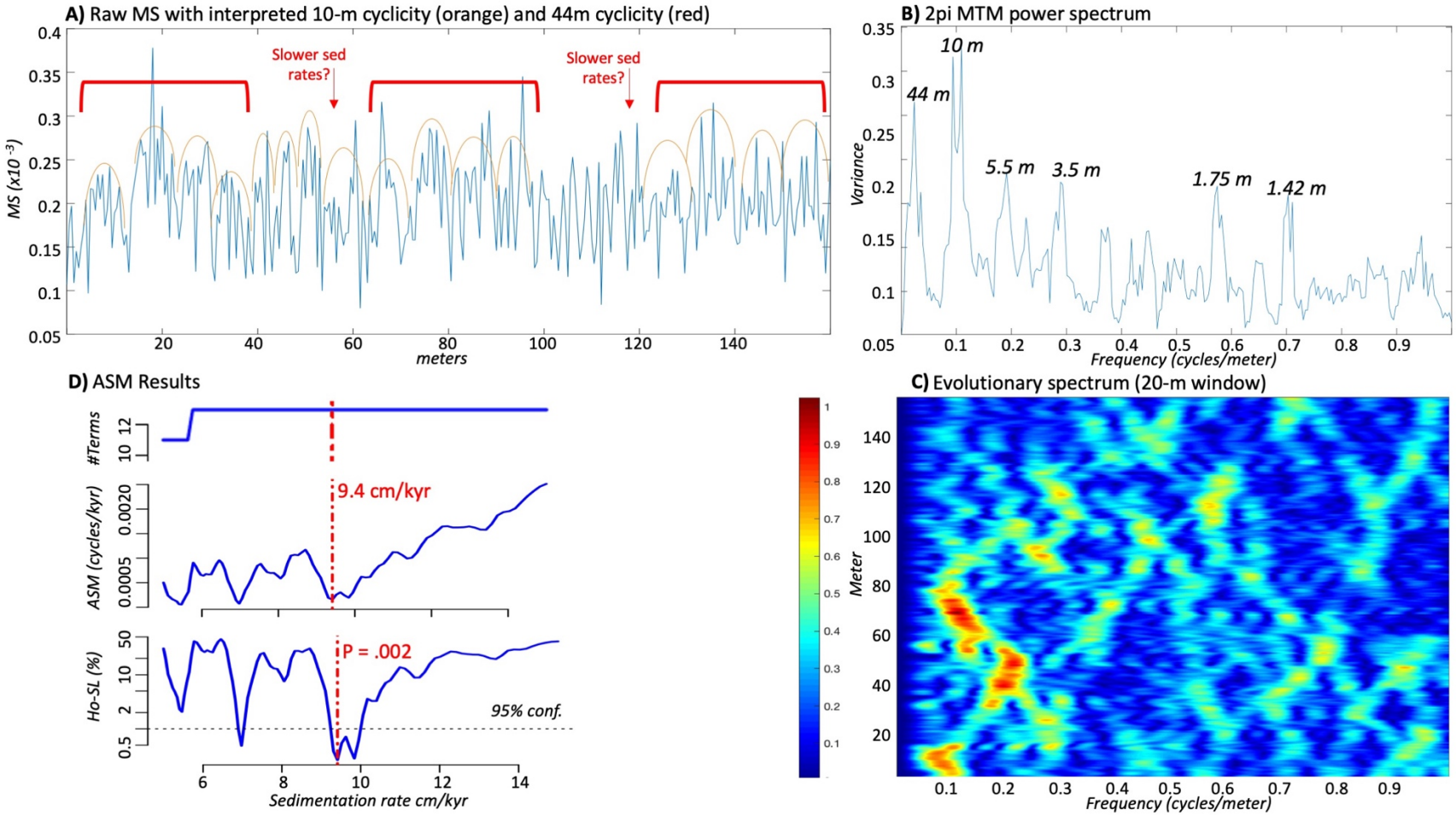
A) Raw MS with interpreted 10-m cyclicity (orange) and 44m cyclicity (red)
Slower sed rates?
Slower sed rates?
MS (x10 -3)
meters
B) 2pi MTM power spectrum
10 m
44 m
5.5 m
3.5 m
1.75 m
1.42 m
Variance
Frequency (cycles/meter)
D) ASM Results
#Terms
9.4 cm/kyr
ASM (cycles/kyr)
P = .002
Ho-SL (%)
95% conf.
Sedimentation rate cm/kyr
C) Evolutionary spectrum (20-m window)
Meter
Frequency (cycles/meter)

**Figure 5** ***(Previous Page).*** Results of time series analysis and modeling for MS data collected in outcrop from the lower Salagou Formation (see stratigraphic context in Figure 3; lower bar). The section is measured in meters (from low to high is moving up-section). (A) Magnetic susceptibility data with interpretations shown by orange arcs [10 m cycles—short (~100 kyr) orbital eccentricity] and red brackets [44 m cycles—long (~405 kyr) orbital eccentricity]. (B) The power spectrum shows the proportion of power (or variance) as a function of frequency (in cycles/m). (C) The FFT spectrogram, computed with a 20 m running window. Warmer (red) colors represent high power and cooler (blue) colors low power. (D) Results of ASM analysis with the optimal sedimentation rate identified by the vertical red dashed curve. Top: number of astronomical frequencies used in the fit; middle: ASM statistic; bottom: statistical significance of Monte Carlo modeling with the critical level shown by the horizontal black dashed line.

**Figure 6** ***(Following Page)***. Results from time series analysis and modeling for MS data collected in outcrop from the mid-upper Salagou Formation (see stratigraphic context in Figure 3; lower bar). The section is measured in meters (from low to high is moving up-section). (A) Magnetic susceptibility data with long-term amplitude variation (~100–130 m cycles). Higher frequency signals are not notable at this scale, but the inset zooms into an interval (590–630 m) to provide an example of the 10 m cycles (interpreted with orange arcs) that are also present in this section. (B) The power spectrum shows the proportion of power (or variance) as a function of frequency (in cycles/m). (C) The FFT spectrogram, computed with a 100 m running window and subtraction of low pass Taner filter with a cutoff frequency of 0.035 cycles/m (see Supplementary Appendix S1 for script). Warmer (red) colors represent high power and cooler (blue) colors low power. (D) Results of ASM analysis with the optimal sedimentation rate identified by the vertical red dashed curve. Top: number of astronomical frequencies used in the fit; middle: ASM statistic; bottom: statistical significance of Monte Carlo modeling with the critical level shown by the horizontal black dashed line.

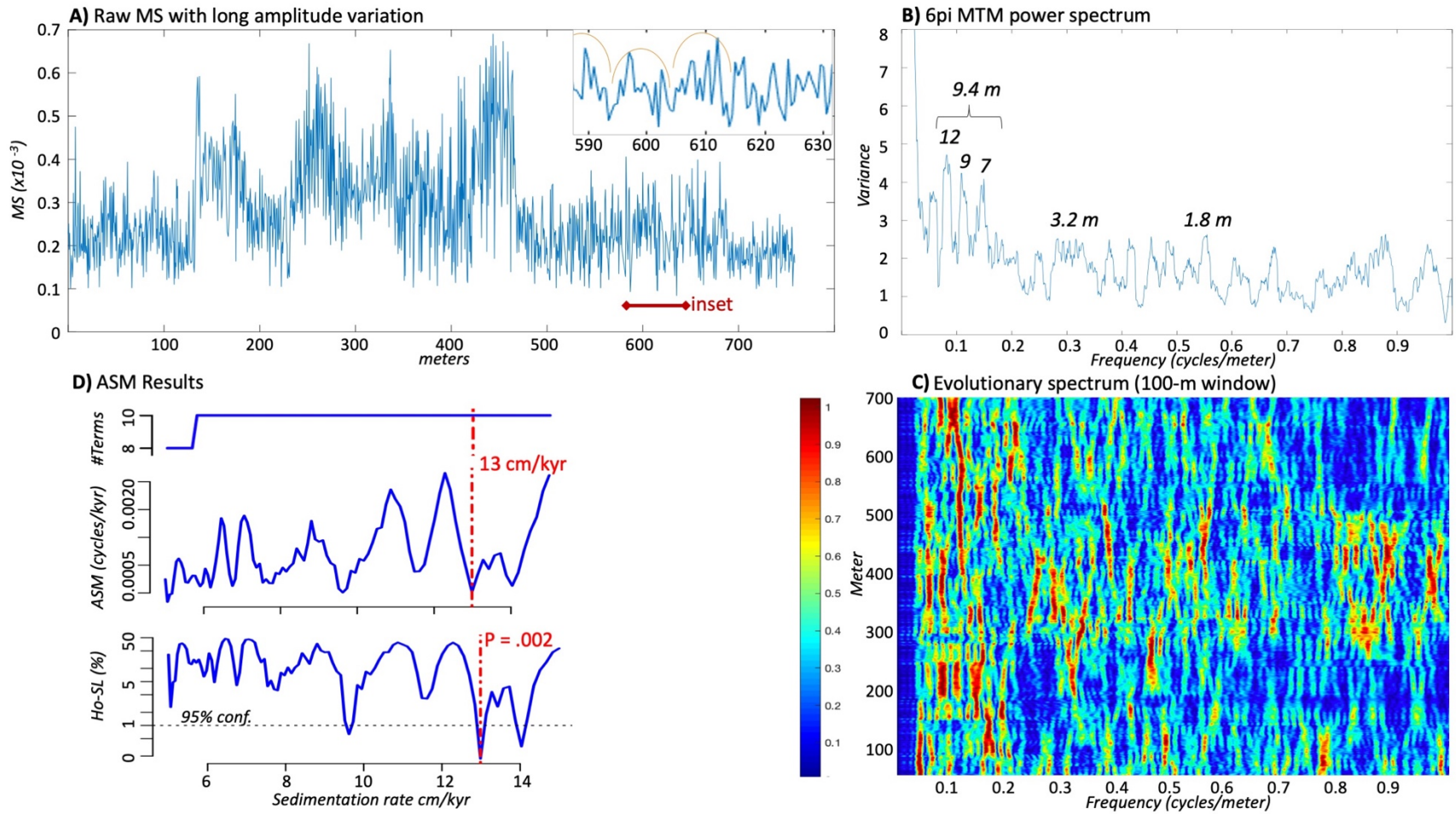
A) Raw MS with long amplitude variation
MS (x10 -3)
meters
inset
B) 6pi MTM power spectrum
Variance
9.4 m
12
9
7
3.2 m
1.8 m
Frequency (cycles/meter)
D) ASM Results
#Terms
13 cm/kyr
ASM (cycles/kyr)
Ho-SL (%)
P = .002
95% conf.
Sedimentation rate cm/kyr
C) Evolutionary spectrum (100-m window)
Meter
Frequency (cycles/meter)

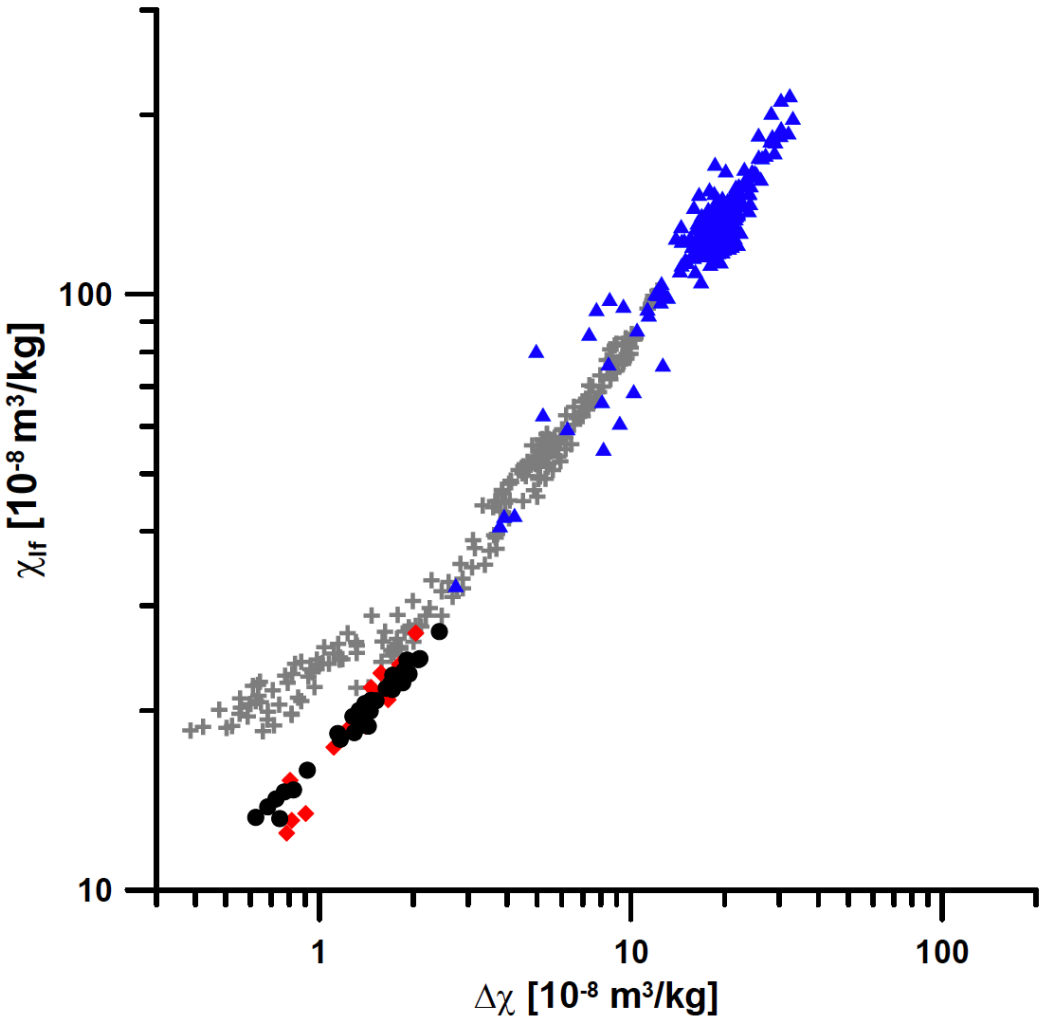


**Figure 7.** Frequency-dependent susceptibility (χlf vs. Δχ) of the Salagou Formation loess samples (red spades from Figure 3B; black circles from Figure 3C) compared to data from the Quaternary CLP red clay (blue triangles; Song et al., 2007) and a loess-paleosol section from Romania (gray crosses; Zeeden et al., 2016).

## REFERENCES CITED


Ahmed, I. A. M., and Maher, B. A. (2017). Identification and paleoclimatic significance of magnetite nanoparticles in soils. PNAS 115:201719186. doi: 10. 1073/pnas.1719186115

Basarin, B., Buggle, B., Hambach, U., Markoviæ, S. B., Dhand, K. O., Kovaèeviæ, A., et al. (2014). Time-scale and astronomical forcing of Serbian loess-palaeosol sequences. Glob. Planet. Change 122, 89–106. doi: 10.1016/j.gloplacha.2014. 08.007

Beget, J. E., Stone, D. B., and Hawkins, D. B. (1990). Paleoclimatic forcing of magnetic susceptibility variations in Alaskan loess during the Quaternary. Geology 18, 40–43.

Berger, A., and Loutre, M. F. (1994). Astronomical forcing through geological time. Spec. Publs Int. Ass. Sediment. 19, 15–24. doi: 10.1002/9781444304039.ch2

Chlachula, J. (2003). The Siberian loess record and its significance for reconstruction of Pleistocene climate change in north-central Asia. Q. Sci. Rev. 22, 1879–1906. doi: 10.1016/s0277-3791(03)00182-3

Cogoini, M., Elmore, R. D., Soreghan, G. S., and Lewchuk, M. T. (2001). Contrasting rock-magnetic characteristics of two upper Paleozoic loessite-paleosol profiles. Phys. Chem. Earth 26, 905–910. doi: 10.1016/s1464-1895(01)00140-5

Copard, Y., Disnar, J. R., Becq-Giraudon, J.-F., and Boussafir, M. (2000). Evidence and effects of fluid circulation on organic matter in intramontane coalfields (Massif Central, France). Int. J. Coal Geol. 44, 49–68. doi: 10.1016/s0166- 5162(99)00049-x

Domeier, M., and Torsvik, T. H. (2014). Plate tectonics in the late Paleozoic. Geosci. Front. 5, 303–350. doi: 10.1016/j.gsf.2014.01.002

Evans, M. E. (2012). Magnetostratigraphy of the Lodève Basin, France: Implications for the Permo-Carboniferous reversed superchron and the geocentric axial dipole. Stud. Geophys. Geodaetica 56, 725–734. doi: 10.1007/s11200-010- 0082-y

Evans, M. E., and Heller, F. (2001). Magnetism of loess/paleosol sequences: Recent developments. Earth Sci. Rev. 54, 129–144. doi: 10.1016/s0012-8252(01)00044-7

Foster, T. M., Soreghan, G. S., Soreghan, M. J., Benison, K. C., and Elmore, R. D. (2014). Climatic and paleogeographic significance of eolian sediment in the Middle Permian Dog Creek Shale (Midcontinent U.S.). Palaeogeogr. Palaeoclimatol. Palaeoecol. 402, 12–29. doi: 10.1016/j.palaeo.2014.02.031

Gao, X., Hao, Q., Oldfield, F., Bloemendal, J., Deng, C., Wang, L., et al. (2019). New high-temperature dependence of magnetic susceptibility-based climofunction for quantifying paleoprecipitation from Chinese loess. Geochem. Geophys. Geosyst. 20, 4273–4291. doi: 10.1029/2019GC008401

Giles, J. M., Soreghan, M. J., Benison, K. C., Soreghan, G. S., and Hasiotis, S. T. (2013). Lakes, loess, and paleosols in the Permian Wellington Formation of Oklahoma, USA: implications for paleoclimate and paleogeography of the midcontinent. J. Sediment. Res. 83, 825–846. doi: 10.2110/jsr.2013.59

Hayward, R. K., and Lowell, T. V. (1993). Variations in loess accumulation rates in the mid-continent, United States, as reflected by magnetic susceptibility. Geology 21, 821–824.

Heller, F., and Liu, T.-S. (1982). Magnetostratigraphical dating of loess deposits in China. Nature 300, 431–433. doi: 10.1038/300431a0

Heller, F., and Liu, T.-S. (1984). Magnetism of Chinese loess deposits. Geophys. J. R. Astron. Soc. 77:125. doi: 10.1111/j.1365-246x.1984.tb01928.x

Heller, F., and Liu, T.-S. (1986). Palaeoclimatic and sedimentary history from magnetic susceptibility of loess in China. Geophys. Res. Lett. 13, 1169–1172. doi: 10.1029/gl013i011p01169

Huang, H., Gao, Y., Jones, M. M., Tao, H., Alan, R., Ibarra, D. E., et al. (2020). Astronomical forcing of Middle Permian terrestrial climate recorded in a large paleolake in northwestern China. Palaeogeogr. Palaeoclimatol. Palaeoecol. 2020:109735. doi: 10.1016/j.palaeo.2020.109735

Jia, J. (2020). Magnetic properties of upper Paleozoic loessite-paleosol couplets in the Western USA: The role of pedogenic hematite in magnetic enhancement. Q. Int. 544, 57–64. doi: 10.1016/j.quaint.2020.02.014

Johnson, S. Y. (1989). Significance of loessite in the Maroon Formation (Middle Pennsylvanian to lower Permian), Eagle Basin, Northwest Colorado. J. Sediment. Petrol. 59, 782–791.

Katz, B., Elmore, R. D., Cogoini, M., and Ferry, S. (1998). Widespread chemical remagnetization: Orogenic fluids or burial diagenesis of clays. Geology 26, 603–606.

Kessler, J. L. P., Soreghan, G. S., and Wacker, H. J. (2001). Equatorial aridity in western Pangea: Lower Permian loessite and dolomitic paleosols in northeastern New Mexico. J. Sediment. Res. 71, 818–833.

Kiersnowski, H. (2013). "Late Permian Aeolian sand seas from the Polish Upper Rotliegend Basin in the context of palaeoclimatic periodicity," in Palaeozoic Climate Cycles: Their Evolutionary and Sedimentological Impact, Vol. 376, eds A. Gasiewicz and M. Słowakiewicz (London: Geological Society Special Publication), 431–456. doi: 10.1144/SP376.20

KT-10 manual (2017). KT-10 v2 Magnetic Susceptibility, Conductivity and Combined Magnetic Susceptibility-Conductivity Meter with GeoView: User's Guide. Version 2.2. Terraplus Geophysical Equipment Supplier. Available online at: http://www.terraplus.ca (accessed May, 2018).

Kukla, G. (1987). Loess stratigraphy in central China. Q. Sci. Rev. 6, 191–219. doi: 10.1016/0277-3791(87)90004-7

Kukla, G., and An, Z. S. (1989). Loess stratigraphy in central China. Palaeogeogr. Palaeoclimatol. Palaeoecol. 72, 203–225. doi: 10.1016/0031-0182(89)90143-0

Kukla, G., Heller, F., Liu, X. M., Xu, T. C., Liu, T. S., and An, Z. S. (1988). Pleistocene climates in China dated by magnetic susceptibility. Geology 16, 811–814.

Laskar, J., Robutel, P., Joutel, F., Gastineau, M., Correia, A. C. M., and Levrard, B. (2004). A long-term numerical solution for the insolation quantities of the Earth. Astron. Astrophys. 428, 261–285. doi: 10.1051/0004-6361

Li, Y., Shi, W., Aydin, A., Beroya-Eitner, M. A., and Gao, G. (2019). Loess genesis and worldwide distribution. Earth-Sci. Rev. 2019:102947. doi: 10.1016/j.earscirev.2019.102947

Lindquist, A. K., Feinberg, J. M., and Waters, M. R. (2011). Rock magnetic properties of a soil developed on an alluvial deposit at Buttermilk Creek, Texas, USA. Geochem. Geophys. Geosyst. 12, 1–12. doi: 10.1029/2011GC003848

Liu, T. (1985). Loess and the Environment. Beijing: China Ocean Press.

Liu, X. M., Shaw, J., Liu, T. S., and Heller, F. (1993). Magnetic susceptibility of the Chinese loess-paleosol sequence: Environmental change and pedogenesis. Geol. Soc. Lond. 150, 583–588. doi: 10.1144/gsjgs.150.3.0583

Mack, G. H., and Dinterman, P. A. (2002). Depositional environments and paleogeography of the Lower Permian (Leonardian) Yeso and correlative formations in New Mexico. Mountain Geol. 39, 75–88.
Mack, G. H., James, W. C., and Monger, H. C. (1993). Classification of paleosols. GSA Bull. 105, 129–136. doi: 10.1130/0016-7606(1993)105<0129:cop>2.3.co;2
Maher, B. (1986). Characterisation of soils by mineral magnetic measurements. Phys. Earth Planet. Inter. 42, 76–92. doi: 10.1016/s0031-9201(86)80010-3
Maher, B. A. (1998). Magnetic properties of modern soils and Quaternary loessic palaeosols: Palaeoclimatic implications. Palaeogeogr. Palaeoclimatol. Palaeoecol. 137, 2554. doi: 10.1016/S0031-0182(97)00103-X
Maher, B. A. (2016). Palaeoclimatic records of the loess/palaeosol sequences of the Chinese Loess Plateau. Q. Sci. Rev. 154, 23–84. doi: 10.1016/j.quascirev.2016. 08.004
Maher, B. A., and Possolo, A. (2013). Statistical models for use of palaeosol magnetic properties as proxies of palaeorainfall. Glob. Planet. Change 111, 280–287. doi: 10.1016/j.gloplacha.2013.09.017
Maher, B. A., and Taylor, R. M. (1988). Formation of ultrafine-grained magnetite in soils. Nature 336, 368–370. doi: 10.1038/336368a0
Maher, B. A., and Thompson, R. (1991). Mineral magnetic record of the Chinese loess and paleosols. Geology 19, 3–6.
Maher, B. A., and Thompson, R. (1992). Paleoclimatic significance of the mineral magnetic record of the Chinese loess and paleosols. Q. Res. 37, 155–170. doi: 10.1016/0033-5894(92)90079-x
Maher, B. A., Thompson, R., and Zhou, L. P. (1994). Spatial and temporal reconstructions of changes in the Asian palaeomonsoon: A new mineral magnetic approach. Earth Planet. Sci. Lett. 125, 462–471.
Matasova, G. G., and Kazansky, A. Y. (2004). Magnetic properties and magnetic fabrics of Pleistocene loess/palaeosol deposits along west-central Siberian transect and their palaeoclimatic implications. Geol. Soc. Lond. Spec. Publ. 238, 145–173. doi: 10.1144/GSL.SP.2004.238.01.11
Meyers, S. R. (2014). Astrochron: An R Package for Astrochronology. Available online at: https://cran.r-project.org/package=astrochron (accessed March, 2019).
Meyers, S. R., and Sageman, B. B. (2007). Quantification of deep-time orbital forcing by average spectral misfit. Am. J. Sci. 307, 773–792. doi: 10.2475/05. 2007.01
Michel, L. A., Tabor, N. J., Montanez, I. P., Schmitz, M. D., and Davydov, V. I. (2015). Chronostratigraphy and Paleoclimatology of the Lodève Basin, France: Evidence for a pan-tropical aridification event across the Carboniferous– Permian boundary. Palaeogeogr. Palaeoclimatol. Palaeoecol. 430, 118–131. doi: 10.1016/j.palaeo.2015.03.020
Muhs, D. R. (2007). “Loess deposits, origins, and properties,” in Encyclopedia of Quaternary Science, eds C. J. Mock, and S. Elias (Amsterdam: Elsevier), 1405. doi: 10.1016/b0-444-52747-8/00158-7
Murphy, K. (1987). Eolian origin of upper Paleozoic red siltstones at Mexican Hat and Dark Canyon. 127. Utah M.S. Thesis, University of Nebraska-Lincoln, Lincoln.
Muttoni, G., and Kent, D. V. (2019). Adria as promontory of Africa and its conceptual role in the Tethys twist and Pangea B to Pangea A transformation in the Permian. Res. Paleontol. Stratigr. 12, 249–269.

Parrish, J. T. (1993). Climate of the Supercontinent Pangea. J. Geol. 101, 215–233. doi: 10.1086/648217

Pfeifer, L. S., Soreghan, G. S., Pochat, S., and Van Den Driessche, J. (2020). Loess in eastern equatorial Pangea archives a dusty atmosphere and possible upland glaciation. GSA Bull. doi: 10.1130/B35590.1

Pfeifer, L. S., Soreghan, G. S., Pochat, S., Van Den Driessche, J., and Thomson, S. N. (2016). Permian exhumation of the Montagne Noire core complex recorded in the Graissessac-Lodève Basin. Basin Res. 30, 1–14. doi: 10.1111/bre. 12197

Pochat, S., and Van Den Driessche, J. (2011). Filling sequence in Late Paleozoic continental basins: A chimera of climate change? A new light shed given by the Graissessac – Lodève basin (SE France). Palaeogeogr. Palaeoclimatol. Palaeoecol. 302, 170–186. doi: 10.1016/j.palaeo.2011.01.006

Porter, S. C. (2001). Chinese loess record of monsoon climate during the last glacial–interglacial cycle. Earth Sci. Rev. 54, 115–128. doi: 10.1016/s0012- 8252(01)00043-5

Porter, S. C., Hallet, B., Wu, X., and An, Z. (2001). Dependence of near-surface magnetic susceptibility on dust accumulation rate and precipitation on the Chinese Loess Plateau. Q. Res. 55, 271–283. doi: 10.1006/qres.2001.2224

Reynolds, R., Belnap, J., Reheis, M., Lamothe, P., and Luiszer, F. (2001). Aeolian dust in Colorado Plateau soils: Nutrient inputs and recent change in source. Proc. Natl. Acad. Sci. 98, 7123–7127. doi: 10.1073/pnas.12109 4298

Schneider, J. W., Körner, F., Roscher, M., and Kroner, U. (2006). Permian climate development in the northern peri-Tethys area —The Lodève basin, French Massif Central, compared in a European and global context. Palaeogeogr. Palaeoclimatol. Palaeoecol. 240, 161–183. doi: 0.1016/j.palaeo.2006.03.057

Schneider, J. W., Lucas, S. G., Scholze, F., Voigt, S., Marchetti, L., Werneburg, R., et al. (2019). Late paleozoic-early mesozoic continental biostratigraphy - links to the standard global chronostratigraphic scale. Palaeoworld. 531, 1–53.

Schneider, J. W., Lucas, S. G., Werneburg, R., and Rößler, R. (2010). Euramerican Late Pennsylvanian / Early Permian arthropleurid/tetrapod associations – implications for the habitat and paleobiology of the largest terrestrial arthropod in Lucas, S. G., Schneider, J. W. and Spielmann, J. A., eds, Carboniferous-Permian transition in Canõn del Cobre, northern New Mexico. New Mexico Museum Nat. History Sci. Bull. 49, 49–70.

Shackleton, N. J., Berger, A., and Peltier, W. R. (1990). An alternative astronomical calibration of the lower Pleistocene timescale based on ODP Site 677. Trans. R. Soc. Edinb. Earth Sci. 81, 251–261. doi: 10.1017/s0263593300020782

Singer, M. J., Verosub, K. L., Fine, P., and TenPas, J. D. (1996). A conceptual model for the enhancement of magnetic susceptibility in soils. Quat. Int. 3436:243248. doi: 10.1016/1040-6182(95)00089-85

Song, Y., Fang, X., Torii, M., Ishikawa, N., Li, J., and An, Z. (2007). Late Neogene rock magnetic record of climatic variation from Chinese eolian sediments related to uplift of the Tibetan Plateau. J. Asian Earth Sci. 30, 324–332. doi: 10.1016/j.jseaes.2006.10.004

Soreghan, G. S., Elmore, R. D., Katz, B., Cogoini, M., and Banerjee, S. (1997). Pedogenically enhanced magnetic susceptibility variations preserved in Paleozoic loessite. Geology 25, 1003–1006.

Soreghan, G. S., Elmore, R. D., and Lewchuk, M. T. (2002). Sedimentologic– magnetic record of western Pangean climate in Upper Paleozoic loessite (Lower Cutler Beds, Utah). Geol.

Soc. Am. Bull. 114, 1019–1035. doi: 10.1130/0016-7606(2002)114<1019:smrowp>2.0.co;2
Soreghan, G. S., Soreghan, M. J., and Hamilton, M. A. (2008a). Origin and significance of loess in late Paleozoic western Pangaea: a record of tropical cold. Palaeogeogr. Palaeoclimatol. Palaeoecol. 268, 234–259. doi: 10.1016/j.palaeo. 2008.03.050
Soreghan, G. S., Soreghan, M. J., Poulsen, C. J., Young, R. A., Sweet, D. E., and Davogustto, O. C. (2008b). Anomalous cold in Pangaean tropics. Geology 36, 659–662.
Soreghan, G. S., Sweet, D. E., and Heavens, N. G. (2014). Upland Glaciation in tropical pangaea: geologic evidence and implications for late paleozoic climate modeling. J. Geol. 122, 1–30.
Soreghan, M. J., Heavens, N., Soreghan, G. S., Link, P. K., and Hamilton, M. A. (2014). Abrupt and high-magnitude changes in atmospheric circulation recorded in the Permian Maroon Formation, tropical Pangaea. Geol. Soc. Am. Bull. 126, 569–584. doi: 10.1130/B30840.1
Soreghan, M. J., and Soreghan, G. S. (2007). Whole-rock geochemistry of Upper Paleozoic loessite, Western Pangea: implications for paleo-atmospheric circulation. Earth Planet. Sci. Lett. 255, 117–132. doi: 10.1016/j.epsl.2006.12.010
Stevens, T., and Lu, H. (2009). Optically stimulated luminescence dating as a tool for calculating sedimentation rates in Chinese loess: comparisons with grain-size records. Sedimentology 56, 911–934. doi: 10.1111/j.1365-3091.2008.01004.x
Sweet, A. C., Soreghan, L. S., Sweet, D. E., Soreghan, M. J., and Madden, A. S. (2013). Permian dust in Oklahoma: source and origin for middle Permian (Flowerpot-Blaine) redbeds in Western Tropical Pangaea. Sediment. Geol. 28, 181–196. doi: 10.1016/j.sedgeo.2012.12.006
Tabor, N. J., and Myers, T. S. (2015). Paleosols as Indicators of Paleoenvironment and Paleoclimate. Annu. Rev. Earth Planet. Sci. 43, 333–363. doi: 10.1146/ annurev-earth-060614-105355
Tramp, K. L., Soreghan, G. S., and Elmore, R. D. (2004). Paleoclimatic inferences from paleopedology and magnetism of the Permian Maroon Formation. GSA Bull. 116, 671–686. doi: 10.1130/B25354.1
Woods, S., Elmore, R. D., and Engel, M. (2002). Paleomagnetic dating of the smectite-to-illite conversion: Testing the hypothesis in Jurassic sedimentary rocks, Skye, Scotland. J. Geophys. Res. 107, 2–9. doi: 10.1029/2000JB000053
Yang, S. L., and Ding, Z. L. (2004). Comparison of particle size characteristics of the Tertiary "red clay" and Pleistocene loess in the Chinese Loess Plateau: Implications for origin and sources of the "red clay.". Sedimentology 51, 77–93. doi: 10.1046/j.1365-3091.2003.00612.x
Zeeden, C., Hambach, U., Obreht, I., Hao, Q., Abels, H. A., Veres, D., et al. (2018). Patterns and timing of loess-paleosol transitions in Eurasia: Constraints for paleoclimate studies. Glob. Planet. Change 162, 1–7. doi: 10.1016/j.gloplacha. 2017.12.021
Zeeden, C., Kels, H., Hambach, U., Schulte, P., Protze, J., Eckmeier, E., et al. (2016). Three climatic cycles recorded in a loess-palaeosol sequence at Semlac (Romania) – Implications for dust accumulation in south-eastern Europe. Quat. Sci. Rev. 154, 130–142. doi: 10.1016/j.quascirev.2016.11.002
Zheng, H., Oldfield, F., Yu, L., Shaw, J., and An, Z. (1991). The magnetic properties of particle-sized samples from the Luo Chuan loess section: evidence for pedogenesis. Phy. Earth Planet. Inter. 68, 250–258. doi: 10.1016/0031-9201(91)90044-i

Zhou, L. P., Oldfield, F., Wintle, A. G., Robinson, S. G., and Wang, J. T. (1990). Partly pedogenic origin of magnetic variations in Chinese Loess. Nature 346, 737–739. doi: 10.1038/346737a0

CHAPTER III

# ICE-CRYSTAL TRACES IMPLY EPHEMERAL FREEZING IN EARLY PERMIAN EQUATORIAL PANGEA

# ICE-CRYSTAL TRACES IMPLY EPHEMERAL FREEZING IN EARLY PERMIAN EQUATORIAL PANGEA


## ABSTRACT

Delicate impressions in lacustrine strata of the lower Permian (lower Cisuralian) Usclas Formation record ephemeral freezing in equatorial Pangea. These sediments accumulated in the paleoequatorial and intramontane Lodève Basin (southern Massif Central, France) during peak icehouse conditions (Late Paleozoic Ice Age). Experimental replication of these features corroborates the interpretation that they are ice-crystal molds. Evidence for films of ice in marginal-lacustrine sediment at such low latitudes and inferred low-moderate altitudes (< 2 km) calls for a reevaluation of climate conditions in eastern equatorial Pangea. Ephemeral freezing implies either cold tropical temperatures (~5°C cooler than the Last Glacial Maximum) and/or lapse rates that exceeded those of the Last Glacial Maximum. Extreme continentality of the Lodève Basin as portrayed by a Pangea B configuration would have amplified seasonality, albeit the climatic forcing(s) necessary to promote cold temperatures in equatorial Pangea remain enigmatic.


## INTRODUCTION

The Graissessac-Lodève Basin is a small continental rift basin in France's Massif Central (Fig. 1). Delicate crystal molds in multiple bedding-plane exposures of the lower Permian Usclas Formation have been interpreted to record traces of either gypsum crystals, implying evaporative conditions (Odin, 1986), or ice crystals, implying ephemeral freezing conditions (Becq-Giraudon et al., 1996) during the late Paleozoic icehouse (LPIA). Here, we document and characterize the primary morphologies of these features, and conduct laboratory analyses to empirically reproduce sediment impressions left by freezing of water-saturated mud. The paleoenvironmental conditions of formation (ephemeral freezing) implied by these results demand a reevaluation of climate models in low-latitude early Permian Pangea.

## BACKGROUND

Pangean assembly resulted in uplift of the Central Pangean Mountains which spanned the equator from North America (Appalachian-Ouachita-Marathon belt) to Western Europe (Variscan belt). Syn-orogenic extension in the late stages of the Variscan Orogeny (~300 Ma) produced several rift basins (Menard and Molnar, 1988; Burg et al., 1994) that remained within the equatorial belt throughout the late Paleozoic (Fig. 1; Domeier and Torsvik, 2014; Kent and Muttoni, 2018). Among them, the Lodève Basin (southern Massif Central) preserves an upper Carboniferous - Permian record of regional paleoequatorial climate from apex to collapse of the LPIA.

The abundance of ice-contact deposits across southern Gondwana implies that Asselian-Sakmarian (early Permian; ~298 – 295 Ma) time records the most intense phase of the LPIA (e.g. Fielding et al., 2008). Evidence for periglacial and proglacial conditions at paleoequatorial latitudes have also been hypothesized in both western (Ancestral Rocky Mountains; Soreghan et al., 2008ab; 2014ab) and eastern Pangea (Variscan paleomountains; Julien, 1895; Becq-Giraudon

and Van Den Driessche, 1994; Becq-Giraudon et al., 1996; Pfeifer et al., 2020). However, these claims remain controversial because they imply colder conditions than models can replicate (e.g. Soreghan et al., 2008a; Heavens et al. 2012; 2015).

The lower Permian (lower Cisuralian) Usclas Formation (Lodève Basin) consists primarily of organic-rich mudstone and tan siltstone of lacustrine origin (Pochat and Van Den Driessche, 2011). Delicate, stellate features occur on multiple bedding-plane exposures here, and in coeval strata of the nearby Gabian-Neffies Basin (Montenat and Dolle, 1986) and in Germany (Martinstein-Nahe; Reineck, 1955).

## METHODS

Three detailed sections of the Usclas Formation (totaling 5.4 m; Fig. 1) containing an abundance of delicate impressions were measured at cm-scale resolution. The impressions were classified into three morphologies. Thin sections were made of representative samples and compositional analyses (Energy Dispersive Spectroscopy; EDS) were acquired with a Cameca SX100 electron probe micro-analyzer. Laboratory experiments of freezing saturated mud (with distilled water-to dilute NaCl solutions) were designed to simulate ice-crystal growth and test the hypothesis that the features represent traces of ice (see Appendix I for experimental set up and variables).

## RESULTS

### Morphological documentation of delicate traces

The Usclas Formation (Fig. 1) comprises massive to locally laminated, thinly-bedded mudstone to tuffaceous mudstone (mode 25-30 μm; Appendix II). The bedding-plane traces (occurring as both molds and casts) exhibit three morphologies (Fig. 2), designated as Morphology "*SR*" (stubby rods), "*FN*" (fanned needles), and "*DC*" (delicate, complex), albeit these represent a continuum. Morphologies *FN* and *DC* (most common) co-occur (Fig. 1) and exist as molds. Morphology *SR* occurs near the top of the section and exist as casts. All impressions contain secondary minerals (Fig. 2): Potassium feldspar replaces dolomite in *SR*, and potassium feldspar lines molds of *FN* and *DC*.

***Morphology SR*** forms composite, rod-like, stubby needles (6-10 mm). Bundles commonly intersect at 60°, 90°, or 180° angles.

***Morphology FN*** consists of needles (2-5 mm) occurring most commonly as 60-120° fans. Less common are feather-like features (up to 20-25 mm) that fan in preferred directions from a linear center with rare curvature.

***Morphology DC*** consists of delicate blades that form well-developed 60-120° semi-radial "bowtie" -to full-360° radial fans. Some fans comprise straight needles (3-10 mm), while others are feather-like to dendritic, with smaller curved branches emanating from the main needles. Bowtie features (60-120°) are longer (up to 25-30 mm).

## Laboratory simulation of ice growth in sediment

Morphologies of experimental ice (formed at -15°C in saturated mud) match the scale and form of bedding-plane impressions from the Usclas Formation (Fig. 2). The variable that most influences morphology is sediment water saturation, and to a lesser extent, water chemistry. *SR* generally forms in mud saturated or super-saturated (for shorter, deeper impressions) with distilled water. *FN* forms in mud with very dilute NaCl (0.1-0.5%) -saturated conditions, and *DC* forms in mud saturated with 0.5-1% NaCl solution. Note that natural growth rates are much slower (0.01—0.1"/h; Barns and Laudise, 1985), so the rate of freezing (in comparison to natural systems) is also a variable, just not within our experimental design.

# DISCUSSION

## Interpretation of Usclas Formation features as ice-crystal traces

Empirical replication of the observed Usclas Formation morphologies using fully-saturated mud beneath a film (≤ 1.5 mm thick) of water (with up to 1% NaCl) corroborates the interpretation that these features represent ice-crystal molds. Furthermore, the common morphological features that define both ice crystal traces from modern mudflats (e.g. Table 1; Fig. 3,a-c) and inferred ice crystal traces from the ancient record (e.g. Table 1; Fig. 3,d-l) reinforce this interpretation. Generally, these characteristics include straight, tapered, needle-like traces in bundled-to-radial habits that exhibit intersecting or overlapping patterns. Experiments reproduced several of the particular sizes and forms of each morphology, including the short, higher-relief features of *SR*, 60-120° fans of *FN*, and delicate, radial blades and dendritic branches of *DC* (Fig. 2). *DC* morphologies visually replicate irrefutable ice-crystal marks from modern playas (e.g., Fig. 3,c). *FN* morphologies resemble shapes of inferred Pleistocene ice crystal traces (e.g., Fig. 3,d-e) and cryostructures (e.g., Fig. 3,f). The rod-like forms of *SR* resemble *Fucoides graphica* features in early interpretations of peritidal ground ice (Hall, 1843; Clarke, 1918).

Empirical results show that the primary controls on crystal morphology (notably, aspect ratio) are fluid saturation of the mud, and water depth. Water chemistry also influences crystal shape, with more complex (curved, feathery, dendritic) forms (Fig. 2; *DC*) resulting from dilute NaCl solutions (0.1-1%). Previous observations of ice crystallization in both laboratory (e.g. Allan, 1926; Mark, 1932; Reineck, 1955) and natural settings (e.g. Fig. 3,a-c; Table 1; Reineck and Singh, 1980) also emphasized the influence of water saturation of the host sediment on crystal size and morphology. The very fine grain size of the Usclas Formation enhanced preservation of the delicate traces (as in a Lagerstätte).

Odin (1986) interpreted the bedding-plane traces in the Usclas Formation as the result of evaporite (gypsum) crystallization, supported by other evidence for shallow water and dry conditions (e.g. desiccation features) elsewhere in this unit. However, the morphologies of Usclas Formation traces are inconsistent with the prismatic, pyramidic habits or "brainlike" textures that characterize gypsum crystals (cf. Magee, 1991; Benison and Bowen, 2013). Additionally, abundant evidence for wet paleoenvironmental conditions in this section of the Usclas Formation (Fig. 1; organic-rich black mudstone) refute the prevalence of strongly evaporitic conditions necessary for the precipitation of gypsum (or other salts) in this setting.

**Paleoclimate implications for the early Permian**

Empirical replication of ice crystal molds supports the inference that the ice crystals formed in—at most—very shallow films (< 2 mm) of water, and displaced sediment downward and outward during growth. This is consistent with ephemeral freezing along paleoshorelines of the Usclas Formation lake (cf. Fig. 3,c) which is a common occurrence in modern playa lakes in climates subject to freezing temperatures (e.g. Racetrack Playa, Death Valley), but unknown in low-elevation equatorial regions.

Ephemeral freezing during cold seasons and at equatorial latitudes during the early Permian implies either (1) substantial elevation to achieve freezing temperatures or (2) markedly cooler equatorial conditions than exist today, or even during the last glacial maximum (LGM). Persistent freezing —and even glacial— conditions exist in the tropics today (down to ~4500 m; Porter, 2001) and expanded during the LGM (to ~3500 m, or rarely to as low as 2100-2400 m in high-precipitation regions; Kaser and Osmaston 2002; Hastenrath, 2009). Variscan Mountain paleoelevations remain debated (see Appendix III), but recent investigations (e.g. Rabin et al. 2015; Pfeifer et al., 2018) indicate that the highest elevations in the southern Massif Central (ca. 308 Ma) were ~2500 m. Subsequent (308 – 295 Ma) extensional subsidence-to-gravity collapse (Menard and Molnar, 1988) resulted in an estimated mean elevation of the Lodève Basin during deposition of the Usclas Formation (ca. 295 Ma) of ~1500 m (Appendix III).

Given moderate-to-low elevations (≤ 1500 m), seasonal freezing in the Usclas Formation calls for cooler tropical conditions than most models consider for low-latitude Pangea. LPIA climate simulation of peak icehouse conditions show that $pCO_2$ <150 ppm under a cold summer orbit could produce equatorial MAT of 0-10°C, consistent with upland glaciation (Feulner, 2017), and thus ephemeral freezing at lower elevations. Furthermore, Soreghan et al. (2019) suggested that frequent and widespread explosive volcanism in central-western Europe (at low-latitude) ca. 300 Ma may have intensified or sustained cool temperatures, even as $pCO_2$ began to rise. Evidence in support of coeval volcanism is found in the Usclas Formation at this locality: Mudstone beds containing the impressions have illite-rich clay mineral compositions (Michel, 2009), potentially consistent with a component of distal volcanic ash, and they also occur directly below crystalline, tuffaceous units (Fig. 1).

Average tropical air temperatures (25°C) and lapse rates (-6.7°C/km) from the LGM (e.g. Loomis et al., 2017) could not produce even ephemeral freezing at < 2 km elevation (Fig. 4). However, either (a) temperatures averaging ~5°C cooler than the LGM, with an LGM lapse rate (Fig. 4a) or (b) LGM-temperatures with a dry tropical lapse rate (-9.8°C/km; MacLennan et al., 2020; Fig. 4b) are both consistent with ephemeral freezing at < 2 km elevation. Under a "Pangea B" configuration for 300 Ma (Fig. 1; Kent and Muttoni, 2018) the extreme continentality of the Lodève Basin would magnify seasonality, potentially enabling a drier (steeper) lapse rate (Fig. 4b). The climatic forcing(s) necessary to impact tropical precipitation patterns and promote anomalously cold conditions in equatorial Pangea remain poorly understood (Heavens et al., 2015). To date, examples of ice-crystal traces in the low-latitude geological record date exclusively from the upper Carboniferous – lower Permian (Table 1), calling for exploration of a potentially widespread phenomenon that has long been overlooked owing to the seeming improbability of freezing conditions at equatorial latitudes during the Phanerozoic.

## CONCLUSIONS

Laboratory analyses empirically reproduce sediment impressions left by freezing of water-saturated mud and corroborate the interpretation that morphologically identical features from the lower Permian Usclas Formation (Lodève Basin, France) represent ice-crystal traces. Evidence for films of ice on the paleoshoreline of a low-latitude lake record ephemeral freezing in equatorial Pangea during peak icehouse conditions (LPIA). Given the relatively low elevation (< 2 km) of the Lodève Basin during this time, these conditions require either cold tropical temperatures (~5°C cooler than those of the Last Glacial Maximum) and/or lapse rates that exceeded those of the Last Glacial Maximum. The forcing(s) necessary to promote cold climate conditions in equatorial Pangea remain enigmatic, but the extreme continentality of the Lodève Basin as portrayed by Pangea B would have magnified strong seasonality. This work reinforces the presently sparse—yet temporally unique—recognition of low-latitude ice traces in the Phanerozoic (exclusively upper Paleozoic) record and calls for further investigation of evidence for anomalously cold equatorial temperatures, and explanations thereof.

## ACKNOWLEDGMENTS

This research was supported by the U.S. National Science Foundation: NSF IRES Grant No. 1658614 (G.S. Soreghan, M.J. Soreghan) and NSF Grant No. 1338331 (G.S. Soreghan). Thanks to L. Alaniz, J. Mueller, J. Langston, S. Huntsman, E. Simpson, V. Smith, and K. Yeager for field assistance, L. Hunt, A. Roche, and Z. Tomlinson for microprobe sample preparation and analysis, and M. Elwood-Madden, P. Getty, N. Heavens, J. Obrist-Farner, F. Oboh-Ikuenobe, M. Soreghan, J. Trop, C. Ver Straeten, and S. Voigt for discussions.

**Supplemental Material.** Provided in dissertation section “Supplemental Material for Ch. III”.

## FIGURES AND TABLES

**Table 1.** Summary of existing interpretations of ice crystal trace markings (modern - ancient). See Fig. 3 for photos and references. Paleolatitudes are approximate, converted from modern latitudes using the paleogeography of Torsvik et al. (2012; paleolatitude.org).

| Time | Location | Paleo-lat | Paleo-alt | Substrate | Bed | Citation | App. III |
|---|---|---|---|---|---|---|---|
| Modern | Germany | 49.8 | SL | mud | | Hänzschel, 1935 | |
| Modern | Illinois, US | 41.5 | 500' | loess | | Udden, 1918 | A |
| Modern | Northeast US | 42.3 | SL | clay | | Shaler-W., 1896 | |
| Modern | NW Idaho, US | 46.7 | 1800' | loess | | Mark, 1932 | |
| Modern | Tidal bay, CA | 47.3 | SL | sand - mud | | Dionne, 1985 | |
| Pleistocene | Utah, US | 40.2 | 4200' | fine sands | surface | Mark, 1932 | DE |
| U. Cretaceous | South Dakota, US | 46.7 | SL | silt - clay | surface | Udden, 1918 | |
| U. Cretaceous | Texas, US | 33.8 | SL | lime - clay | surface | Udden, 1918 | HI |
| M. Permian | New Mexico, US | 9.2 | SL | limestone | surface | Lang, 1937 | G |
| L. Permian | Germany | 3.9 | ~ 1000' | silt - clay | surface | Reineck, 1955 | |
| L. Carboniferous | De L'aïr, Niger | -50 | < 1000' | mud-silt | surface | Lang et al., 1991 | L |
| U. Devonian | New York, US | -33 | SL | sand - mud | base | Clarke, 1917 | |
| U. Ordovician | Libya | -62 | < 1000' | mud | surface | Girard et al., 2015 | K |
| U. Ordovician | Morocco | -80 | < 1000' | sandy mud | surface | Nutz et al., 2013 | J |

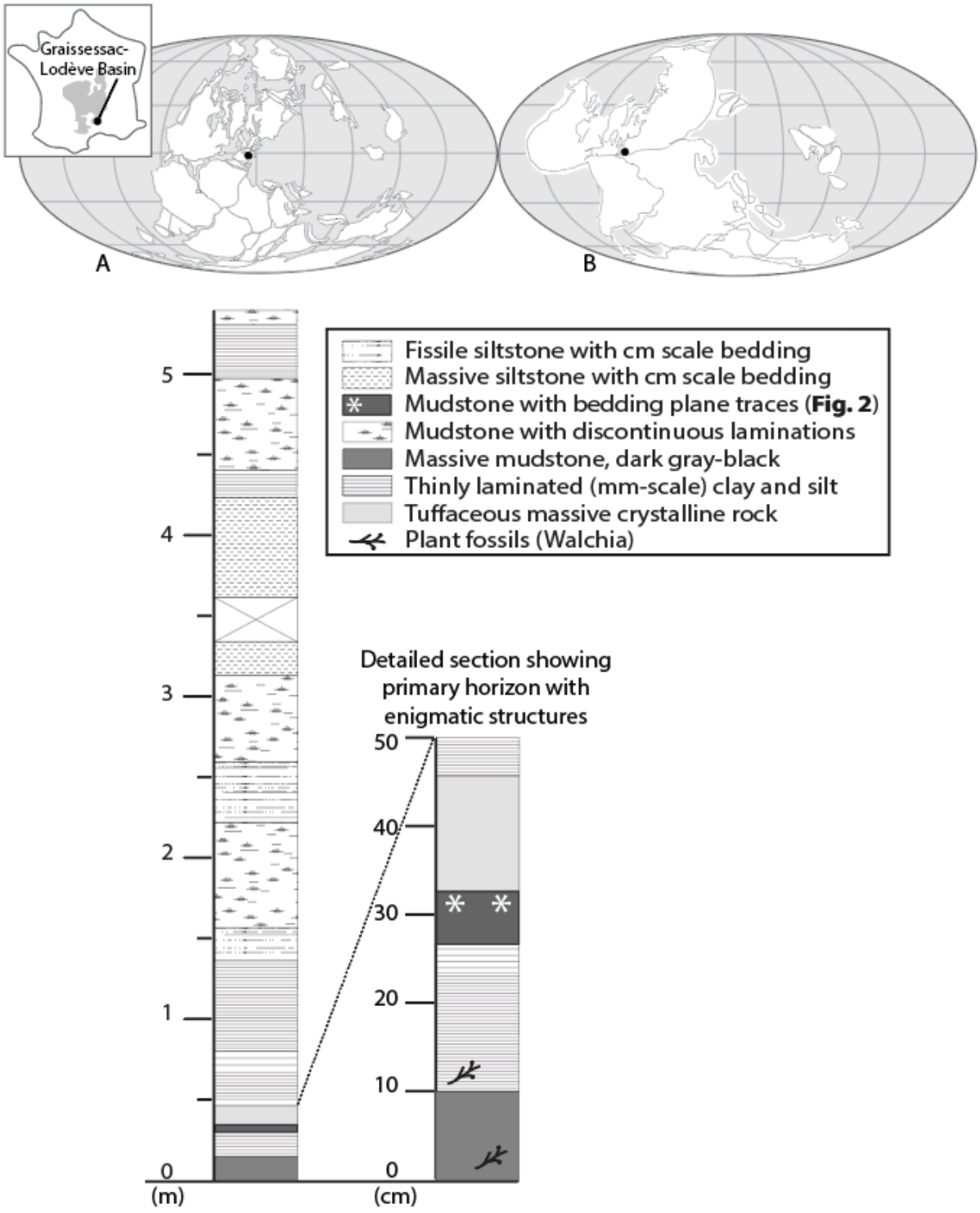


**Figure 1.** *Upper:* Early Permian (~290 Ma) paleogeographic reconstructions of (A) Domeier and Torsvik (2014) and (B) Kent and Muttoni (2018), Pangea B. Black circles show the equatorial location of the Graissessac-Lodève Basin (south-central France) ~0-2°S (A) to 0-2°N (B). The proximity to the PaleoTethys Sea varies substantially. *Lower:* Stratigraphic section (concatenation of three exposures) of the Usclas Formation, Lodève Basin. The detailed log on the right shows the first 0.5 meters at cm-scale resolution where most of the features are found.

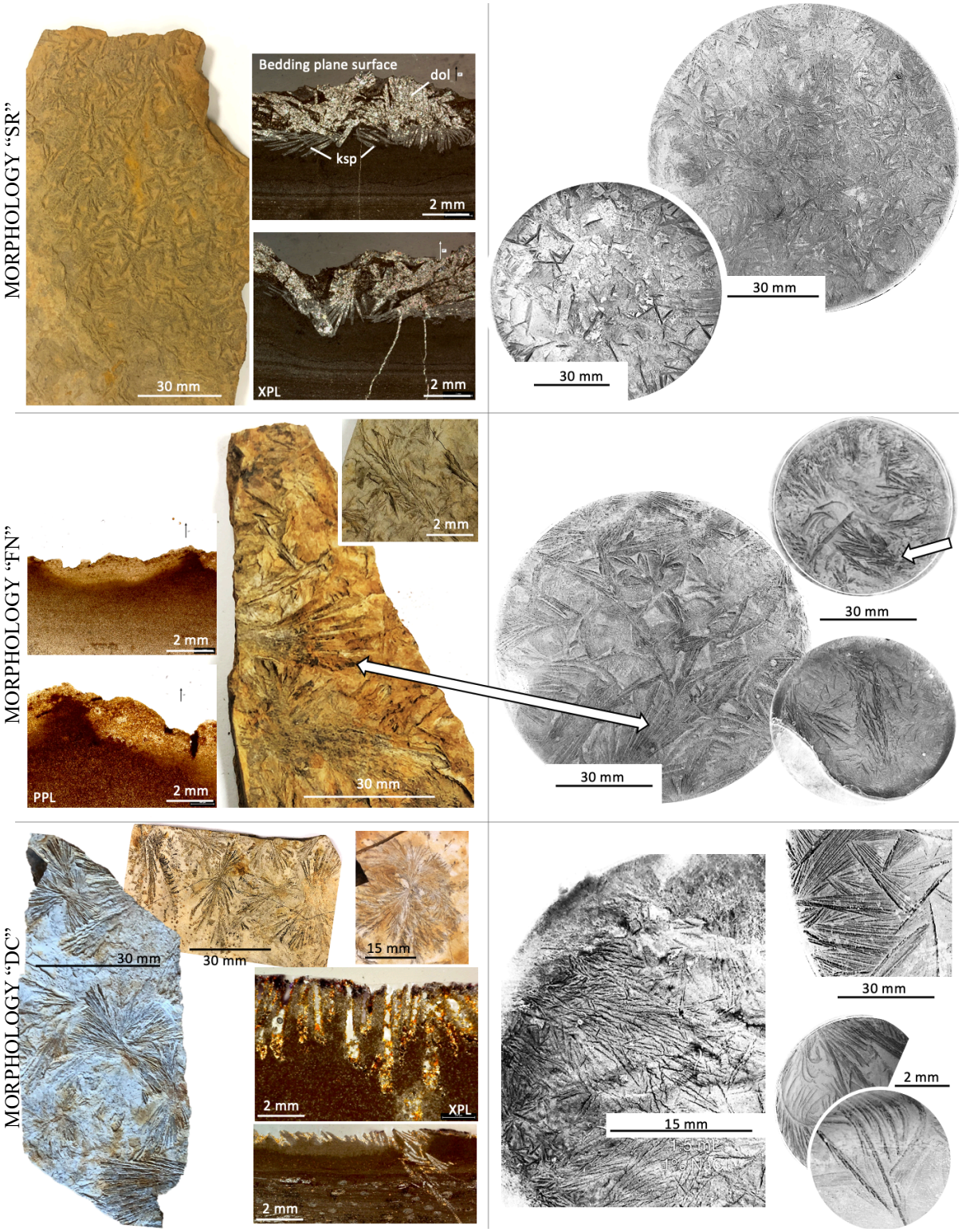


**Figure 2.** Summary of morphologic characteristics of features from the Usclas Formation *(left)* adjacent to examples from experimental results *(right)* that replicate features in each morphology, respectively.

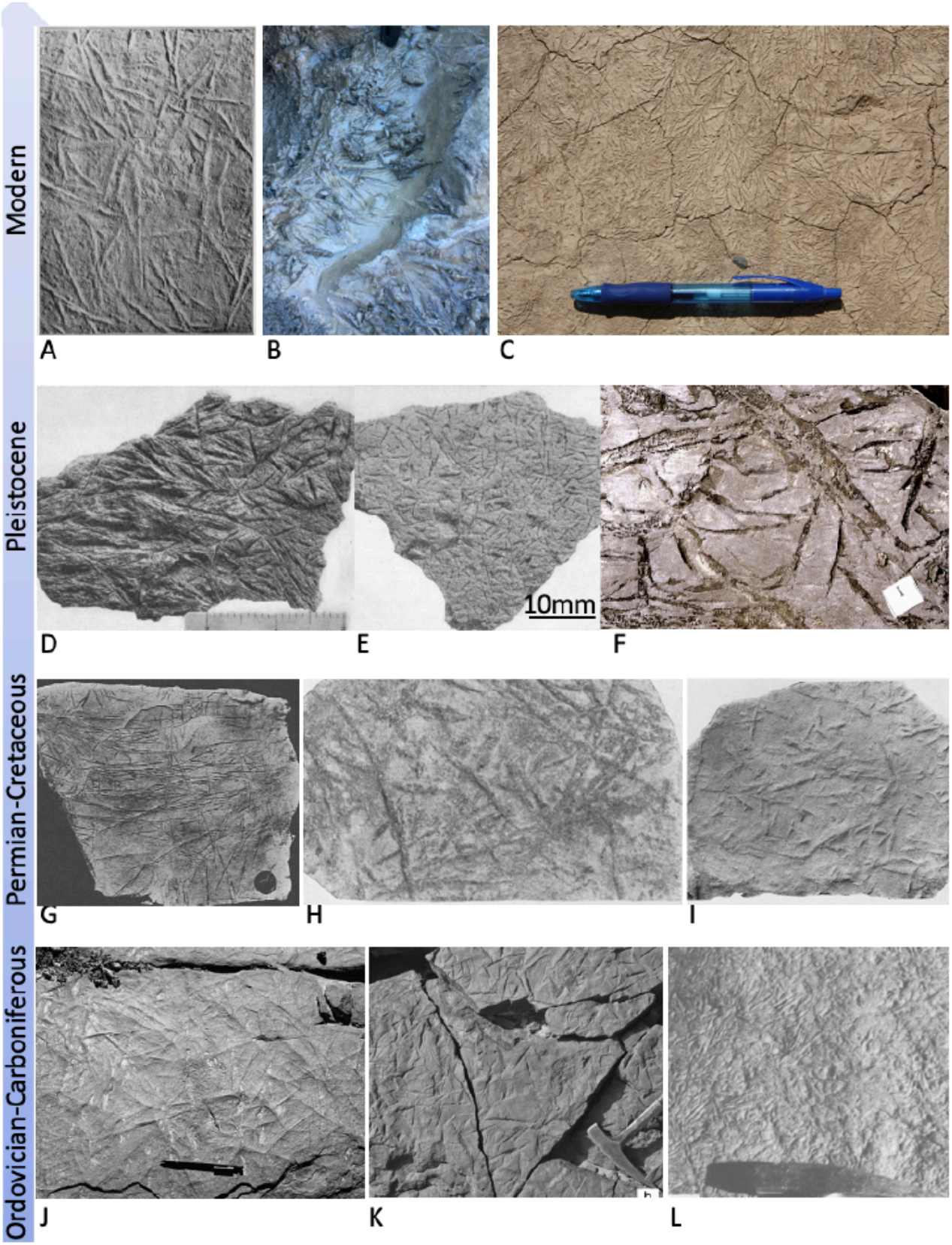
Modern
Pleistocene
Permian-Cretaceous
Ordovician-Carboniferous
A
B
C
D
E
10mm
F
G
H
I
J
K
L

**Figure 3** ***(previous page).*** Select photos through geologic time from the literature of markings interpreted as ice crystals (see also: Table 1). Photo descriptions in order as follows: (A) Modern, casts of ice crystals in loess, IL, U.S. (Udden, 1918), (B) Modern, in mud, Svalbaard (Photo by G.S. Soreghan), (C) Modern, in high-altitude playa lake, western Argentina (Photo by G.S. Soreghan), (D-E) Late Pleistocene, in fine sands, UT, U.S. (from Mark, 1932), (F) Pleistocene, reticulate-chaotic cryostructures in ice-rich, lake-bottom muds (from French and Shur, 2010), (G) Middle-Permian, in Carlsbad limestone, Guadalupe Mts., U.S. (from Lang, 1937), (H-I) Upper Cretaceous, in Eagleford limestone – clays, TX, U.S. (from Udden, 1918), (J) Upper Ordovician, in sand-mud, Morocco (from Nutz et al., 2013), (K) Upper Ordovician, in mud, Libya (from Girard et al., 2015), (L) Lower Carboniferous, in mud-silt, De L'aïr, Niger (from Lang et al., 1991).

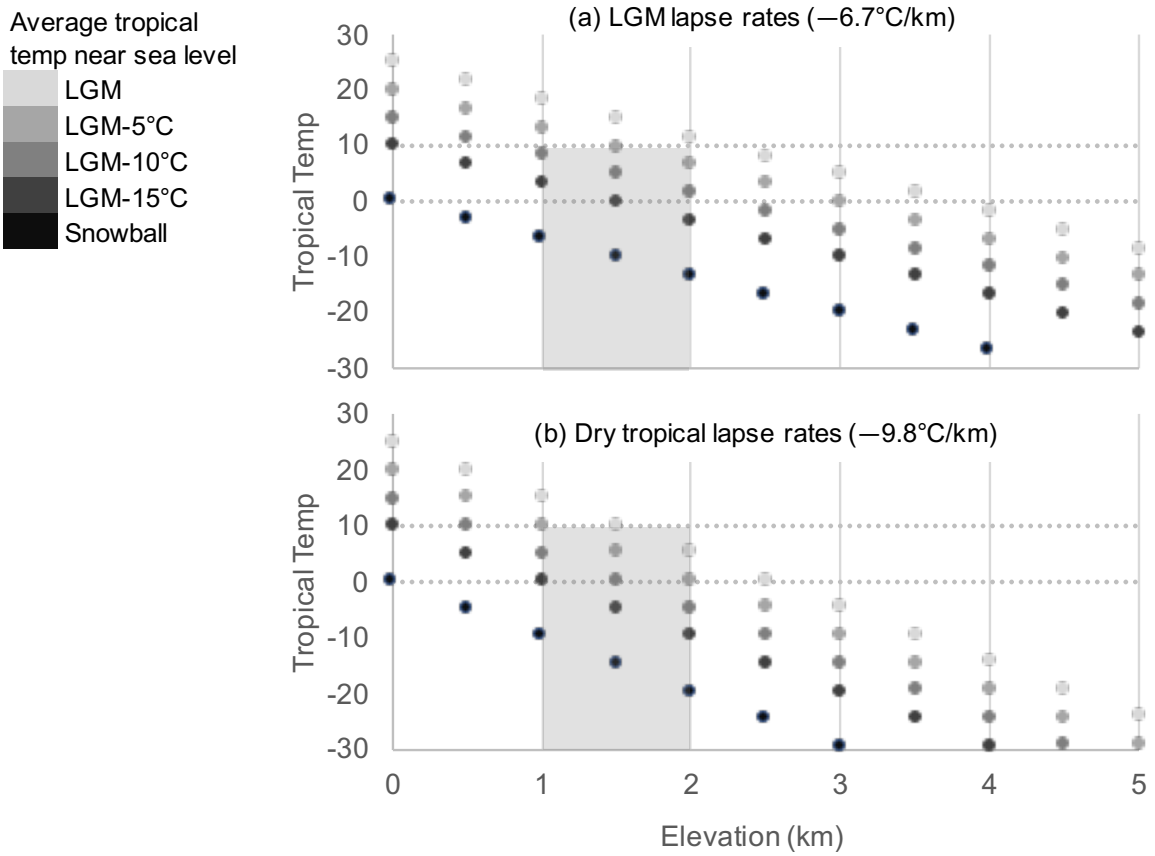


**Figure 4.** Plots of possible tropical temperature conditions in the Permian at different elevations using (a) the same adiabatic lapse rate as the LGM (-6.7°C/km; Loomis et al., 2017) and (b) a "dry" tropical lapse rate (-9.8°C/km; MacLennan et al., 2020). The grey zone represents possible paleoelevations (within error) of the Lodève Basin ca. 295 Ma during Usclas Formation deposition (see discussion in text). Average tropical temperatures near sea level range from LGM temperatures (lightest grey) to 15°C cooler than LGM (darkest grey). LGM-15°C is the coolest end of the range of estimates proposed by Soreghan et al., 2014a (0-15°C cooler than LGM) to have ~1000 m glacial conditions in western equatorial Pangea. The dotted horizontal lines represent average equatorial MAT (0-10°C) that could support upland glaciation in low-latitude Pangea (Feulner et al., 2017).

## REFERENCES CITED


Allan, J.A., 1926, Ice Crystal Markings: The American Journal of Science, ser. 5, v. 11, p. 494-500.

Barns, R. L., and Laudise, R. A., 1985, Size and perfection of crystals in lake ice. Journal of Crystal Growth, v. 71, n. 1, p. 104–110. https://doi.org/10.1016/0022-0248(85)90049-1

Becq-Giraudon, J.-F. and Van Den Driessche, J., 1994, Dépôts périglaciaires dans le Stephano-Autunien du Massif Central, Comptes Rendus de l'Académie Des Sciences, v. 318, n. 6, p. 675.

Becq-Giraudon, J.-F., Montenat, C., and Van Den Driessche, J., 1996, Hercynian high-altitude phenomena in the French Massif Central: tectonic implications, Palaeogeography, Palaeoclimatology, Palaeoecology, v. 122, p. 227–241.

Benison, K.C., and Bowen, B.B., 2013, Extreme sulfur-cycling in acid brine lake environments of Western Australia, Chemical Geology, v. 351, p. 154–167. https://doi.org/10.1016/j.chemgeo.2013.05.018

Burg J.P., Van Den Driessche J., and Brun J.P., 1994, Syn-to post-thickening extension in the Variscan Belt of Western Europe: modes and structural consequences, Comptes Rendus de l'Academie des Sciences Paris, v. 319, p. 1019-1032.

Clarke, J.M., 1918, Strand and Undertow Markings of Upper Devonian Time as Indications of the Prevailing climate, New York State Museum Bulletin, p. 199–210.

Dionne, J.C., 1985, Formes, figures et facies sédimentaires glaciels des estrans vaseux des régions froids, Palaeogeography, Palaeoclimatology, Palaeoecology, v. 51, p. 415–451.

Domeier, M., and Torsvik, T.H., 2014, Plate tectonics in the late Paleozoic, Geoscience Frontiers, v. 5, p. 303–350. http://doi.org/10.1016/j.gsf.2014.01.002anddomain=pdf.

Feulner, G., 2017, Formation of most of our coal brought Earth close to global glaciation: Proceedings of the National Academy of Sciences of the United States of America, v. 26, p. 1–5, https://doi .org/10.1073/pnas.1712062114.

Fielding, C.R., Frank, T.D., Isbell, J.L., 2008, The Late Paleozoic Ice Age—a Review of Current Understanding and Synthesis of Global Climate Patterns. In: Fielding, C.R., Frank, T.D., Isbell, J.L. (Eds.), Geological Society of America Special Papers, v. 441, p. 343–354.

French, H., and Shur, Y., 2010, The principles of cryostratigraphy. Earth-Science Reviews, v. 101, n. 3–4, p. 190–206. https://doi.org/10.1016/j.earscirev.2010.04.002

Girard, F., Ghienne, J., Du-bernard, X., and Rubino, J., 2015, Sedimentary imprints of former ice-sheet margins : Insights from an end-Ordovician archive (SW Libya), Earth Science Reviews, v. 148, p. 259–289. https://doi.org/10.1016/j.earscirev.2015.06.006

Hall, J., 1843, The survey of the fourth geological district, Geology of New-York, Part IV.

Hänzschel, W., 1935, Recent ice crystals in marine sediments and fossil traces of ice crystals, Senckenbergiana, v. 17, p. 151-177.

Hastenrath, S., 2009, Past glaciation in the tropics, Quaternary Science Reviews, v. 28, p. 790-798.

Heavens, N.G., Mahowald, N.M., Soreghan, G.S., Soreghan, M.J., and Shields, C.A., 2012, Glacial- interglacial variability in tropical Pangaean precipitation during the late Paleozoic ice age: simulations with the Community Climate System Model. Climate of the Past Discussions, v. 8, n. 3, p. 1915–1972, doi:10.5194/cpd-8-1915-2012.

Heavens, N.G., Mahowald, N.M., Soreghan, G.S., Soreghan, M.J., and Shields, C.A., 2015, A model-based evaluation of tropical climate in Pangaea during the late Palaeozoic icehouse.

Palaeogeography, Palaeoclimatology, Palaeoecology, v. 425, p. 109–127. https://doi.org/10.1016/j.palaeo.2015.02.024
Julien, A., 1895, Ancien glaciers de la période houillère dans le plateau central de la France, Ann. Club Alp. Fr., v. 21, p. 1–28.
Kaser, G., and Osmaston, H., 2002, Tropical Glaciers, Cambridge University Press.
Kent, D.V., and Muttoni, G., 2018, Pangea B and the Late Paleozoic Ice Age, Palaeogeography, Palaeoclimatology, Palaeoecology, https://doi.org/10.1016/j.palaeo.2020.109753
Lang, P.J., Dijon, M., Yahaya, M., El Hamet, M.O., and Besombes, J.C.M., 1991, Depots glaciaires du Carbonifere inferieur a l'Ouest de l'Air (Niger). Geologische Rundschau, v. 80, n. 3, p. 611–622.
Lang, W.B., 1937, The Permian Formations of the Pecos Valley of New Mexico and Texas, Bulletin of the American Association of Petroleum Geologists, v. 21, n. 7, p. 833–898.
Loomis, S.E., Russell, J.M., Verschuren, D., Morrill, C., Cort, G. De, Damsté, J.S. S., Olago, D., Eggermont, H., Street-perrott, F.A., Kelly, M.A., 2017, The tropical lapse rate steepened during the Last Glacial Maximum, Science Advances, v. 3, p. 1–8.
Maclennan, S.A., Eddy, M.P., Merschat, A.J., Mehra, A.K., Crockford, P.W., Maloof, A.C., Southworth, C.S., and Schoene, B., 2020, Geologic evidence for an icehouse Earth before the Sturtian global glaciation, Science Advances, v. 6, p. 1–6.
Magee, J.W., 1991, Late quaternary lacustrine, groundwater, aeolian and pedogenic gypsum in the Prungle Lakes, southeastern Australia. Palaeogeography, Palaeoclimatology, Palaeoecology, v. 84, n. 1–4, p. 3–42. https://doi.org/10.1016/0031-0182(91)90033-N
Mark, W.D., 1932, Fossil Impressions of Ice Crystals in Lake Bonneville Beds, The Journal of Geology, v. 40, n. 2, p. 171–176.
Menard, G., and Molnar, P., 1988, Collapse of a Hercynian Tibetan Plateau into a late Palaeozoic European Basin and Range province, Nature, v. 334, p. 235–237.
Michel, L.A., 2009, Petrographic, petrologic, and isotopic study of paleosol carbonates from the permo-pennsylvanian Lodève Basin, France [Thesis].
Montenat, C., Dolle, P., 1986, Des traces de gel dans l'Autunien du Midi de la France? In: Coll. Paleozoique superieur continental, Lille, p. 51.
Nutz, A., Ghienne, J., and Storch, P., 2013, Circular, cryogenic structures from the hirnantian deglaciation sequence (Anti-Atlas, Morocco), Journal of Sedimentary Research, v. 83, p. 115–131. https://doi.org/10.2110/JSR.2013.11
Odin, B., 1986, Les formations permiennes, Autunien supérieur à Thuringienne, du ‘‘Bassin’’ de Lodève (Hérault, France): Stratigraphie, mineralogie, paleoenvironnements, correlations. Thèse, Université Aix-Marseille III, p. 392.
Pfeifer L.S., Soreghan, G.S., Pochat S., Van Den Driessche, J. and Thomson S.N., 2016-2018, Permian exhumation of the Montagne Noire core complex recorded in the Graissessac-Lodève Basin, France. Basin Research, v. 30, p. 1-14.
Pfeifer, L.S., Soreghan, G.S., Pochat, S., Van Den Driessche, J., 2020, Loess in eastern equatorial Pangea archives a dusty atmosphere and possible upland glaciation, Geological Society of America Bulletin, https://doi.org/10.1130/B35590.1.
Pochat, S. and Van Den Driessche, J., 2011, Filling sequence in Late Paleozoic continental basins: a chimera of climate change? A new light shed given by the Graissessac-Lodève basin, Palaeogeography, Palaeoclimatology, Palaeoecology, v. 302, p. 170–186.
Porter, S.C., 2001, Snowline depression in the tropics during the Last Glaciation, Quaternary Science Reviews, v. 20, p. 1067-1091.

Rabin, M., Trap, P., Carry, N., Fréville, K., Cenki-tok, B., Lobjoie, C., Goncalves, P., Marquer, D., 2015, Strain partitioning along the anatectic front in the Variscan Montagne Noire massif (southern French Massif Central), Tectonics, p. 1–27. https://doi.org/10.1002/2014TC003790.Received

Reineck, H.E., and Singh, I.B., 1980, Depositional sedimentary environments, Springer-Verlag, Berlin, p. 551.

Reineck, H.E., 1955, Marken, Spuren und Fährten in den Waderner Schichten (ro) bei Martinstein/Nahe. Neues Jb. Geol. Palaont. Abh, v. 101, p. 75-90.

Shaler, N.S., Woodworth, J.B., and Marbut, C.F., 1806, The glacial brick of Rhode Island and Sotheastern Massachusetts, 17th annual report, director US Geological Survey, p. 951.

Soreghan, G.S., Soreghan, M.J., Poulsen, C.J., Young, R.A., Eble, C.F., Sweet, D.E., and Davogustto, O.C., 2008a, Anomalous cold in the Pangaean tropics, Geology, v. 36, n. 8, p. 659–662. https://doi.org/10.1130/G24822A.1

Soreghan, G.S., Soreghan, M.J., and Hamilton, M.A., 2008b, Origin and significance of loess in late Paleozoic western Pangaea: A record of tropical cold?, Palaeogeography, Palaeoclimatology, Palaeoecology, v. 268, p. 234–259, doi: 10.1016/j.palaeo.2008.03.050

Soreghan, G.S., Sweet, D.E., and Heavens, N.G., 2014a, Upland glaciation in tropical Pangaea: Geologic evidence and implications for Late Paleozoic climate modeling, Journal of Geology, v. 122, p. 137-163.

Soreghan, M.J., Heavens, N., Soreghan, G.S., Link, P.K., Hamilton, M.A., 2014b, High resolution record of Permian atmospheric circulation changes inferred from geochemical, magnetic, and sedimentologic indicators in the Maroon formation, Geological Society of America Bulletin, v. 126, n. 3-4, p. 569–584.

Soreghan, G.S., Soreghan, M.J., Heavens, N.G., 2019, Explosive volcanism as a key driver of the late Paleozoic ice age. Geology, 47 (7), 1–5.

Udden, J.A., 1918, Fossil Ice Crystals, University of Texas Bulletin, n. 1821, p. 3–39

CHAPTER IV

# ACTIVATION OF THE MULTICONTEXT MODEL IN A FIELD-BASED PROGRAM FOR TRADITIONALLY UNDERSERVED STUDENTS



Citation:
*Pfeifer, L.S., Soreghan, M.J., Feille, K., Soreghan, G.S., Weissmann, G.S., Ibarra, R.A., and Stroud, W.A. (2020). Activation of the Multicontext model in a field-based program for traditionally underserved students, Journal of Geoscience Education, doi: 10.1080/10899995.2020.1838850.*

# ACTIVATION OF THE MULTICONTEXT MODEL IN A FIELD-BASED PROGRAM FOR TRADITIONALLY UNDERSERVED STUDENTS


## ABSTRACT

This paper presents results from our multi-year NSF-IRES program: a four-week, field-based summer program involving the participation and mentorship of U.S. undergraduate geoscience cohorts to develop knowledge and skills in sedimentary geology while immersed in an international research collaboration. Student participants in our program are predominantly first-generation college students, largely from historically underrepresented groups in STEM, and most have a "high context" orientation. Academic culture (especially in STEM) tends to favor the "low-context" approach of scientific inquiry (task-oriented, linear, individuated), but many students bring different cultural values from personal or community-based experiences that tend to be higher-context (process-oriented, systems-thinking, integrated). Herein we discuss how activating a Multicontext model—one that recognizes and includes a broader spectrum of "knowing and doing" (Ibarra, 2001; Weissmann et al., 2019)—resulted in measurable advances, especially for higher-context students, from the first to second year of the program in terms of self-efficacy in field and analytical competencies, as well as in student engagement. To balance cultural frameworks (Chávez and Longerbeam, 2016), specific implementations in the field curriculum included (1) a non-linear, learning cycle-structured orientation prior to fieldwork that clearly introduces research objectives early, and promotes scientific inquiry and peer-to-peer interaction, (2) frequent discussions during fieldwork to place low-context tasks such as making field measurements into a broader context, and (3) a pre-defined mini-project option that allows students to set an individual intent for growth as a scientist in this experience. Leaders of similar programs to NSF IRES that support undergraduate students from underrepresented groups in STEM research might enhance program quality, student engagement, and inclusivity by recognizing and adapting to a broader spectrum of culturally-based learning perspectives. This study represents a small segment within the Multicontext system for redefining and expanding diversity and inclusion—a theory that has broad implications for the entirety of academic culture.


### Purpose and learning goals

At all degree levels, the geosciences remain the least diverse of all STEM fields, with almost no change in number of geoscience PhDs attained by Native American and Black (non-Hispanic) minorities in over 40 years (Bernard and Cooperdock, 2018; Dutt, 2020). Weissmann et al. (2019), Chávez and Longerbeam (2016), and Ibarra (1999, 2001) describe how activation of Multicontext Theory can broaden academic (and geoscience) culture to create an inclusive environment that values a *spectrum* of cultural strengths for all students. Participants in our month-long, summer field program (NSF-IRES) are students from racial/ethnic minority groups, low socioeconomic status, and/or are non-traditional students, and mostly have a "high context" orientation (discussed below). We applied a Multicontext model to instructional sequence design in the second year of the program as an intervention to evaluate whether action taken to recognize a broader spectrum of context orientation could positively impact the participating student cohort. Success of this adjustment is defined by measurable advances in student self-efficacy for all program participants. This paper presents a comparison of student survey

responses and auxiliary qualitative data from the first and second field seasons (FS1 and FS2, respectively) in order to evaluate how adjustments in instructional sequence design affected student engagement and self-efficacy. Our results suggest that adopting this approach could make a significant positive difference in analogous programs.

## Literature context

### *The Multicontext Theory*

Both the challenges of science education in underrepresented communities, and in turn, the low numbers of underrepresented people in STEM fields relate largely to the incompatibility between traditional science cultures and cultures of underrepresented groups (Aikenhead, 1996, 1997; Murray, 1997; Riggs, 1998; Riggs and Semken, 2001; Semken and Morgan, 1997; Wolfe and Riggs, 2017). As the numbers of minority populations grow and scholarship programs for underrepresented groups in geoscience are more available, this cultural dichotomy becomes increasingly apparent. Educational research has shown a continued motivation to find ways to *"make teaching and learning relevant and responsive to the languages, literacies, and cultural practices of students across categories of difference and (in)equality"* (Paris, 2012 p. 93, and references therein), but academic culture is slow to adapt. Hall (1959, 1966, 1976) defined the *cultural context* of people from different backgrounds along a spectrum according to the way they prefer to approach, interpret and perceive information according to family or community influences. The defining characteristics of high (HC) vs. low (LC) context are summarized in Table 1. Academic culture (especially in STEM) favors the "low-context" approach of scientific inquiry as articulated by Weissmann et al. (2019), Ibarra (1999, 2001), and others (Chávez and Longerbeam, 2016; Halverson, 1993), but many students (e.g. women and underrepresented minority populations) bring different cultural values from personal or community-based experiences that tend to be higher-context (Chávez and Longerbeam, 2016; Hall, 1959, 1966, 1976; Ibarra, 2001). Low-context cultures tend to be task-oriented, apply linear thought processes, and compartmentalize information, whereas high-context cultures tend to be process-oriented, think in terms of systems, and value information in a broader context and with integrated topics. Low-context cultures require less social context to interact and interpret the world than high-context cultures (Hall, 1976). Though they are termed "low" and "high," both are equally valued and valid (and complimentary) approaches to understanding and interacting with the world and should not be used to stereotype (Weissmann et al., 2019). Furthermore, Ibarra (2001) recognized that despite an inclination for either end of the context spectrum, individuals often have the flexibility to act across the spectrum situationally or through time.

The Multicontext Theory has broad implications for redefining and expanding diversity and inclusion within the entire *system* of prevailing academic culture in the United States (see Weissmann et al., 2019), but this paper specifically emphasizes the impact of balanced cultural frameworks for teaching effectively at a "classroom level" in the specific academic community of geoscience. Chávez and Longerbeam (2016) described how teaching and learning relationships are embedded in culture and noted methods for teaching on a continuum, from individuated (LC) to integrated (HC) world views, in order to engage the cultural strengths of all learners. To teach with a mixed, Multicontexted framework—one that recognizes, embraces, and *includes* a broader spectrum of "knowing and doing" (Ibarra, 2001; Weissmann et al., 2019)—enriches learning, fosters a sense of belonging (Moore, 2020), provides more equal opportunities

for all students to thrive in academia, and creates a more well-rounded and dynamic workforce in STEM.

### *A note about field education as Multicontexted potential*

Many have recognized that field experiences in geoscience are more effective at helping students to understand concepts than classroom-based courses (e.g. Boyle et al., 2007; Feig et al., 2019; Orion and Hofstein, 1994; Riggs et al., 2009; Stokes and Boyle, 2009; Thrift, 1975; Waldron et al., 2016; Whitmeyer et al., 2009) but the measurements of educational benefits are difficult to quantify. Streule and Craig (2016) and Kortz et al. (2019) attributed the value of field education in the context of the social framework it provides: one where students develop independent thinking skills, versatility, and self-efficacy. Mogk and Goodwin (2012) posited that it is the immersive nature of learning in the field that allows it to be so effective, and similarly, Elkins and Elkins (2007) suggested the social novelty of the field setting motivates student learning. However, it is important to consider that inaccessibility, unfamiliarity, or unappealing perceptions of fieldwork conditions and logistics introduce barriers for many (O'Connell and Holmes, 2011; Sherman-Morris and McNeal, 2016). Integration of field-based training, for example, in small liberal arts courses (e.g. Knapp et al., 2006) or Earth science education programs designed for adult learners in Indigenous communities (e.g. Riggs, 2005; Semken and Morgan, 1997), has shown to be broadly impactful when appropriately applied for the student population.

Compton (2016; p. 1) posited that "*field studies are founded on three kinds of information*": (1) Objective data: simple, straightforward facts from direct observation and measurement, (2) Interpretive data: founded on perception and experience, where genetic insight clarifies a host of interrelated data, and (3) Age relations: organizing facts and interpretations into an order of events. Note the symmetry of factual (detailed, operational, observational, literal) and philosophical (interpretive, interrelated, contexted, imaginative) data: A *Multicontext* unity. There is space in the field for students across the spectrum to practice their strengths, and it requires flexibility to adapt to their non-preferred context (high context learners must be meticulous about detailed descriptions and data acquisition; low context learners must be able to interconnect past environments and depositional systems). Field education can be taught with a very low-context approach, but education in the field setting has already presented us with an ideal potential for balanced cultural frameworks in teaching—We just have to activate it.

## Study population and setting

*Landscapes of Deep Time in the Red Earth of France* (NSF International Research Experience for Students) is a four-week**,** field-based summer program that aims to mentor U.S. undergraduate science students from underserved populations in geological research. Planned as a three-year project, it involves recruitment of a new undergraduate cohort for each season and includes a stipend in addition to full financial support (for travel and living expenses). The program is designed to mentor students in developing basic skillsets (e.g. sedimentologic field techniques and analyses) while being exposed to an interdisciplinary research collaboration and international cultural experience. Initially, recruitment was focused on Native American populations in Oklahoma, but we found local recruitment state-wide to be a challenge owing to the narrow applicant pool and the cultural burden of international travel requiring an extended

period of time away from home (e.g. family and tribal obligations). Native American students are the least likely group to attend college or participate in study abroad programs (Field, 2016; Wanger et al., 2012) owing to a desire for support systems that recognize and align values with those of their families and communities (Guillory, 2009; HeavyRunner and DeCelles, 2002). Due to the low response rate from local Native American communities, the recruitment and participation of students expanded nationwide through advertising with the Geoscience Alliance, GeoForce, and other geoscience society forums (e.g. Geological Society of America, American Geophysical Union, NSF Research Experiences for Undergraduate students, Earth Science Women's Network, American Indian Science and Engineering Society). The FS1 and FS2 student cohorts (Table 2; n=4 per summer, n=8 total) were composed of undergraduates (rising juniors and seniors) pursuing a B.S. or B.A. in geoscience (or natural resources) where 7/8 were first-generation college students, 7/8 were women, 6/8 were Native American, Hispanic, or African American, and about half were also either non-traditional students in the sense of age, sexual orientation, or parental status. Students originated from a wide range of rural, suburban, and urban communities. According to the cultural context inventory (Halverson, 1993), the majority (5/8) were high-context-preferred, and the others were low-context-preferred (as assessed at the beginning of the field season). Academic ranks varied, but most (6/8) students were rising seniors. Previous backgrounds in relevant coursework, undergraduate research or field experience varied considerably by student (ranging from training at large universities with formal geoscience majors to smaller colleges or tribal schools with integrated environmental programs), and slightly by cohort (with FS2 students being slightly more experienced on average upon entry).

**Materials and implementation: Activation of the Multicontext Theory**

Instructional sequences (Fig. 1) were developed prior to two separate four-week field seasons of the IRES program (FS1 and FS2 respectively). The FS1 curriculum was designed with little focus paid to learning philosophies and in retrospect, the pedagogical goals and itinerary preferentially served low-context ways of learning and doing. The program orientation was lecture heavy and sequentially ordered from detailed descriptions of field methods to big-picture, contextual talks presented mid-way through the program (after substantial fieldwork). The majority of the field work curriculum for FS1 involved students conducting detailed, unimodal data collection (e.g. measuring stratigraphic section) with linear analysis of the data (e.g. building stratigraphic profiles) and little integration of multiple datasets.

The aim of our program (structured according to NSF IRES objectives) is twofold—Aside from the education and pedagogy aspect (to attract underrepresented students to STEM), there is a significant component of conducting geological research and collecting new and publishable data to answer questions about ancient climates. Given that (1) our fieldwork takes place internationally with complicated logistics and limited resources, (2) aside from teaching, we had to acquire a large amount of data in a brief time, and (3) our student cohorts did not belong to any one underrepresented demographic (Table 2), it was not possible to adjust the FS2 curriculum design to include elements proven effective for specific cultures (e.g. for Indigenous populations: place-based curricula in traditional homelands, integration of Indigenous knowledge, explicit involvement of Indigenous leaders/educators; Johnson et al., 2014; Murray, 1997; Riggs, 2005; Riggs and Semken, 2001; Semken and Morgan, 1997; Semken, 2005; Semken et al., 2017; Unsworth et al., 2012; Wildcat, 2018). Instead, we focused on a strategy to

recognize and include a broad spectrum of culturally-based learning approaches. Guidance for building a Multicontextual classroom (Chávez and Longerbeam, 2016; Ibarra, 2001; Weissmann et al., 2019; Table 1) heavily influenced the revision of the instructional sequence from FS1 to FS2.

The framework for the FS2 instructional sequence (Fig. 1) started with a one-week mixed lecture and application orientation structured according to the BSCS (Biological Science Curriculum Study) 5E Instructional Model (Bybee and Landes, 1990; Bybee et al., 2006). Our decision to rely on the framework of the 5E *learning-cycle* approach for FS2 is grounded in theoretical foundations which veer from traditional teaching methodologies and emphasize the development and application of student-centered lessons (Abraham, 1997; Duran and Duran, 2004). While traditional pedagogical approaches stress the progression of skills towards a pre-determined outcome, learning cycles are based on "constructivist-learning"—emphasizing the investigation of phenomena and use of evidence to support conclusions (Abraham, 1997; Duran and Duran, 2004). There are more opportunities in the 5E learning cycle approach for students to self-reflect, redefine and elaborate, and interact with peers to solve problems (Bybee, 1997). It is more of a non-linear systems approach that holds a greater emphasis on integrated ideas and applications: A traditionally high-context cultural value. The 5E Model consists of five stages (Engage, Explore, Explain, Elaborate, and Evaluate) in which students formulate a better understanding of scientific processes and skills based on first-hand experiences (Açışlı et al., 2011; Newby, 2004). The *Engage* phase is meant for the instructor to assess and connect to prior knowledge and introduce a new concept through the use of short activities that stimulate curiosity. In *Explore*, a common experience is provided so that the students can apply prior knowledge to generate new ideas and begin investigation. In the *Explanation* phase, students are given the opportunity to demonstrate their conceptual understanding and the instructor corrects misconceptions before moving onto *Elaboration* wherein students have an opportunity to apply their understanding of the concept to a different situation or activity. Finally, in *Evaluate,* students are encouraged to assess their understanding and abilities to complete a final exercise or activity that allows the instructor to evaluate student progress overall. Figures 1-2 detail specific lectures and activities included in each of the 5E steps for FS2 orientation. This model provides shared experiences (e.g. workbooks with exercises to compliment lectures, card-sort activities, sketching, journaling) that place application before theory (HC-preferred; Table 1). Lectures are ordered from overarching research questions to basic concepts and field skills (opposite of FS1, as requested in FS1 student feedback; Table 5) and are completed before the start of work in the field. This way, students gain awareness of relevant background knowledge and major research questions *prior* to beginning field work, enabling all *new* data and information—first-hand experiences in the field—to be evaluated in a broader context (HC-preferred; Table 1).

After the 5E-structured orientation, it is important to continue integration of the Multicontext model in field pedagogy. Skills and concepts taught in the field are coupled with discussion (and frequent review) to specify the contribution of the process or data to the overarching research questions. For example, "we are doing this [low-context activity] today, but with integration of [other datasets] it relates to the broader context by addressing [this primary research question]." This way, data collection—which tends to be repetitive, detailed, low-context work—is *able* to be perceived in a more process-oriented, relevant, and interconnected way (HC-preferred; Table 1). Furthermore, additional equipment (e.g. Gigapan for outcrop imaging and lithostratigraphic correlation, portable DinoLite microscope for hand sample and thin section analysis, drafting software; Fig. 2) and data from FS1 (e.g. thin sections,

geochemical data) are available for students to pursue an *optional* predefined individual "mini-project." This added an element to FS2 for students to interpret and integrate multiple data sets (e.g. stratigraphy and magnetic susceptibility), opening doors for systems thinking and analysis (HC-preferred; Table 1).

**Evaluation**

Students did not receive course credit or grades for their participation in the IRES program, so while exam performance is the quantitative standard for evaluating student success in academic environments, here we focus on the quantitative measurement of gains in student self-confidence through exposure to the change in curriculum from FS1 to FS2. The social cognitive theory investigates how perceived self-efficacy affects human action and thought. From Bandura (1986, p. 367-368*): "Self-efficacy scales do not measure skill; they measure what people believe they can do under varied circumstances, whatever skills they possess, or the particular skills required by the task… Judgements of operative self-efficacy are concerned not with the skills one has, but with beliefs about what one can do with the sub skills one possesses in dealing with continuously changing realities, most of which contain ambiguous, unpredictable, and stressful elements."*

Student participants each summer (FS1 and FS2) completed identical surveys that served as pre and post measures of self-efficacy and a culminating attitudinal survey to evaluate the quality of the overall program. The questions and structure did not change between FS1 to FS2. The surveys were developed by the authors prior to the first field season and were administered by the same instructor on the mornings of the first and last days of the program. No time limit was enforced for completing the survey; with both the survey questions and follow-up short answer questions, the typical student took about one hour to complete the survey. The identical pre and post survey includes ~12 items (Table 3) designed to measure development of self-efficacy in research applications and content knowledge (e.g. understanding of past climates, sedimentological skillsets). For each item, students self-rank their level of confidence (1-3 from highest to lowest) in each concept or skill. The attitudinal survey—taken only at the conclusion of each field season (at the same time as the post-survey above)—asks students to rate ~10 aspects of the program on a scale 0-3 from lowest to highest quality (Table 3). Quantitative data from surveys (Table 3) were analyzed in R Studio using paired t-tests, and t-tests to assess differences between two populations (Table 4).

In addition to the surveys described above, qualitative data sources include (1) instructor logs from informal, weekly reflections (group share) and (2) short-answer responses at the end of pre- and post-surveys (described above). The informal, weekly reflections were held as a group (all students and mentors) and were meant to encourage self-reflection and career development discussion. The students were asked to reflect on their experience weekly through journaling, but sharing was optional. Participant responses during informal reflections were transcribed by the instructor and unitized into unique data pieces. A constant comparative approach (Glaser, 1965) was used to identify key themes in areas of program improvement (from a student perspective). Select data units that exemplified this theme are summarized in Table 5 for each field season. Each (pre- and post-survey) includes six short answer questions: Most are intended to obtain background (e.g., coursework or motivation to participate in the program) or general career goal (e.g., intent to apply to grad school) information. However, two of the open-ended questions prompted responses from the FS2-student cohort that were characteristic in nature according to

their context inventory (selected for summary in Table 6). Students in FS2 took the cultural context inventory survey (Halverson, 1993) at the beginning of the season to document preferred context and associated work ethic/learning behaviors, and students in FS1 were asked to complete it retroactively. All survey instruments are accessible in the Supplemental Materials.

## Results

Student participants in the NSF IRES program are from racial/ethnic minority groups, low socioeconomic status, and/or are non-traditional students, and are primarily high context-preferred learners (Table 2). In the final attitudinal survey (Table 3), students rated the overall quality of the program higher in FS2 (mean 28) than in FS1 (mean 26). Findings from the pre-to-post self-rated assessments suggest that student participation in the program, regardless of year or cultural context, resulted in advancement of student confidence in research application, independent field work, and their ability to contribute to science (Table 3; all but one student show positive gains from the beginning to end of the field season). As shown in Table 4*a,* this overall positive gain in pre-to-post survey scores (mean +7.5) for all students (n=8) both years, is statistically significant ($p << 0.05$). Within this group, HC (n=5) and LC (n=3) students each improved (~+7.0; Table 4*b*-*c*) by insignificant ($p = 0.07$-$0.08$) gains, but there is no statistical difference ($p = 0.94$) in the mean gain between context groups overall.

Establishing significance is not possible with analysis by distinct year *and* context orientation due to small sample sizes, but the improvements are still quantitatively measurable. For example, the pre-to-post difference in mean scores (+3.0) for all students from FS1 (n=4) to FS2 (n=4) indicates self-rated improvement overall in FS2, though not by a statistically significant margin ($p = 0.50$; Table 4*d*-*e*). However, if we isolate the data to examine only those students who tested as high context, the increase in mean pre-to-post-survey gains (+7.3) from FS1 (n=3) to FS2 (n=2) is closer to being statistically significant ($p = 0.24$; Table 4*f*-*g*), but not quite due to the small numbers of students. In contrast, students who tested as low context at the beginning of the field season saw a minor decline in mean pre-to-post gains (-4.0) from FS1 (n=1) to FS2 (n=2), but it is not possible to assess significance with only one student in FS1 (Table 4*h*-*i*).

Key themes in qualitative data are identified and reported in Tables 5-6. Table 5 summarizes areas for program improvement (from a student perspective) that influenced changes in instructional sequence design for each subsequent field season. Table 6 summarizes open-ended responses (from FS2 only) to select questions from the pre- and post-survey that demonstrate the expected nature of student participants as predicted by their context inventory.

## Discussion

The Multicontext Theory does not suggest that one way of knowing and doing (high or low context) is better than the other. However, because academia (and especially STEM) traditionally favors low context approaches, the objective for FS2 was to integrate more aspects into the instructional design that are typically high-context-favorable (see Table 1), especially given the demographic of the students in the program. We consider that the overall success of the program is defined by the ability to have *all* participating students improve by quantifiable (pre-to-post survey) margins *and* to observe qualitative behaviors that demonstrate a connection and engagement to the work. In this discussion, we will first review components of the FS2

Multicontext model, and the data (quantitative and qualitative) that largely support its positive impact. Then we will assess other factors that possibly contributed to the change in student experience from FS1 to FS2.

Student participation in the program *in general* results in measurable and significant advances in student self-efficacy (Table 4*a*), but to assess the impact of Multicontext activation in curriculum design in FS2 (with the particular objective of being more inclusive of higher-context modes), we must analyze the results by year and by preferred context orientation. From FS1 to FS2 we see an increase in the pre-to-post survey margin (+3.0; Table 4*d*-*e*) of self-assessed student confidence (e.g. in relevant skills/competencies, research application, independent field work, scientific thinking) and in the student-rated overall quality of the program. Despite the inability to determine statistical significance due to small sample size, substantial gains in student self-efficacy from FS1 to FS2 were reported by higher-context students (+7.3; Table 4*f*-*g*) while lower-context students reported a slight decline (-4.0; Table 4*h*-*i*). Based on these data and observations, we interpret that FS1 was more supportive of low-context students, and that activation of a Multicontext approach in FS2 (Fig. 1) resulted in a more inclusive environment, especially for higher-context students.

Observationally, there was a stark contrast between FS1 and FS2 in individual student level of focus and engagement through the field season. FS1 student feedback (Table 5) suggested a lack of clarity around how their work fit into the broader research questions. It is likely that instruction of content and skills without a broader context (e.g. how/where data collected in the field would eventually be applied) resulted in a potentially challenging and unsupportive learning environment, especially for higher-context students. Balancing across cultural frameworks (Chávez and Longerbeam, 2016; Weissmann et al., 2019) in the instructional design for FS2 (Fig. 1) resulted in improved student engagement. Defining research objectives *early* (week one pre-field 5E-structured orientation) and revisiting them often (discussing *how* data collected throughout the field season fits into broader research questions) resulted in a strong understanding of the purpose of the research before beginning work in the field. During the 5E orientation, high-context students were particularly animated and tended to lead the group in activities like the card sort (Fig. 2), not just because it was "active" but because it involved systems thinking about how detailed observations (sedimentary structures) were produced in different systems (depositional environments) and speculation about contextually significant implications (regional climate). For example, while lower-context students focused on assigning the correct name and paleocurrent direction to each feature, higher-context students would ask questions like: "*Why can't this feature belong to both fluvial and glacial systems?"* and *"Why can't this feature indicate paleoflow going in multiple different directions?"* The answer to both being that they can! It is a perfect example of how in science there is "no one right answer"— but there is also no single "right" way of *thinking*. It is hard to determine how the prevailing role of higher-context students in these scenarios impacted the learning environment for lower-context students: But it did seem to positively influence lower-context students to consider alternative solutions (usually further outside of the textbook definitions). The option to have ownership of individual projects/products, access to equipment, and continued mentorship associated with evening (after-field) work also fostered a better overall student connection to the research in FS2 by allowing them to take direction in their learning experience.

Survey responses from FS2 (Table 6) characterize the typical or expected nature of student behavior as predicted by their context inventory. Lower-context students were very goal-

specific and product-focused—almost disappointed if they did not fully complete the assembly of a poster presentation during their time (Table 6; row 4, 8, col 2)—whereas higher-context students had intentions to absorb diversified aspects of the entire system (and consider all the data) rather than being limited to an individual project. Lower-context students excelled at data collection, drawing upon an inherent inclination to metrics and detail, whereas higher-context students struggled to maintain focus during these activities, but asked relevant and impactful questions such as *"Why did we choose this locality?"* and *"What does this feature mean about the climate at the time of deposition?"* Questions, group discussions, and student-lead initiatives to conduct literature reviews and practice petrography skills (with the DinoLite microscope) showed a level of interest and engagement in and out of the field that was not apparent in FS1. The quality and quantity of work produced by students during FS2 was impressive. Three students (a mix of higher- and lower-context) continued work on individual research projects after their return from the field program and have presented at undergraduate research symposia (at their home institutions) as well as at Geological Society of America conferences (Birkett et al., 2020; Mueller et al., 2020).

The development of a positive or negative team chemistry was also a driving element in the overall learning experience in regard to student level of focus and engagement. It is possible that activation of a Multicontext approach reduced competition and individuation, cultivating a more integrated student cohort in FS2. On the other hand, an initially more cohesive cohort in FS2 could have also contributed to the margin of improvement over FS1 (effectively minimizing the importance of the change in instructional approach). In FS1, an abrupt shift from excitement and euphoria to arguments and alienation among student participants occurred in the second week. This shift, known as "forming" to "storming" according to Tuckman's small group dynamics hypothesis (Tuckman, 1965, Tuckman and Jensen, 1977), negatively impacted the learning environment and contributed to a degradation in student engagement despite its intangibility. Integration and discussion of personality assessment data (Myers-Briggs; Briggs, 1987) at the beginning of the field season, coupled with a more naturally-cohesive cohort, generally resulted in a more positive team dynamic and sustained engagement. The personality assessment included a brief discussion on context orientation, but it would be interesting to elaborate on cultural context and the Multicontext model at the beginning of FS3 to see if there is an influence on group dynamic with improved comprehension of self and teammate tendencies in respect to the cultural context spectrum. With work like this that involves small-group collaboration in a field context where different personalities are forced to work closely and interact both in a working *and* living space, we can expect that student focus and engagement will be affected in part by team chemistry and dynamic.

Additional factors that potentially influence the improvement from FS1 to FS2 include: (1) the varied academic background of students upon entering the program. However, the FS2 cohort had more previous experience in geoscience-specific courses and experiences, so this is likely *not* a driving factor, as we would expect to see *smaller* pre-to-post assessment gains in FS2 than in FS1. Also, note that the mean total self-assessed pre-score for FS1 and FS2 match (Table 4*d*-*e*). (2) Another factor could be adaptability (e.g. culturally or intense fieldwork) that was covert. These aspects could have varied with time—by individual or by group—and may have influenced some assessment responses as well. Finally, (3) as noted above, the field setting is inherently underlain by Multicontexted potential.

## Limitations

Some of the most valued intentions of this experience are inherently difficult to measure (e.g., improved understanding of the scientific process, a stimulated passion to pursue a STEM career, student interest/engagement), especially with the limitations of a particularly small and diverse sample size (four students annually). A more robust sample set in terms of number of students and number of survey questions may have changed or enhanced the significance of results. Additionally, several variables are difficult to control (e.g. the impact of small group dynamic, changes in the applicant pool or recruitment/selection procedures, varying levels of prior experience by student). Finally, the data are acquired through means of self-reporting so it is subjective, and we are limited to discussion about improvements in self-efficacy. To obtain a more direct read of student skill acquisition or concept retention, an objective method of measurement is required (e.g. formal exams or demonstrations in the field), but likely not possible for this program given the lack of formal grading or option to obtain coursework credit. All of these potential limitations should be considered in the interpretation of results and in planning for the final field season (FS3).

## Implications and future study

This study is only one example of how a short field-based program like IRES can benefit from a broadened spectrum of context teaching frameworks. Future plans include continued implementation of the Multicontext model for the final season of the NSF IRES program (FS3) to assess whether results are reproducible with a different group and/or location. Pre- and post-survey formats will be preserved to keep data comparable between successive field seasons. Changes will include expanding on the informal reflections, lunch discussions, and integration of "mini lectures" into the field day. The integration of mini in-field lectures for brief skillset review (e.g. map-reading) is based on FS2 student feedback (Table 5) and serves as an opportunity to continue tying the selection of field locations and data collection plans back to broader context research questions (as discussed in FS2). Students in FS3 will complete the same context inventory survey (Halverson, 1993), as well as a more comprehensive scaled Context Diversity matrix developed by Ibarra *(pers. commun. 2019).* An introduction to the Multicontext Theory will be shared with the students at the beginning of the field season so they can begin to recognize when they are engaged in higher- or lower-contexted work. We are interested to (1) test which (if either) of the context inventory tests is more insightful, and (2) observe the fluidity of student context orientation over the four-week timeframe. We expect that if the students have some awareness of the Multicontext model, and where tasks fit on the spectrum, we will observe shifts over the course of the field season in their context-inventory results, indicating their adaptability to use both perspectives in comprehension and application.

## Conclusions

Programs (like NSF IRES) that support undergraduate students from historically underrepresented groups in international STEM research might find more success in student engagement when leaders and instructors recognize and activate the Multicontexted culture of their research group. With heavy (international) travel logistics, a different student cohort each year, and a relatively short field season, it is challenging to assess context orientation, manage

interpersonal group dynamics, and provide students a meaningful educational experience that is well-balanced with productive data collection. We found it important to fuse typical (by definition) "high" and "low" (integrated and individuated) context teaching frameworks because students may shift higher or lower on the spectrum situationally or through time, and the ultimate goal is to create *Multi*contextual thinkers (both low and high context are equally as important, but the full spectrum must be valued).

Separate cohorts for the first two years of our program are mostly first-generation college students from historically underrepresented groups in STEM, and most are "high context"-preferred learners. From FS1 to FS2, there are measurable improvements in student self-efficacy overall (e.g. in concept comprehension, field/analytical competencies, research application), but they are dominantly reported by high-context students. Associated with these quantitative (survey-derived) gains, observational transformations into FS2 include a higher quality of work, and a positive, productive and integrated group dynamic that we interpret to reflect higher levels of student engagement and inclusion as scientists. These improvements (quantitative and qualitative) can be attributed partially to the shift from an FS1 low context-preferred instructional framework to a more balanced, Multicontexted culture in FS2. The FS2 instructional sequence includes (1) a mixed lecture-application 5E-structured orientation prior to fieldwork that clearly introduces the broad research objectives early, (2) frequent discussions during fieldwork to place low-context tasks in a broader context (e.g. explain how the current dataset will be integrated with other information and ultimately impact major research questions) and (3) a pre-defined mini-project *option* that allowed students to set an individual intent for growth in this experience (e.g. integrating multiple datasets to focus on a single idea vs. applying diversified field methods to contribute to several ideas). Weissmann et al. (2019, p. 7) stated that *"activation of the Multicontexted approach requires systemic, institutional cultural change by broadening values to be inclusive of high contexted approaches."* Within the Multicontext *system*—a theory that has broad implications for the entirety of academic culture—this study represents a small segment of how *awareness* of the Multicontext Theory as an instructor, coupled with relatively minor adjustments to balance across cultural frameworks in teaching, results in a more inclusive environment for students to apply their individual strengths and cultural context to effect an enhanced learning experience.

## ACKNOWLEDGMENTS

This chapter is derived from an article published in Journal of Geoscience Education, 2020, copyright National Association of Geoscience Teachers (NAGT). This work was supported by the National Science Foundation under International Research Experiences for Students (IRES) grant No. 1658614 (G.S. Soreghan, M.J. Soreghan) and National Science Foundation grant No. 1338331 (G.S. Soreghan). Additional support was provided by the Eberly Family Chair in Geosciences at the University of Oklahoma (G.S. Soreghan). Thanks to NSF IRES student participants (2018 and 2019) and M. Powell for review and assistance with statistical analysis. Thanks to reviewers (A. Aitken, M. Moore, M. Powell, and others) and editors at JGE for their assistance improving this work. University of Oklahoma Office of Human Research Participant Protection/Institutional Review Board (IRB No. 9330).

**Supplemental Material.** Provided in dissertation section "Supplemental Material for Ch. IV". Also available in the data repository for the publication (through JGE).

## FIGURES AND TABLES

**Table 1.** Summary of high context (HC) and low context (LC) cultural values modified from Weissmann et al. (2019), Chávez and Longerbeam (2016), and Ibarra (2001).

| **Thinking style** | |
|---|---|
| LC | HC |
| Information compartmentalized/possibly separate from contex | Information only meaningful when evaluated in context with integrated topics |
| Examination of isolated ideas valued over real world applicatio | Real world application of knowledge valued over examination of isolated ideas |
| Linear thinking and analysis | Interconnected (nonlinear) systems thinking and analysis |
| Interact using direct communication and fact | Interact using indirect communication and embellishment of fact |
| Task oriented (success evaluated on completion of task) | Process oriented (success evaluated on how well group conducted work) |
| Time - emphasis on schedules, timelines, deadlines | Time - Time may not fit in a specific schedule; deadlines are flexible |
| Space - personal property is shared less | Space - personal property is shared more |
| | |
| **Teaching style** | |
| LC | HC |
| Individual | Social context |
| Isolated components and their attributes | Systems, relationships and connections |
| Less interactive | Interactive |
| Teacher-oriented | Student-oriented |
| Theory before application | Application before theory |
| Multiple choice | Open-ended, place-based |
| Small to big picture: Understand concept and process first then determine how findings fit into context. | Big to small picture: Understand purpose first; concepts without context are challenging. |

**Table 2.** Context inventory survey results (Halverson, 1993; Supplemental Materials) and corresponding demographic information for students in FS1 and FS2. The exact student number on this table does not correspond with the exact student numbers in Table 3: Given the small sample size, numbers were shuffled for confidentiality on demographic information.

| | HC/LC | First gen/low income | Native American, Hispanic, Black | Female | Other (LGBTQ, parent status, Age) | FS |
|---|---|---|---|---|---|---|
| Student 1 | Low | x | | x | | FS1 |
| Student 2 | High | x | x | x | x | FS1 |
| Student 3 | High | x | x | x | x | FS1 |
| Student 4 | High | x | x | x | x | FS1 |
| Student 5 | Low | x | | | x | FS2 |
| Student 6 | High | x | x | x | | FS2 |
| Student 7 | High | x | x | x | | FS2 |
| Student 8 | Low | | x | x | | FS2 |

**Table 3** ***(next page).*** Raw data from pre-post and attitudinal assessments (Supplemental Materials). Questions from each survey are provided at the bottom of the table. Total Pre and Total Post is the score total per student for the whole assessment. The score for each question on the pre-post assessment is between 1-3 where 1 indicates highest confidence (1= yes, I understand this sufficiently so that I can do or explain this independently, 2= I can follow this in class or when I have an example but am confused when I work on my own, and 3= I recognize what this is referring to, but I don't understand or know how to do it). The score for each question on the attitudinal survey (comprehensive program evaluation) is between 0-3 where 3 indicates the highest rating (3= Excellent/very satisfied, 2= Very good/satisfied, 1= Average/neutral, and 0= Below average/dissatisfied).

| | | | Pre-Post self-rated assessment | | | Attitudinal Survey |
|---|---|---|---|---|---|---|
| Student ID | Year | Context | Total Pre | Total Post | Gains (Pre-Post) | Total Score |
| Student 1 | FS1 | High | 27 | 16 | 11 | 25 |
| Student 2 | FS1 | Low | 23 | 13 | 10 | 26 |
| Student 3 | FS1 | High | 19 | 12 | 7 | 25 |
| Student 4 | FS1 | High | 16 | 20 | -4 | 28 |
| Student 5 | FS2 | High | 27 | 13 | 14 | 30 |
| Student 6 | FS2 | Low | 15 | 12 | 3 | 30 |
| Student 7 | FS2 | High | 22 | 12 | 10 | 28 |
| Student 8 | FS2 | Low | 21 | 12 | 9 | 23 |

Pre-Post self-rated assessment questions *(n=12)*

Defining what a sedimentary basin is and why we're interested in studying one
Understanding of what the continents looked like 250 million years ago.
Understanding of global icehouse vs. greenhouse paleoclimate conditions.
Ability to use a Jacob's staff to measure and record a stratigraphic section.
Ability to thoroughly describe and identify sedimentary rocks in outcrop
Ability to identify sed structures in outcrop and hypothesize about formation.
Understanding/IDing sediment transport mechanisms + associated structures
Ability to hypothesize about sed transport/depositional environs based on obs
Confidence in formulating several hypotheses based on observations
Confidence in developing a methodical scientific approach to testing hypothese
Ability to integrate mult. datasets to make well-supported interpretations
Conducting independent geological fieldwork.

Attitudinal survey questions: Program evaluation *(n=10)*

This international REU program was well organized as a whole.
The international component of program added value to scientific experience.
I would recommend this program to others.
I would recommend my mentor(s) for future projects.
The value of your project to your future graduate school or professional career
Information presented during orientation (workbooks, evening lecture series)
The program in providing a broader view of what geoscience is
The program in providing you with skillsets that make you more confident in field
The program in helping you understand uncertainty and interpretation in science
Your acceptance into the research group as a contributing member

**Table 4.** Summary of pre-post self-rated assessment (Supplemental Materials) statistical analysis. Shaded cells indicate where gains are statistically significant.

| | | Year | Context | Total Pre | Total Post | Gains (Pre-Post) | | P-value* |
|---|---|---|---|---|---|---|---|---|
| *a* | Mean *(n=8)* | All | All | 21.3 | 13.8 | 7.5 | | < 0.01 |
| *b* | Mean *(n=5)* | All | High | 22.2 | 14.6 | 7.6 | | 0.07 |
| *c* | Mean *(n=3)* | All | Low | 19.7 | 12.3 | 7.3 | | 0.08 |
| | *Signif. of gains FS1 to FS2* | | | | | | Difference | P-value** |
| *d* | Mean *(n=4)* | FS1 | All | 21.3 | 15.3 | 6.0 | | |
| *e* | Mean *(n=4)* | FS2 | All | 21.3 | 12.3 | 9.0 | 3.0 | 0.50 |
| | *Signif. of gains FS1 to FS2, HC vs. LC* | | | | | | Difference | P-value** |
| *f* | Mean *(n=3)* | FS1 | High | 20.7 | 16.0 | 4.7 | | |
| *g* | Mean *(n=2)* | FS2 | High | 24.5 | 12.5 | 12.0 | 7.3 | 0.24 |
| *h* | Single *(n=1)* | FS1 | Low | 23.0 | 13.0 | 10.0 | | |
| *i* | Mean *(n=2)* | FS2 | Low | 18.0 | 12.0 | 6.0 | -4.0 | N/A |

*using paired t-test

**using t-test

**Table 5.** Select student feedback from informal weekly reflections. These statements represent key themes regarding areas of improvement from a student perspective (by field season).

| ***FS1*** | ***FS2*** |
|---|---|
| *Evening lectures were a valuable part of the learning experience, but I wish they were given in reverse order.* | *Mini lectures every so often IN the field (e.g. map-reading) would be helpful.* |
| *Assigned readings of overview papers would've been helpful to prepare for the field season.* | *The onboarding series and order of lectures provided a good foundation prior to field work.* |
| *Big picture lectures would've provided a better foundation before fieldwork.* | |

**Table 6.** Open-ended survey responses from select questions on the pre-and post-assessments (Supplemental Materials) by context inventory (FS2 only).

| | | |
|---|---|---|
| "What are your goals?" (pre-assessment) vs. "Were your goals accomplished?" (post-assessment) | | |
| | *Pre-Assessment* | *Post-Assessment* |
| High | I want to become more prepared for my future career | Yes, I made a poster outline and learned about fieldwork in geology |
| High | Learn how to conduct paleoclimate research and field research skills | Yes, I learned how to complete geological fieldwork and use different techniques in formulating hypotheses and how to test them. |
| Low | I would like to learn more about the methodology of paleoclimatology to help decide between that and paleoecology | Yes, fully. |
| Low | I'd like to have a good experience in field research and interpretation so that I know what to expect in the future and feel comfortable to conduct fieldwork independently. | Yes, my main goal was to have a real research experience - field work, discussion, interpretation, written product. I am looking forward to continued work on my mini project at home and eventually presenting. |
| What do you like about science (e.g. fieldwork/research/sedimentology/paleoclimate) how would you rate your ability to think scientifically/work independent research projects? (pre vs. post assessments) | | |
| | *Pre-Assessment* | *Post-Assessment* |
| High | I think I understand research well and can think independently | I like the mystery and problem solving. I would rate my abilities at adequate but needs improvement. |
| High | I love that science is very methodological and the concepts are concrete but it can also be examined and reshaped. I love the interdisciplinary nature of science. | I had a great time doing fieldwork. I would rate my ability at a 8/10 |
| Low | I adore learning new things and science is the best way to do that; I am not sure how good I am, but I do work alone often. | I enjoy learning new things in a scientific process and in sed/paleoclimate I can understand the history of earth was like at the time. I would note that my ability to work independently is high. |
| Low | I like being able to interpret what happened in the past and then apply it to the future. I would say that I can think scientifically and work well independently. | I look at science as a "healthy challenge"—I can think very well scientifically and ask good questions. I am excited to pursue a small independent research project with guidance. |

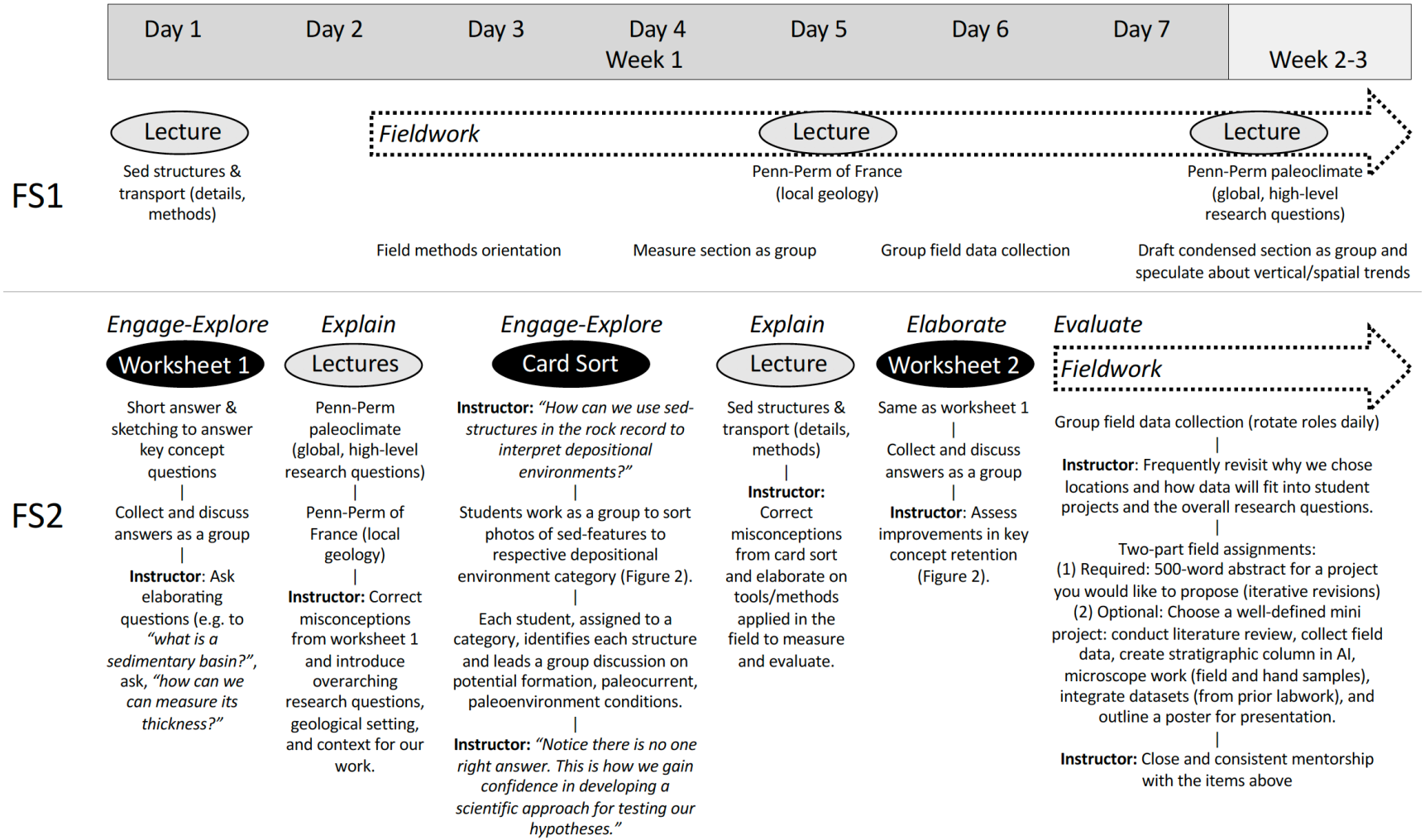
Day 1
Day 2
Day 3
Day 4
Week 1
Day 5
Day 6
Day 7
Week 2-3
FS1
Lecture
Sed structures & transport (details, methods)
Fieldwork
Lecture
Penn-Perm of France (local geology)
Lecture
Penn-Perm paleoclimate (global, high-level research questions)
Field methods orientation
Measure section as group
Group field data collection
Draft condensed section as group and speculate about vertical/spatial trends
FS2
Engage-Explore
Worksheet 1
Short answer & sketching to answer key concept questions
Collect and discuss answers as a group
Instructor: Ask elaborating questions (e.g. to "what is a sedimentary basin?", ask, "how can we can measure its thickness?"
Explain
Lectures
Penn-Perm paleoclimate (global, high-level research questions)
Penn-Perm of France (local geology)
Instructor: Correct misconceptions from worksheet 1 and introduce overarching research questions, geological setting, and context for our work.
Engage-Explore
Card Sort
Instructor: "How can we use sed-structures in the rock record to interpret depositional environments?"
Students work as a group to sort photos of sed-features to respective depositional environment category (Figure 2).
Each student, assigned to a category, identifies each structure and leads a group discussion on potential formation, paleocurrent, paleoenvironment conditions.
Instructor: "Notice there is no one right answer. This is how we gain confidence in developing a scientific approach for testing our hypotheses."
Explain
Lecture
Sed structures & transport (details, methods)
Instructor: Correct misconceptions from card sort and elaborate on tools/methods applied in the field to measure and evaluate.
Elaborate
Worksheet 2
Same as worksheet 1
Collect and discuss answers as a group
Instructor: Assess improvements in key concept retention (Figure 2).
Evaluate
Fieldwork
Group field data collection (rotate roles daily)
Instructor: Frequently revisit why we chose locations and how data will fit into student projects and the overall research questions.
Two-part field assignments:
(1) Required: 500-word abstract for a project you would like to propose (iterative revisions)
(2) Optional: Choose a well-defined mini project: conduct literature review, collect field data, create stratigraphic column in AI, microscope work (field and hand samples), integrate datasets (from prior labwork), and outline a poster for presentation.
Instructor: Close and consistent mentorship with the items above

**Figure 1** ***(previous page).*** Instructional sequences and corresponding timeline from FS1 *(top)* and FS2 *(bottom)*.


**Figure 2.** Photos display examples of elements implemented in FS2. *Top right:* Pre-to-post field season improvements in Pangea sketches from the Engage-Elaborate phases of 5E orientation. Bottom right: A card sort activity *"how can we use sedimentary structures in the rock record to interpret depositional environments?"* in the Explore-Explain phases of 5E orientation. *Left:* Examples of students using equipment in the field (Gigapan outcrop imaging) and at home (DinoLite microscope) to pursue individual projects.

## REFERENCES CITED


Abraham, M.R. 1997. The learning cycle approach to science instruction (Research matters - To the science teacher, No. 9701). Columbia, MO: The National Association for Research in Science Teaching.

Açışlı, S., Yalçın, S.A., Turgut, U. 2011. Effects of the 5E learning model on students' academic achievements in movement and force issues. Procedia - Social and Behavioral Sciences, 15, 2459–2462.

Aikenhead, G.S. 1996. Science education: Border crossing into the subculture of science. Studies in Science Education, 27, 1–52.

Aikenhead, G.S. 1997. Toward a First Nations cross-cultural science and technology curriculum. Science Education, 81 (2), 217–238.

Bandura, A. 1986. The explanatory and predictive scope of self-efficacy theory. Journal of social and clinical psychology, 4 (3), 359-373.

Bernard, R.E., Cooperdock, H.G. 2018. No progress on diversity in 40 years. Nature Geoscience, 11 (5), 292–295. doi:10.1038/s41561-018-0116-6.

Birkett, B.A., Pfeifer, L.S., Pochat, S., Van den Driessche, J., Soreghan, G.S., Soreghan, M.J. 2020. Hypothesized freezing in low-latitude lakes of the early Permian: Examples from the Usclas Formation, Graissessac-Lodéve Basin, France. Geological Society of America Abstracts with Programs.

Boyle, A., Maguire, S., Martin, A., Milsom, C., Nash, R., Rawlinson, S., Turner, A., Wurthmann, S., Conchie, S. 2007. Fieldwork is good: The student perception and the affective domain. Journal of Geography in Higher Education, 31: 299–317.

Briggs, K.C. 1987. Myers-Briggs type indicator. Form G. Palo Alto, Calif., Consulting Psychologists Press.

Bybee, R.W., Landes, N.M. 1990. Science for life and living: An elementary school science program from Biological Sciences Improvement Study (BSCS). The American Biology Teacher, 52 (2), 92-98.

Bybee, R.W. 1997. Achieving scientific literacy: From purposes to practices. Portsmouth, NH: Heinemann Publications.

Bybee, R.W., Taylor, J.A., Gardner A., Scotter, P.V., Powell, J.C., Westbrook, A. Landes, N. 2006. The BCBS 5E instructional model: origins and effectiveness. Office Of Science Education National Institutes Of Health. 1-80.

Chávez, A.F., Longerbeam, S.D. 2016. Teaching Across Cultural Strengths: A guide to balancing integrated and individuated cultural frameworks in college teaching, Stylus Press, Sterling VA, 241.

Compton, R.R. 2016. Geology in the Field. Earthspun Books. 1-2.

Dutt, K. 2020. Race and racism in the geosciences. Nature Geoscience. 13 (2–3), https://doi.org/10.1038/s41561-019-0519-z

Duran, L.B., Duran, E. 2004. The Science Education Review, 3 (2), 49-58.

Elkins, J.T., Elkins, N.M.L. 2007. Teaching Geology in the Field: Significant Geoscience Concept Gains in Entirely Field-based Introductory Geology Courses. Journal of Geoscience Education, 55 (2), 126–132.

Feig, A.D., Atchison, C.L., Stokes, A., Gilley, B. 2019. Achieving Inclusive Field-based Education: Results and Recommendations from an Accessible Geoscience Field Trip. Journal of the Scholarship of Teaching and Learning. 19 (2), 66-87.

Field, K. 2016. For native students, educations promise has long been broken: Chronicle of Higher Ed, 62 (41), 26.
Glaser, B. G. (1965). The constant comparative method of qualitative analysis. Social Problems, 12(4), 436--445. http://www.jstor.org/stable/798843
Guillory, R.M. 2009. American Indian/Alaska Native college student retention strategies. Journal of Developmental Education, 33, 12-19.
Hall, E.T. 1959. The silent language, Anchor books.
Hall, E.T. 1966. The Hidden dimension, Anchor books.
Hall, E.T. 1976. Beyond Culture, Anchor books.
Halverson, C.B. 1993. Cultural-context inventory: the effects of culture on behavior and work style, in Pfeiffer, JW (ed), The 1993 Annual: Developing Human Resources, San Diego, Pfeiffer and Company, 131-145.
HeavyRunner, I., DeCelles, R. 2002. Family Education Model: Meeting the student retention challenge. Journal of American Indian Education, 41 (2), 29-37.
Ibarra, R.A. 1999. Multicontextuality: A new perspective on minority underrepresentation in SEM academic fields. Making Strides, 1, 1–9.
Ibarra, R.A. 2001. Beyond Affirmative Action: Reframing the Context of Higher Education, University of Wisconsin Press, Madison, 323.
Johnson, A.N., Sievert, R., Durglo, M., Finley, V., Adams, L., Hofmann, M.H. 2014. Indigenous knowledge and geoscience on the flathead Indian reservation, northwest Montana: Implications for place-based and culturally congruent education. Journal of Geoscience Education, 62, 187-202.
Knapp, E.P., Greer, L., Connors, C.D., Harbor, D.J. 2006. Field-based Instruction as Part of a Balanced Geoscience Curriculum at Washington and Lee University, Journal of Geoscience Education, 54 (2), 103-108. doi: 10.5408/knappetal-v54p1.
Kortz, K.M., Cardace, D., Savage, B. 2020. Affective factors during field research that influence intention to persist in the geosciences, Journal of Geoscience Education, 68 (2), 133-151. doi:10.1080/10899995.2019.1652463
Mogk, D.W., Goodwin, C. 2012. Learning in the field: Synthesis of research on thinking and learning in the geosciences. In Kastens, K.A., Manduca, C.A., eds., Earth and mind II: A synthesis of research on thinking and learning in the geoscience. Geological Society of America Special Paper, 486: 131–163.
Moore, M.Z. 2020. Fostering a Sense of Belonging Using a Multicontext Approach. Journal of College Student Retention, 0 (0), 1-18. doi: 10.1177/1521025120944828
Mueller, J.M., Pfeifer, L.S., Soreghan, G.S., Soreghan, M.J. 2020. Identification of weakly develop paleosols in a Permian loess using micromorphology, geochemistry, and magnetic susceptibility. Geological Society of America Abstracts with Programs.
Murray, J.J. 1997. Ethnogeology and its implications for the aboriginal geoscience curriculum. Journal of Geoscience Education, 45, 117–122.
Newby, D.E. 2004. Using inquiry to connect young learners to science. http://www.nationalcharterschols.org/uploads/pdf/resource20040617125804using%20Inguiry.pdf (18.05.2008).
O'Connell, S., Holmes, A. 2011. Obstacles to the recruitment of minorities into the geosciences: A call to action. GSA Today, 21 (6), 52–53. https://doi.org/10.1130/G105GW.1
Orion, N., Hofstein, A. 1994. Factors that influence learning during a scientific field trip in a natural environment. Journal of Research in Science Teaching, 31 (10), 1097–1119.

Paris, D. 2012. Culturally Sustaining Pedagogy: A Needed Change in Stance, Terminology, and Practice. Educational Researcher, 41 (3), 93–97. doi: 10.3102/0013189X12441244
Riggs, E.M. 1998. Toward an understanding of the roles of scientific, traditional, and spiritual knowledge in our "demon-haunted world." American Indian Culture and Research Journal, 22, 213– 226.
Riggs, E.M., Semken, S.C. 2001. Earth science for Native Americans. Geotimes, 49 (9), 14 – 17.
Riggs, E.M. 2005. Field-Based Education and Indigenous Knowledge: Essential Components of Geoscience Education for Native American Communities. In: Krugly-Smolska, K., Taylor, P.C Culture and comparative studies.
Riggs, E.M., Lieder, C.C., Balliet, R. 2009. Geologic Problem Solving in the Field: Analysis of Field Navigation and Mapping by Advanced Undergraduates. Journal of Geoscience Education, 57 (1), 48-63.
Semken, S.C., Morgan, F. 1997. Navajo pedagogy and Earth systems. Journal of Geoscience Education, 45, 109– 112.
Semken, S.C. 2005. Sense of Place and Place-Based Introductory Geoscience Teaching for American Indian and Alaska Native Undergraduates, Journal of Geoscience Education, 53 (2), 149-157.
Semken, S.C., Ward, E.G., Moosavi, S., Chinn, P.W.U. 2017. Place-Based Education in Geoscience: Theory, Research, Practice, and Assessment. Journal of Geoscience Education, 65, 542–562.
Sherman-Morris, K., Mcneal, K.S. 2016. Understanding Perceptions of the Geosciences Among Minority and Nonminority Undergraduate Students. Journal of Geoscience Education, 64 (2), 147–156. https://doi.org/10.5408/15-112.1.
Stokes, A., Boyle, A.P. 2009. The undergraduate geoscience fieldwork experience: Influencing factors and implications for learning. In Whitmeyer, S.J., Mogk, D.W., and Pyle, E.J., eds., Field geology education: Historical perspectives and modern approaches. Geological Society of America Special Paper, 461: 291–311.
Streule, M.J., Craig, L.E. 2016. Social Learning Theories—An Important Design Consideration for Geoscience Fieldwork. Journal of geoscience education 64, 101–107.
Thrift, D. 1975. Field Trips: A priceless ingredient. Journal of Geological Education, 23, 137–139.
Tuckman, B.W. 1965. Developmental sequence in small groups. Psychological Bulletin, 63 (6). 384-399.
Tuckman, B.W., Jensen, M.C. 1977. Stages of Small-Group Development Revisited. Group and Organization Studies. 2 (4), 419-427.
Unsworth, S., Riggs, E.M., Chávez, M. 2012. Creating pathways toward geoscience education for Native American youth: The importance of cultural relevance and self-concept. Journal of geoscience education, 60, 384 – 392.
Waldron, J.W., Locock, A.J., Pujadas-Botey, A. 2016. Building an Outdoor Classroom for Field Geology: The Geoscience Garden. Journal of geoscience education 64, 215-230.
Wanger, S.P., Minthorn, R.S., Weinland, K.A., Appleman, B., James, M., Arnold, A., 2012. Native American student participation in study abroad: American Indian culture and research journal, 36, 127-151.
Weissmann, G.S., Ibarra, R.A., Howland-Davis, M., Lammey, M.V. 2019. The Multicontext path to redefining how we access and think about diversity, equity, and inclusion in

STEM. Journal of Geoscience Education, 67 (4), 320–329. https://doi.org/10.1080/10899995.2019.1620527.
Whitmeyer, S.J., Mogk, D.W., Pyle, E.J. (Eds). 2009. Field Geology Education: Historical Perspectives and Modern Approaches: Geological Society of America Special Paper 461, 356.
Wildcat, D. 2018. Exploring Applications of Indigenuity: Incorporating Indigenous perspectives in the geoscience classroom. Earth Educators' Rendezvous Workshop. Lawrence, KS.
Wolfe, B.A., Riggs, E.M. 2017. Macrosystem analysis of programs and strategies to increase underrepresented populations in the geosciences. Journal of Geoscience Education, 65 (4), 577-593.

**SUPPLEMENTAL MATERIALS**
**Chapter I**

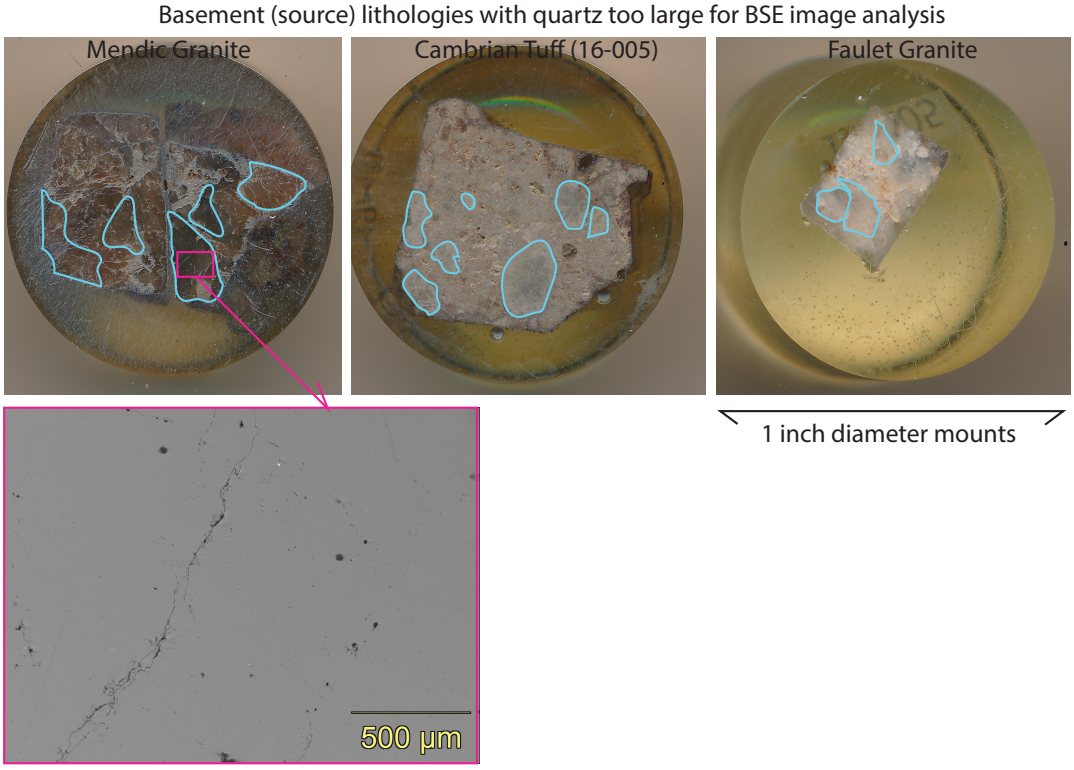


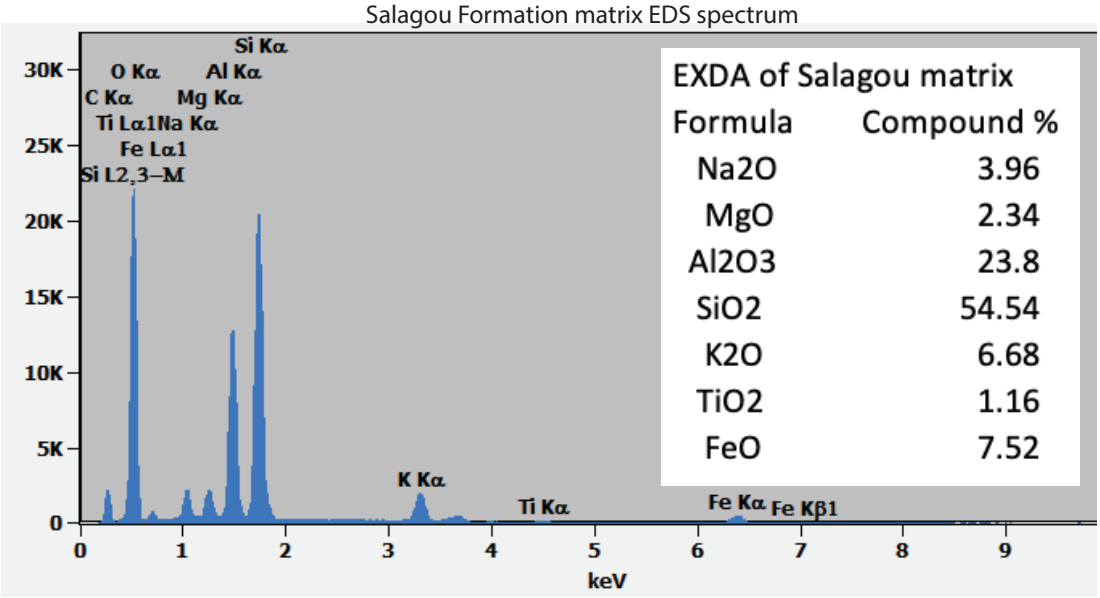


**Appendix I.** Additional microprobe data, including quartz grain sizes in basement source samples that were too large for 2D BSE quartz grain size analysis *(top)* and EDS spectra and compositional table for the illite-rich matrix of the Salagou Formation *(bottom)*.

**GPS Location Data**

**I. Locations of Section Lines**

GPS Coordinates for "Boar Basin"
Lower-most Salagou (north of Rabieux)
Measured June 6-7, 2018
LSALBB

| lat (N) | long (E) | Ref m |
|---|---|---|
| 43.703510 | 3.450141 | 0 |
| 43.703422 | 3.451212 | 10 |
| 43.702818 | 3.451168 | |
| 43.702935 | 3.451594 | |
| 43.702999 | 3.452095 | |
| 43.702904 | 3.452042 | |
| 43.702662 | 3.452178 | |
| 43.702477 | 3.452146 | |
| 43.702319 | 3.452218 | |
| 43.702269 | 3.452168 | |
| 43.702534 | 3.452907 | |
| 43.702218 | 3.453075 | |
| 43.702118 | 3.453316 | |
| 43.702122 | 3.453626 | |
| 43.701972 | 3.453895 | |
| 43.701597 | 3.454433 | |
| 43.701553 | 3.454694 | |
| 43.701623 | 3.454996 | |
| 43.701905 | 3.455363 | |
| 43.701646 | 3.455413 | |
| 43.701519 | 3.455656 | |
| 43.701201 | 3.456163 | |
| 43.700985 | 3.456229 | |
| 43.700806 | 3.456123 | |
| 43.700483 | 3.456511 | |
| 43.700154 | 3.456935 | 130 |
| 43.700079 | 3.456920 | |
| 43.699860 | 3.457058 | |
| 43.700016 | 3.457573 | |
| 43.699544 | 3.457733 | 161 |

GPS Coordinates for "Hog Hill"
Lower Salagou
Measured June 17, 2018
LSALHH

| lat (N) | long (E) | Ref m |
|---|---|---|
| 43.683235 | 3.432288 | 0 |
| 43.683075 | 3.431964 | |
| 43.682436 | 3.431939 | |
| 43.682423 | 3.431829 | |
| 43.681602 | 3.431370 | |
| 43.681504 | 3.431089 | |
| 43.681077 | 3.431136 | |
| 43.680753 | 3.430453 | |
| 43.680584 | 3.430150 | |
| 43.680457 | 3.429756 | 70 |

GPS Coordinates for "The Peninsula"
Mid-Upper Salagou (E. of Octon, "La Sure")
Measured June 4, 2018
MUSAL

| lat (N) | long (E) | Ref m |
|---|---|---|
| 43.657362 | 3.347601 | 0 |
| 43.656937 | 3.347432 | 10 |
| 43.656809 | 3.347526 | |
| 43.656591 | 3.347459 | |
| 43.656479 | 3.347526 | |
| 43.656323 | 3.347492 | |
| 43.656219 | 3.347031 | 40 |
| 43.656102 | 3.347042 | |
| 43.655925 | 3.346988 | |
| 43.655017 | 3.348165 | |
| 43.654823 | 3.347205 | |
| 43.655086 | 3.346638 | |
| 43.655015 | 3.346372 | |
| 43.654866 | 3.346298 | 100 |

GPS Coordinates for "The Ranch"
Lower-Middle Salagou (east of Octon)
Measured June 2-3, 5 2018
LSALE

| lat (N) | long (E) | Ref m |
|---|---|---|
| 43.675317 | 3.335809 | 0 |
| 43.674943 | 3.336263 | 5 |
| 43.674663 | 3.336497 | |
| 43.674528 | 3.336772 | |
| 43.674011 | 3.337181 | |
| 43.673999 | 3.337384 | |
| 43.673924 | 3.337399 | |
| 43.674000 | 3.337719 | |
| 43.673928 | 3.338021 | |
| 43.673622 | 3.337928 | |
| 43.673413 | 3.338125 | 80 |
| 43.673246 | 3.338254 | |
| 43.673063 | 3.338275 | |
| 43.672948 | 3.338372 | |
| 43.672766 | 3.338498 | |
| 43.672607 | 3.338545 | |
| 43.672481 | 3.338440 | |
| 43.672342 | 3.338519 | |
| 43.672075 | 3.338770 | 130 |

GPS Coordinates for Octon
Upper Salagou
Measured June 13, 2018
USALOB

| lat (N) | long (E) | Ref m |
|---|---|---|
| 43.645994 | 3.299409 | 0 |
| 43.645643 | 3.299263 | 20 |
| 43.644924 | 3.298998 | |
| 43.644875 | 3.298321 | |
| 43.644744 | 3.298861 | |
| 43.644688 | 3.298352 | |
| 43.644691 | 3.298274 | |
| 43.643981 | 3.300121 | |
| 43.643660 | 3.300378 | |
| 43.643356 | 3.299859 | |
| 43.642696 | 3.299505 | 120 |

GPS Coordinates for "The Labyrinth"
Upper Salagou (S. of Peninsula) June 9-10
Measured June 9-10, 2018
USAL

| lat (N) | long (E) | Ref m |
|---|---|---|
| 43.652694 | 3.342276 | 0 |
| 43.649827 | 3.343290 | 10 |
| 43.649010 | 3.343417 | |
| 43.647400 | 3.342933 | |
| 43.646652 | 3.345230 | |
| 43.646322 | 3.345263 | |
| 43.646094 | 3.344828 | |
| 43.645332 | 3.345125 | |
| 43.645449 | 3.344069 | |
| 43.645136 | 3.344025 | 81.5 |
| 43.644855 | 3.343356 | |
| 43.644653 | 3.343276 | |
| 43.644342 | 3.343451 | |
| 43.644193 | 3.343292 | 110 |

GPS Coordinates for Merifons
Upper-most Salagou
Measured June 20, 2018
USALME

| lat (N) | long (E) | Ref m |
|---|---|---|
| 43.634079 | 3.277059 | 0 |
| 43.633829 | 3.277023 | |
| 43.633584 | 3.276725 | 20 |
| 43.633353 | 3.276712 | 30 |
| 43.633416 | 3.276291 | 38 |
| 43.633382 | 3.276343 | 40 |
| 43.633219 | 3.276365 | 50 |
| 43.633020 | 3.276600 | |
| 43.632925 | 3.276484 | 60 |
| 43.632940 | 3.276180 | 70 |

GPS Coordinates for WOCTON
Upper Salagou
Measured June 18-19, 2018
USALWO

| lat (N) | long (E) | Ref m |
|---|---|---|
| 43.641229 | 3.304007 | 0 |
| 43.640997 | 3.304038 | |
| 43.640689 | 3.303933 | 21 |
| 43.640573 | 3.303969 | |
| 43.640366 | 3.304091 | 30 |
| 43.640121 | 3.304386 | 36 |
| 43.639833 | 3.304502 | |
| 43.639206 | 3.304966 | |
| 43.639179 | 3.304847 | 73.5 |
| 43.639197 | 3.304380 | 80 |
| 43.638942 | 3.304724 | 85 |
| 43.638826 | 3.304558 | 90.5 |
| 43.638913 | 3.304324 | 91 |
| 43.638393 | 3.304505 | 106 |
| 43.639284 | 3.289774 | 110 |
| 43.639156 | 3.289469 | 120 |
| 43.638693 | 3.289306 | |
| 43.638547 | 3.289355 | |
| 43.638271 | 3.289456 | 145 |
| 43.638052 | 3.289559 | |
| 43.638009 | 3.289615 | |
| 43.637888 | 3.289451 | 161 |
| 43.637557 | 3.289166 | 178 |
| 43.637443 | 3.288964 | |
| 43.637266 | 3.288853 | 190 |
| 43.637169 | 3.288648 | |
| 43.637134 | 3.288491 | 200 |
| 43.637174 | 3.288254 | 204 |
| 43.636824 | 3.288367 | |
| 43.636713 | 3.288106 | 220 |
| 43.636566 | 3.288337 | |
| 43.636460 | 3.288169 | 225 |

## II. Detrital zircon samples

GPS Coordinates for detrital zircon samples (n=3)
Salagou Formation
Collected June, 2012
Analyzed 2012-2013

| *Strat. Position* | *Sample* | *lat (N)* | *long (E)* |
|---|---|---|---|
| Upper Salagou | R2B-B | 43.64482 | 3.235133 |
| Mid-Upper Salagou (Octon Mbr.) | R2B-G | 43.64435 | 3.289017 |
| Basal Salagou | R2B-F | 43.68885 | 3.411000 |

## III. Grain size samples

GPS Coordinates for grain size analysis
Salagou Formation (red mudstone)
Collected June, 2018
Analyzed 2018-2019

| *Strat. Position* | *Sample* | *lat (N)* | *long (E)* |
|---|---|---|---|
| Lowermost | LSALBB 0 | 43.703510 | 3.450141 |
| Lower | LSALHH 30 | 43.682423 | 3.431829 |
| Lower-Mid | LSALE 0 | 43.675317 | 3.335809 |
| Lower-Mid | LSALE 25 | 43.674528 | 3.336772 |
| Lower-Mid | LSALE 50 | 43.674000 | 3.337719 |
| Lower-Mid | LSALE 75 | 43.673413 | 3.338125 |
| Lower-Mid | LSALE 100 | 43.672948 | 3.338372 |
| Lower-Mid | LSALE 125 | 43.672075 | 3.338770 |
| Mid-Upper | MUSAL 0 | 43.657362 | 3.347601 |
| Mid-Upper | MUSAL 10 | 43.656937 | 3.347432 |
| Upper | USAL 0 | 43.652694 | 3.342276 |
| Upper | USAL 150 | 43.644193 | 3.343292 |
| Upper | USALOB | 43.645994 | 3.299409 |

GPS Coordinates for grain size analysis
Montagne Noire Basement (rep. lithologies)
Collected June, 2018
Analyzed 2018-2019

| *Type* | *Sample* | *lat (N)* | *long (E)* |
|---|---|---|---|
| Granite | 16-004 | 43.64472222 | 2.96472222 |
| Granite | 16-003 | 43.64055556 | 2.96916667 |
| Tuff | K1A | 43.73111111 | 3.33194444 |
| Schist | K2MN+K3MN | 43.66166667 | 3.09916667 |
| Schist | X10+X11 | 43.66305556 | 3.07972222 |

**III. Geochemical samples**

GPS Coordinates for geochem analysis
Salagou Formation (red mudstone)
Collected June, 2018
Analyzed 2018-2019

| *Strat. Position* | *Sample* | *lat (N)* | *long (E)* |
|---|---|---|---|
| Upper | USALWO 90 | 43.638826 | 3.304558 |
| Upper | USALWO 74 | 43.639179 | 3.304847 |
| Upper | USALWO 70 | 43.639179 | 3.304847 |
| Upper | USALWO 60 | 43.639206 | 3.304966 |
| Lower-Mid | LSALE 16.5 | 43.674943 | 3.336263 |
| Paleosol top | R4 (LSALE) | 43.674943 | 3.336263 |
| Paleosol | R3 (LSALE) | 43.674943 | 3.336263 |
| Paleosol | R2 (LSALE) | 43.674943 | 3.336263 |
| Paleosol base | R1 (LSALE) | 43.674943 | 3.336263 |
| Lower-Mid | LSALE 10 | 43.674943 | 3.336263 |
| Lower-Mid | LSALE 5 | 43.674943 | 3.336263 |
| Lower | LSALBB 75 | 43.701597 | 3.454433 |
| Lower | LSALBB 55 | 43.702534 | 3.452907 |
| Lower | LSALBB 16 | 43.703422 | 3.451212 |

**Paleosol samples (n=4) are 30-cm apart*

GPS Coordinates for geochem analysis
Montagne Noire Basement (rep. lithologies)
Collected June, 2018
Analyzed 2018-2019

| *Type* | *Sample* | *lat (N)* | *long (E)* |
|---|---|---|---|
| Schist | X10 | 43.6630556 | 3.07972222 |
| Schist | X11 | 43.6605556 | 3.06916667 |
| Granite | Faulat | 43.7963889 | 3.08055556 |
| Granite | Mendic | 43.7186111 | 3.15333333 |

**SUPPLEMENTAL MATERIALS**
**Chapter II**

**MATLAB and R commands**
MATLAB commands associated with the manuscript 'Rock magnetic cyclostratigraphy of Permian loess in eastern equatorial Pangea (Salagou Formation, south-central France)' by Pfeifer et al., 2020.
Note: *tanerfilter.m* and *evofft.m* are available at:
http://mason.gmu.edu/~lhinnov/cyclostratigraphytools.html
and all other MATLAB functions are available in the MATLAB Signal and Curve Fitting toolboxes.
##################################

***Lower ("boarbasin")***
*General Notes:* Power spectrum is 2pi multi-taper (MTM) without padding. 6pi MTM with padding looks very similar. Evolutionary spectrogram is with a 20m window and shows true variance values (not normalized to the max frequency).

```
figure; plot(boarbasin(:,1),boarbasin(:,2));
diffboarbasin=diff(boarbasin(:,1));
figure;plot(diffboarbasin);
mean(diffboarbasin)
median(diffboarbasin)
dd=0.5;
depthint=boarbasin(1,1):dd:boarbasin(317,1);
depthint=depthint';
boarbasinint=interp1(boarbasin(:,1),boarbasin(:,2),depthint);
figure;plot(depthint,boarbasinint);
```

*Power spectrum without padding*

```
[p,w]=pmtm(detrend(boarbasinint),2,321);
f=w/(2*pi*dd);
figure;plot(f,p);
```

*Evolutionary spectrum (window is 20)*

```
s=evofft(data,window,step,dt,fmin,fmax,unit,norm)
s=evofft(data,20,dd,dd,0,1,'m',1);
```

***Upper ("composite-upper")***
*General Notes:* Raw data is pre-whitened. Power spectrum is 6pi MTM. Evolutionary spectrum is with a 100m window and shows true variance values (not normalized to the max frequency). The evolutionary spectrum is after Taner band filters were applied to focus on high-frequency variability.

*Pre-whitening*

```
span350=350/dd;
smoothupper350=smooth(upperint,span350,'loess');
```

```
hold all; plot(depthint,smoothupper350);
upperintres350=upperint-smoothupper350;
figure;plot(depthint,upperintres350);

Power spectrum with padding
[p,w]=pmtm(upperintres350,6);
f=w/(2*pi*dd);
figure;plot(f,p);

Evolutionary spectrum (window is 100)
s=evofft([depthint upperintres350],100,dd,dd,0,1,'m',1);

Taner low-pass filter removal to focus on higher-frequency signal
[tanerbandx,filtout,f]=tanerfilter(upperintres350,dd,0,-0.035,0.035);
hold all; plot(depthint,tanerbandx);
upperintres350restanner=upperintres350-tanerbandx;
figure;plot(depthint,upperintres350restanner);

Power spectrum, 6pi MTM
[p,w]=pmtm(upperintres350restanner,6);
f=w/(2*pi*dd);
figure;plot(f,p);

Evolutionary spectrogram (window is 100)
s=evofft([depthint upperintres350restanner],100,dd,dd,0,1,'m',1);
s=evofft([depthint upperintres350restanner],100,dd,dd,0,1,'m',0);
```

**R commands**

```
# R commands associated with the manuscript 'Rock magnetic cyclostratigraphy of Permian
loess in eastern equatorial Pangea (Salagou Formation, south-central France)' by Pfeifer et al.
# code written by Linda Hinnov 2018-2019
###################################
# investigate cyclicity in the Lower ("boarbasin")
# General notes: Astronomical target has 13 astronomical frequencies
# load library 'astrochron' which must be installed
library(astrochron)

# load data into R
boarbasin=read()

# set time step for interpolation
dt=0.5

# linearly interpolate depth series (is required for time series analysis)
boarbasinint=linterp(boarbasin,dt)
```

```
# apply Evolutive Harmonic Analysis
EHAboarbasin=eha(boarbasinint,tbw=2, win=180, demean=T, detrend=T, sigID=T,
siglevel=0.95,
pl=2, output=5, fmin=0., fmax=1., xlab="Frequency (cycles/m)", ylab="Height (m)")

# set parameters for Astronomical Spectral Misfit
freq <- data.frame(EHAboarbasin)
rayleigh <- 0.00443459
nyquist <- 1
target <- c(1/405.091,1/131,1/123.4,1/98.9, 1/94.5,1/44.84,1/34.331, 1/33.441,
1/26.155,1/21.296,
1/20.234,1/17.521, 1/17.392)

# apply Astronomical Spectral Misfit
asm(freq=freq,target=target,rayleigh=rayleigh,nyquist=nyquist,sedmin=5,sedmax=15,numsed=
100,linLog=1,iter=100000,output=FALSE)

# investigate cyclicity in the middle-upper (“composite”)
# General notes: Astronomical target has 10 astronomical frequencies
# load library 'astrochron' which must be installed
library(astrochron)

# load data into R
composite=read()

# set time step for interpolation
dt=0.5

# linearly interpolate depth series (is required for time series analysis)
compositeint=linterp(composite,dt)

# apply Evolutive Harmonic Analysis
EHAcomposite=eha(compositeint,tbw=2, win=758.5, demean=T, detrend=T, sigID=T,
siglevel=0.95,
pl=2, output=5, fmin=0., fmax=1., xlab="Frequency (cycles/m)", ylab="Height (m)")

# set parameters for Astronomical Spectral Misfit
freq <- data.frame(EHAcomposite)
rayleigh <- 0.00443459
nyquist <- 1
target <- c(1/405.091,1/131,1/123.4,1/98.9,1/44.84,1/34.331,1/26.155,1/21.296,1/17.521,
1/17.392)

# apply Astronomical Spectral Misfit
asm(freq=freq,target=target,rayleigh=rayleigh,nyquist=nyquist,sedmin=5,sedmax=15,numsed=
100,linLog=1,iter=100000,output=FALSE)  # end script
```

**Raw MS data**

***Lower section***

| *Meter* | *MS ($x10^{-3}$)* | 19.5 | 0.227 | 38 | 0.184 |
|---|---|---|---|---|---|
| 0 | 0.107 | 20 | 0.311 | 38.5 | 0.138 |
| 0.5 | 0.176 | 20.5 | 0.21 | 39 | 0.119 |
| 1 | 0.197 | 21 | 0.234 | 39.5 | 0.224 |
| 1.5 | 0.109 | 21.5 | 0.161 | 40 | 0.201 |
| 2 | 0.145 | 22 | 0.257 | 40.5 | 0.23 |
| 2.5 | 0.126 | 22.5 | 0.207 | 41 | 0.2 |
| 3 | 0.15 | 23 | 0.196 | 41.5 | 0.118 |
| 3.5 | 0.169 | 23.5 | 0.159 | 42 | 0.283 |
| 4 | 0.204 | 24 | 0.182 | 42.5 | 0.167 |
| 4.5 | 0.097 | 24.5 | 0.23 | 43 | 0.122 |
| 5 | 0.217 | 25 | 0.249 | 43.5 | 0.172 |
| 5.5 | 0.216 | 25.5 | 0.209 | 44 | 0.197 |
| 6 | 0.192 | 26 | 0.227 | 44.5 | 0.148 |
| 6.5 | 0.233 | 26.5 | 0.239 | 45 | 0.21 |
| 7 | 0.205 | 27 | 0.122 | 45.5 | 0.26 |
| 7.5 | 0.233 | 27.5 | 0.243 | 46 | 0.247 |
| 8 | 0.174 | 28 | 0.222 | 46.5 | 0.271 |
| 8.5 | 0.193 | 28.5 | 0.244 | 47 | 0.141 |
| 9 | 0.242 | 29 | 0.266 | 47.5 | 0.163 |
| 9.5 | 0.149 | 29.5 | 0.271 | 48 | 0.12 |
| 10 | 0.189 | 30 | 0.216 | 48.5 | 0.122 |
| 10.5 | 0.195 | 30.5 | 0.129 | 49 | 0.182 |
| 11 | 0.219 | 31 | 0.111 | 49.5 | 0.25 |
| 11.5 | 0.172 | 31.5 | 0.187 | 50 | 0.206 |
| 12 | 0.152 | 32 | 0.177 | 50.5 | 0.287 |
| 12.5 | 0.164 | 32.5 | 0.232 | 51 | 0.27 |
| 13 | 0.121 | 33 | 0.212 | 51.5 | 0.209 |
| 13.5 | 0.199 | 33.5 | 0.238 | 52 | 0.266 |
| 15.5 | 0.273 | 34 | 0.124 | 52.5 | 0.127 |
| 16 | 0.255 | 34.5 | 0.23 | 53 | 0.252 |
| 16.5 | 0.259 | 35 | 0.207 | 53.5 | 0.1 |
| 17 | 0.195 | 35.5 | 0.137 | 54 | 0.196 |
| 17.5 | 0.27 | 36 | 0.215 | 54.5 | 0.191 |
| 18 | 0.378 | 36.5 | 0.185 | 55 | 0.201 |
| 18.5 | 0.199 | 37 | 0.15 | 55.5 | 0.165 |
| 19 | 0.274 | 37.5 | 0.114 | 56 | 0.207 |

| | | | | | |
|---|---|---|---|---|---|
| 56.5 | 0.132 | 76.5 | 0.279 | 97 | 0.196 |
| 57 | 0.196 | 77 | 0.211 | 97.5 | 0.225 |
| 57.5 | 0.17 | 77.5 | 0.284 | 98 | 0.126 |
| 58 | 0.152 | 78 | 0.228 | 98.5 | 0.133 |
| 58.5 | 0.166 | 78.5 | 0.172 | 99 | 0.197 |
| 59 | 0.166 | 79 | 0.266 | 99.5 | 0.238 |
| 59.5 | 0.23 | 79.5 | 0.223 | 100 | 0.212 |
| 60 | 0.211 | 80 | 0.178 | 100.5 | 0.204 |
| 60.5 | 0.295 | 80.5 | 0.111 | 101 | 0.205 |
| 61 | 0.206 | 81 | 0.209 | 101.5 | 0.136 |
| 61.5 | 0.08 | 81.5 | 0.235 | 102 | 0.186 |
| 62 | 0.203 | 82 | 0.241 | 102.5 | 0.158 |
| 62.5 | 0.17 | 82.5 | 0.163 | 103 | 0.123 |
| 63 | 0.109 | 83 | 0.135 | 103.5 | 0.169 |
| 63.5 | 0.209 | 83.5 | 0.237 | 104 | 0.221 |
| 64 | 0.155 | 84 | 0.227 | 104.5 | 0.184 |
| 64.5 | 0.168 | 84.5 | 0.2 | 105 | 0.116 |
| 65 | 0.15 | 85 | 0.236 | 105.5 | 0.227 |
| 65.5 | 0.21 | 85.5 | 0.242 | 106 | 0.253 |
| 66 | 0.316 | 86 | 0.195 | 106.5 | 0.221 |
| 66.5 | 0.279 | 86.5 | 0.16 | 107 | 0.177 |
| 67 | 0.217 | 87 | 0.292 | 107.5 | 0.136 |
| 67.5 | 0.239 | 87.5 | 0.226 | 108 | 0.154 |
| 68 | 0.218 | 88 | 0.26 | 108.5 | 0.184 |
| 68.5 | 0.224 | 88.5 | 0.306 | 109 | 0.242 |
| 69 | 0.207 | 89 | 0.231 | 109.5 | 0.219 |
| 69.5 | 0.174 | 90 | 0.146 | 110 | 0.159 |
| 70 | 0.13 | 90.5 | 0.221 | 110.5 | 0.131 |
| 70.5 | 0.146 | 91 | 0.15 | 111 | 0.155 |
| 71 | 0.163 | 91.5 | 0.199 | 111.5 | 0.247 |
| 71.5 | 0.166 | 92 | 0.218 | 112 | 0.084 |
| 72 | 0.197 | 92.5 | 0.149 | 112.5 | 0.218 |
| 72.5 | 0.158 | 93 | 0.273 | 113 | 0.222 |
| 73 | 0.158 | 93.5 | 0.191 | 113.5 | 0.188 |
| 73.5 | 0.229 | 94 | 0.146 | 114 | 0.144 |
| 74 | 0.212 | 94.5 | 0.199 | 114.5 | 0.219 |
| 74.5 | 0.258 | 95 | 0.254 | 115 | 0.269 |
| 75 | 0.225 | 95.5 | 0.345 | 115.5 | 0.2 |
| 75.5 | 0.22 | 96 | 0.242 | 116 | 0.283 |
| 76 | 0.286 | 96.5 | 0.213 | 116.5 | 0.254 |

| | | | | | |
|---|---|---|---|---|---|
| 117 | 0.182 | 131.5 | 0.209 | 146 | 0.209 |
| 117.5 | 0.123 | 132 | 0.146 | 146.5 | 0.164 |
| 118 | 0.185 | 132.5 | 0.189 | 147 | 0.253 |
| 118.5 | 0.216 | 133 | 0.299 | 147.5 | 0.214 |
| 119 | 0.148 | 133.5 | 0.229 | 148 | 0.176 |
| 119.5 | 0.292 | 134 | 0.163 | 148.5 | 0.174 |
| 120 | 0.201 | 134.5 | 0.212 | 149 | 0.18 |
| 120.5 | 0.22 | 135 | 0.206 | 149.5 | 0.188 |
| 121 | 0.156 | 135.5 | 0.315 | 150 | 0.271 |
| 121.5 | 0.169 | 136 | 0.205 | 150.5 | 0.11 |
| 122 | 0.168 | 136.5 | 0.18 | 151 | 0.194 |
| 122.5 | 0.199 | 137 | 0.187 | 151.5 | 0.228 |
| 123 | 0.209 | 137.5 | 0.253 | 152 | 0.181 |
| 123.5 | 0.212 | 138 | 0.194 | 152.5 | 0.163 |
| 124 | 0.114 | 138.5 | 0.227 | 153 | 0.193 |
| 124.5 | 0.202 | 139 | 0.23 | 153.5 | 0.206 |
| 125 | 0.187 | 139.5 | 0.253 | 154 | 0.254 |
| 125.5 | 0.184 | 140 | 0.165 | 154.5 | 0.173 |
| 126 | 0.219 | 140.5 | 0.153 | 155 | 0.254 |
| 126.5 | 0.21 | 141 | 0.155 | 155.5 | 0.197 |
| 127 | 0.239 | 141.5 | 0.223 | 156 | 0.197 |
| 127.5 | 0.186 | 142 | 0.192 | 156.5 | 0.181 |
| 128 | 0.237 | 142.5 | 0.169 | 157 | 0.293 |
| 128.5 | 0.177 | 143 | 0.208 | 157.5 | 0.182 |
| 129 | 0.184 | 143.5 | 0.187 | 158 | 0.157 |
| 129.5 | 0.12 | 144 | 0.194 | 158.5 | 0.187 |
| 130 | 0.181 | 144.5 | 0.275 | 159 | 0.12 |
| 130.5 | 0.185 | 145 | 0.173 | 159.5 | 0.185 |
| 131 | 0.219 | 145.5 | 0.214 | 160 | 0.248 |

***Mid-Upper section***

| ***Meter*** | ***MS (x10$^{-3}$)*** | 755 | 0.164 | 751 | 0.225 |
|---|---|---|---|---|---|
| 758.5 | 0.16 | 754.5 | 0.193 | 750.5 | 0.237 |
| 758 | 0.18 | 754 | 0.179 | 750 | 0.227 |
| 757.5 | 0.172 | 753.5 | 0.185 | 749.5 | 0.164 |
| 757 | 0.142 | 753 | 0.151 | 749 | 0.226 |
| 756.5 | 0.106 | 752.5 | 0.138 | 748.5 | 0.142 |
| 756 | 0.215 | 752 | 0.202 | 748 | 0.23 |
| 755.5 | 0.243 | 751.5 | 0.19 | 747.5 | 0.172 |

| | | | | | |
|---|---|---|---|---|---|
| 747 | 0.222 | 725 | 0.234 | 702.5 | 0.219 |
| 746.5 | 0.181 | 724.5 | 0.194 | 702 | 0.121 |
| 746 | 0.248 | 723.5 | 0.126 | 701.5 | 0.148 |
| 745.5 | 0.155 | 723 | 0.172 | 701 | 0.191 |
| 745 | 0.148 | 722.5 | 0.176 | 700.5 | 0.204 |
| 744.5 | 0.147 | 722 | 0.196 | 700 | 0.183 |
| 744 | 0.136 | 721.5 | 0.106 | 699.5 | 0.145 |
| 743.5 | 0.203 | 721 | 0.161 | 699 | 0.182 |
| 743 | 0.273 | 720.5 | 0.11 | 698.5 | 0.196 |
| 742.5 | 0.208 | 719.5 | 0.207 | 698 | 0.177 |
| 742 | 0.187 | 719 | 0.153 | 697.5 | 0.166 |
| 741.5 | 0.17 | 718.5 | 0.1 | 697 | 0.204 |
| 741 | 0.203 | 718 | 0.175 | 696.5 | 0.189 |
| 740.5 | 0.214 | 717.5 | 0.173 | 696 | 0.164 |
| 740 | 0.232 | 717 | 0.192 | 695.5 | 0.158 |
| 739.5 | 0.103 | 716.5 | 0.221 | 695 | 0.128 |
| 739 | 0.204 | 716 | 0.199 | 694.5 | 0.145 |
| 738.5 | 0.182 | 715.5 | 0.206 | 694 | 0.231 |
| 738 | 0.204 | 715 | 0.256 | 693.5 | 0.142 |
| 737.5 | 0.181 | 714.5 | 0.151 | 693 | 0.19 |
| 737 | 0.174 | 714 | 0.181 | 692.5 | 0.21 |
| 736.5 | 0.207 | 713.5 | 0.181 | 692 | 0.167 |
| 736 | 0.177 | 713 | 0.172 | 691.5 | 0.17 |
| 735.5 | 0.245 | 712.5 | 0.135 | 691 | 0.124 |
| 735 | 0.203 | 712 | 0.193 | 690.5 | 0.207 |
| 734.5 | 0.162 | 711.5 | 0.209 | 690 | 0.174 |
| 734 | 0.123 | 711 | 0.203 | 689.5 | 0.157 |
| 733.5 | 0.177 | 710.5 | 0.154 | 689 | 0.141 |
| 733 | 0.195 | 710 | 0.168 | 688.5 | 0.194 |
| 732.5 | 0.163 | 709.5 | 0.167 | 688 | 0.238 |
| 732 | 0.132 | 709 | 0.195 | 687.5 | 0.216 |
| 731.5 | 0.13 | 708.5 | 0.192 | 687 | 0.293 |
| 731 | 0.122 | 708 | 0.158 | 686.5 | 0.309 |
| 730.5 | 0.187 | 707.5 | 0.167 | 686 | 0.279 |
| 730 | 0.264 | 707 | 0.147 | 685.5 | 0.235 |
| 729.5 | 0.191 | 706.5 | 0.168 | 685 | 0.175 |
| 729 | 0.181 | 706 | 0.156 | 684.5 | 0.179 |
| 728.5 | 0.197 | 705.5 | 0.155 | 684 | 0.283 |
| 728 | 0.168 | 705 | 0.22 | 683.5 | 0.246 |
| 727.5 | 0.186 | 704.5 | 0.153 | 682.5 | 0.283 |
| 727 | 0.19 | 704 | 0.163 | 682 | 0.217 |
| 726 | 0.168 | 703.5 | 0.16 | 681.5 | 0.275 |
| 725.5 | 0.202 | 703 | 0.198 | 681 | 0.284 |

| | | | | | |
|---|---|---|---|---|---|
| 680.5 | 0.394 | 655 | 0.177 | 630.5 | 0.365 |
| 680 | 0.264 | 654.5 | 0.227 | 630 | 0.244 |
| 679.5 | 0.286 | 654 | 0.223 | 629.5 | 0.213 |
| 678 | 0.202 | 653.5 | 0.267 | 629 | 0.211 |
| 677.5 | 0.223 | 653 | 0.307 | 628.5 | 0.208 |
| 676.5 | 0.121 | 652.5 | 0.227 | 628 | 0.162 |
| 675.5 | 0.279 | 652 | 0.211 | 624 | 0.233 |
| 675 | 0.195 | 651.5 | 0.379 | 623.5 | 0.137 |
| 674.5 | 0.124 | 651 | 0.228 | 622.5 | 0.165 |
| 674 | 0.148 | 650.5 | 0.242 | 622 | 0.143 |
| 673.5 | 0.264 | 650 | 0.227 | 621.5 | 0.204 |
| 673 | 0.201 | 649.5 | 0.175 | 621 | 0.234 |
| 672 | 0.196 | 649 | 0.331 | 620.5 | 0.236 |
| 671.5 | 0.164 | 648.5 | 0.29 | 620 | 0.253 |
| 671 | 0.205 | 646.5 | 0.343 | 619 | 0.26 |
| 670 | 0.188 | 645.5 | 0.336 | 618.5 | 0.277 |
| 669.5 | 0.227 | 645 | 0.274 | 618 | 0.257 |
| 669 | 0.182 | 644.5 | 0.261 | 617.5 | 0.144 |
| 668.5 | 0.183 | 644 | 0.256 | 617 | 0.3 |
| 668 | 0.223 | 643 | 0.276 | 616.5 | 0.248 |
| 667.5 | 0.187 | 642.5 | 0.196 | 616 | 0.206 |
| 667 | 0.164 | 642 | 0.16 | 615.5 | 0.095 |
| 666.5 | 0.193 | 641.5 | 0.235 | 615 | 0.097 |
| 666 | 0.291 | 641 | 0.203 | 614.5 | 0.218 |
| 665.5 | 0.373 | 640.5 | 0.205 | 614 | 0.131 |
| 665 | 0.201 | 640 | 0.229 | 613.5 | 0.216 |
| 664.5 | 0.346 | 639.5 | 0.236 | 613 | 0.351 |
| 664 | 0.275 | 639 | 0.251 | 612.5 | 0.193 |
| 663.5 | 0.109 | 638.5 | 0.362 | 612 | 0.217 |
| 663 | 0.31 | 638 | 0.208 | 611.5 | 0.335 |
| 662.5 | 0.149 | 637.5 | 0.206 | 611 | 0.346 |
| 662 | 0.244 | 637 | 0.192 | 610.5 | 0.252 |
| 661.5 | 0.207 | 636.5 | 0.172 | 610 | 0.295 |
| 661 | 0.162 | 636 | 0.196 | 609.5 | 0.267 |
| 660.5 | 0.119 | 635.5 | 0.084 | 609 | 0.259 |
| 659.5 | 0.156 | 635 | 0.206 | 608.5 | 0.18 |
| 659 | 0.262 | 634.5 | 0.253 | 608 | 0.246 |
| 658.5 | 0.126 | 633.5 | 0.13 | 607.5 | 0.243 |
| 658 | 0.172 | 633 | 0.154 | 607 | 0.224 |
| 657.5 | 0.399 | 632.5 | 0.235 | 606.5 | 0.295 |
| 657 | 0.179 | 632 | 0.188 | 606 | 0.343 |
| 656 | 0.205 | 631.5 | 0.247 | 605.5 | 0.332 |
| 655.5 | 0.223 | 631 | 0.268 | 605 | 0.217 |

| | | | | | |
|---|---|---|---|---|---|
| 604.5 | 0.188 | 577 | 0.202 | 554.5 | 0.177 |
| 604 | 0.275 | 576.5 | 0.279 | 554 | 0.152 |
| 603.5 | 0.215 | 576 | 0.221 | 553.5 | 0.149 |
| 603 | 0.29 | 575.5 | 0.221 | 553 | 0.222 |
| 602.5 | 0.254 | 575 | 0.135 | 552.5 | 0.208 |
| 602 | 0.22 | 574.5 | 0.317 | 552 | 0.25 |
| 601.5 | 0.285 | 574 | 0.251 | 551.5 | 0.2 |
| 601 | 0.263 | 573.5 | 0.206 | 551 | 0.551 |
| 600.5 | 0.296 | 573 | 0.22 | 550.5 | 0.304 |
| 600 | 0.37 | 572.5 | 0.21 | 550 | 0.3 |
| 599.5 | 0.238 | 571.5 | 0.238 | 549.5 | 0.185 |
| 599 | 0.221 | 571 | 0.276 | 549 | 0.251 |
| 598.5 | 0.283 | 570.5 | 0.214 | 548.5 | 0.181 |
| 598 | 0.199 | 570 | 0.215 | 548 | 0.276 |
| 597.5 | 0.255 | 569 | 0.185 | 547.5 | 0.336 |
| 597 | 0.175 | 568.5 | 0.343 | 547 | 0.169 |
| 596.5 | 0.298 | 568 | 0.308 | 546.5 | 0.248 |
| 595.5 | 0.195 | 567.5 | 0.217 | 546 | 0.374 |
| 595 | 0.302 | 567 | 0.286 | 545.5 | 0.242 |
| 594.5 | 0.318 | 566.5 | 0.23 | 545 | 0.135 |
| 594 | 0.17 | 566 | 0.181 | 544.5 | 0.177 |
| 593 | 0.225 | 565.5 | 0.222 | 544 | 0.102 |
| 592.5 | 0.233 | 565 | 0.219 | 543.5 | 0.137 |
| 592 | 0.284 | 564.5 | 0.121 | 543 | 0.3 |
| 591.5 | 0.249 | 564 | 0.149 | 542.5 | 0.257 |
| 591 | 0.206 | 563.5 | 0.17 | 542 | 0.281 |
| 590.5 | 0.274 | 563 | 0.172 | 541.5 | 0.316 |
| 590 | 0.26 | 562.5 | 0.246 | 541 | 0.158 |
| 589.5 | 0.247 | 562 | 0.195 | 540.5 | 0.168 |
| 589 | 0.189 | 561.5 | 0.26 | 540 | 0.236 |
| 587 | 0.093 | 561 | 0.33 | 539.5 | 0.208 |
| 586.5 | 0.188 | 560.5 | 0.306 | 539 | 0.106 |
| 586 | 0.335 | 560 | 0.207 | 538.5 | 0.199 |
| 585.5 | 0.327 | 559.5 | 0.222 | 538 | 0.148 |
| 585 | 0.21 | 559 | 0.207 | 537.5 | 0.18 |
| 584.5 | 0.168 | 558.5 | 0.237 | 537 | 0.257 |
| 584 | 0.199 | 558 | 0.22 | 536.5 | 0.298 |
| 583.5 | 0.216 | 557.5 | 0.19 | 536 | 0.23 |
| 583 | 0.333 | 557 | 0.137 | 535.5 | 0.167 |
| 582.5 | 0.406 | 556.5 | 0.238 | 534.5 | 0.12 |
| 582 | 0.128 | 556 | 0.102 | 534 | 0.309 |
| 578 | 0.197 | 555.5 | 0.277 | 533.5 | 0.166 |
| 577.5 | 0.282 | 555 | 0.234 | 533 | 0.179 |

| | | | | | |
|---|---|---|---|---|---|
| 532.5 | 0.262 | 506 | 0.343 | 483.5 | 0.257 |
| 532 | 0.243 | 505 | 0.339 | 483 | 0.276 |
| 531.5 | 0.21 | 504.5 | 0.17 | 482.5 | 0.238 |
| 531 | 0.236 | 504 | 0.2 | 482 | 0.27 |
| 530.5 | 0.272 | 503.5 | 0.33 | 481.5 | 0.274 |
| 530 | 0.244 | 503 | 0.12 | 481 | 0.197 |
| 529.5 | 0.221 | 502.5 | 0.121 | 480.5 | 0.14 |
| 529 | 0.189 | 502 | 0.142 | 480 | 0.273 |
| 528.5 | 0.292 | 501 | 0.147 | 479.5 | 0.29 |
| 528 | 0.284 | 500.5 | 0.135 | 479 | 0.168 |
| 527.5 | 0.14 | 500 | 0.194 | 478.5 | 0.215 |
| 527 | 0.181 | 499.5 | 0.179 | 478 | 0.254 |
| 526.5 | 0.293 | 499 | 0.22 | 477.5 | 0.191 |
| 526 | 0.162 | 498.5 | 0.183 | 477 | 0.212 |
| 525.5 | 0.111 | 498 | 0.167 | 476.5 | 0.311 |
| 525 | 0.118 | 497.5 | 0.158 | 476 | 0.254 |
| 524.5 | 0.263 | 497 | 0.234 | 475.5 | 0.293 |
| 524 | 0.251 | 496.5 | 0.24 | 475 | 0.308 |
| 523.5 | 0.298 | 496 | 0.215 | 474.5 | 0.206 |
| 523 | 0.188 | 495.5 | 0.26 | 474 | 0.268 |
| 522.5 | 0.193 | 495 | 0.315 | 473.5 | 0.247 |
| 522 | 0.233 | 494.5 | 0.285 | 473 | 0.209 |
| 521.5 | 0.254 | 494 | 0.253 | 472.5 | 0.236 |
| 521 | 0.133 | 493.5 | 0.149 | 472 | 0.289 |
| 516 | 0.255 | 493 | 0.196 | 471.5 | 0.214 |
| 515 | 0.154 | 492.5 | 0.202 | 471 | 0.28 |
| 514.5 | 0.21 | 492 | 0.176 | 470.5 | 0.185 |
| 514 | 0.296 | 491.5 | 0.17 | 470 | 0.295 |
| 513.5 | 0.13 | 491 | 0.207 | 469.5 | 0.274 |
| 513 | 0.192 | 490.5 | 0.152 | 469 | 0.246 |
| 512.5 | 0.244 | 490 | 0.228 | 468.5 | 0.183 |
| 512 | 0.172 | 489.5 | 0.201 | 468 | 0.272 |
| 511.5 | 0.188 | 489 | 0.252 | 467.5 | 0.318 |
| 511 | 0.165 | 488.5 | 0.202 | 467 | 0.313 |
| 510.5 | 0.195 | 488 | 0.161 | 466.5 | 0.397 |
| 510 | 0.204 | 487.5 | 0.213 | 466 | 0.403 |
| 509.5 | 0.102 | 487 | 0.112 | 465.5 | 0.387 |
| 509 | 0.235 | 486.5 | 0.184 | 465 | 0.5 |
| 508.5 | 0.225 | 486 | 0.246 | 464.5 | 0.332 |
| 508 | 0.231 | 485.5 | 0.296 | 464 | 0.606 |
| 507.5 | 0.196 | 485 | 0.314 | 463.5 | 0.951 |
| 507 | 0.238 | 484.5 | 0.282 | 463 | 0.717 |
| 506.5 | 0.238 | 484 | 0.14 | 462.5 | 0.573 |

| | | | | | |
|---|---|---|---|---|---|
| 462 | 0.139 | 437 | 0.186 | 412.5 | 0.31 |
| 461.5 | 0.433 | 436.5 | 0.628 | 412 | 0.344 |
| 459.5 | 0.572 | 436 | 0.635 | 411.5 | 0.255 |
| 459 | 0.649 | 435.5 | 0.353 | 411 | 0.534 |
| 458.5 | 0.296 | 435 | 0.354 | 410.5 | 0.161 |
| 458 | 0.507 | 434.5 | 0.536 | 410 | 0.563 |
| 457.5 | 0.517 | 434 | 0.487 | 409.5 | 0.245 |
| 457 | 0.473 | 433.5 | 0.575 | 409 | 0.336 |
| 456.5 | 0.471 | 433 | 0.521 | 408.5 | 0.24 |
| 456 | 0.517 | 432.5 | 0.298 | 408 | 0.365 |
| 455.5 | 0.404 | 432 | 0.437 | 407.5 | 0.592 |
| 455 | 0.478 | 431.5 | 0.218 | 407 | 0.319 |
| 454.5 | 0.525 | 431 | 0.343 | 406.5 | 0.152 |
| 454 | 0.673 | 430.5 | 0.33 | 406 | 0.35 |
| 453.5 | 0.476 | 430 | 0.618 | 405.5 | 0.329 |
| 453 | 0.351 | 429.5 | 0.464 | 405 | 0.252 |
| 452.5 | 0.29 | 429 | 0.43 | 404.5 | 0.114 |
| 452 | 0.32 | 428.5 | 0.337 | 404 | 0.155 |
| 450.5 | 0.627 | 428 | 0.39 | 403.5 | 0.317 |
| 450 | 0.49 | 425 | 0.472 | 403 | 0.278 |
| 448.5 | 0.532 | 424 | 0.317 | 402.5 | 0.162 |
| 448 | 0.482 | 423.5 | 0.478 | 402 | 0.248 |
| 447.5 | 0.449 | 423 | 0.295 | 401.5 | 0.285 |
| 447 | 0.577 | 422.5 | 0.47 | 401 | 0.141 |
| 446.5 | 0.663 | 422 | 0.331 | 400.5 | 0.132 |
| 446 | 0.486 | 421.5 | 0.428 | 400 | 0.315 |
| 445.5 | 0.306 | 421 | 0.149 | 399.5 | 0.474 |
| 445 | 0.17 | 420.5 | 0.222 | 399 | 0.217 |
| 444.5 | 0.588 | 420 | 0.159 | 398.5 | 0.452 |
| 444 | 0.368 | 419.5 | 0.356 | 398 | 0.196 |
| 443.5 | 0.69 | 419 | 0.186 | 397.5 | 0.197 |
| 443 | 0.504 | 418.5 | 0.273 | 397 | 0.191 |
| 442.5 | 0.529 | 418 | 0.264 | 396.5 | 0.359 |
| 442 | 0.487 | 417.5 | 0.307 | 396 | 0.22 |
| 441.5 | 0.662 | 417 | 0.114 | 395.5 | 0.237 |
| 441 | 0.442 | 416.5 | 0.12 | 395 | 0.235 |
| 440.5 | 0.332 | 416 | 0.191 | 394.5 | 0.2 |
| 440 | 0.498 | 415.5 | 0.276 | 394 | 0.236 |
| 439.5 | 0.615 | 415 | 0.493 | 393.5 | 0.211 |
| 439 | 0.54 | 414.5 | 0.425 | 393 | 0.185 |
| 438.5 | 0.293 | 414 | 0.192 | 392.5 | 0.291 |
| 438 | 0.478 | 413.5 | 0.59 | 392 | 0.164 |
| 437.5 | 0.556 | 413 | 0.307 | 391.5 | 0.257 |

| | | | | | |
|---|---|---|---|---|---|
| 391 | 0.258 | 369.5 | 0.141 | 348 | 0.189 |
| 390.5 | 0.505 | 369 | 0.381 | 347.5 | 0.274 |
| 390 | 0.282 | 368.5 | 0.138 | 347 | 0.401 |
| 389.5 | 0.377 | 368 | 0.389 | 346.5 | 0.238 |
| 389 | 0.277 | 367.5 | 0.245 | 346 | 0.194 |
| 388.5 | 0.429 | 367 | 0.249 | 345.5 | 0.309 |
| 388 | 0.256 | 366.5 | 0.142 | 345 | 0.243 |
| 387.5 | 0.201 | 366 | 0.442 | 344.5 | 0.181 |
| 387 | 0.353 | 365.5 | 0.365 | 344 | 0.314 |
| 386.5 | 0.413 | 365 | 0.466 | 343.5 | 0.253 |
| 386 | 0.324 | 364.5 | 0.359 | 343 | 0.319 |
| 385.5 | 0.107 | 364 | 0.327 | 342.5 | 0.329 |
| 385 | 0.229 | 363.5 | 0.464 | 342 | 0.46 |
| 384.5 | 0.307 | 363 | 0.361 | 341.5 | 0.201 |
| 384 | 0.264 | 362.5 | 0.397 | 341 | 0.281 |
| 383.5 | 0.279 | 362 | 0.253 | 340.5 | 0.295 |
| 383 | 0.153 | 361.5 | 0.251 | 340 | 0.413 |
| 382.5 | 0.297 | 361 | 0.156 | 339.5 | 0.506 |
| 382 | 0.383 | 360.5 | 0.103 | 339 | 0.344 |
| 381.5 | 0.347 | 360 | 0.493 | 338.5 | 0.462 |
| 381 | 0.278 | 359.5 | 0.318 | 338 | 0.531 |
| 380.5 | 0.322 | 359 | 0.325 | 337.5 | 0.288 |
| 380 | 0.266 | 358.5 | 0.346 | 337 | 0.356 |
| 379.5 | 0.377 | 358 | 0.309 | 336.5 | 0.653 |
| 379 | 0.196 | 357.5 | 0.347 | 336 | 0.574 |
| 378.5 | 0.307 | 357 | 0.172 | 335.5 | 0.588 |
| 378 | 0.331 | 356.5 | 0.441 | 335 | 0.243 |
| 377.5 | 0.12 | 356 | 0.273 | 334.5 | 0.417 |
| 377 | 0.284 | 355.5 | 0.318 | 334 | 0.509 |
| 376.5 | 0.378 | 355 | 0.308 | 333.5 | 0.468 |
| 376 | 0.461 | 354.5 | 0.308 | 333 | 0.333 |
| 375.5 | 0.341 | 354 | 0.428 | 332.5 | 0.488 |
| 375 | 0.468 | 353.5 | 0.27 | 332 | 0.317 |
| 374.5 | 0.273 | 353 | 0.335 | 331.5 | 0.392 |
| 374 | 0.267 | 352.5 | 0.41 | 331 | 0.284 |
| 373.5 | 0.344 | 352 | 0.13 | 330.5 | 0.286 |
| 373 | 0.242 | 351.5 | 0.289 | 330 | 0.422 |
| 372.5 | 0.419 | 351 | 0.119 | 329.5 | 0.471 |
| 372 | 0.225 | 350.5 | 0.428 | 329 | 0.54 |
| 371.5 | 0.348 | 350 | 0.369 | 328.5 | 0.324 |
| 371 | 0.329 | 349.5 | 0.233 | 328 | 0.323 |
| 370.5 | 0.373 | 349 | 0.311 | 327.5 | 0.419 |
| 370 | 0.295 | 348.5 | 0.23 | 327 | 0.478 |

| | | | | | |
|---|---|---|---|---|---|
| 326.5 | 0.331 | 305 | 0.328 | 283.5 | 0.405 |
| 326 | 0.359 | 304.5 | 0.301 | 283 | 0.459 |
| 325.5 | 0.321 | 304 | 0.298 | 282.5 | 0.335 |
| 325 | 0.328 | 303.5 | 0.281 | 282 | 0.24 |
| 324.5 | 0.273 | 303 | 0.335 | 281.5 | 0.306 |
| 324 | 0.357 | 302.5 | 0.25 | 281 | 0.326 |
| 323.5 | 0.378 | 302 | 0.366 | 280.5 | 0.318 |
| 323 | 0.407 | 301.5 | 0.386 | 280 | 0.356 |
| 322.5 | 0.39 | 301 | 0.341 | 279.5 | 0.211 |
| 322 | 0.355 | 300.5 | 0.284 | 279 | 0.226 |
| 321.5 | 0.368 | 300 | 0.257 | 278.5 | 0.298 |
| 321 | 0.333 | 299.5 | 0.301 | 278 | 0.423 |
| 320.5 | 0.305 | 299 | 0.343 | 277.5 | 0.283 |
| 320 | 0.362 | 298.5 | 0.338 | 277 | 0.532 |
| 319.5 | 0.257 | 298 | 0.31 | 276.5 | 0.35 |
| 319 | 0.315 | 297.5 | 0.329 | 276 | 0.454 |
| 318.5 | 0.482 | 297 | 0.324 | 275.5 | 0.409 |
| 318 | 0.408 | 296.5 | 0.306 | 275 | 0.294 |
| 317.5 | 0.34 | 296 | 0.392 | 274.5 | 0.588 |
| 317 | 0.348 | 295.5 | 0.264 | 274 | 0.202 |
| 316.5 | 0.415 | 295 | 0.292 | 273.5 | 0.505 |
| 316 | 0.453 | 294.5 | 0.296 | 273 | 0.284 |
| 315.5 | 0.301 | 294 | 0.392 | 272.5 | 0.27 |
| 315 | 0.306 | 293.5 | 0.333 | 272 | 0.433 |
| 314.5 | 0.313 | 293 | 0.43 | 271.5 | 0.314 |
| 314 | 0.36 | 292.5 | 0.289 | 271 | 0.366 |
| 313.5 | 0.387 | 292 | 0.305 | 270.5 | 0.437 |
| 313 | 0.382 | 291.5 | 0.315 | 270 | 0.528 |
| 312.5 | 0.394 | 291 | 0.378 | 269.5 | 0.297 |
| 312 | 0.315 | 290.5 | 0.216 | 269 | 0.26 |
| 311.5 | 0.302 | 290 | 0.354 | 268.5 | 0.534 |
| 311 | 0.32 | 289.5 | 0.519 | 268 | 0.575 |
| 310.5 | 0.324 | 289 | 0.267 | 267.5 | 0.474 |
| 310 | 0.354 | 288.5 | 0.334 | 267 | 0.419 |
| 309.5 | 0.33 | 288 | 0.339 | 266.5 | 0.269 |
| 309 | 0.317 | 287.5 | 0.441 | 266 | 0.522 |
| 308.5 | 0.308 | 287 | 0.209 | 265.5 | 0.424 |
| 308 | 0.298 | 286.5 | 0.357 | 265 | 0.506 |
| 307.5 | 0.471 | 286 | 0.255 | 264.5 | 0.355 |
| 307 | 0.413 | 285.5 | 0.189 | 264 | 0.567 |
| 306.5 | 0.316 | 285 | 0.393 | 263.5 | 0.55 |
| 306 | 0.214 | 284.5 | 0.246 | 263 | 0.5 |
| 305.5 | 0.259 | 284 | 0.439 | 262.5 | 0.424 |

| | | | | | |
|---|---|---|---|---|---|
| 262 | 0.513 | 240 | 0.299 | 218.5 | 0.23 |
| 261.5 | 0.596 | 239.5 | 0.358 | 218 | 0.287 |
| 261 | 0.289 | 239 | 0.327 | 217.5 | 0.285 |
| 260.5 | 0.444 | 238.5 | 0.279 | 217 | 0.197 |
| 260 | 0.613 | 238 | 0.489 | 216.5 | 0.151 |
| 259.5 | 0.362 | 237.5 | 0.402 | 216 | 0.298 |
| 259 | 0.574 | 237 | 0.303 | 215.5 | 0.239 |
| 258.5 | 0.492 | 236.5 | 0.251 | 215 | 0.279 |
| 258 | 0.387 | 236 | 0.302 | 214.5 | 0.318 |
| 257.5 | 0.288 | 235.5 | 0.235 | 214 | 0.241 |
| 257 | 0.313 | 235 | 0.309 | 213.5 | 0.197 |
| 256.5 | 0.516 | 234.5 | 0.291 | 213 | 0.253 |
| 256 | 0.403 | 234 | 0.269 | 212.5 | 0.248 |
| 255.5 | 0.492 | 233.5 | 0.315 | 212 | 0.308 |
| 255 | 0.391 | 233 | 0.397 | 211.5 | 0.246 |
| 254.5 | 0.321 | 232.5 | 0.288 | 211 | 0.268 |
| 254 | 0.468 | 232 | 0.305 | 210.5 | 0.107 |
| 253.5 | 0.432 | 231.5 | 0.231 | 210 | 0.291 |
| 253 | 0.469 | 231 | 0.127 | 209.5 | 0.314 |
| 252 | 0.274 | 230.5 | 0.136 | 209 | 0.312 |
| 251.5 | 0.668 | 230 | 0.16 | 208.5 | 0.234 |
| 251 | 0.406 | 229.5 | 0.13 | 208 | 0.186 |
| 250.5 | 0.309 | 229 | 0.124 | 207.5 | 0.273 |
| 250 | 0.477 | 228.5 | 0.203 | 207 | 0.289 |
| 249.5 | 0.386 | 228 | 0.21 | 206.5 | 0.313 |
| 249 | 0.56 | 227.5 | 0.288 | 206 | 0.32 |
| 248.5 | 0.364 | 227 | 0.337 | 205.5 | 0.321 |
| 248 | 0.388 | 226.5 | 0.318 | 205 | 0.306 |
| 247.5 | 0.202 | 226 | 0.31 | 204.5 | 0.235 |
| 247 | 0.346 | 225.5 | 0.261 | 204 | 0.232 |
| 246.5 | 0.512 | 225 | 0.266 | 203.5 | 0.288 |
| 246 | 0.358 | 224.5 | 0.237 | 203 | 0.233 |
| 245.5 | 0.347 | 224 | 0.182 | 202.5 | 0.363 |
| 245 | 0.343 | 223.5 | 0.208 | 202 | 0.194 |
| 244.5 | 0.263 | 223 | 0.194 | 201.5 | 0.277 |
| 244 | 0.34 | 222.5 | 0.105 | 201 | 0.284 |
| 243.5 | 0.282 | 222 | 0.269 | 200.5 | 0.284 |
| 243 | 0.447 | 221.5 | 0.318 | 200 | 0.378 |
| 242.5 | 0.276 | 221 | 0.241 | 199.5 | 0.255 |
| 242 | 0.397 | 220.5 | 0.214 | 199 | 0.189 |
| 241.5 | 0.342 | 220 | 0.235 | 198.5 | 0.205 |
| 241 | 0.493 | 219.5 | 0.31 | 198 | 0.265 |
| 240.5 | 0.411 | 219 | 0.191 | 197.5 | 0.204 |

| | | | | | |
|---|---|---|---|---|---|
| 197 | 0.283 | 175 | 0.164 | 134 | 0.536 |
| 196.5 | 0.238 | 174.5 | 0.551 | 133 | 0.385 |
| 196 | 0.234 | 174 | 0.445 | 132 | 0.169 |
| 195.5 | 0.324 | 173.5 | 0.478 | 131.5 | 0.138 |
| 195 | 0.306 | 173 | 0.409 | 131 | 0.151 |
| 194.5 | 0.196 | 172 | 0.489 | 130.5 | 0.352 |
| 194 | 0.224 | 171 | 0.477 | 130 | 0.224 |
| 193.5 | 0.259 | 170 | 0.318 | 129.5 | 0.212 |
| 193 | 0.237 | 169 | 0.454 | 129 | 0.162 |
| 192.5 | 0.166 | 168 | 0.27 | 128.5 | 0.163 |
| 192 | 0.293 | 167 | 0.221 | 128 | 0.159 |
| 191.5 | 0.299 | 166 | 0.232 | 127.5 | 0.166 |
| 191 | 0.205 | 165 | 0.299 | 127 | 0.174 |
| 190.5 | 0.295 | 164 | 0.434 | 126.5 | 0.185 |
| 190 | 0.333 | 163 | 0.396 | 126 | 0.326 |
| 189.5 | 0.311 | 162 | 0.475 | 125.5 | 0.263 |
| 189 | 0.196 | 161 | 0.316 | 125 | 0.155 |
| 188.5 | 0.309 | 160 | 0.264 | 124.5 | 0.155 |
| 188 | 0.257 | 159 | 0.41 | 124 | 0.225 |
| 187.5 | 0.302 | 158 | 0.33 | 123.5 | 0.16 |
| 187 | 0.185 | 157 | 0.421 | 123 | 0.255 |
| 186.5 | 0.31 | 156 | 0.258 | 122.5 | 0.17 |
| 186 | 0.31 | 155 | 0.442 | 122 | 0.179 |
| 185.5 | 0.308 | 154 | 0.333 | 121 | 0.197 |
| 185 | 0.381 | 153 | 0.352 | 120.5 | 0.142 |
| 184.5 | 0.399 | 152 | 0.429 | 120 | 0.15 |
| 184 | 0.418 | 151 | 0.303 | 119.5 | 0.18 |
| 183.5 | 0.282 | 150 | 0.44 | 119 | 0.207 |
| 183 | 0.395 | 149 | 0.453 | 118.5 | 0.142 |
| 182.5 | 0.254 | 148 | 0.4 | 118 | 0.143 |
| 182 | 0.35 | 147 | 0.439 | 117.5 | 0.184 |
| 181.5 | 0.398 | 146 | 0.308 | 117 | 0.261 |
| 181 | 0.298 | 145 | 0.302 | 116.5 | 0.161 |
| 180.5 | 0.303 | 144 | 0.338 | 116 | 0.185 |
| 180 | 0.326 | 143 | 0.463 | 115.5 | 0.208 |
| 179.5 | 0.288 | 142 | 0.389 | 115 | 0.123 |
| 179 | 0.465 | 141 | 0.415 | 114.5 | 0.167 |
| 178.5 | 0.426 | 140 | 0.293 | 114 | 0.338 |
| 178 | 0.398 | 139 | 0.359 | 113.5 | 0.31 |
| 177 | 0.429 | 138 | 0.263 | 113 | 0.354 |
| 176.5 | 0.24 | 137 | 0.592 | 112.5 | 0.151 |
| 176 | 0.41 | 136 | 0.454 | 112 | 0.16 |
| 175.5 | 0.476 | 135 | 0.59 | 111.5 | 0.124 |

| | | | | | |
|---|---|---|---|---|---|
| 111 | 0.257 | 89 | 0.343 | 67 | 0.214 |
| 110.5 | 0.11 | 88.5 | 0.226 | 66.5 | 0.102 |
| 110 | 0.209 | 88 | 0.207 | 66 | 0.23 |
| 109.5 | 0.208 | 87.5 | 0.312 | 65.5 | 0.188 |
| 109 | 0.234 | 87 | 0.271 | 65 | 0.237 |
| 108.5 | 0.287 | 86.5 | 0.261 | 64.5 | 0.216 |
| 107.5 | 0.183 | 86 | 0.188 | 64 | 0.252 |
| 107 | 0.197 | 85.5 | 0.25 | 63.5 | 0.224 |
| 106.5 | 0.202 | 85 | 0.275 | 63 | 0.175 |
| 106 | 0.241 | 84.5 | 0.259 | 62.5 | 0.204 |
| 105.5 | 0.193 | 84 | 0.258 | 62 | 0.394 |
| 105 | 0.125 | 83 | 0.224 | 61.5 | 0.238 |
| 104.5 | 0.149 | 82.5 | 0.186 | 61 | 0.272 |
| 104 | 0.217 | 82 | 0.279 | 60.5 | 0.189 |
| 103.5 | 0.249 | 81.5 | 0.139 | 60 | 0.207 |
| 103 | 0.121 | 81 | 0.292 | 59.5 | 0.315 |
| 102.5 | 0.264 | 80.5 | 0.25 | 59 | 0.155 |
| 102 | 0.177 | 80 | 0.24 | 58.5 | 0.22 |
| 101.5 | 0.29 | 79.5 | 0.219 | 58 | 0.322 |
| 101 | 0.249 | 79 | 0.219 | 57.5 | 0.295 |
| 100.5 | 0.227 | 78.5 | 0.127 | 57 | 0.183 |
| 100 | 0.19 | 78 | 0.232 | 56.5 | 0.23 |
| 99.5 | 0.165 | 77.5 | 0.231 | 56 | 0.178 |
| 99 | 0.243 | 77 | 0.154 | 55.5 | 0.19 |
| 98.5 | 0.143 | 76.5 | 0.251 | 55 | 0.15 |
| 98 | 0.281 | 76 | 0.241 | 54.5 | 0.208 |
| 97.5 | 0.271 | 75.5 | 0.241 | 54 | 0.218 |
| 97 | 0.224 | 75 | 0.284 | 53.5 | 0.17 |
| 96.5 | 0.264 | 74.5 | 0.221 | 53 | 0.203 |
| 96 | 0.225 | 74 | 0.246 | 52.5 | 0.15 |
| 95.5 | 0.231 | 73.5 | 0.209 | 52 | 0.128 |
| 95 | 0.193 | 73 | 0.203 | 51.5 | 0.143 |
| 94.5 | 0.2 | 72.5 | 0.171 | 51 | 0.184 |
| 94 | 0.245 | 72 | 0.159 | 50.5 | 0.277 |
| 93.5 | 0.361 | 71.5 | 0.17 | 50 | 0.188 |
| 93 | 0.181 | 71 | 0.229 | 49.5 | 0.269 |
| 92.5 | 0.239 | 70.5 | 0.263 | 49 | 0.222 |
| 92 | 0.216 | 70 | 0.244 | 48.5 | 0.252 |
| 91.5 | 0.284 | 69.5 | 0.276 | 48 | 0.254 |
| 91 | 0.277 | 69 | 0.233 | 47.5 | 0.347 |
| 90.5 | 0.285 | 68.5 | 0.242 | 47 | 0.232 |
| 90 | 0.344 | 68 | 0.202 | 46.5 | 0.323 |
| 89.5 | 0.374 | 67.5 | 0.191 | 46 | 0.171 |

| | | | | | |
|---|---|---|---|---|---|
| 45.5 | 0.251 | 30 | 0.149 | 14.5 | 0.188 |
| 45 | 0.338 | 29.5 | 0.198 | 14 | 0.205 |
| 44.5 | 0.17 | 29 | 0.224 | 13.5 | 0.197 |
| 44 | 0.233 | 28.5 | 0.21 | 13 | 0.176 |
| 43.5 | 0.335 | 28 | 0.228 | 12.5 | 0.372 |
| 43 | 0.27 | 27.5 | 0.142 | 12 | 0.203 |
| 42.5 | 0.259 | 27 | 0.176 | 11.5 | 0.173 |
| 42 | 0.275 | 26.5 | 0.22 | 11 | 0.233 |
| 41.5 | 0.272 | 26 | 0.174 | 10.5 | 0.299 |
| 41 | 0.264 | 25.5 | 0.269 | 10 | 0.29 |
| 40.5 | 0.197 | 25 | 0.238 | 9.5 | 0.161 |
| 40 | 0.279 | 24.5 | 0.248 | 9 | 0.174 |
| 39.5 | 0.305 | 24 | 0.242 | 8.5 | 0.242 |
| 39 | 0.359 | 23.5 | 0.262 | 8 | 0.248 |
| 38.5 | 0.267 | 23 | 0.154 | 7.5 | 0.475 |
| 38 | 0.165 | 22.5 | 0.143 | 7 | 0.173 |
| 37.5 | 0.294 | 22 | 0.154 | 6.5 | 0.192 |
| 37 | 0.351 | 21.5 | 0.216 | 6 | 0.188 |
| 36.5 | 0.177 | 21 | 0.102 | 5.5 | 0.322 |
| 36 | 0.275 | 20.5 | 0.267 | 5 | 0.161 |
| 35.5 | 0.231 | 20 | 0.134 | 4.5 | 0.127 |
| 35 | 0.275 | 19.5 | 0.181 | 4 | 0.156 |
| 34.5 | 0.304 | 19 | 0.199 | 3.5 | 0.177 |
| 34 | 0.208 | 18.5 | 0.182 | 3 | 0.137 |
| 33.5 | 0.153 | 18 | 0.251 | 2.5 | 0.101 |
| 33 | 0.207 | 17.5 | 0.187 | 2 | 0.174 |
| 32.5 | 0.104 | 17 | 0.184 | 1.5 | 0.229 |
| 32 | 0.255 | 16.5 | 0.295 | 1 | 0.191 |
| 31.5 | 0.23 | 16 | 0.17 | 0.5 | 0.251 |
| 31 | 0.219 | 15.5 | 0.261 | 0 | 0.227 |
| 30.5 | 0.246 | 15 | 0.188 | | |

**Raw Rock Magnetic Data**

Ranch section (every 5m with extra at paleosol, 0-80 m) – Acquired May 2019

| | *m* | *χlf* | *χhf* | *χfd or DeltaMS* |
|---|---|---|---|---|
| LBTR0000 | 0 | 20.0351007 | 18.6680214 | 1.36707925 |
| LBTR0005 | 5 | 23.1252275 | 21.5507827 | 1.57444485 |
| LBTR0010 | 10 | 21.4427133 | 19.8588276 | 1.58388568 |
| LBTR0011_1Base | 11 | 20.5746159 | 19.1433382 | 1.43127763 |
| LBTR0011_2 | 11 | 17.3709798 | 16.2584144 | 1.11256545 |
| LBTR0011_3 | 11 | 18.6017478 | 17.3725151 | 1.22923269 |
| LBTR0011_4Top | 11 | 12.4577895 | 11.6729032 | 0.78488637 |
| LBTR0020 | 20 | 18.829932 | 17.4240363 | 1.40589569 |
| LBTR0025 | 25 | 23.1870584 | 21.2718483 | 1.91521012 |
| LBTR0030 | 30 | 23.3011546 | 21.5407912 | 1.76036343 |
| LBTR0031 | 31 | 15.2790036 | 14.4748455 | 0.80415809 |
| LBTR0035 | 35 | 21.8446602 | 20.1456311 | 1.69902913 |
| LBTR0040 | 40 | 19.5770616 | 18.2842368 | 1.29282482 |
| LBTR0045 | 45 | 26.9913987 | 24.9532536 | 2.0381451 |
| LBTR0050 | 50 | 23.7405598 | 21.8924922 | 1.84806753 |
| LBTR0055 | 55 | 13.4438134 | 12.5407318 | 0.90308165 |
| LBTR0060 | 60 | 20.869734 | 19.2098622 | 1.65987187 |
| LBTR0065 | 65 | 13.0892449 | 12.2745995 | 0.81464531 |
| LBTR0070 | 70 | 23.9134507 | 22.1056575 | 1.80779318 |
| LBTR0075 | 75 | 20.3955501 | 18.9407626 | 1.45478749 |
| LBTR0080 | 80 | 21.8713105 | 20.4053522 | 1.46595828 |

Ranch section (every 30 cm, detailed section around paleosol, 10 m total) – Acquired Jan 2020

| *m* | *χlf* | *χhf* | *χfd or DeltaMS* |
|---|---|---|---|
| 0 | 27.15411559 | 24.7285464 | 2.42556918 |
| 0.3 | 24.46180556 | 22.3611111 | 2.10069444 |
| 0.6 | 23.34519573 | 21.4768683 | 1.8683274 |
| 0.9 | 24.36920223 | 22.2912801 | 2.07792208 |
| 1.2 | 21.704947 | 19.9911661 | 1.71378092 |
| 1.5 | 21.77405119 | 20.0794351 | 1.69461606 |
| 1.8 | 20.78301887 | 19.2641509 | 1.51886792 |
| 2.1 | 22.13452915 | 20.4484305 | 1.68609865 |
| 2.4 | 14.22018349 | 13.4954128 | 0.72477064 |
| 2.7 | 18.30948122 | 17.1645796 | 1.14490161 |
| 3 | 13.18024263 | 12.4350087 | 0.74523397 |
| 3.3 | 20.55833333 | 19.1583333 | 1.4 |

| | | | |
|---|---|---|---|
| 3.6 | 18.83968113 | 17.404783 | 1.43489814 |
| 3.9 | 18.91418564 | 17.5394046 | 1.37478109 |
| 4.2 | 22.24888889 | 20.4711111 | 1.77777778 |
| 4.5 | 20.01774623 | 18.6779059 | 1.33984028 |
| 4.8 | | | |
| 5.1 | 22.6367713 | 20.8071749 | 1.82959641 |
| 5.4 | | | |
| 5.7 | 23.0477908 | 21.1091073 | 1.9386835 |
| 5.9 | 22.27436823 | 20.4241877 | 1.85018051 |
| 6 | 21.79785331 | 20.1610018 | 1.63685152 |
| 6.3 | 20.81128748 | 19.3474427 | 1.4638448 |
| 6.6 | 22.94602013 | 21.2259835 | 1.7200366 |
| 6.9 | 19.96363636 | 18.5090909 | 1.45454545 |
| 7.2 | 24.3175736 | 22.4085638 | 1.90900981 |
| 7.5 | 18.37251356 | 17.079566 | 1.29294756 |
| 7.8 | 20.22317597 | 18.806867 | 1.41630901 |
| 8.1 | 17.91248861 | 16.74567 | 1.1668186 |
| 8.4 | 19.55017301 | 18.2698962 | 1.28027682 |
| 8.7 | | | |
| 9 | 13.79106992 | 13.1086773 | 0.68239259 |
| 9.3 | 13.24253076 | 12.6186292 | 0.62390158 |
| 9.6 | 14.61005199 | 13.8388215 | 0.7712305 |
| 9.9 | 15.88709677 | 14.9731183 | 0.91397849 |
| 10.2 | 14.7277677 | 13.9019964 | 0.82577132 |

**SUPPLEMENTAL MATERIALS**
**Chapter III**

## Appendix I: Methods (expanded)

Mud (mode 52-60 µm; Appendix II) was collected from modern lake sediment (Oklahoma) and frozen at -15°C overnight. After preliminary tests of the impact of sediment depth (1-10 mm in 90 mm and 48 mm-diameter petri dishes), and sediment homogeneity (sieved vs. un-sieved), all experiments were set up with pre-sieved (< 850 µm) sediment ~1-10 mm deep (sediment depths did not impact morphology). Experimental variables in this study included (1) solution chemistry: distilled water + NaCl (0%, 0.1%, 0.5%, 1%), and (2) sediment saturation: saturated vs. supersaturated. Saturation was achieved by addition of solution to sediment until pore spaces were full; supersaturation describes saturation plus pooling (≤ 1.5 mm films) of solution above the sediment. Models with dilute NaCl solutions were performed to test the effect of the presence of salts on morphology. We did not simulate growth of evaporitic minerals (e.g. calcium sulfates like gypsum) in sediment due to their moderate-to-low solubility, the time required to grow well-formed crystals (up to a year), uncertainty around paleoclimate-specific variables (e.g. availability of organics, sediment composition), and because this has already been well-documented (e.g. Cody and Cody, 1988; Magee, 1991). Grain size, temperature, and time were held constant in all experiments.

## Appendix II: Grain size

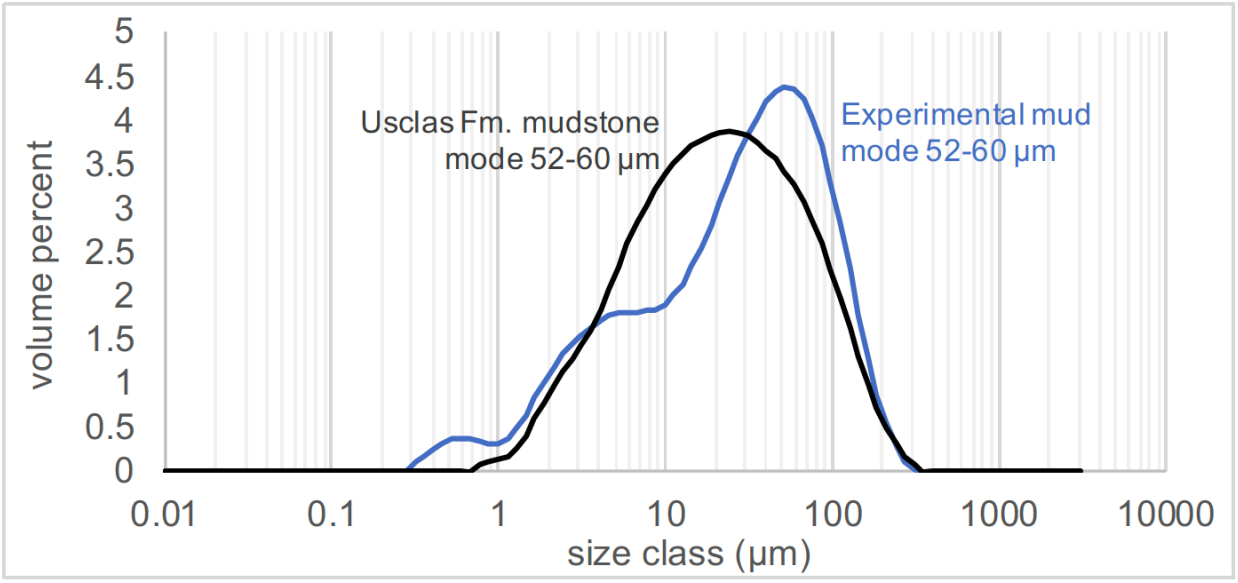


Figure showing the grain size distribution of mud used for laboratory simulation of ice crystal growth after being sieved to <850 µm (blue) and grain size distribution of disaggregated Usclas Formation mudstone (black).

## Appendix III: Variscan Paleoaltitude (expanded)

Mean Variscan paleoaltitude estimations determined using various indirect methods range from 5000 m to 2000 m (Becq-Giraudon et al., 1996; Fluteau et al. 2001; Roscher and Schneider, 2006; Goddéris et al. 2017). This discrepancy is mostly due to the time period considered. From 300 - 260 Ma, continental extension resulted in substantial thinning of thick Variscan crust, initiating the reduction in Variscan belt elevation (e.g. Becq-Giraudon and Van Den Driessche, 1994). In the southern French Massif central, high temperature, low pressure metamorphism developed between 320- 300 Ma (e.g. Roger et al. 2015; Poujol et al., 2017), with retrograde P-T conditions 0.4 Gpa and 700°C at 308 Ma (e.g. Rabin et al. 2015). The current crustal thickness here (30 km) is entirely Variscan-age (no major tectonic event could have affected its thickness since). Therefore, the crustal thickness in the Montagne Noire area at 300 Ma was ~45 km, corresponding to an elevation of 2500 m (assuming a ratio of 1/6 for isostatic compensation of thickening; e.g. Molnar and England, 1990). According to Pfeifer et al. (2018), ~15 km of overburden was removed by 285 Ma, reducing the crust to 30 km-thick and implying a mean elevation near sea level. However, drainage during the Upper Carboniferous and the Permian was internal (e.g. Pochat and Van Den Driessche, 2011) and erosion products were trapped in intramontane basins, so crustal thinning was mainly achieved by lithosphere extension. Concomitant mantle thinning induced the increase of both heat flow and lithosphere buoyancy, and finally surface uplift. Thus, removal of the 15 km overburden did not result in a lowering of elevation to sea level, but likely a buoyancy-sustained mean elevation around 1000 m. In summary, the mean elevation of the Variscan Mountains was reduced by ~1500 m from 308 Ma to 285 Ma. Around 295 Ma it did not exceed 1650 m (assuming persistent lowering through time during extension) or perhaps was much less than 1650 m (assuming exponential subsidence during gravity collapse extension; e.g. Sonder et al., 1987). This implies that the Usclas Formation (295-290 Ma) was deposited at moderate-low elevation (< 1650 m) in a basin surrounded by ranges > 1650 m. Similarities in facies and flora/fauna across the uppermost Carboniferous and the Permian basins in the Variscan domain indicate consistencies in climatic conditions and elevation throughout the Variscan chain.

**SUPPLEMENTAL MATERIALS**
**Chapter IV**

**I. Survey Instruments:** Self-efficacy survey (pre-to-post, self-rated) and Attitudinal survey. Also includes prompt for informal weekly reflection journaling ("formative personal reflections").

Symbol/code: _____

**Student self-rated Pre-Assessment**
Please draw a symbol or code at the top so that I can match this with your post-test (this is anonymous). We do not expect you to already know ANY of these things and the end goal is not for you to become an expert, this is simply to collect data that measures improvements in your ability and confidence while making interpretations and decisions in the field, and also to track how well we are doing at addressing the objectives of the program. Please rate your understanding/competency of each skill or concept by choosing one of the three options.

1. Defining what a sedimentary basin is and why we might be interested in studying one.
   __ Yes, I understand this sufficiently so that I can do or explain this independently.
   __ I can follow this in class or when I have an example but am confused when I work on my own.
   __ I recognize what this is referring to, but I don't understand/know how to do it.

2. Understanding of what the continents looked like 250 million years ago.
   __ Yes, I understand this sufficiently so that I can do or explain this independently.
   __ I can follow this in class or when I have an example but am confused when I work on my own.
   __ I recognize what this is referring to, but I don't understand/know how to do it.

3. Understanding of global icehouse vs. greenhouse paleoclimate conditions.
   __ Yes, I understand this sufficiently so that I can do or explain this independently.
   __ I can follow this in class or when I have an example but am confused when I work on my own.
   __ I recognize what this is referring to, but I don't understand/know how to do it.

4. Ability to use a Jacob's staff to measure and record a stratigraphic section.
   __ Yes, I understand this sufficiently so that I can do or explain this independently.
   __ I can follow this in class or when I have an example but am confused when I work on my own.
   __ I recognize what this is referring to, but I don't understand/know how to do it.

5. Ability to thoroughly describe and identify sedimentary rocks in outcrop (grain size, bedding, mineralogy, etc.)
   __ Yes, I understand this sufficiently so that I can do or explain this independently.
   __ I can follow this in class or when I have an example but am confused when I work on my own.
   __ I recognize what this is referring to, but I don't understand/know how to do it.

6. Ability to identify sedimentary structures in outcrop and hypothesize about their formation.
   __ Yes, I understand this sufficiently so that I can do or explain this independently.
   __ I can follow this in class or when I have an example but am confused when I work on my own.
   __ I recognize what this is referring to, but I don't understand/know how to do it.

7. Understanding several sediment transport mechanisms and the associated characteristics of "representative" deposits that you might expect to identify in outcrop.
   __ Yes, I understand this sufficiently so that I can do or explain this independently.
   __ I can follow this in class or when I have an example but am confused when I work on my own.
   __ I recognize what this is referring to, but I don't understand/know how to do it.

8. Ability to hypothesize about sediment transport mechanisms and paleoenvironmental conditions during deposition based on a variety of outcrop observations.
   __ Yes, I understand this sufficiently so that I can do or explain this independently.
   __ I can follow this in class or when I have an example but am confused when I work on my own.
   __ I recognize what this is referring to, but I don't understand/know how to do it.

9. Confidence in formulating several scientific hypotheses based on your observations when there is no right answer (uncertainty!)
   __ Yes, I understand this sufficiently so that I can do or explain this independently.
   __ I can follow this in class or when I have an example but am confused when I work on my own.
   __ I recognize what this is referring to, but I don't understand/know how to do it.

10. Confidence in developing a methodical scientific approach to testing your hypotheses.
    __ Yes, I understand this sufficiently so that I can do or explain this independently.
    __ I can follow this in class or when I have an example but am confused when I work on my own.
    __ I recognize what this is referring to, but I don't understand/know how to do it.

11. Ability to integrate multiple datasets to make well-supported interpretations and conclusions.
    __ Yes, I understand this sufficiently so that I can do or explain this independently.
    __ I can follow this in class or when I have an example but am confused when I work on my own.
    __ I recognize what this is referring to, but I don't understand/know how to do it.

12. Conducting independent geological fieldwork.
    __ Yes, I understand this sufficiently so that I can do or explain this independently.
    __ I can follow this in class or when I have an example but am confused when I work on my own.
    __ I recognize what this is referring to, but I don't understand/know how to do it.

13. I have taken (select all that apply):
    __ Sed/strat
    __ Field
    __ Structure
    __ Paleoclimate
    __ Undergrad research

14. Please briefly describe your experience in conducting research so far (OK if you say NONE!)

15. Please briefly describe your experience in conducting FIELD research (OK if you say NONE!)

16. What are your goals in participating in this program?

17. What are your career goals? (Grad school? Industry? Academia?) It's ok to not know!

18. What do you like about science (e.g. fieldwork/research/sedimentology/paleoclimate) and how would you rate your ability to think scientifically/work independent research projects?

19. Please rate the likelihood that you will apply for/attend graduate school with 5 being most-certainly, and 1 being certainly not:

    1 2 3 4 5

20. What were the important factors in your decision to participate in this program?

---

Symbol/code: _____

**Student Self-Rated Post-Assessment**

Please draw a symbol or code at the top so that I can match this with your pre-test (this is anonymous). We STILL do not expect you to be experts at any of these things, so just answer in a way that allows us to accurately measure improvements in your ability and confidence while making interpretations and decisions in the field, and also to track how well we are doing at addressing the objectives of the program. Please rate your understanding/competency of each skill or concept by choosing one of the three options.

1. Defining what a sedimentary basin is and why we might be interested in studying one.
   __ Yes, I understand this sufficiently so that I can do or explain this independently.
   __ I can follow this in class or when I have an example but am confused when I work on my own.
   __ I recognize what this is referring to, but I don't understand/know how to do it.

2. Understanding of what the continents looked like 250 million years ago.
   __ Yes, I understand this sufficiently so that I can do or explain this independently.
   __ I can follow this in class or when I have an example but am confused when I work on my own.
   __ I recognize what this is referring to, but I don't understand/know how to do it.

3. Understanding of global icehouse vs. greenhouse paleoclimate conditions.
   __ Yes, I understand this sufficiently so that I can do or explain this independently.
   __ I can follow this in class or when I have an example but am confused when I work on my own.
   __ I recognize what this is referring to, but I don't understand/know how to do it.

4. Ability to use a Jacob's staff to measure and record a stratigraphic section.
   __ Yes, I understand this sufficiently so that I can do or explain this independently.
   __ I can follow this in class or when I have an example but am confused when I work on my own.
   __ I recognize what this is referring to, but I don't understand/know how to do it.

5. Ability to thoroughly describe and identify sedimentary rocks in outcrop (grain size, bedding, mineralogy, etc.)
   __ Yes, I understand this sufficiently so that I can do or explain this independently.
   __ I can follow this in class or when I have an example but am confused when I work on my own.
   __ I recognize what this is referring to, but I don't understand/know how to do it.

6. Ability to identify sedimentary structures in outcrop and hypothesize about their formation.
   __ Yes, I understand this sufficiently so that I can do or explain this independently.
   __ I can follow this in class or when I have an example but am confused when I work on my own.
   __ I recognize what this is referring to, but I don't understand/know how to do it.

7. Understanding several sediment transport mechanisms and the associated characteristics of "representative" deposits that you might expect to identify in outcrop.
   __ Yes, I understand this sufficiently so that I can do or explain this independently.
   __ I can follow this in class or when I have an example but am confused when I work on my own.
   __ I recognize what this is referring to, but I don't understand/know how to do it.

8. Ability to hypothesize about sediment transport mechanisms and paleoenvironmental conditions during deposition based on a variety of outcrop observations.
   __ Yes, I understand this sufficiently so that I can do or explain this independently.
   __ I can follow this in class or when I have an example but am confused when I work on my own.
   __ I recognize what this is referring to, but I don't understand/know how to do it.

9. Confidence in formulating several scientific hypotheses based on your observations when there is no right answer (uncertainty!)
   __ Yes, I understand this sufficiently so that I can do or explain this independently.
   __ I can follow this in class or when I have an example but am confused when I work on my own.
   __ I recognize what this is referring to, but I don't understand/know how to do it.

10. Confidence in developing a methodical scientific approach to testing your hypotheses.
    __ Yes, I understand this sufficiently so that I can do or explain this independently.
    __ I can follow this in class or when I have an example but am confused when I work on my own.
    __ I recognize what this is referring to, but I don't understand/know how to do it.

11. Ability to integrate multiple datasets to make well-supported interpretations and conclusions.
    __ Yes, I understand this sufficiently so that I can do or explain this independently.
    __ I can follow this in class or when I have an example but am confused when I work on my own.
    __ I recognize what this is referring to, but I don't understand/know how to do it.

12. Conducting independent geological fieldwork.
    __ Yes, I understand this sufficiently so that I can do or explain this independently.
    __ I can follow this in class or when I have an example but am confused when I work on my own.
    __ I recognize what this is referring to, but I don't understand/know how to do it.

13. Would you recommend this program to other students?

14. Were your goals (for participating in this program) accomplished?

15. Are there courses or experiences that you wish you had before starting this project?

16. Are there specific courses or other projects you plan in the near future as a result of your project?

17. What do you like about science (e.g. fieldwork/research/sedimentology/paleoclimate) and how would you rate your ability to think scientifically/work independent research projects?

18. How has your participation in this program affected your future career plans or interests?

19. Please rate the likelihood that you will apply for/attend graduate school with 5 being most-certainly, and 1 being certainly not:

    1 2 3 4 5

---

**Attitudinal survey - IRES Program Evaluation**
Please answer each item with a numerical rating using the following scale.

| Rating | Satisfaction Scale | Quality Scale |
|---|---|---|
| 3 | Very Satisfied | Excellent |
| 2 | Satisfied | Very Good |
| 1 | Neutral | Average |
| 0 | Dissatisfied | Below Average |

1. This international REU program was well organized as a whole.

   0 1 2 3

2. The international component(s) of the program added value to the underlying scientific experience.

   0 1 2 3

3. I would recommend this program to others.

   0 1 2 3

4. I would recommend my mentor(s) for future projects.

   0 1 2 3

5. The value of your project to your future graduate school or professional career

   0 1 2 3

6. Information presented during orientation (workbooks, evening lecture series)

   0 1 2 3

7. The program in providing a broader view of what geoscience is

   0 1 2 3

8. The program in providing you with skillsets that make you more confident in field

   0 1 2 3

9. The program in helping you understand uncertainty and interpretation in science

   0 1 2 3

10. Your acceptance into the research group as a contributing member

    0 1 2 3

**Formative Personal Reflections**

The purpose is to encourage self-reflection, career development conversations, and/or to discuss the cultural immersion aspect of this research project. We will ask you to do weekly personal reflections at different points throughout the trip and when we gather you will have the option to share your perspective, thoughts, and/or concerns so that we can make sure we are using our time to be effective mentors.

**Example questions**

- What are you enjoying/not enjoying?
- What skills are you good at/where do you tend to lead? Where could you improve? What have you improved on this week?
- How do you anticipate that this experience could impact your future?
- What impact does this have on you professionally, personally, culturally?
- Do you feel inspired to pursue a career in STEM?
- Do you feel inspired by the international collaboration?

**II. Survey Instruments:** The cultural context inventory survey (Halverson, 1993).

Resiliency Tools presented by Al Siebert Resiliency Center

# Cultural-Context Inventory

Developed by Claire B. Halverson, PhD

For each of the following twenty statements circle 1 (strongly disagree) to 5 (strongly agree) to indicate your tendencies and preferences in a work situation.

| | Disagree | | | | Agree |
|---|---|---|---|---|---|
| 1. When communicating, I tend to use a lot of facial expressions, hand gestures, and body movements rather than to rely mostly on words. | 1 | 2 | 3 | 4 | 5 |
| 2. I pay more attention to the context of a conversation-who said what and under what circumstances-than I do to the words. | 1 | 2 | 3 | 4 | 5 |
| 3. When communicating, I tend to spell things out quickly and directly rather than talk around and add to the point. | 1 | 2 | 3 | 4 | 5 |
| 4. In an interpersonal disagreement, I tend to be more emotional than logical and rational. | 1 | 2 | 3 | 4 | 5 |
| 5. I tend to have a small, close circle of friends rather than a large, but less close, circle of friends. | 1 | 2 | 3 | 4 | 5 |
| 6. When working with others, I prefer to get the job done first and socialize afterward rather than socialize first and then tackle the job. | 1 | 2 | 3 | 4 | 5 |
| 7. I would rather work in a group than by myself. | 1 | 2 | 3 | 4 | 5 |
| 8. I believe rewards should be given for individual accomplishments rather than for group accomplishments. | 1 | 2 | 3 | 4 | 5 |
| 9. I describe myself in terms of my accomplishments rather than in terms of my family and relationships. | 1 | 2 | 3 | 4 | 5 |
| 10. I prefer sharing space with others to having my own private space. | 1 | 2 | 3 | 4 | 5 |
| 11. I would rather work for someone who maintains authority and functions for the good of the group than work for someone who allows a lot of autonomy and individual decision making. | 1 | 2 | 3 | 4 | 5 |
| 12. I believe it is more important to be on time, than to let other concerns take priority. | 1 | 2 | 3 | 4 | 5 |
| 13. I prefer working on one thing at a time to working on a variety of things at once. | 1 | 2 | 3 | 4 | 5 |
| 14. I generally set a time schedule and keep to it rather than leave things unscheduled and go with the flow. | 1 | 2 | 3 | 4 | 5 |
| 15. I find it easier to work with someone who is fast and wants to see immediate results than to work with someone who is slow and wants to consider all the facts. | 1 | 2 | 3 | 4 | 5 |
| 16. In order to learn about something, I tend to consult many sources of information rather than go to the one best authority. | 1 | 2 | 3 | 4 | 5 |
| 17. In figuring out problems, I prefer focusing on the whole situation to focusing on specific parts or taking one step at a time. | 1 | 2 | 3 | 4 | 5 |
| 18. When tackling a new task, I would rather figure it out on my own by experimentation than follow someone else's example or demonstration. | 1 | 2 | 3 | 4 | 5 |
| 19. When making decisions, I consider my likes and dislikes, not just the facts. | 1 | 2 | 3 | 4 | 5 |
| 20. I prefer having tasks and procedures explicitly defined to having a general idea of what has to be done. | 1 | 2 | 3 | 4 | 5 |

# Cultural Context Inventory

## Scoring Sheet:

The purpose of this inventory is to assess your tendencies toward being high- or low-context oriented. Transfer the circled numbers for each statement to the appropriate blank provided below. Then, add the numbers in each column to obtain your scores

| High Context (HC) | Low Context (LC) |
|---|---|
| 1. _____ | 3. _____ |
| 2. _____ | 6. _____ |
| 4. _____ | 4. _____ |
| 5. _____ | 9. _____ |
| 7. _____ | 12. _____ |
| 10. _____ | 13. _____ |
| 11. _____ | 14. _____ |
| 16. _____ | 15. _____ |
| 17. _____ | 18. _____ |
| 19. _____ | 20. _____ |
| TOTALS _____ | _____ |

**Put a check mark in the appropriate blank below to indicate which score is larger:**

_____ High Context _____ Low Context

**Subtract your high context score from your low context score. Record the difference in the blank below:**

_____ Low Context

\- _____ High Context

_____ ***Difference***

A plus number means higher context.
A minus number means lower context.

For more information about cultural context, please see the book *Effective Multicultural Teams: Theory and Practice (Advances in Group Decision and Negotiation)*, Claire B. Halverson (Editor), S. Aqeel Tirmizi (Editor) ©2008 Springer, or the website: **http://www2.pacific.edu/sis/culture/pub/Context_Cultures_High_and_Lo.htm** brought to you by Dr. Bruce LaBrack, at the University of the Pacific School of International Studies.